UNIVERSITAT DE BARCELONA

Funcionalización enzimática de la celulosa bacteriana para su aprovechamiento y valorización

Carolina Buruaga Ramiro

Funcionalización enzimática de la celulosa bacteriana para su aprovechamiento y valorización

Carolina Buruaga Ramiro

Tesis doctoral

Septiembre 2021

Barcelona

UNIVERSITAT DE BARCELONA

Funcionalización enzimática de la celulosa bacteriana para su aprovechamiento y valorización

Carolina Buruaga Ramiro

Programa de doctorado de Biotecnología

Departamento de Genética, Microbiología y Estadística

Facultad de Biología

Funcionalización enzimática de la celulosa bacteriana para su aprovechamiento y valorización

Memoria presentada por Carolina Buruaga Ramiro para optar al grado de Doctora por la Universidad de Barcelona

Directora

Dra. Josefina Martínez Martínez

Directora y tutora

Dra. Pilar Diaz Lucea

Doctoranda

Carolina Buruaga Ramiro

La presente tesis doctoral ha sido financiada mediante la ayuda “Ajut al personal investigador en formació” (APIF-2017), concedida por la Universidad de Barcelona.

Agradecimientos

Llevo casi cuatro años pensando que pondría en esta más que moralmente obligada sección y ahora me quedo sin inspiración, y no será por falta de personal a quien agradecer el haberme aguantado. Y es una pena, porque seguro que va a ser la más leída y la de mayor factor de impacto. Pero igual que con el doctorado, todo es empezar.

Lo primero que quiero aclarar es que la realización de una tesis doctoral no estaba entre mis planes. Por eso mismo, debo agradecer a mis directoras de tesis (o tutoras, o directora y tutora, o al revés, todavía me confundo, pero las jefas al fin y al cabo), las doctoras Josefina Martínez y Pilar Diaz el cambio de rumbo. Aún me acuerdo como hace ya casi cuatro años me acogieron en el laboratorio después de haber pasado una mala racha. Gracias de corazón Josefina, por ayudarme a salir de esa situación tan mala. Gracias a las dos por ser una fuente de inspiración desde el principio de mujeres trabajadoras, fuertes, capaces de todo lo que se ponga por delante. Lo que hoy en día se dice empoderada. Quiero agradecer también vuestra comprensión en momentos difíciles, ajenos a la tesis, que han ocurrido durante este tiempo. También desde el primer día las cosas quedaron muy claras, tal y como dijo Pilar "Mira, aquí somos pobres, pero nos queremos mucho." Desde luego, razón no te faltaba, porque así han sido estos cuatro años, me he sentido en familia. Ahora mismo es esta familia, la de del lab, la que te manda todo el apoyo para salir del pequeño bache en el que estás. Estoy segura de que todo va a ir bien, porque tú puedes con todo.

Siempre me acordaré de las tardes en que nos reuníamos las tres para revisar los resultados. Podíamos pasar desde quince minutos hasta más de horas. O no llegábamos a ninguna conclusión o salían muchísimas más líneas de investigación. En especial me acuerdo del día que llegamos al "nudo gordiano" y las dos asentisteis convencidas. Yo no entendía nada y se instaló el silencio hasta que os dije "Perdonad, pero yo no conozco esa técnica, ¿dónde busco información?". No sé cuánto tiempo os estuvisteis riendo, pero a mí me pareció mucho. Es por eso por lo que puedo afirmar que los conocimientos que se adquieren en una tesis doctoral son multidisciplinarios. Sea como fuere, espero haber estado a la altura de la confianza que depositasteis en mí al inicio de esta aventura. Yo al menos, he aprendido muchísimo en todos los sentidos, tanto si salían los experimentos como si no, que era lo más común.

Quiero también agradecer al doctor Javier Pastor todas sus aportaciones a la tesis y sus puntos de vista. Además de discutir resultados, eres una fuente conocimiento en todos los ámbitos. Tendría que haberte preguntado lo del nudo gordiano. Y si hay algo que tenemos en común toda la familia del laboratorio, es, como no, el amor por la gastronomía. Si alguien no era de buen comer, no entraba en nuestro grupo. Ahora que os jubiláis los tres, ya no es ningún secreto. Y es que nuestros mejores recuerdos se encuentran siempre alrededor de una mesa, como nuestros míticos amigos

invisibles en Navidad o los picapica de verano, o porque simplemente queríamos comer juntos sin más. Hasta en las reuniones de grupo era menester algún refrigerio. En caso contrario, Javier y Pilar tomaban más notas de la presentación. Y espero que esto no lo lea nadie del OSSMA, pero en el laboratorio nunca ha faltado algo para picar, preferentemente de chocolate claro está. El ritual siempre era el mismo: Pilar decía que no le gustaba el dulce, Josefina lo dejaba de postre y Javier quería algo salado de aperitivo para variar. Menos mal que Susana no hacía ascos a nada y se ofrecía la primera ante tanta incertidumbre, y Vero y yo no nos quedábamos atrás. Esto va a ser difícil de reemplazar.

Dicho esto, si no hiciera mención a mis padres me desheredarían, igual que mi tía. Y no les faltaría razón, porque son los que más me han aguantado, tanto si querían como si no. Me sabe mal haberos preocupado en algunas ocasiones, y aunque va a sonar a tópico, esto del doctorado es como una montaña rusa. Pero hasta aquí hemos llegado, y no habría sido posible sin vosotros, el colchón en el que siempre me puedo refugiar. Gracias mamá por ponerme los pies en la tierra, cuidarme (mucho), y decirme las cosas claras. Ahora habrá dos doctoras en la misma casa, ¡no habrá quién nos aguante! Gracias papá por animarme a acabar este proyecto, porque creo que eres el que está más contento de que vaya a ser doctora, incluso más que yo. Como tú dices, lo que se empieza se acaba, y si se hace, se hace bien. Te has sacado la carrera, el máster y ahora el doctorado junto a mí. Sin ti no llegaría a ningún sitio (literalmente). Gracias Martotos, mi tía, madrina, madre y abuela a la vez, por estar pendiente de mí y animarme a base de croquetas y buñuelos. Y… abueli, me hubiera gustado tanto que estuvieras aquí para poder decirte que ya casi soy doctora. Seguro que me habrías contestado "Ai que bien, hija mía, ahora ya puedes pasar consulta como tu madre, y de paso mírame las piernas que se me hinchan mucho". El día que te dije que iba a empezar a trabajar en la universidad, además de asegurarte de que ahora iba a ser cobrando, me preguntaste "Bueno, cuéntame que es lo que haces, que yo me entere". Espero que desde donde quieras que estés, puedas verlo, junto al pequeño Piolín.

Irónicamente, mientras fuera del laboratorio pasé por la peor etapa que he vivido, la tesis iba viento en popa. Sin vosotros, mi otra familia, no sé cómo habría salido del pozo. Vero, Marina, Melina sénior, Noelia, Mari Carmen, Celia, Marc y Arnau: el ambiente que reinó en nuestro laboratorio (o nuestros, cuando aún teníamos suficiente espacio para estirarnos sin meter el codo en el lector de placas) ese año fue mágico, por eso siempre nos quedará Hogwarts, ya lo sabéis. Marina y Melina, inseparables al principio. La confianza que me inspiraste desde el primer momento llegó a asustarme, Marina, parecíamos almas gemelas…decíamos lo mismo, vestíamos igual, éramos las *drama queens* del lab… será porque las dos somos cáncer. Melina, más reservada y tímida al principio, me encanta llamarte ahora amiga con todas las letras. Gracias por seguir soportándome fuera del laboratorio. Noelia, trabajadora a rabiar, no sé qué habría hecho

sin ti en la etapa final de la tesis, y con una pandemia, además. No sabes cuánto he echado de menos tu humor. Mari Carmen, la que más ganas e ilusión ponía, te han llegado a pasar cosas surrealistas durante tu tfg, pandemia aparte. Te va a ir muy bien en esta nueva etapa. Celia, como chocábamos al principio y qué inseparables nos volvimos. Las tardes sin ti no fueron lo mismo, mon amie. Je te souhaite le meilleur! Marc, papá de agapornis, gracias por tu amistad y tu apoyo en momentos difíciles. No lo voy a negar, sigo sin saber jugar a ajedrez. Arnau, sé que todavía me odias por obligarte a escuchar villancicos desde principios de noviembre, pero yo guardo muy buen recuerdo. Ya sabes que las cosas bien hechas y…¡la leche caliente!

A pesar de ser hija única, el doctorado me ha regalado una hermana. Sí, creo que eso es lo mejor del doctorado; la gente que se cruza en tu camino. No sé si tú serás de la misma opinión, pero yo doy gracias, ya sea por la conjunción de los astros, el destino o la divina casualidad, por haberte conocido, Vero. No podría haber tenido mejor compañera, aunque yo sinceramente te considero mi hermana. Me encanta que hablemos de ciencia y acabemos manteniendo tertulias literarias. Y viceversa. O combinado. O de los yogures de Mercadona. O de cuantos huevos necesitás para hacer una buena tortilla de patatas. Y mezclando español con inglés, portugués, guaraní, francés, alemán y chino. La tesis sin ti era muy aburrida, ¡ahora ya se puede decir! Anda que no hemos vivido cosas juntas, parece mentira. Como dice la canción (rectifico, la polka rock paraguaya), "si ya nos vamos conociendo, ingrata de mis ensueños…". Sólo espero que con la tesis me venga también la doble nacionalidad española-paraguaya. En resumen, que te quiero mucho, compañera Lourdes, que te mereces un monumento por aguantarme, y bien grande. Ya falta poco para que acabes tú también. ¡Vos vas a poder!

No puedo no agradecer a tu wifie, Jesi, todo el apoyo y compañía que me dio durante mi primer año. Gracias Jesi, por tu eterna sonrisa y tus buenos consejos. También te puse la cabeza como un bombo, he de reconocerlo. Fuiste una revolución para el lab, con tu alegría, espontaneidad y tus habilidades sociales (algo que a otros les falta, y no diré quién soy), que contrastaba con la tranquilidad de Xavi. Gracias Xavi por trabajar tan bien. Seguro que eres un profe genial.

Desde que entré como alumna interna colaboradora (ya empieza a hacer años de esto) fui recibida de manera muy cálida, la esencia del lab2. Ahí nos conocimos, Liliana Alexandra, Lily para los amigos. Pensabas que me había olvidado, ¿eh? No sabes cuánto te admiraba (y lo sigo haciendo) y todo lo que aprendí de ti. En ese año no pude tener más nombres: Caro, Karo, Carito, Carola…herencia tuya y de Majo y Dani, junto a Sergi, Alba, Marc, Anna, Judit y Mónica. Sé que el día de mi tesis estarás aquí, sólo espero que no lloremos demasiado. Sencillamente, me encanta ser tu amiga. Julia, Guillem sénior, Guillem Jr, Andrea, Riccardo y Pau…también fuimos una familia de lo más diversa, y además asistimos al evento del año: ¡la tesis de Lily! Julia, tan "cerca" que vivimos y no hay manera de verse. Guillem, sé que no fuiste tú quien me robó la crema de manos, o eso quiero seguir creyendo.

Ian y Melina Jr, hemos coincidido no sólo en la recta final de la tesis, sino también del lab. Sin vosotros el lab hubiera estado muy vacío este último año. Ya sabéis que os toca escribir el libro de la historia del lab2, así que ya podéis sacar a relucir vuestras dotes literarias. ¿Os acordáis cuando literalmente se cayó la pared del lab? Ése podría ser un buen capítulo.

Si hay un denominador común en todos estos años, eres tú Susana. Gracias por tus charlas motivacionales y tu pragmatismo. Creo que eres de las personas de las que más he aprendido en todos los ámbitos, no sólo en cuestiones técnicas y del dichoso SAP. Gracias por haberme enseñado a enseñar. Mónica, muchas gracias también por guiarme al principio de la tesis y darme unas cuantas directrices para el doctorado. Gracias también al resto de compañeros de pasillo, tanto de la Fase I como de la lejana Fase II, en especial a Robert, a Arantxa y a Hafida. Ai Robert, cuando me decías "mírame bien porque en mí te convertirás" me dabas un poco de miedo. He de decir que cada vez te entiendo más. Gracias Javier por tus cafés y tus consejos desde las catacumbas, como tú dices. A la plantilla de secretaría también la voy a echar mucho de menos. Ha sido un placer conoceros y tratar con vosotros, Susana, Rosario, Mónica (aunque nos hayamos visto poquito), Manolo y Bea.

Y gracias a verdaderos amigos, que tanto si hubiera emprendido la aventura de hacer el doctorado como si no, sé que están ahí. Maite, Alex, Maria, Miguel, Marc, Esther, gracias por vuestros puntos de vista. Cuando una va más perdida que pimiento en sangría (refrán paraguayo), no hay nada más reconfortante hablar con ellos. Mucho mejor que las valerianas a las que me he hecho adicta en los últimos tiempos.

Gracias Ana y María, mes chéries, por estar ahí, por sacarme a pasear y a airearme, cuando se podía, por vuestros valiosos consejos y sobre todo, por vuestra amistad. Las clases de francés también han sido un buen caldo de cultivo, sobre todo en el bar flamenco. Gracias también a Mario, Belén, Toni, Marisa, Fernando, Montse, Silvia, Iratxe, Marta. Han sido muchos años juntos, más que un doctorado de hecho. Me ha encantado presumir de la celulosa bacteriana con vosotros.

Y por último, gracias a los profesores que he tenido desde la secundaria hasta hoy. Por vuestra vocación y entusiasmo, tanto, que casi hago hasta letras en vez de ciencias. Gracias por aportarme valores más allá de las clases, en especial al doctor Joan Giménez, a quien admiro profundamente.

Y lo dejo aquí. ¡Esto va por todos vosotros!

Índice

Contenidos **Páginas**

Agradecimientos . . . . . I - IV
Índice **1**
Listado de abreviaturas **3**
Abstract . . . . . **5 - 6**
Resumen . . . . . **7 - 8**
1. Introducción . . . . . **9 - 44**
1.1. Celulosa bacteriana . . . . . 12 - 20
1.1.1.Funcionalización de la celulosa bacteriana . . . . . 19 - 20
1.2. Lipasas bacterianas . . . . . 20 - 29
1.2.1.Aplicaciones de las lipasas bacterianas . . . . . 23 - 24
1.2.2.Bacillus sp. JR3 y LipJ . . . . . 24 - 28
1.2.3.Actividad lipasa termófila de E.coli . . . . . 28 - 29
1.3. Inmovilización de enzimas en celulosa bacteriana . . . . . 30 - 35
1.3.1.Inmovilización de lipasas. 33
1.3.2.Inmovilización de lisozima. . . . . . 34 - 35
1.4. Nanocristales de celulosa bacteriana. . . . . 35 - 43
1.4.1.Enzimas disruptoras de la celulosa. . . . . . 39 - 40
1.4.2.Monoxigenasas líticas de polisacáridos y SamLPMO10C. . . . . . 40 - 42
1.4.3.Funcionalización de la CB con SamC para la obtención de nanocristales 43
2. Objetivos . . . . . **45 - 48**
3. Informes . . . . . **49 - 56**
3.1. Listado de publicaciones. 51
3.2. Informe sobre el factor de impacto . . . . . 52 - 53
3.3. Informe de participación en las publicaciones. . . . . 54 - 55
4. Artículos . . . . . **57 - 150**
4.1. Capítulo 1. Caracterización de lipasas bacterianas. . . . . 59 - 86
4.1.1.Artículo 1. . . . . . 61 - 73
4.1.2.Artículo 2 . . . . . 75 - 85
4.2. Capítulo 2. Funcionalización de la celulosa bacteriana: inmovilización de enzimas. . . . . 87 - 114
4.2.1.Artículo 3. . . . . . 89 - 104
4.2.2.Artículo 4. . . . . . 105 - 114
4.3. Funcionalización de la celulosa bacteriana: obtención de nanocristales con un tratamiento enzimático. . . . . 115 - 148
4.3.1.Artículo 5. . . . . . 117 - 150
5. Discusión general . . . . . **151 - 164**
6. Conclusiones . . . . . **165 - 168**
7. Referencias bibliográficas . . . . . **169 - 186**

Listado de abreviaturas

AA - Actividad auxiliar

BC – *Bacterial Cellulose*

BCNC – *BC nanocrystals*

BCS - *BC in aqueous suspension*

BCP – *BC paper*

BED - *Backscattered electron detector* (detector de electrones retrodispersados)

C1 - Carbono 1

C4 - Carbono 4

CAZy - *Carbohydrate-Active enZYmes*

CB - Celulosa bacteriana

CBM - Módulos de unión a carbohidratos

CDH - Celobiosa deshidrogenasa

CNC – *Cellulose nanocrystals*

CNF – *Cellulose nanofibrils*

EDS - *Energy-Dispersive X-ray Spectroscopy*

FDA - *Food and Drug Administration (*Administración de Alimentos y Medicinas)

GRAS - *Generally Recognized As Safe*

LPMO - *Lytic Polysaccharide Monooxygenase* (Monooxigenasa lítica de polisacáridos)

MALDI-TOF - *Matrix- assisted Laser Desorption/Ionization-Time of Flight*

NCC – Nanocristales de celulosa

NCCB - Nanocristales de celulosa bacteriana

NFC - Nanofibrillas de celulosa

SEM - *Scanning Electron Microscopy* (Microscopía electrónica de barrido)

TEM - *Transmission Electron Microscopy* (Microscopía electrónica de transmisión)

XRD – *X – Ray Diffraction* (Difracción de rayos X)

Abstract

Recently, interest in cellulose has shifted to nanoscale materials including cellulose nanofibrils (CNF), cellulose nanocrystals (CNC) and bacterial cellulose (BC). BC is an exopolysaccharide synthesized by some bacteria, with the same chemical structure than that of vegetable cellulose, but with different conformation and physicochemical properties. BC has a higher degree of purity, a higher crystallinity index and a greater water retention capacity. In addition, it has great elasticity and good mechanical resistance and is biocompatible. According to all these features, BC is a promising biomaterial that can meet the needs of different fields. Due to its three-dimensional structure of nanofibers, BC have a high superficial area, a feature that makes BC a suitable material to entrap different types of molecules. The main goal of this thesis, the functionalization of BC in a framework of more environmentally friendly methodologies, has been approached by enzyme immobilization and the obtention of CNC in a compendium of five research articles.

Prior to studying the suitability of different bacterial cellulose matrices lipase enzyme carriers, LipJ, a previously cloned lipase from *Bacillus cereus* JR3 was genetically improved. This stain deserved great interest for industrial applications because of its remarkably high tolerance to the extreme temperatures of its lipolytic system. However, even though its sequence has a markedly similarity to thermophilic lipases, LipJ showed the highest activity levels at 30°C, with no signs of being a thermophilic lipase. In the first study, with the objective of reversing its mesophilic activity into thermophilic trough a point directed mutation essay and through the construction of a NNK degenerancy library in the H110 position, a putative position involved in temperature dependent activation of thermophilic lipases. The obtained variants showed a a general shift in specificity towards longer chain-length substrates, but without thermophilic traits. These circumstances, in addition to the low activity of native LipJ lipase, led to reject this enzyme for immobilization onto BC. This difficulty in discriminating between the activity due to LipJ or the intrinsic activity of the host strain, *Escherichia coli*, aimed the purpose of the second study of the thesis. Even if this *E.coli*'s basal lipolytic activity is widely known in the scientific community, it has been barely explored. For these reasons, this activity was deeply characterized in the most common strains of *E.coli* used in the cloning and heterologous expression of lipases.

Then, as it is described in the third article, a commercial lipase was used to standardize the immobilization process on two BC matrices: BC in aqueous suspension (BCS) and BC paper (BCP). Once the Lipase BC by physical adsorption, it was found that neither the morphology nor the crystallinity were affected. The specific activity was measured under different conditions and the operational properties were evaluated. The Lipase / BCP nanocomposite showed great thermal stability, reusability and durability. Besides, it remained active after being storaged at room temperature for more than a month, which indicated that it could be a key element in the development of bioactive papers for simple, portable and disposable devices. Following the same methodology, the next research was focused on the production of a functional BC paper with antimicrobial and antioxidant activities through the immobilization of lysozyme. At room temperature, the immobilized enzyme showed greater stability than free lysozyme, apart from conserving all of its activity for almost three months. Due to the intrinsic nature of its components, Lysozyme-BCP is biodegradable and biocompatible, which makes it a great candidate for the design of new packaging materials in the food industry.

Finally, in the last article, NCC from BC (BCNC) were produced by an easier and more environmentally friendly process than traditional harsh acid hydrolysis. The combination of a lytic polysaccharide monooxygenase, who provided BC with negative charges and lead to a better stability, and a mixture of glycosyl hydrolases, BCNC with a length ranging from 80 nm to 2 μm and a width of 9 nm were obtained. Their properties allowed their use as a coating agent in two different pre-existing cellulosic materials, providing them with different degrees of barrier and mechanical properties.

Resumen

Recientemente, el interés en la celulosa se ha desplazado hacia materiales de la nanoescala que incluyen las nanofibrillas de celulosa (NFC), los nanocristales de celulosa (NCC) y la celulosa bacteriana (CB). La CB es un exopolisacárido sintetizado por algunas bacterias. Su composición química es la misma que la de la celulosa vegetal, pero su conformación y sus propiedades fisicoquímicas son diferentes. La CB presenta un mayor grado de pureza, tiene índices de cristalinidad más elevados y mayor capacidad de retención de agua. Además, presenta una gran elasticidad, buena resistencia mecánica y es biocompatible. Todas estas propiedades le confieren una gran aplicabilidad en campos muy diversos. La CB se produce en forma de una red tridimensional de nanofibras que genera una estructura con una elevada área superficial con potencial para la adhesión y retención de moléculas. El objetivo de esta tesis, la funcionalización de la CB dentro de un marco de tecnologías amigables con el medio ambiente, se ha abordado desde dos vertientes: la inmovilización de enzimas y la generación de NCC, todo ello reflejado en un compendio de cinco artículos.

Previamente al estudio de la idoneidad de diferentes matrices de CB como soporte para la inmovilización de enzimas lipasas, se procedió a la mejora genética de la lipasa LipJ de *Bacillus cereus* JR3. Esta cepa exhibía una actividad lipasa hipertermófila en su sobrenadante, una característica de gran interés de cara a una aplicación industrial. Sin embargo, LipJ, a pesar de su similitud de secuencia con otras lipasas termófilas bacterianas, no era la responsable de esta actividad. La meta del primer estudio fue, pues, revertir este comportamiento mesófilo a termófilo a través de una mutagénesis dirigida en los dominios de su centro catalítico y en el péptido señal y a través de la creación de una librería de degeneración NNK en la posición H110, implicada en la activación dependiente de la temperatura de lipasas termófilas. Las diferentes variantes obtenidas con ambas estrategias mostraron un cambio de tendencia en la especificidad de sustrato, pero sin rasgos de termofilia. Estas circunstancias, unidas a la baja actividad de la lipasa original, condujo a su descarte como enzima a inmovilizar sobre la CB. La dificultad en discriminar entre la actividad debida a LipJ o a la actividad intrínseca de la cepa hospedadora, *Escherichia coli,* inspiró el objetivo del segundo estudio de la tesis. Esta actividad basal, aunque conocida por la comunidad científica, apenas se encuentra documentada, y es la causa de interferencias en la caracterización de lipasas. Por estas

razones, se procedió a la caracterización de esta actividad en las cepas más comunes de *E.coli* empleadas en la clonación y expresión heteróloga de lipasas.

Como se describe en el tercer artículo, se empleó una lipasa comercial para estandarizar el proceso de inmovilización por adsorción física sobre dos matrices de CB: CB en suspensión acuosa (BCS, por sus siglas en inglés *Bacterial Cellulose Suspension*) y papel de CB (BCP por sus siglas en inglés *Bacterial Cellulose Paper*). Los nanocomposites de Lipasa/CB obtenidos presentaron excelentes propiedades operacionales. Los nanocomposites Lipasa/BCP mostraron una gran estabilidad térmica, reusabilidad y durabilidad, además de mantenerse activos después de ser almacenados durante más de un mes a temperatura ambiente, por lo que podrían ser potenciales candidatos en la elaboración de papeles bioactivos de dispositivos simples, portátiles y desechables. Siguiendo la misma metodología, en la siguiente investigación se generó un papel de CB funcional con actividad antimicrobiana y antioxidante, mediante la inmovilización de la lisozima. A temperatura ambiente, la enzima inmovilizada mostró una mayor estabilidad que la lisozima libre, aparte de conservar la totalidad de su actividad durante casi tres meses. Debido a la naturaleza intrínseca de sus componentes, el papel Lisozima/BCP es biodegradable y biocompatible, lo que lo convierte en candidato ideal para el diseño de nuevos materiales de envasado en la industria alimentaria.

Finalmente, en el último artículo se describe la producción de NCC de CB (NCCB), a partir de un proceso más sencillo y respetuoso con el medioambiente que la tradicional hidrólisis ácida con ácido sulfúrico o ácido clorhídrico. Mediante un tratamiento con monooxigenasas líticas de polisacáridos (LPMOs), responsables de aportar cargas negativas y proporcionar una mayor estabilidad, y una digestión con glucosil hidrolasas, se obtuvieron unos NCCB de entre 80 nm y 2 μm de longitud y 9 nm de ancho. Sus propiedades permitieron su uso como agentes de recubrimiento sobre soportes celulósicos de origen vegetal, aportándoles propiedades barrera al agua y al aceite, además de mejorar sus cualidades mecánicas.

1. INTRODUCCIÓN

1. Introducción

La creciente demanda de productos sostenibles y renovables independientes de los derivados del petróleo ha hecho que aumente el interés en los materiales "verdes". Para satisfacer esta demanda, los esfuerzos se han centrado en materiales que se obtienen directamente de los recursos naturales, como plantas, moluscos, crustáceos, bacterias y algas (Reid, Villalobos and Cranston, 2017). Entre ellos, los compuestos poliméricos constituyen una fuente renovable de materiales de alto rendimiento debido a su gran diversidad y sus propiedades, y la mayoría de ellos son biológicamente inertes, seguros para la salud humana y se encuentran en abundancia en la naturaleza (Kalia and Avérous, 2011; Zinge and Kandasubramanian, 2020). Aunque polisacáridos renovables como la celulosa, la quitina y el caucho natural, se han utilizado durante siglos, el reciente "movimiento verde" ha llevado a reorientar muchos de estos recursos hacia aplicaciones innovadoras de alto rendimiento (Domínguez *et al.*, 2021). Desde este punto de vista, los nanomateriales renovables constituyen un campo en rápido crecimiento con un gran potencial en la generación de nuevos biomateriales. Al igual que otros nanomateriales, los nanomateriales renovables tienen una alta relación superficie-volumen y propiedades únicas de la nanoescala que no están presentes en los materiales macroscópicos (Reid, Villalobos and Cranston, 2017).

Este trabajo se ha centrado en aprovechar las propiedades de la nanocelulosa bacteriana sometiéndola a diferentes modificaciones. La adhesión de proteínas a la superficie de la CB, concretamente la inmovilización de enzimas, constituye una de las dos grandes funcionalizaciones que se han llevado a cabo en esta tesis. La otra consiste en la generación de nanocristales de CB mediante el uso exclusivo de enzimas, en oposición al tratamiento clásico con ácido sulfúrico o clorhídrico. Entre las enzimas de interés biotecnológico para su inmovilización destacan las lipasas, por este motivo la primera parte del trabajo se centra en la optimización de la lipasa LipJ, previamente descrita en el grupo de investigación. Un efecto colateral de este estudio llevó a la caracterización de una lipasa presente en las cepas de *Escherichia coli* que frecuentemente se utilizan para la clonación de proteínas. Finalmente, el estudio de inmovilización de enzimas en matrices de nanocelulosa bacteriana se llevó a cabo con la lipasa Callera^{TM} Trans L y con la lisozima. Con ello, este tipo de soporte celulósico obtuvo funcionalidad catalítica y actividad antimicrobiana, respectivamente. El segundo propósito de este trabajo fue la obtención de nanocristales sometiendo a la celulosa bacteriana a un tratamiento con

enzimas disruptoras de la celulosa, monoxigenesas líticas de polisacáridos (LPMOs) y celulasas. En los siguientes apartados se tratan todos estos elementos para un mejor entendimiento.

1.1. Celulosa bacteriana

La celulosa es el polímero natural más abundante en la naturaleza y se encuentra ampliamente distribuido en las plantas, donde desempeña un papel esencial en el mantenimiento de la estructura de las paredes celulares (Habibi, Chanzy and Vignon, 2006). Se trata de un homopolisacárido lineal compuesto de unidades de β-D-glucopiranosa unidas entre sí por enlaces β-1-4 cuya unidad de repetición es un dímero de glucosa, conocido como celobiosa (**Figura 1*a***). Las cadenas de polímeros individuales se ensamblan en fibras a través de puentes de hidrógeno intermoleculares e interacciones hidrofóbicas (J. H. Kim *et al.*, 2015; Thomas *et al.*, 2018). Dentro de las fibras de celulosa hay regiones donde las cadenas de celulosa están dispuestas en una estructura altamente ordenada (cristalinas) y regiones desordenadas (amorfas) (Moon *et al.*, 2011) (**Figura 1*b***, ***c*)**. La celulosa además de formar parte de la pared celular de los vegetales se puede encontrar en animales marinos, hongos, bacterias, invertebrados e incluso amebas (Habibi, Chanzy and Vignon, 2006).

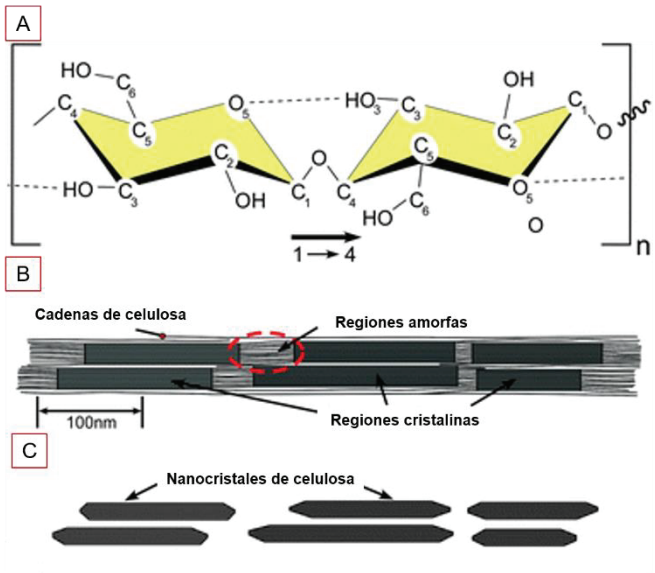

Figura 1. ***a)*** Unidad de repetición de una cadena de celulosa mostrando la direccionalidad del enlace β-1-4. ***b)*** Representación de una microfibrilla de celulosa en la que se muestra la ordenación de zonas cristalinas y amorfas. ***c)*** Representación de los nanocristales de celulosa que se obtienen después de una hidrólisis en la que se eliminaron las regiones amorfas. De Moon *et al.,* 2011.

La celulosa bacteriana (CB) fue inicialmente reportada por Brown en 1886 (Brown, 1886) como una membrana gelatinosa sobre la superficie de un caldo de fermentación de vinagre. La bacteria responsable, denominada *Acetobacter xylinus*, producía esta película membranosa en un cultivo en reposo y en presencia de oxígeno y glucosa. Esta especie, renombrada como *Gluconacetobacter xylinus*, actualmente es conocida como *Komagataeibacter xylinus* (Yamada *et al.*, 2012). Es una bacteria gramnegativa perteneciente a la familia *Acetobactereaceae*, aerobia estricta que realiza la oxidación incompleta de diversos azúcares y alcoholes (fermentación oxidativa). Su hábitat natural son las frutas y vegetales en proceso de descomposición (Pacheco *et al.*, 2004).

La CB dispone de una estructura químicamente equivalente a la celulosa vegetal, pero con una gran pureza química al carecer de hemicelulosa y lignina asociadas (Chawla *et al.*, 2009). Para eliminar estos componentes, la celulosa vegetal debe ser purificada mediante procesos enzimáticos, químicos y/o mecánicos, lo que genera un coste económico y ambiental alto, además de cambiar su funcionalidad y limitar su aplicabilidad. Sin embargo, para obtener la CB pura simplemente tiene que ser lavada de restos de células bacterianas con un tratamiento alcalino suave (Castro *et al.*, 2014; Vasconcelos *et al.*, 2017). La CB es producida de forma extracelular por distintas bacterias de los géneros *Agrobacterium* (Matthysse *et al.*, 2005), *Pseudomonas* (Ude *et al.*, 2006), *Rhizobium* (Yang *et al.*, 2013), y el ya mencionado *Komagataeibacter* (Brown, 1886; Gullo *et al.*, 2006), para los que se han descrito diversas funciones fisiológicas. En especies de los géneros *Rhizobium* y *Agrobacterium* facilita la adhesión celular en interacciones simbióticas e infecciosas (Matthysse *et al.*, 2005). En *Komagataeibacter xylinus* tiene una función de protección mecánica, química y biológica dentro del hábitat natural (Ross, Mayer and Benziman, 1991). La disposición de las microfibrillas de celulosa permite a las bacterias flotar en la interfase aire/líquido para obtener con mayor facilidad el oxígeno necesario para su crecimiento (Jonas and Farah, 1998). Adicionalmente, su carácter altamente higroscópico le permite retener humedad previniendo la desecación del sustrato (Pacheco *et al.*, 2004). Otras funciones reportadas son el refuerzo del suministro de nutrientes a las bacterias ya que éstos se concentran mejor debido a su capacidad de absorción (Ross, Mayer and Benziman, 1991; Bielecki *et al.*, 2005), como ayuda a los microorganismos aerobios estrictos por tal de que estén cerca de la fase gaseosa y como almacenamiento de alimento para utilizar en momentos de escasez (Okamoto *et al.*, 1994; Tahara *et al.*, 1998).

Los estudios sobre el proceso de biosíntesis de la celulosa bacteriana se han llevado a cabo especialmente con el género *Komagataeibacter*, que sintetiza celulosa a partir de diferentes fuentes de carbono como glucosa, sacarosa, glicerol, manitol o arabitol (Ishihara *et al.*, 2002; Keshk, 2014), tanto en condiciones de cultivo en agitación como estático. *K. xylinus* es considerada como arquetipo en la biogénesis de la CB ya que es la especie más estudiada y una de las pocas con un rendimiento de producción de celulosa importante como para ser explotada comercialmente (Lin *et al.*, 2013). Durante el proceso de síntesis de la CB, la glucosa se polimeriza y se extruye fuera de la célula a través de la enzima celulosa sintasa asociada a la membrana celular (**Figura 2*a***). Previamente a esta extrusión, es necesaria la conversión de la fuente de carbono en uridin difosfato glucosa (UPD- glucosa). Para ello, la glucosa, que es el sustrato primario, ha de ser convertida en glucosa-6-fosfato por la enzima glucoquinasa. Posteriormente actúa una fosfoglucomutasa convirtiéndolo en glucosa-1-fosfato; y para la excreción al medio este producto es convertido en UDP-glucosa en presencia de la enzima UDPG pirofosforilasa (Ross, Mayer and Benziman, 1991). Por último, el complejo celulasa sintasa excreta el polímero a través de la membrana plasmática al espacio extracelular (**Figura 2*b***).

El complejo de la celulosa sintasa está conformado por cuatro subunidades proteicas, denominadas BcsA, B, C y D, cuyos genes se encuentran en el operón *bcs* (*bacterial cellulose synthesis*) (Pacheco *et al.*, 2004) y se se transcriben como un mRNA policistrónico (Wong *et al.*, 1990). Este operón ha sido estudiado en las bacterias productoras de celulosa más conocidas, y se ha observado que para la formación de la cadena del polisacárido *in vitro* son necesarias solo dos subunidades: la BcsA y BcsB (Römling and Galperin, 2015). BcsA es la subunidad catalítica cuyo gen se encuentra más conservado, y se encuentra anclada en la membrana interna por la subunidad periplásmica BcsB (Omadjela *et al.*, 2013) (Figura 2*a*). En *K. xylinus* se han encontrado genes adicionales, como el *bcsZ,* cuya función aún no está del todo claro (Römling and Galperin, 2015). La presencia de los genes que codifican estas proteínas no es exclusiva de las bacterias acéticas y está muy extendida entre otros géneros bacterianos productores (Ortiz *et al*., 2004).

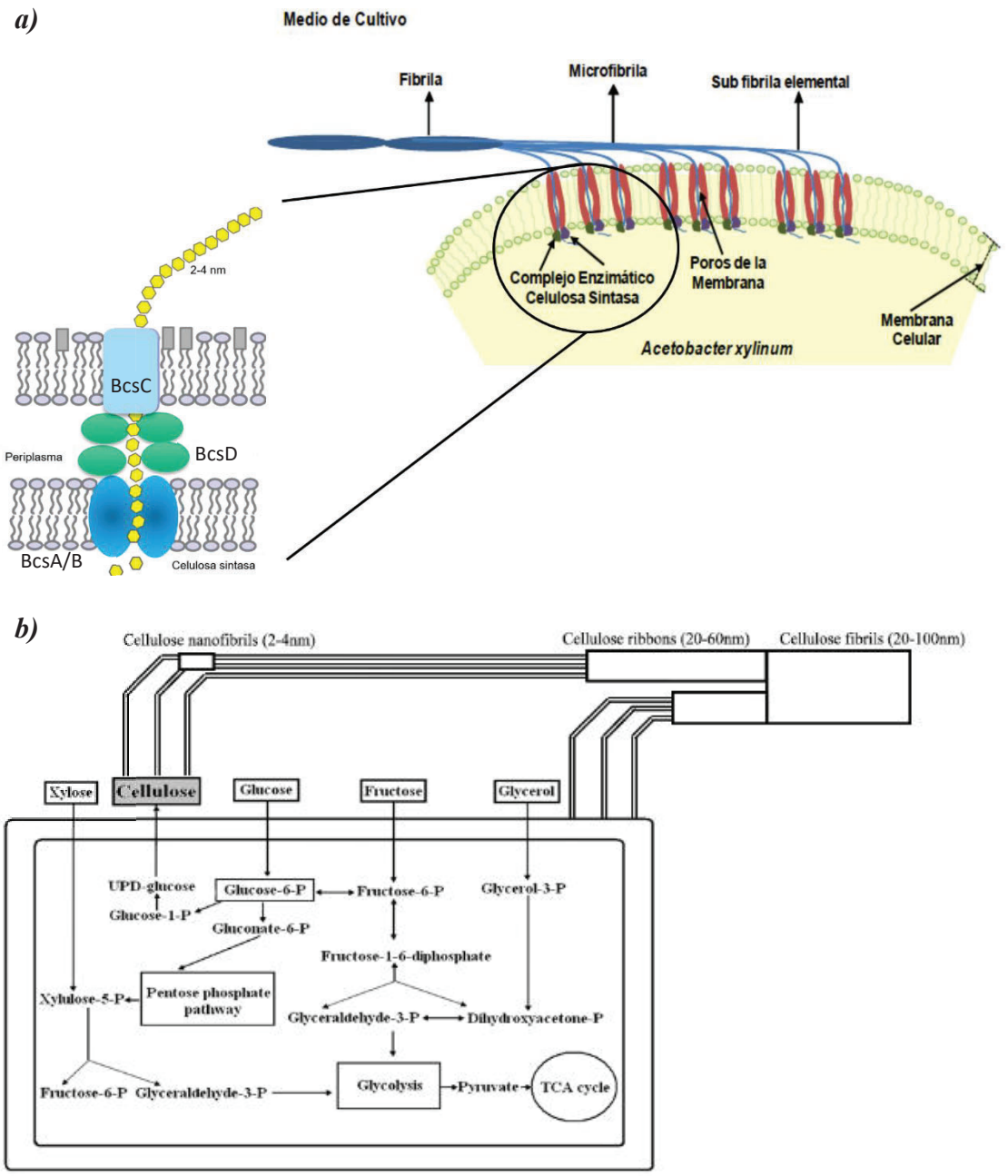

Figura 2. Representación de la síntesis y extrusión de la CB a través del complejo celulosa sintasa. ***a)*** Ilustración esquemática de la biosíntesis intracelular de las moléculas de celulosa y el posterior ensamblaje extracelular de éstas en nanofibras a través de los poros de la membrana celular. Modificado de Carreño Pineda, 2011. ***b)*** Esquema del proceso bioquímico de la formación de las fibras de CB. Modificado de Stepanov and Efremenko, 2018.

Las cadenas de celulosa individuales se unen por puentes de hidrógeno entre los numerosos grupos hidroxilo en protofibrillas, que tienen un diámetro de aproximadamente 2 - 4 nm y que a su vez se unen con otras protofibrillas adyacentes, dando lugar a microfibrillas de 20 – 70 nm de ancho (Lee *et al.*, 2014). El resultado es

una red tridimensional de nanofibrillas de celulosa que, en condiciones estáticas de cultivo, se acumula en la interfaz aire-líquido en forma de una película o membrana, mientras que en condiciones de cultivo agitado se produce en masas irregulares esféricas (Hestrin and Schramm, 1954) (**Figura 3**).

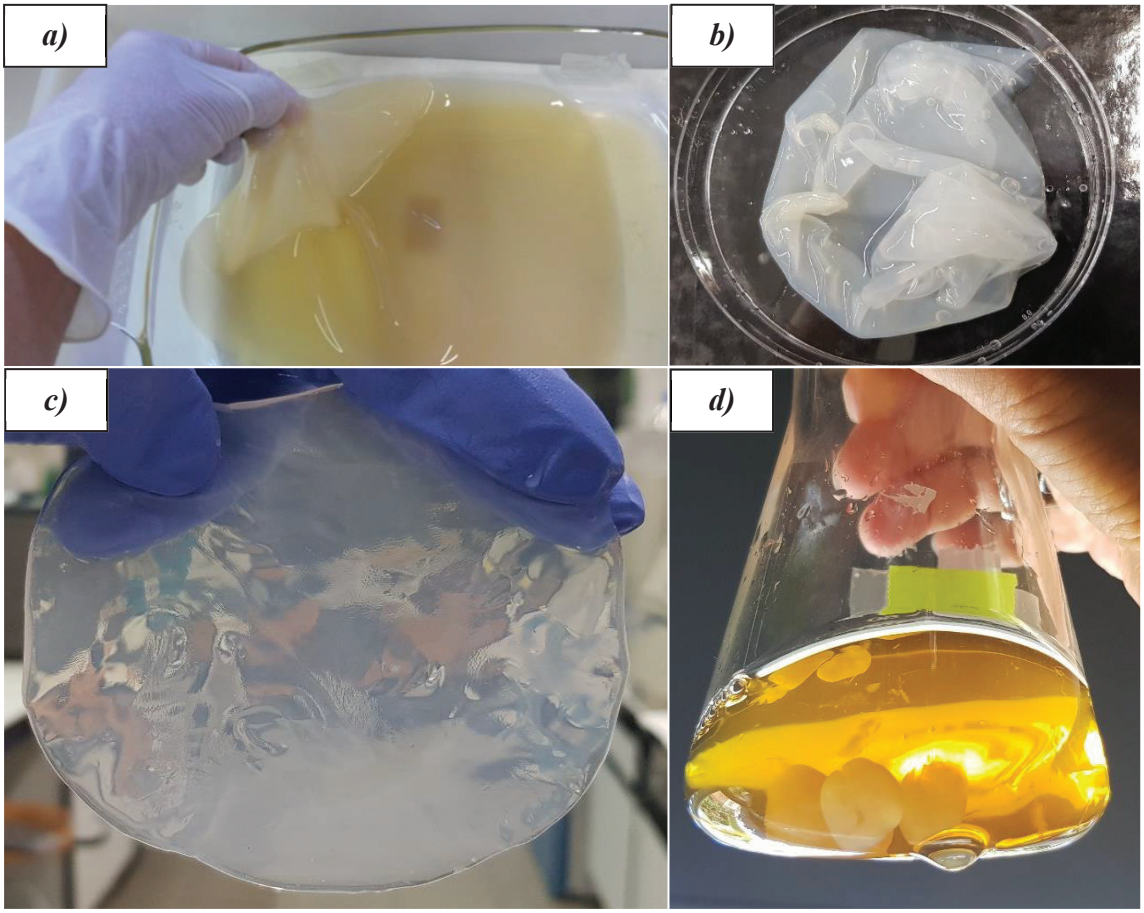

Figura 3. Membranas de CB de *Komagateibacter intermedius* JF2 ***a)*** producidas en condiciones estáticas en la interfase aire – líquido del medio sin purificar y ***b)***, ***c)*** purificadas, con textura uniforme. ***d)*** CB producida en un cultivo con agitación.

Estas nanofibras, de alto grado de polimerización y elevada cristalinidad, forman una estructura tridimensional altamente porosa (Chawla *et al.*, 2009; Maria *et al.*, 2010; Gama, Gatenholm and Klemm, 2016) y estable (Kalia *et al.*, 2011) (**Figura 4**). Esta nanoestructura única proporciona a la CB numerosas propiedades excelentes como alta capacidad de retención de agua (Dahman, 2009; Saibuatong and Phisalaphong, 2010), alta resistencia mecánica (Castro *et al.*, 2011), gran elasticidad y elevada resistencia a la tracción (Keshk, 2014; Santos *et al.*, 2015). Además, la CB es biocompatible y biodegradable (Chawla *et al.*, 2009).

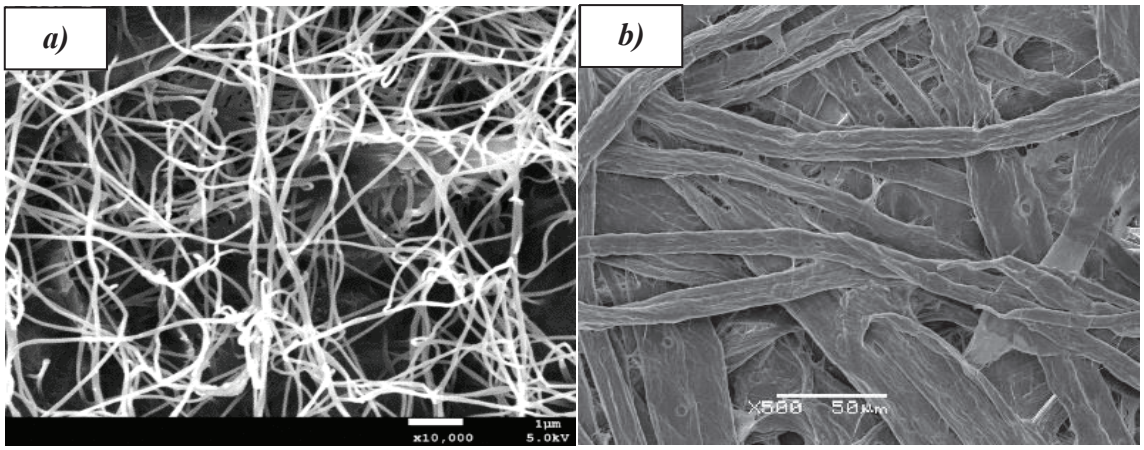

Figura 4. Imágenes de microscopía electrónica de barrido de la membrana (SEM) de CB *(a)* y de fibras de eucalipto *(b)*. Nótese la típica estructura porosa y reticulada de fibras ultrafinas de la CB, en comparación a la celulosa vegetal.

El conjunto de estas características hace de la CB un material interesante para diversas aplicaciones. Se ha propuesto una larga lista de aplicaciones como por ejemplo, refuerzo de materiales poliméricos y papel (Zimmermann, Bordeanu and Strub, 2010; Miao and Hamad, 2013), agente espesante y estabilizador de alimentos (Shi *et al.*, 2014), envasado de alimentos (Spence *et al.*, 2010), en la producción de probióticos (Jayani *et al.*, 2020), como biomaterial para la fabricación de cosméticos (Bianchet *et al.*, 2020), para la elaboración de piel artificial (Fu, Zhang and Yang, 2013; Kingkaew *et al.*, 2014), vasos sanguíneos artificiales e ingeniería de tejidos (Klemm *et al.*, 2001; Gao *et al.*, 2012; Ramani and Sastry, 2014; Scherner *et al.*, 2014; Islam *et al.*, 2021), en diafragmas para altavoces (Nishi *et al.*, 1990; Ciechańska, 2004), para la preparación de películas ópticamente transparentes (Palaninathan *et al.*, 2014), conductores eléctricos y materiales magnéticos (Zhang *et al.*, 2011; Charreau, L. Foresti and Vazquez, 2012; Santos *et al.*, 2015). A mayores, la alta pureza y cristalinidad de la CB, junto con sus dimensiones, lo convierten en un material de partida prometedor para el aislamiento de nanocristales de celulosa (Satyamurthy *et al.*, 2011; Vasconcelos *et al.*, 2017).

En el escalado industrial de la producción de CB es necesario tener un elevado rendimiento en la conversión de la fuente de carbono en celulosa y una alta productividad del microorganismo productor (Çakar *et al.*, 2014). Concerniente al primero objetivo, los principales factores extrínsecos que afectan a la producción y a las propiedades de la CB son los nutrientes, el diseño del reactor, la temperatura, la disponibilidad de oxígeno, el pH y los aditivos (Hu *et al.*, 2014). El diseño óptimo de los medios de cultivo no sólo es importante para el crecimiento de los microorganismos sino también para la estimulación

de la formación de celulosa (Chawla *et al.*, 2009; Fernandes *et al.*, 2020). Por ello, los medios de crecimiento contienen una elevada concentración de azúcares, lo que encarece el proceso (Zhuang *et al.*, 2007). Así, uno de los factores claves a mejorar en el proceso de producción de CB para permitir su aplicación a gran escala es la reducción en los costes de materia prima (Blanco Parte *et al.*, 2020). Hay muchas investigaciones centradas en aumentar, o al menos mantener, la productividad y el rendimiento con nutrientes más económicos, usando, por ejemplo, subproductos de otros procesos industriales (Chawla *et al.*, 2009). Otra estrategia es la búsqueda y el aislamiento de nuevas cepas altamente productoras (He *et al.*, 2020). En el grupo de investigación, se aislaron cuatro nuevas cepas productoras de CB a partir de vinagre comercial. Una de ellas, en base a su caracterización fisiológica, su secuencia del gen 16S rRNA y el análisis de su huella genética por espectrometría de masas MALDI-TOF, fue identificada como *Komagataeibacter intermedius*, llamada JF2 (Fernández *et al.*, 2019). *Komagataeibacter intermedius* JF2 tiene una eficiencia de producción de CB superior a la de *K.xylinus*, la cepa de referencia, además de producir más cantidad en menos tiempo. La CB obtenida por ambas cepas presentaba la misma estructura molecular, si bien las nanofibras de la celulosa procedente de la cepa JF2 mostró una mayor cristalinidad y una distribución más homogénea (**Figura 5**). Por todas estas características, la cepa JF2 ha sido la empleada en los estudios presentados en esta tesis.

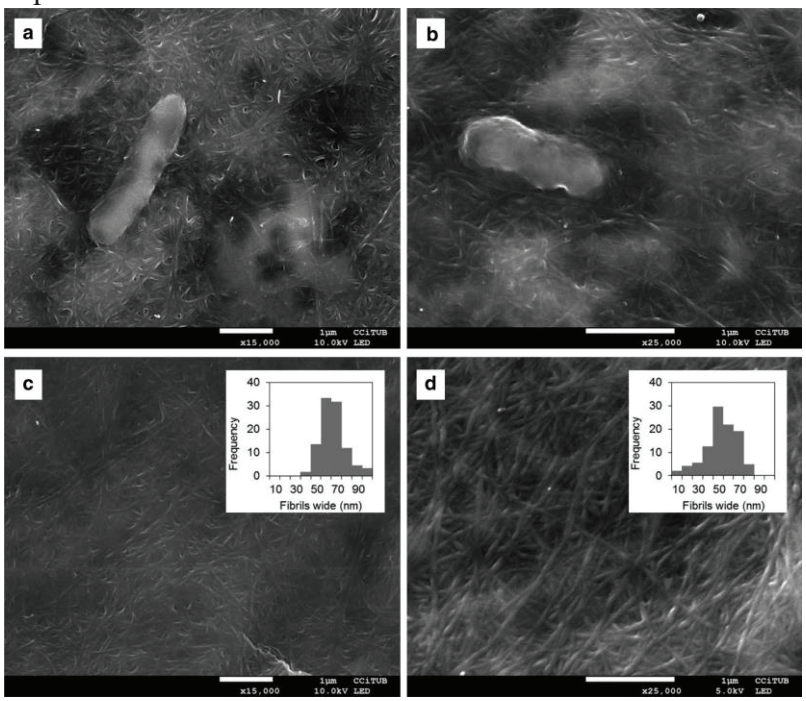

Figura 5. Imágenes de SEM de células de ***a)*** *K. intermedius* JF2 y ***b)*** *K. xylinus* produciendo CB en ***c)*** y ***d)***, respectivamente. En los insertos de c) y d) pueden observarse la distribución del tamaño de las fibras. De Fernández *et al*., 2019.

1.1.1. Funcionalización de la celulosa bacteriana

La aplicabilidad industrial y biotecnológica de la CB, igual que la de otros polisacáridos, se puede ver limitada por características inherentes, siendo algunas de ellas su baja solubilidad en agua a pH neutro, dificultad para su dispersión en medios acuosos y su equilibro entre hidrofilicidad - hidrofobicidad (Karaki *et al.*, 2016). En otros casos, interesa aportar nuevas características, como la actividad antimicrobiana (Chen, Zou and Hong, 2015; Morena *et al.*, 2019) o antioxidante (Cabañas-Romero *et al.*, 2020). En este contexto, una modificación química de su estructura podría no sólo mejorar sus propiedades sino hacer aún más amplio su abanico de potenciales aplicaciones. De hecho, la modificación química de la molécula de celulosa es habitualmente un requisito previo para proporcionarle nuevas funciones (Vikhoreva, Gorbacheva and Gal'braikh, 1994; Fernandes *et al.*, 2020). Los grupos hidroxilo que aportan a la CB de un elevado carácter hidrofílico (Liu *et al.*, 2008) son precisamente la diana de preferencia para reacciones tales como la oxidación, sulfonación, esterificación o amidación, entre otras (Yang, Xie and He, 2011; Vasconcelos *et al.*, 2020). La oxidación mediada por el radical TEMPO (2,2,6,6-tetrametilpiperidina-1-oxilo) en combinación con NaBr/NaOCl en condiciones alcalinas, se puede considerar uno de los métodos más eficientes para la modificación de la celulosa ya que permite introducir cantidades significativas de grupos carboxilo (Saito and Isogai, 2005). Sin embargo, este tratamiento presenta algunas desventajas como la generación de residuos químicos y la falta de selectividad (Karaki *et al.*, 2016).

En este aspecto, teniendo en cuenta factores como la reducción energética, el impacto ambiental y una elevada especificidad y propiedades selectivas, los procesos enzimáticos de modificación de la CB suponen una alternativa más amigable para con el medio ambiente a los procesos químicos (Karaki *et al.*, 2016). Un ejemplo de la transición de la modificación química de la CB a la enzimática es el paso de la oxidación de la CB mediante el reactivo TEMPO, mencionado anteriormente, a la oxidación mediada por el sistema Lacasa-TEMPO realizada en el grupo de investigación (Morena *et al.*, 2019; Valls *et al.*, 2019). Sin disminuir la eficiencia del proceso, el tratamiento Lacasa/TEMPO permite sustituir el empleo de NaBr/NaOCl por la enzima oxidativa lacasa. La CB funcionalizada mediante este sistema se utilizó como soporte para la generación de nanopartículas de plata (**Figura 6**), que confirieron actividad antimicrobiana a la CB,

ausente en la CB nativa (Morena *et al.*, 2019).

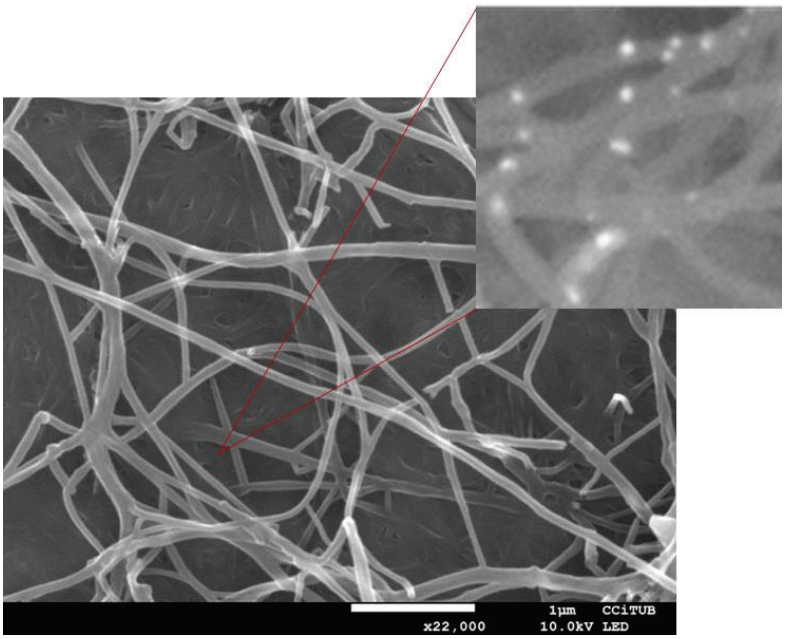

Figura 6. Imagen SEM de los composites BC-Ag, visualizados con filtro LED. En detalle, con filtro BED (detector de electrones retrodispersados, en inglés *backscattered electron detector*), se encuentran las nanopartículas de plata generadas. De Morena *et al*., 2019.

1.2. Lipasas bacterianas

Las lipasas (EC 3.1.1.3, triacilglicerol hidrolasas) se encuentran ampliamente distribuidas en la naturaleza y constituyen un grupo diverso de enzimas que catalizan la hidrólisis de los enlaces ésteres formados entre un ácido y un alcohol (Ro *et al.*, 2004) (**Figura 7**). Sin embargo, en un medio orgánico pueden catalizar su síntesis, mediante reacciones de esterificación, interesterificación o transesterificación (Jaeger, Dijkstra and Reetz, 1999; Bornscheuer, 2002; Ferrer *et al.*, 2015) de diferentes acilglicéridos, alcoholes, ésteres, glicósidos y aminas (Sharma and Kanwar, 2014). Se trata, pues, de una reacción de equilibrio que puede revertirse modificando las condiciones del medio (Jaeger, Dijkstra and Reetz, 1999; Stathopoulou *et al.*, 2013), lo que hace de las lipasas enzimas muy atractivas dentro del campo de la biotecnología (Guncheva and Zhiryakova, 2011). De hecho, su versatilidad justifica la presencia de enzimas lipolíticas en todos los grupos biológicos: en animales, su función básica es catalizar la absorción de grasas; en plantas, la fabricación de reservas energéticas (Seth *et al.*, 2014); en arqueas y bacterias, donde realizan funciones relacionadas con el metabolismo, el transporte y la señalización

lipídicos o la absorción de carbono, entre otros; e incluso en virus (Gupta, Gupta and Rathi, 2004).

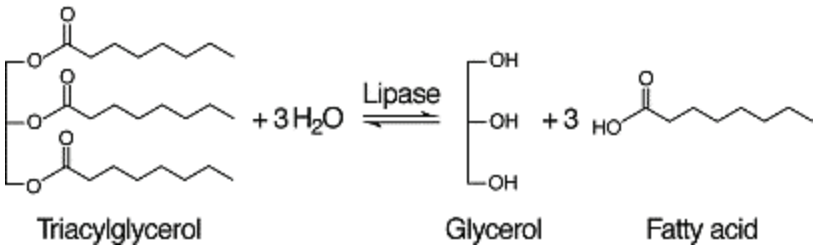

Figura 7. Esquema de la reacción catalizada por las lipasas. De Sharma and Kanwar, 2014.

Todas las enzimas lipolíticas tienen un plegamiento típico de las α/β hidrolasas, con una estructura central generalmente de 8 láminas β interconectadas por hélices α. El centro activo tiene tres aminoácidos, con una posición conservada en el interior del plegamiento, que son la serina nucleofílica, un ácido aspártico (o ácido glutámico) y una histidina, unida al residuo ácido por puentes de hidrógeno (**Figura 8**).

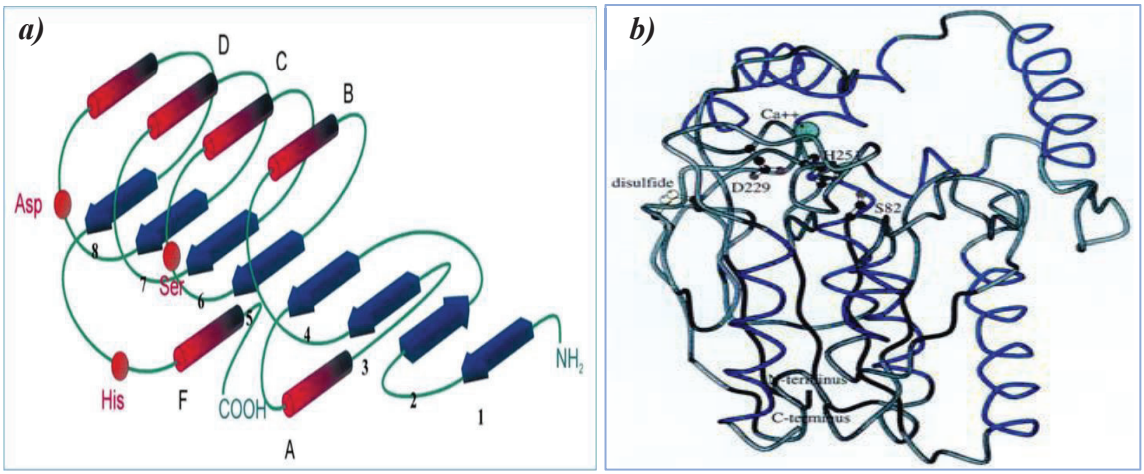

Figura 8. Estructura de las lipasas microbianas. ***a)*** Estructura obtenida por rayos X de la lipasa LipA de *Pseudomonas aeruginosa*. Se indican los extremos N y C terminales y la tríada catalítica formada por el residuo nucleófilo (S82), el residuo ácido (D229) y la histidina (H251). De Nardini *et al.*, 2000. ***b)*** Representación esquemática del plegamiento α/β hidrolasa. Las láminas β (1-8) son mostradas como flechas azules, mientras que las hélices α (A-F) están representadas por columnas rojas. La posición relativa de los tres aminoácidos catalíticos está indicada por los círculos rojos. De Bornscheuer *et al*., 2002.

La serina nucleofílica está generalmente incluida en el pentapéptido conservado Gly-X-Ser-X-Gly, donde las X pueden ser cualquier aminoácido (Dartois *et al.*, 1992; Ruiz, Pastor and Diaz, 2003). Estas características, sin embargo, varían en las lipasas descritas en el género *Bacillus*, que tienen en común que un residuo de alanina reemplaza la

primera glicina del pentapéptido conservado, seguido por una histidina: Ala-His-Ser-X-Gly (Arpigny and Jaeger, 1999; Ruiz *et al.*, 2002; Ruiz, Pastor and Diaz, 2005) en que X puede ser una metionina o un glutamato (Guncheva and Zhiryakova, 2011). El tamaño de las lipasas puede variar entre 20 y 77kDa, donde las lipasas más pequeñas conocidas corresponden a las de *Bacillus* sp (Arpigny and Jaeger, 1999; Asoodeh, Emtenani and Emtenani, 2014).

Un gran número de lipasas del género *Bacillus* han sido aisladas hasta la fecha, pero la mayoría de ellas sólo han sido caracterizadas a un nivel muy básico. El género *Bacillus* representa un grupo muy diverso de microorganismos con representantes que habitan en los lugares más extremos del planeta como desiertos, suelos volcánicos, casquetes polares, etc. Debido a que las células se han adaptado a vivir en estas condiciones, sus enzimas, y en particular sus lipasas, han evolucionado adquiriendo propiedades excepcionales.

Tradicionalmente las enzimas lipolíticas se clasificaban de forma genérica como lipasas y esterasas o carboxilesterasas, de manera que las lipasas son específicas para acilgliceroles con ácidos grasos de cadena larga (más de 10 carbonos) mientras que las esterasas actúan sobre acilgliceroles de cadena corta (menos de 10 carbonos) (Akoh *et al.*, 2004), aunque la mayoría de lipasas son capaces de hidrolizar también sustratos típicos de esterasas. La clasificación más utilizada actualmente es la de Arpigny y Jaeger de 1999, formada por 8 familias basadas en la secuencia aminoacídica y en las propiedades biológicas, que han sido ampliadas hasta 19 recientemente (Jaeger and Eggert, 2002; A Bassegoda, Pastor and Diaz, 2012; Castilla *et al.*, 2017). La clasificación de las lipasas en la familia I (lipasas verdaderas) se basa en dos criterios: la activación interfacial y la presencia de tapa (*lid* en inglés). La mayoría de las verdaderas lipasas tienen esta tapa en la superficie de la enzima, que está constituida por una α-hélice, cubriendo el sitio activo de la enzima y que se abre en presencia de una concentración mínima de sustrato (Jaeger, Dijkstra and Reetz, 1999). Hasta que no se llega a esta concentración, no se forma una emulsión con triglicéridos, necesaria para su activación. Este fenómeno es lo que se conoce como activación interfacial. Debido a esta brusca activación, al alcanzarse cierta concentración de sustrato, las lipasas no siguen una cinética de Michaelis-Menten, a diferencia de las esterasas.

1.2.1. Aplicaciones de las lipasas microbianas

Durante los últimos años, el uso de las lipasas en las industrias alimentaria, cosmética, detergente, farmacéutica, de combustible y de productos químicos finos ha ido en aumento, ya que permiten procesos más ecológicos y sostenibles al sustituir procesos realizados con químicos poco respetuosos con el medio ambiente (Jaeger and Reetz, 1998; Jaeger, Dijkstra and Reetz, 1999; Bornscheuer, 2002; Gupta, Gupta and Rathi, 2004; Bornscheuer and Kazlauskas, 2006; Drepper *et al.*, 2006; Antranikian, Bornscheuer and Liese, 2010; Reetz, 2013; Gupta *et al.*, 2015; Angajala, Pavan and Subashini, 2016; Kourist *et al.*, 2017). Las lipasas microbianas son el segundo grupo más amplio de biocatalizadores industriales después de las enzimas amilolíticas. Han sido aplicadas con éxito como aditivos en la formulación de detergentes cuando su pH óptimo es ligeramente alcalino en el caso de las obtenidas de *Bacillus licheniformis*, *B.subtilis* y *B.pumilus* (Nthangeni *et al.*, 2001), o en la industria textil en combinación con proteasas (cuando su pH óptimo es ácido) para la obtención de pieles (Guncheva and Zhiryakova, 2011). Su uso en la industria alimentaria se encuentra en la modificación de grasas y aceites por tal de obtener un mayor valor nutricional y unas mejores texturas y propiedades físicas del producto, en la alteración del sabor y la textura de panes y quesos, y en la síntesis de substitutos de sabor (Aravindan, Anbumathi and Viruthagiri, 2007). Las lipasas termófilas y con variedad de sustratos se aplican en el procesamiento de la pasta de papel para eliminar resinas y ceras procedentes de la madera (Castro-Ochoa *et al.*, 2005). Otros usos se encuentran en la producción de reactivos para la industria farmacéutica, en el tratamiento de aguas residuales (Gupta, Gupta and Rathi, 2004) y en procesos químicos en que se requieren altas temperaturas para obtener una mayor tasa de conversión y reducir las probabilidades de contaminación microbiana (Castro-Ochoa *et al.*, 2005).

Las lipasas de origen microbiano son, además, las más indicadas para las aplicaciones industriales por su bajo precio, por la simplicidad en su producción debido a que la mayoría son extracelulares, por su susceptibilidad a ser expresadas en células huésped, por su gran espectro de sustratos y finalmente, por su amplio rango de condiciones óptimas de pH y temperatura (Sharma, Chisti and Banerjee, 2001). Mientras que su especificidad de sustrato puede ser modificada mediante técnicas de mutagénesis, se ha demostrado que su inmovilización aumenta su resistencia a la temperatura y al pH (Hernandez and Fernandez-Lafuente, 2011). En conjunto, esta gran versatilidad, así como las diferencias en estructura y función de las enzimas lipolíticas, justifican la búsqueda y

la exploración de nuevas fuentes biológicas de estas enzimas, así como la necesidad de caracterizarlas de forma individualizada y evaluar sus propiedades para una posible aplicación industrial.

En general, las lipasas son enzimas robustas que pueden ser usadas en condiciones suaves sin necesidad de añadir cofactores, otra característica que abunda en su interés industrial desde el punto de vista económico (Gupta, Gupta and Rathi, 2004; Drepper *et al.*, 2006; Kapoor and Gupta, 2012; Gupta *et al.*, 2015). Aunque muy explotadas, siguen existiendo procesos que requieren de enzimas lipasas que presenten una mayor tolerancia a condiciones extremas o que actúen sobre sustratos con residuos acil de cadena larga (Narancic *et al.*, 2015; Siddiqui, 2015). Para obtenerlas, se pueden seguir distintas estrategias: el aislamiento de nuevas enzimas (Falcocchio *et al.*, 2005; Prim *et al.*, 2005; Ruiz, Pastor and Diaz, 2005) o alternativamente, su modificación por tal de mejorarlas (Bassegoda *et al.*, 2010; Bassegoda, Cesarini and Diaz, 2012; Cesarini *et al.*, 2012; Fillat *et al.*, 2014, 2015; Siddiqui, 2015). Y por supuesto, se pueden combinar ambas técnicas por tal de producir el biocatalizador deseado para un proceso determinado (Bassegoda, Cesarini and Diaz, 2012).

1.2.2. Bacillus sp. JR3 y LipJ

En trabajos previos a esta tesis, se describió el aislamiento de la cepa mesófila *Bacillus* sp. JR3 de un suelo volcánico de la laurisilva de la isla El Hierro, en las Islas Canarias. El sobrenadante de la cepa mostraba actividad lipasa termófila (entre 80 y 100 ºC), manteniendo una elevada actividad relativa después de 96 h de incubación (Ribera *et al.*, 2017). LipJ, una lipasa con un ORF de 1242 pares de bases, 413 aminoácidos, y con un peso de 39 kDa, fue clonada en *Escherichia coli* y posteriormente caracterizada en las mismas condiciones que el sobrenadante de la cepa original. Sorprendentemente mostró su máxima actividad a 30 ºC, sin ningún rasgo de termofília, sugiriendo que LipJ es probablemente una esterasa intracelular que solo puede detectarse en *Bacillus* sp. JR3 después de la lisis de las células, pero no en el sobrenadante. Sin embargo, el análisis filogenético y estructural de LipJ asignaron esta esterasa a la familia I.5 (**Figura 9*a***), aunque posicionada en otro clado, similar a la lipasa LipAT (también llamada AZ) de *Actinibacillus thermoaerophilus* (Masomian *et al.*, 2016; Ribera *et al.*, 2017). La subfamilia I.5, junto con la subfamilia I.4, constituyen las dos familias en que se encuentran clasificadas las lipasas del género *Bacillus*. Las lipasas de la familia I.5 se caracterizan por la secuencia conservada del pentapéptido catalítico (Ala-His-Ser-Gln-

Gly), por la existencia del péptido señal común en todas las lipasas extracelulares de *Bacillus* (Jaeger, Dijkstra and Reetz, 1999), por tener un tamaño aproximado de 40 - 45 kDa, por ser lipasas termoestables cuya temperatura óptima se encuentra entre 60 y 75 ºC, por sus dominios de unión a los iones Ca^{2+} y Zn^{2+}, y por actuar sobre sustratos de cadena media y larga (Carrasco-López *et al.*, 2009). De todas estas propiedades, LipJ sólo conserva el tamaño (39 kDa) y los dominios de unión a zinc, ya que la secuencia de su pentapéptido catalítico es Gly-His-Ser-Met-Gly (**Figuras 10** y **11**). De hecho, LipJ sería el resultado de una rareza evolutiva en que una serie de cambios han convertido la enzima originalmente termófila en mesófila e intracelular, ya que actualmente su pentapéptido tiene más similitud con la secuencia del pentapéptido de la subfamilia I.4 (Ala-His-Ser-Met-Gly), que se caracteriza por albergar lipasas que no son termoestables de un tamaño alrededor de los 19-20 kDa y actuar sobre sustratos de cadena corta y media.

Paralelamente al análisis de la secuencia, la superimposición del modelo 3D de LipJ con las estructuras de las lipasas termofílicas más cercanas de la familia I.5 de *Pelosinus fermentans* (pdb: *5ah0*) (Biundo *et al.*, 2016) y *Geobacillus stearothermophilus* L1 (pdb: *1ku0*) (Jeong *et al.*, 2002) mostró un dominio putativo de unión a iones Ca^{2+} y Zn^{2+} (Ribera *et al.*, 2017), un rasgo común encontrado entre las lipasas bacterianas termófilas con tapa (Jeong *et al.*, 2002; Carrasco-López *et al.*, 2009; Timucin *et al.*, 2015) (**Figura 9*b***). Aún así, la presencia de estos iones no incrementó de manera significativa la actividad termófila de LipJ, llegando incluso a disminuir con la adición de Zn^{2+} (Ribera *et al.*, 2017). Alternativamente, teniendo en cuenta que la coordinación de los iones metálicos como es el Zn^{2+} ha sido descrita como relevante en la regulación de la apertura de la *lid* de las lipasas termófilas (Jeong *et al.*, 2002; Carrasco-López *et al.*, 2009; Rahman *et al.*, 2012; Timucin *et al.*, 2015; Biundo *et al.*, 2017; Varejão *et al.*, 2018), se trató de encontrar diferencias en los residuos putativos más significativos envueltos en la activación dependiente de la temperatura de lipasas termófilas. Todos los aminoácidos descritos implicados directamente en la termofilicidad se pudieron encontrar en la secuencia de LipJ, manteniendo además la misma posición y distancia que en las otras secuencias comparadas. Los cuatro residuos D86, H106, H112, D260 y los triptófanos W85 y W232 se encontraron no sólo en la secuencia, sino también en el modelo 3D de LipJ. Otros residuos de las alfa-hélices 6 y 7, sugeridos como relevantes para la formación de "stabilizing salt bridges" (Carrasco-López *et al.*, 2009) también se encontraron en la secuencia de la proteína, excepto en el residuo H110, diferente en las lipasas más

próximas de *Pelosinus fermentans* y *Clostridium botulinum*. En la bibliografía, el residuo correspondiente en *C.botulinum* (F182) fue modificado, obteniéndose un mutante (F182Y) cuya termofilicidad se vio aumentada, sugiriendo que este aminoácido juega un papel importante en la activación dependiente de temperatura (Biundo *et al.*, 2017).

El conjunto de todos estos antecedentes; la similitud de su secuencia con otras lipasas termófilas de los géneros *Bacillus* y *Geobacillus* y el análisis *in silico* de su estructura, parecen aportar suficiente evidencia de un hipotético origen termófilo para esta enzima. Su origen podría estar relacionado con otra hipotética lipasa extracelular hipertermófila, responsable de la actividad lipolítica hipertermófila detectada en el sobrenadante. Ambas podrían estar codificadas por genes paralógos, producto de la duplicación de un gen ancestral de una lipasa termófila (Ribera *et al.*, 2017). Estos genes habrían evolucionado de manera diferente: LipJ habría perdido su comportamiento termófilo y secuencia péptido señal, conservando ciertos motivos termófilos, mientras que la otra, en cambio, habría retenido la elevada actividad termófila, perdiendo algunos caracteres de su secuencia que hace que sea difícil su clonación mediante el diseño de iniciadores específicos.

Con estos antecedentes y para indagar en el posible origen termófilo de la enzima LipJ, en este trabajo se decidió realizar dos ensayos de mutagénesis, con el objetivo de revertir el comportamiento mesófilo a termófilo. El primero se centró en la creación de una librería NNK modificando el residuo H110 mediante mutagénesis de saturación iterativa por su posible implicación en la coordinación del ión Zn^{2+}. El otro estudio consistió en una mutagénesis dirigida; de las tres mutaciones introducidas en el gen *lipJ*, dos fueron en el pentapéptido conservado en la posición 136 y 139, y la tercera en el hipotético péptido señal.

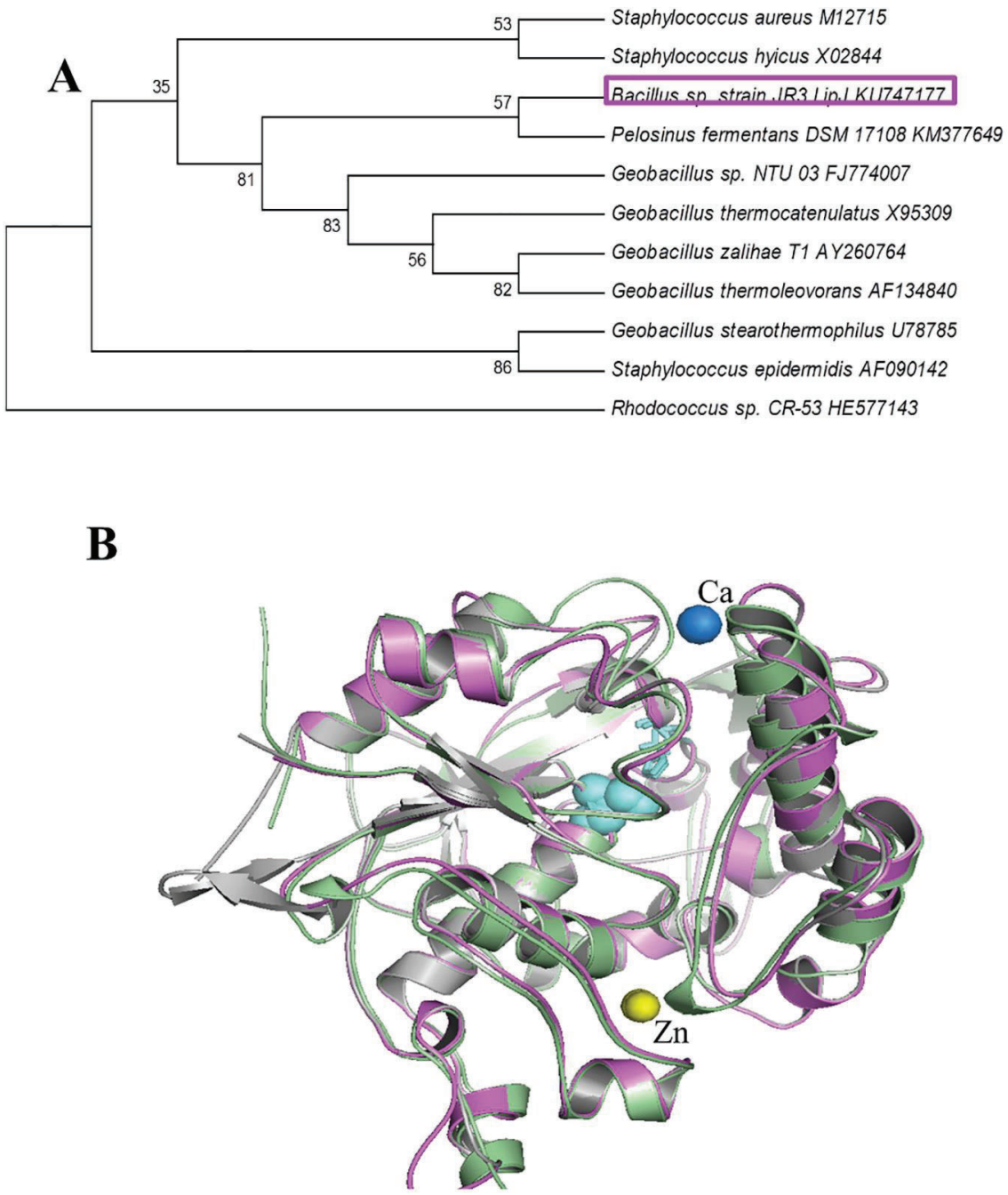

Figura 9. Análisis *in silico* de LipJ. *a)* Árbol filogenético de LipJ usando el *software* MEGA 7 ref y las lipasas más próximas de la familia I.5 y la lipasa PfL1 de *Pelosinus fermentans.* La caja señala la posición de LipJ, incluyéndola en el mismo clúster de las lipasas termófilas de la familia I.5. Una lipasa de la familia X de *Rhodococcus sp*. *CR53* fue incluida en el árbol para "extreme rooting". ***b)*** Modelo de la estructura 3D de LipJ (en lila), alineada y superpuesta a los de L1 de *G. stearothermophilus* (en verde) y PfL1 de *Pelosinus fermentans* (en gris). Las tres estructuras muestran una alineación casi completa a excepción de las dos láminas β externas de PfL1 (en la derecha). Los residuos implicados en la catálisis aparecen en la misma posición en las tres estructuras y están subrayadas en cián. Los iones Zn^{2+} y Ca^{2+} (esferas amarillas y azules, respectivamente) muestran la posición de las cavidades putativas de unión, que deben de estar presentes también en LipJ. De Ribera *et al.,* 2017.

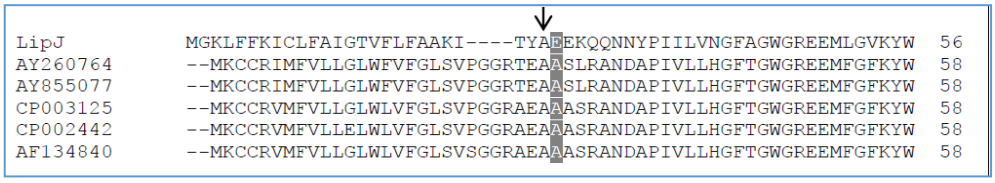

Figura 10. Alineamiento múltiple de la secuencia de LipJ con la de otras lipasas termófilas. Se muestra el punto de corte del péptido señal (flecha) y el aminoácido (sombreado) diferente entre estas secuencias. De Ribera *et al.*, 2017.

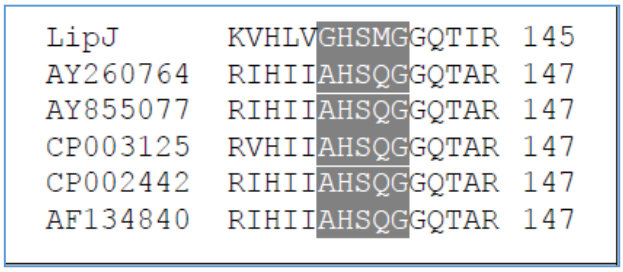

Figura 11. Diferencias observadas en el pentapéptido que incluye la serina catalítica entre la secuencia de LipJ y otras lipasas termófilas. *Geobacillus zalihae* (AY260764), *Bacillus sp*. L2 (AY855077), *Geobacillus thermoleovorans* (CP003125), *Geobacillus* sp. Y412MC52 (CP002442), *Geobacillus thermoleovorans* (AF134840). De Ribera *et al.,* 2017.

1.2.3. Actividad lipasa termófila de E.coli

Escherichia coli ha sido empleada como el huésped de preferencia para la expresión heteróloga de múltiples enzimas, entre las cuales se han aislado, clonado y caracterizado muchas enzimas lipolíticas (Prim *et al.*, 2006; Ruiz *et al.*, 2007; Bofill *et al.*, 2010; Bassegoda *et al.*, 2013; Infanzón *et al.*, 2014). Sin embargo, poca atención se ha prestado a la actividad lipolítica intrínseca de ésta, cuya existencia, aún sin ninguna caracterización profunda publicada, ha sido documentada (Nantel and Proulx, 1973; E *et al.*, 2005; Ribera *et al.*, 2017) (**Figura 12**). En general, en todas estas investigaciones, las enzimas de interés clonadas han conseguido ser producidas y se han mantenido activas con éxito, permitiendo de esta manera proseguir con su caracterización y futuras aplicaciones (A Bassegoda, Pastor and Diaz, 2012). No obstante, en el caso de aquellas lipasas clonadas que exhiben poca actividad, esta actividad de enzimas putativas lipolíticas tendría que tenerse en cuenta (Nantel and Proulx, 1973; Ribera *et al.*, 2017). Éste fue el caso de las últimas investigaciones del grupo, cuando se clonó una nueva lipasa, LipG, aislada de *Bacillus* sp. JR3 (Ribera *et al.*, 2017), la cual mostraba una estructura sin precedentes (resultados sin publicar). LipG, aunque poseía la mayoría de los rasgos de una lipasa,

incluyendo el pentapétido consenso G(A)-X-S-X-G y la típica tríada catalítica constituida por una serina como residuo nucleofílico, un ácido aspártico y una histidina como donador de protones, no mostró una actividad lipolítica significativa. Consecuentemente, se concluyó que la actividad detectada no era debida a la putativa enzima clonada. Teniendo en cuenta estos resultados y los obtenidos previamente, que indican la existencia de una actividad lipolítica basal en las cepas de *E.coli* habitualmente empleadas para la clonación y expresión de esterasas y lipasas, se decidió profundizar en esta actividad intrínseca llevando a cabo su caracterización detallada. En este trabajo se midió la actividad lipolítica de diferentes *E.coli* para confirmar este hecho, y se realizó una comparación entre ellas. Se seleccionó el extracto celular procedente de la cepa *E.coli* BL21 star (DE3) para el posterior análisis de las propiedades operacionales.

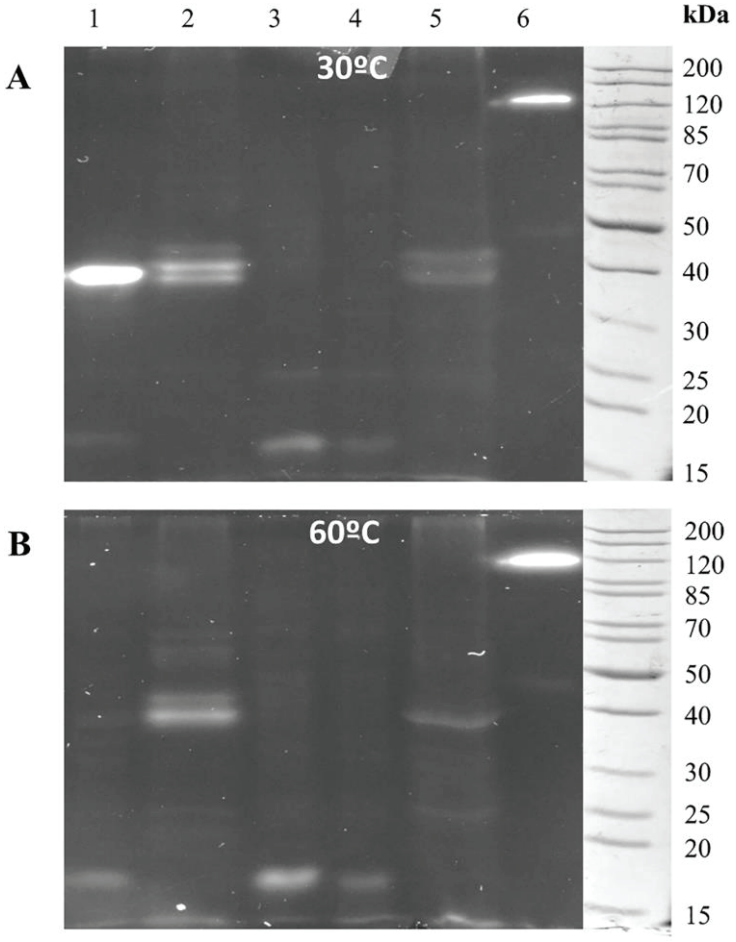

Figura 12. Análisis de zimograma de los extractos celulares de la lipasa clonada LipJ y del sobrenadante de la cepa JR3, llevado a cabo a 30 ºC *(a)* y a 60 ºC *(b)*. En todos los carriles se encuentra presente una banda con actividad lipasa, atribuida a la actividad basal de *E.coli.* Carril 1: extracto celular crudo de *E.coli* expresando LipJ; Carril 2: sobrenadante de *B. cereus* 131; Carriles 3-4: extracto celular soluble (3) e insoluble (4) de *E.coli* sin el inserto de LipJ, usado como control negativo; Carriles 5-6: sobrenadante concentrado (5) y extracto celular crudo de JR3. De Ribera *et al.,* 2017.

1.3. Inmovilización de enzimas en celulosa bacteriana

El uso de enzimas en procesos industriales es habitual y está aumentando últimamente en diferentes campos de la industria, principalmente por el hecho de poder sustituir procesos químicos contaminantes para el medio ambiente por otros más sostenibles, además de ofrecer al mismo tiempo más especificidad de reacción y mayor pureza del producto (Romero-Fernández *et al.*, 2018)**.** La introducción de tecnologías basadas en el uso de enzimas como catalizadores biológicos en procesos de transformación contribuye a un uso más eficiente y racional de las materias primas, al aprovechamiento de los subproductos industriales para su conversión en productos de alto valor añadido, y a la obtención de materiales de calidad a través de tecnologías menos costosas y mucho menos nocivas para el entorno (Prim, 2002; Zhu, Wu and Wang, 2011; Picart, De María and Schallmey, 2015).

Las enzimas más usadas en la industria son los procedentes de microorganismos, ya que la cantidad de enzima obtenida es mucho más elevada a la producida por plantas o animales, además de ser su extracción mucho más fácil, en especial cuando se trata de enzimas extracelulares, lo que abarata el coste de la producción industrial (Ibrahim, 2008; Treichel *et al.*, 2010). Las tecnologías moleculares permiten modificar estas enzimas para cambiar sus características catalíticas por tal de maximizar la pureza del producto y la economía de la producción (Cherry and Fidantsef, 2003). A pesar de este hecho, existe la necesidad constante de la búsqueda y la caracterización de nuevas enzimas, ya que la mayoría de enzimas microbianas que se utilizan son producidas por un número reducido de microorganismos, estimándose que sólo un porcentaje ínfimo de los microorganismos han sido analizados como fuente de enzimas. Algunos de los requisitos buscados en estas enzimas son la tolerancia a elevadas o bajas temperaturas y a pH ácidos o básicos (Joshi and Satyanarayana, 2015), ya que muchos de los procesos industriales en que se usan se llevan a cabo bajo estas mismas condiciones extremas (Salle *et al.*, 2015). Las posibles aplicaciones de estas enzimas son el blanqueo y reciclaje del papel, el desarrollo de nuevas energías sostenibles o la industria alimentaria. Las más usadas en la actualidad en el sector industrial incluyen las lipasas, las esterasas, las celulasas, las xilanasas, las proteasas, las pectinasas y las amilasas (Salle *et al.*, 2015).

Una enzima o una proteína inmovilizada es aquella que está adherida a un material inerte e insoluble (Mohamad *et al.*, 2015). El término de enzima inmovilizada se empezó a

acuñar a principios del siglo XX como referencia a enzimas unidas directamente a matrices. En el presente, sirve para designar a enzimas unidas directamente a una matriz y a enzimas que necesitan un agente intermediario para ser inmovilizadas (Cao, van Langen and Sheldon, 2003). La inmovilización de enzimas aporta una serie de ventajas tales como el aumento del rendimiento de la reacción, una mayor reproducibilidad de los ensayos, la posibilidad de reusar la enzima, un incremento de la estabilidad de la misma, un tiempo mínimo de reacción y la disminución del coste del proceso (Wang, 2006; Omagari *et al.*, 2009; Kadokawa, 2012). Estas características han promovido el uso de enzimas inmovilizadas en la industria, en el campo de la biomedicina, en la detección de contaminantes ambientales o en la monitorización de procesos de calidad alimentaria (Monosik *et al.*, 2012; Nigam and Shukla, 2015; Rocchitta *et al.*, 2016). Algunos ejemplos de sus numerosas aplicaciones prácticas en diferentes ámbitos son los siguientes:

- Producción industrial de antibióticos (Vandamme, 1983) y bebidas alcohólicas (Kourkoutas *et al.*, 2004)
- Aplicaciones biomédicas (Chang, 1976; Kim and Herr, 2013)
- Industria alimentaria en el procesado de alimentos y bebidas (Mariotti *et al.*, 2008; Panesar, Kumari and Panesar, 2010).
- Industria textil en la decoloración de tintes (Yanto, Tachibana and Itoh, 2014) y producción de tejidos antimicrobianos (Coradi *et al.*, 2018)
- Producción de biodiésel (Zhao *et al.*, 2015)
- Tratamiento de aguas residuales (Arca-Ramos *et al.*, 2016)
- Productos de limpieza como detergentes, con proteasas y lipasas inmovilizadas (Soleimani, Khani and Najafzadeh, 2012)
- Elaboración de biosensores (Nguyen *et al.*, 2019; Pohanka, 2019)

Entre las matrices más empleadas para la inmovilización destacan los nanomateriales (Gupta *et al.*, 2011), el óxido de grafeno (Zhang *et al.*, 2010; Troncoso and Torres, 2020) y polímeros como el alginato (Heichal-Segal, Rappoport and Braun, 1995) o el colágeno (Coulet and Gautheron, 1981), que conducen a la formación de nanocomposites funcionales, cuyo interés para aplicaciones biotecnológicas ha ido en aumento desde la última década. Los nanocomposites se entienden como la combinación de dos materiales independientes, la matriz y el material embebido en ella, siendo al menos uno de ellos de dimensión nanométrica. Normalmente, la matriz actúa como soporte de moléculas

orgánicas con actividad biológica (Mohamad *et al.*, 2015). Mientras que la primera aporta las características físico - químicas del nanocomposite, la última le confiere propiedades biológicas. Si bien el uso de nanomateriales como soporte de enzimas inmovilizadas ha expandido aún más su uso y potenciales aplicaciones (Molinero-Abad *et al.*, 2014), aún es necesario ahondar más en el desarrollo de nuevos nanomateriales que sean económicos, de elevada pureza y sin toxicidad (Kim *et al.*, 2015). En esta línea, la CB es un candidato atractivo para la inmovilización de enzimas. Su red porosa y ultrafina proporciona una elevada accesibilidad al sitio activo de la enzima, ya que ofrece una baja resistencia a la difusión, una fácil recuperación y potencia las aplicaciones de operación continua (Sulaiman *et al.*, 2015). Además, la CB es considerada no sólo más segura sino más amigable con el medio ambiente que otros nanomateriales (Lu *et al.*, 2013). La inmovilización de enzimas en CB ha sido descrita previamente por otros autores, como es el caso de la lisozima en fibras de CB en suspensión (Bayazidi, Almasi and Asl, 2018), de una lipasa en cristales de CB (Kim *et al.*, 2015) y de nisina, lacasa o lipasas en membranas de CB (Wu, Wu and Su, 2017; dos Santos *et al.*, 2018; Yuan *et al.*, 2018).

Existen muchos métodos para la inmovilización de enzimas en una superficie sólida, tanto químicos como físicos (Mohamad *et al.*, 2015). Una inmovilización enzimática efectiva puede conseguirse por métodos químicos, con uniones covalentes o uniones cruzadas (*cross linking* en inglés) (Yao *et al.*, 2013; Lin and Dufresne, 2014). Ya sea a través de modificaciones químicas de la matriz o bien con el uso de conectores (*linkers* en inglés), se puede limitar la funcionalidad del nanocomposite además de generar residuos peligrosos para el medio ambiente (Castro *et al.*, 2014). Aunque en los últimos años están surgiendo nuevas técnicas, conocidas como inmovilización inteligente, que abarcan desde el uso de partículas metálicas (Vaghari *et al.*, 2016), inmovilizaciones por fotoactivación (Holden, Jung and Cremer, 2004) hasta inmovilizaciones activadas térmicamente (Huber *et al.*, 2003), entre otros, el método más extendido a la par que efectivo es la inmovilización física por adsorción. Éste consiste en la adhesión de la proteína al soporte en condiciones acuosas mediante fuerzas de van der Waals, interacciones iónicas y puentes de hidrógeno (Credou and Berthelot, 2014; Jesionowski, Zdarta and Krajewska, 2014). Al no haber modificación química alguna ni de la matriz ni de la enzima, el cambio configuracional de ésta última es mínimo (Choi, 2004). Los primeros en utilizar esta metodología fueron Nelson y Griffin, utilizando carbón como soporte de una invertasa (Nelson and Griffin, 1916).

1.3.1. Inmovilización de lipasas

Uno de los objetivos de este trabajo ha sido la preparación de nanocomposites Enzima/CB para evaluar la idoneidad de matrices de CB como soportes para la inmovilización de enzimas por adsorción física. Como se ha comentado, entre la gran variedad de enzimas, las lipasas han ganado mucha atención como biocatalizadores en campos como la industria alimentaria, formulación de detergentes y de sabores, producción de medicamentos y síntesis de biofuel, entre otros (Angajala, Pavan and Subashini, 2016). Debido a su relevancia en el desarrollo de bioensayos y biorreactores (Pohanka, 2019), se escogieron como modelo a inmovilizar sobre diferentes matrices de CB (**Figura 13**). Concretamente, se inmovilizó la lipasa Callera^{TM} Trans L, la formulación comercial de la lipasa de *Thermomyces lanuginosus* (Nordblad *et al.*, 2014) de Novozymes, previa purificación por cromatografía de intercambio iónico. Una vez obtenidos los nanocomposites Lipasa/CB, se evaluaron tanto la eficiencia de retención de la enzima como su actividad hidrolítica en diferentes condiciones de temperatura y pH, en comparación siempre con la lipasa libre. Las matrices seleccionadas fueron las fibras de CB en suspensión y el papel de CB. El papel de CB es una matriz que combina la elevada relación área/volumen de las fibras de CB con la firmeza y las propiedades mecánicas del papel convencional, lo que puede conducir al diseño de dispositivos de alto rendimiento.

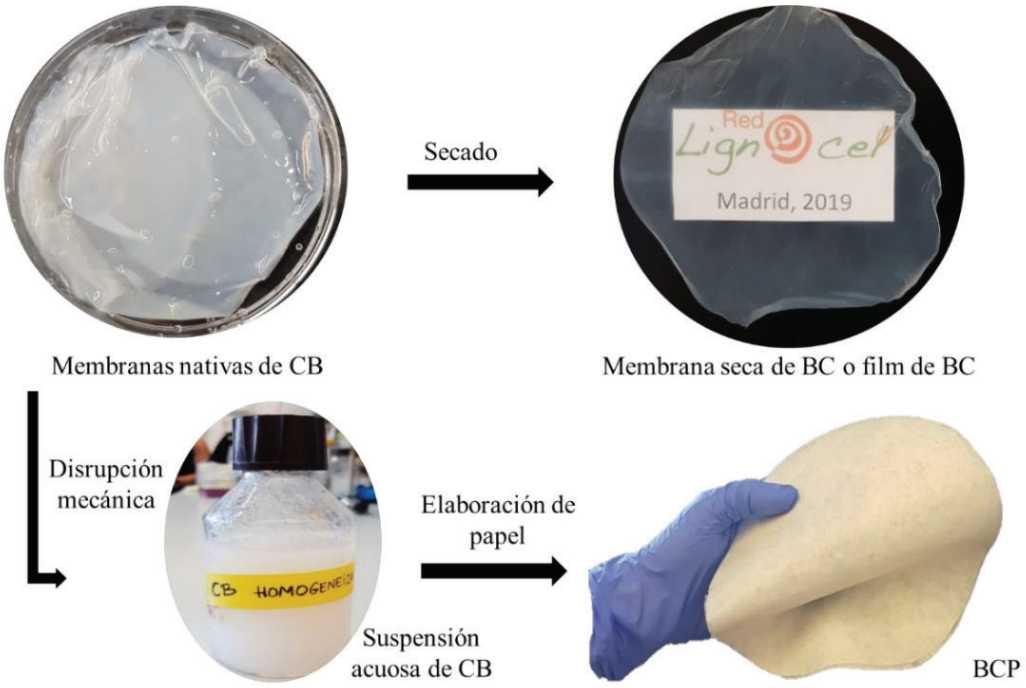

Figura 13. Diferentes matrices de CB. A partir de las membranas de CB se pueden obtener los films al evaporarse el agua de las membranas purificadas. Por otro lado, después de la trituración y homogeneización de las membranas, se consigue una suspensión de las fibras. Al filtrar y secar estas fibras se puede elaborar el papel de CB (BCP).

1.3.2. Inmovilización de lisozima

La lisozima es una enzima con actividad antimicrobiana que se puede encontrar abundantemente en la naturaleza, producida por plantas, hongos, bacterias, aves y mamíferos (Branen and Davidson, 2004). Debido a su actividad selectiva contra la pared celular de una gran variedad de bacterias grampositivas y gramnegativas (Ibrahim, Thomas and Pellegrini, 2001; Rudra, Dave and Haynie, 2006), esta enzima se encuentra actualmente extensamente empleada en la industria alimentaria y está clasificada como GRAS (*Generally Recognized As Safe,* por sus siglas en inglés, es un acrónimo creado en 1958 por la Administración de Alimentos y Medicinas (*Food and Drug Administration*, FDA) que permite la regulación de sustancias añadidas a los alimentos, previamente consideradas como seguras para la salud humana por un panel de expertos) (CAGRI, USTUNOL and RYSER, 2004; Mangalassary *et al.*, 2008; Sung *et al.*, 2011; Hanušová *et al.*, 2013). La lisozima es efectiva en la preservación de quesos, leche de vaca, cerveza (Makki and Durance, 1996), fruta fresca y vegetales, carne y pescado y vino (GILL and HOLLEY, 2000). Sin embargo, añadirla directamente puede implicar una pérdida de su efectividad debido a su alta sensibilidad y rápida inactivación bajo según qué condiciones ambientales (Rose *et al.*, 1999; Bayazidi, Almasi and Asl, 2018). Como se ha comentado con anterioridad, las enzimas inmovilizadas en matrices poliméricas suelen ganar en estabilidad respecto a pH y temperatura, entre otros factores (Fang *et al.*, 2011).

Paralelamente, la CB no sólo es considerada un buen soporte para la inmovilización de enzimas, tal y como se ha descrito con anterioridad, sino que también está creciendo el interés en su uso como material de envasado activo, portador de agentes antimicrobianos. Y es que el envasado de alimentos es uno de los puntos más críticos en términos de seguridad alimentaria. Aquel tipo de envasado que, además de ofrecer una barrera física hacia el medio exterior, lleva a cabo otro tipo de función, es lo que se considera como envasado activo (*active packaging* en inglés) (Vermeiren *et al.*, 1999). Un envasado activo puede proporcionar propiedades antimicrobianas como antioxidantes a través de la interacción directa de determinados compuestos con el alimento, además de ayudar a la eliminación de algunos factores negativos, como oxígeno o vapor de agua (Bajpai *et al.*, 2018), mejorando su estabilidad (Dasgupta *et al.*, 2015). La adición de sustancias antimicrobianas de origen natural está recibiendo cada vez más atención por tal de inactivar células bacterianas o bien ralentizar su crecimiento a la par que se mantienen la calidad y la seguridad alimentarias (Gill, 2003; Guerra *et al.*, 2005).

Una de las muchas matrices en que puede tratarse la CB, como es el papel de CB, es una muy buena candidata para la adsorción física de moléculas biológicamente activas. Aunque la inmovilización de lisozima en diferentes soportes de CB ha sido descrita (Bayazidi, Almasi and Asl, 2018), esta sería la primera vez que se combina esta forma de CB y lisozima. El principal objetivo de este trabajo fue la producción de un papel bioactivo de CB con lisozima, la evaluación de sus actividades antimicrobianas y antioxidantes y la caracterización de sus propiedades operacionales. Este estudio podría ser la semilla para el diseño de un nuevo material de empaquetamiento activo.

1.4. Nanocristales de celulosa bacteriana

La celulosa y sus derivados tienen una larga tradición de aplicaciones en la industria y se han incorporado a innumerables productos y procesos (Klemm *et al.*, 2011; Choi and Shin, 2020). Recientemente, el interés en la celulosa se ha desplazado hacia materiales de la nanoescala que incluyen la celulosa bacteriana (CB), las nanofibrillas de celulosa (NFC) y los nanocristales de celulosa (NCC), cuyas propiedades se recogen en la **Tabla 1**. La nanocelulosa, debido a sus características físico-mecánicas superiores, ha recibido una atención tremenda para una variedad de aplicaciones, incluyendo la industria alimentaria, cosmética, industria papelera, implantes biomédicos, industria química, electrónica, materiales ópticos, membranas de separación, etc. (Xue, Mou and Xiao, 2017).

Tabla 1. Características de los 3 tipos de nanocelulosa: celulosa bacteriana (CB), nanofibrillas de celulosa (NFC) y nanocristales de celulosa (NCC). Modificado de Moon *et al.,* 2011 y Klemm *et al.,* 2011.

Tipo de partícula	Longitud (µm)	Tamaño de la partícula		Cristalinidad (%)	Método de obtención
		Anchura (nm)	Altura (nm)		
CB	> 1	20 - 100	6 - 10	65 - 79	Síntesis bacteriana
NFC	0.5 - 2	5 - 70	4 - 20	-	Tratamiento mecánico de fibras vegetales
NCC	0.05 - 2	3 - 70	3 - 8	54 - 100	Hidrólisis de fibras vegetales, NFC, celulosa de tunicados o CB

Los NCC son partículas rígidas con forma de varilla que cuentan con una anchura que oscila entre los 3 - 70 nm y un largo de entre 50 nm y varias micras dependiendo del origen y el procedimiento de obtención (Klemm *et al.*, 2011; Moon *et al.*, 2011) (**Figura 14**). Se trata de partículas compuestas 100% de celulosa y que son altamente cristalinas. Tienen propiedades interesantes tales como baja densidad, alta área superficial y capacidad de ser modificables debido a los grupos laterales reactivos -OH (Roy *et al.*, 2009; Balea *et al.*, 2020). Las ventajas del uso de NCC están relacionadas no sólo con sus propiedades físicas y químicas sino también con su biodegradabilidad, renovabilidad, sostenibilidad, abundancia y biocompatibilidad (Dogan and McHugh, 2007; Müller, Laurindo and Yamashita, 2009; Peng *et al.*, 2011). Además, sus dimensiones, de escala nanométrica, abren una amplia gama de posibles propiedades por descubrir ya que, a nivel nanométrico, algunas propiedades de los materiales se ven afectadas por las leyes de la física atómica y no son las mismas que en los materiales tradicionales (Brinchi *et al.*, 2013).

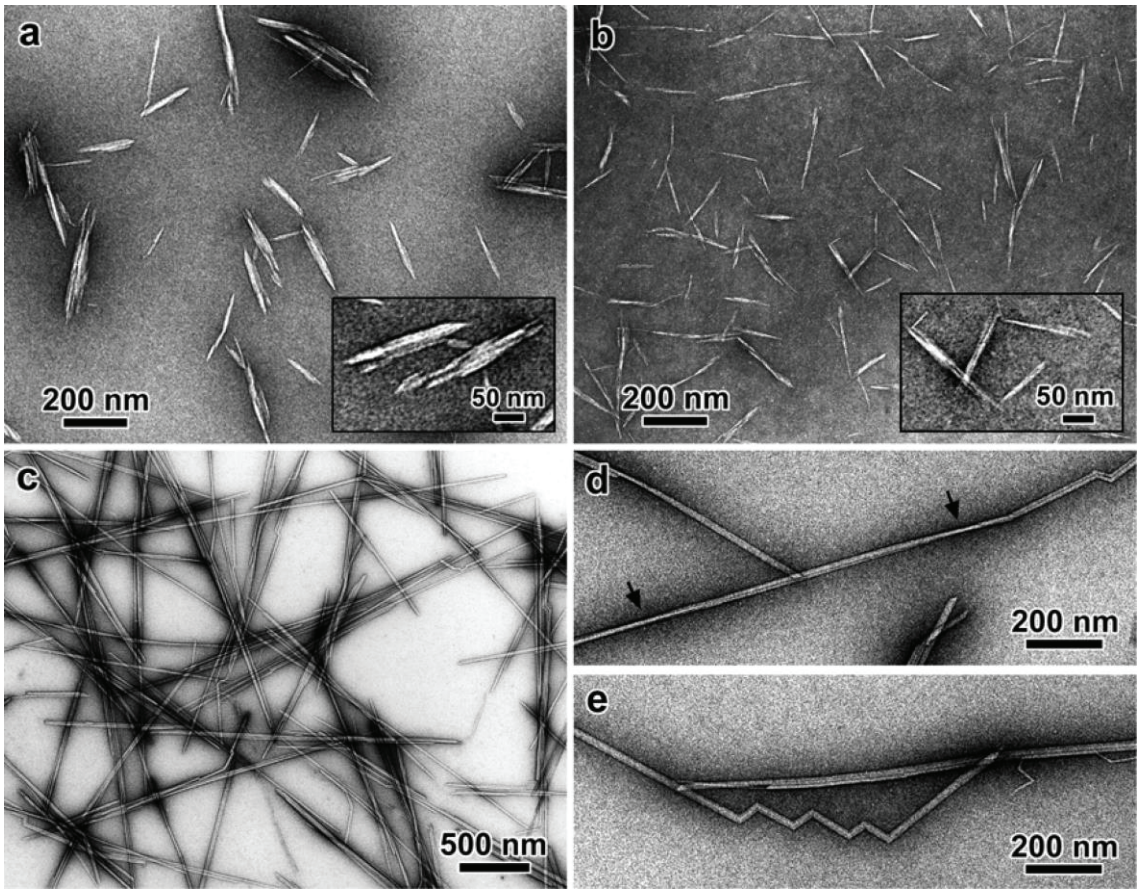

Figura 14. Microfotografías de microscopía electrónica de transmisión (TEM) de tinciones negativas de nanocristales de celulosa obtenidos por hidrólisis ácida con ácido sulfúrico de *a)* algodón, ***b)*** Avicel, microcelulosa cristalina parcialmente despolimerizada, ***c-e)*** celulosa de tunicados. Las flechas en *d)* señalan zonas donde los nanocristales se ven de canto. De Elazzouzi-Hafraoui *et al.*, 2008.

Las aplicaciones de los NCC se pueden dividir en dos categorías. La primera de ellas implica su uso como un potencial nanomaterial en campos tan diversos como la inmovilización enzimática, síntesis de materiales antimicrobianos, tecnologías "verdes", sensores de pH y síntesis de fármacos, entre otros (Roman *et al.*, 2009; Lam *et al.*, 2012). No obstante, su empleo como agente reforzante o de recubrimiento sobre otros polímeros, generando los NCC-nanocomposites, puede ampliar aún más toda la lista de potenciales aplicaciones (Nielsen *et al.*, 2010; Belbekhouche *et al.*, 2011; Kalashnikova *et al.*, 2012; Zinge and Kandasubramanian, 2020; Nascimento *et al.*, 2021), sobre todo en la industria papelera y de envasado (Choi and Shin, 2020). Sus propiedades únicas junto a sus nanodimensiones antes mencionadas, pueden producir nuevos materiales con propiedades mecánicas mejoradas, todo ello a muy bajas concentraciones (George and Sabapathi, 2015).

Los nanocristales de celulosa se han aislado previamente de diferentes fuentes de tipo vegetal, pero estas contienen celulosa junto con hemicelulosa, lignina y otras impurezas. La obtención a partir de CB es más simple gracias a su composición pura, sin lignina ni hemicelulosas (Abral *et al.*, 2018). Los nanocristales derivados de la CB, BCNC por sus siglas en inglés (*Bacterial Cellulose Nanocrystals*), pueden ser físicamente incorporados en otras matrices poliméricas para formar nanocomposites poliméricos. Entre las principales aplicaciones, destacan su uso en la industria papelera como aditivo (Azeredo, Rosa and Mattoso, 2017; Tayeb *et al.*, 2018), restauración de libros (Campano *et al.*, 2019) o como vehículo de otras moléculas inmovilizadas, como enzimas (Santos *et al.*, 2017; Balea *et al.*, 2018; Casas *et al.*, 2018). Cuando son añadidos a otras celulosas de origen vegetal, disminuye su porosidad y mejora sus propiedades barrera de ésta (Mazhari Mousavi *et al.*, 2017; Wang, Tavakoli and Tang, 2019). Para ello, se pueden mezclar con la pasta vegetal antes de la elaboración de superficies planas o bien adicionarlos sobre soportes sólidos ya formados, lo que permite economizar en gastos energéticos y asegura su retención (Mörseburg and Chinga-Carrasco, 2009).

Actualmente, la estrategia principal para obtener NCC de fibras celulósicas todavía depende de la hidrólisis ácida que lo que hace es eliminar la celulosa amorfa para obtener celulosa altamente cristalina, aparte de reducir su tamaño (Bai, Holbery and Li, 2009) (**Figura 15**). Después de la hidrólisis ácida, la dilución y el lavado repetido con agua acompañados de centrifugación y diálisis extensa se llevan a cabo para la eliminación de

moléculas de ácido libre y / o impurezas. Posteriormente, las partículas de NCC se dispersan como suspensiones uniformes mediante un tratamiento mecánico, por ejemplo, sonicación (Xue, Mou and Xiao, 2017). Así, su obtención es energéticamente costosa y genera una gran cantidad de residuos contaminantes. Además, el método con sulfúrico da como resultado la producción de nanocristales que contienen sulfato lo que compromete su biocompatibilidad y hace que muestren una menor estabilidad térmica en comparación con la celulosa nativa, un parámetro importante para su uso como materiales de refuerzo. Una alternativa para obtener NCC mediante un proceso más amigable con el medioambiente sería la utilización de enzimas disruptoras de las fibras celulósicas. Este sería un proceso con una producción de residuos mucho menor y, además, permite obtener NCC inalterados, que mantendrán su estabilidad térmica y biocompatibilidad mejorando su alcance en aplicaciones biomédicas y farmacéuticas (George *et al.*, 2011; Satyamurthy *et al.*, 2011). A mayores, el uso de enzimas permitiría simplificar el protocolo de obtención de NCC ya que no serían necesarios los procedimientos para la eliminación del ácido, consiguiendo que el proceso de producción sea más seguro, con menos contaminantes y con menor consumo de energía (Cui *et al.*, 2016).

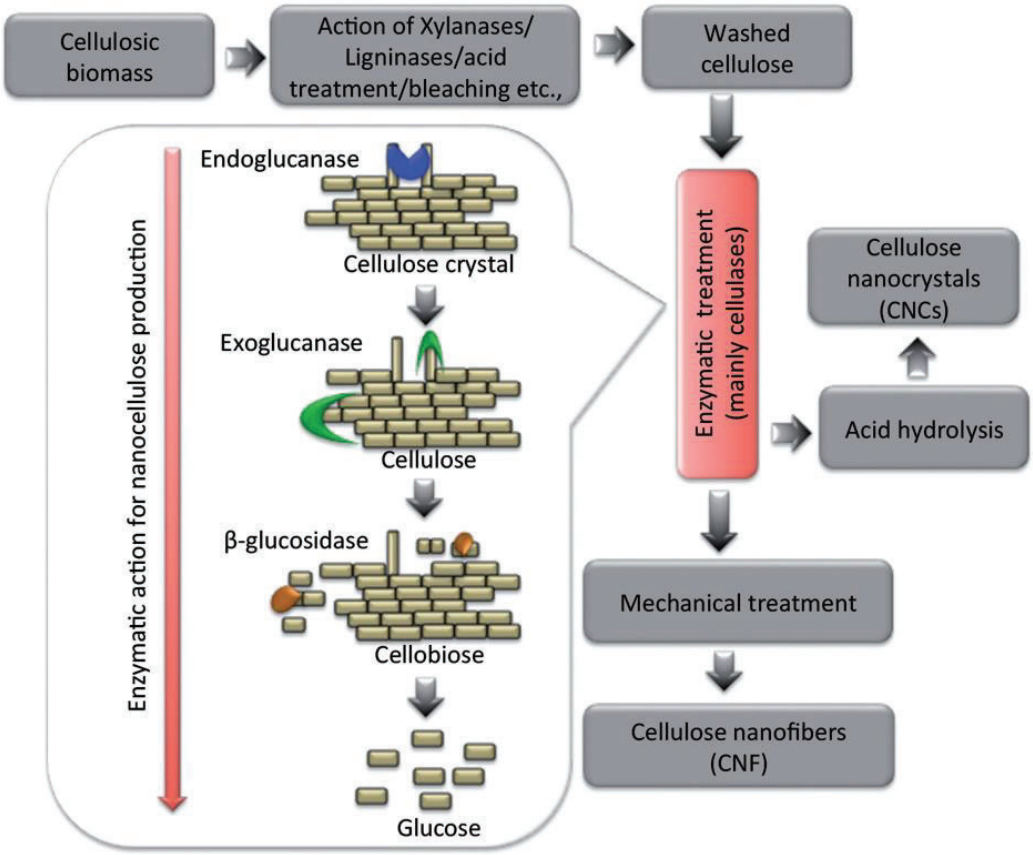

Figura 15. Ruta esquemática del aislamiento de NCC a partir de biomasa celulósica vegetal. El uso de enzimas tiene un papel relevante en la hidrólisis de la lignina y la hemicelulosa y en la posterior conversión de la celulosa obtenida en los NCC. De Karim *et al.*, 2017.

1.4.1. Enzimas disruptoras de la celulosa

Muchos hongos y bacterias producen enzimas que les permiten degradar el material lignocelulósico para poder utilizarlo como nutriente (Johansen, 2016). Las celulasas son enzimas capaces de degradar la celulosa. Clásicamente distinguimos celulasas de acción endo, conocidas como endoglucanasas (EC 3.2.1.4), que cortan aleatoriamente en el interior de la cadena de la celulosa y celulasas procesadoras exo, llamadas exoglucanasas (EC 3.2.1.91) que degradan los extremos de la cadena de celulosa; además también existen las β -glucosidasas (EC 3.2.1.91) que degrada la celobiosa a glucosa (**Figura 16**). Todas estas enzimas son hidrolíticas y se conocen como glucosil hidrolasas (Vaaje-Kolstad *et al.*, 2010).

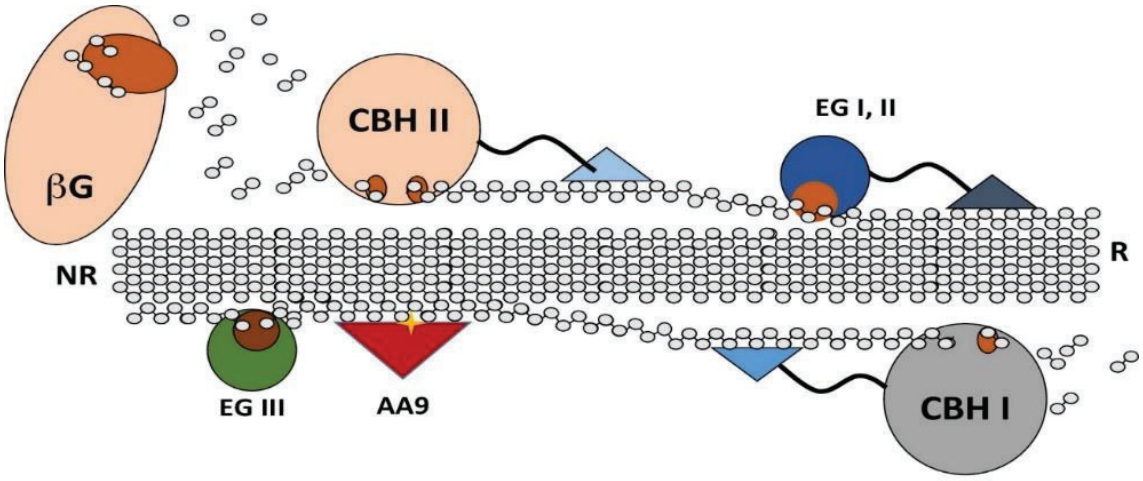

Figura 16. Acción de las diferentes enzimas modificadoras de la celulosa. La β-glucosidasa (βG) libera glucosa de la celobiosa; las exoglucanasas (CBH I y CBH II) liberan celobiosa del extremo reductor (R) y no reductor (NR) respectivamente y las endoglucanasas (EG I, II y III) rompen el enlace glucosídico interno, creando puntos de acción para CBH I y CBH II. En rojo se muestran las enzimas con actividad auxiliar (AA), en concreto las monooxigenasas líticas de polisacárido (LPMOs). Algunas celulasas contienen módulos de unión a celulosa, representados aquí como triángulos azules. De Johansen, 2016.

Aunque este modelo es generalmente aceptado, sigue siendo difícil entender cómo las glucosil hidrolasas podrían actuar en la zona cristalina de la celulosa, por lo que inicialmente se especuló sobre la existencia de un factor disruptor del sustrato que podría hacer que el sustrato cristalino sea más accesible para las enzimas hidrolíticas (Reese, Siu and Levinson, 1950). En 2010 se describió la ruptura oxidativa de los enlaces glucosídicos llevada a cabo por enzimas conocidas hoy como monooxigenasas líticas de polisacáridos, denominadas, por sus siglas en inglés, LPMO (*Lytic Polysacharide Monoxigenase*). Las LPMOs son enzimas dependientes de cobre que son capaces de romper el enlace

glucosídico que une las unidades de glucosa que conforman la celulosa mediante un mecanismo de oxidación del carbono 1 (C1) y/o el carbono 4 (C4) de la glucosa, aumentando la accesibilidad de las celulasas al sustrato (Li *et al.*, 2012; Vermaas *et al.*, 2015; Eibinger *et al.*, 2017; Villares *et al.*, 2017). Estas enzimas se han encontrado en bacterias y hongos y se clasifican dentro de la familia de actividades auxiliares (AA). Si bien su función biológica aún es objeto de investigación, su abundancia en los genomas de organismos degradadores de la biomasa vegetal sugiere la gran importancia de las LPMO en el procesamiento de ésta (Forsberg *et al.*, 2014b). Aún así, se están llevando cabo estudios para dilucidar su papel como factores de virulencia en infecciones virales (Chiu *et al.*, 2015) y en procesos de patogenicidad bacteriana (Paspaliari *et al.*, 2015).

Como se puede ver en el esquema presentado en la **Figura 17**, en un medio acuoso la oxidación del C1 da lugar a una lactona que espontáneamente se transforma en ácido aldónico por la hidrólisis del anillo, mientras que la oxidación del C4 resulta en una cetoaldosa que espontáneamente da lugar a la formación de un grupo diol en dicho carbono. Si se produce la oxidación de ambos carbonos (C1 y C4) se produce un grupo diol en el extremo no reductor y un ácido glucónico en el extremo reductor (Vaaje-Kolstad *et al.*, 2017). El mecanismo de reacción no es del todo conocido, pero recientes investigaciones sugieren que requiere oxígeno molecular y un donador de electrones como, por ejemplo, el ácido ascórbico, para despolimerizar las cadenas de azúcares (Sani and Krishnaraj, 2017).

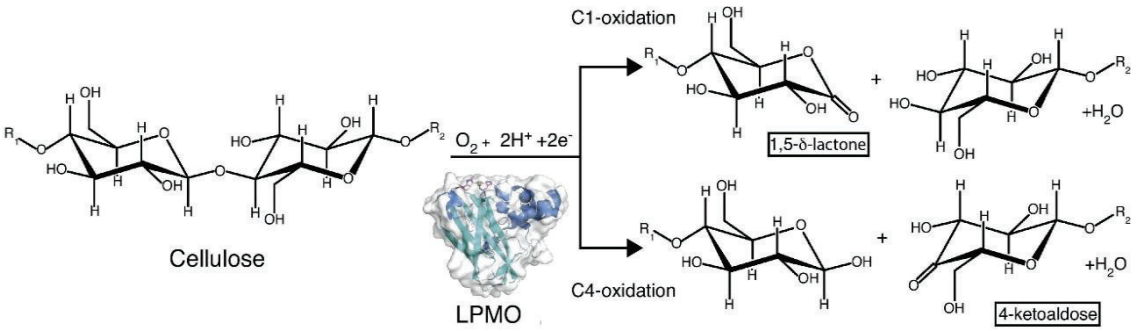

Figura 17. Mecanismo de reacción de las LPMOs. Oxidación del carbono 1 o carbono 4 de la celulosa con la ruptura del enlace glucosídico entre glucosas. De Vaaje-Kolstad et al. 2017.

1.4.2. Monoxigenasas líticas de polisacáridos y SamLPMO10C

Antes del descubrimiento de las monoxigenasas líticas de polisacáridos, la ruptura de polímeros naturales recalcitrantes se atribuía únicamente a la hidrólisis del enlace glicosídico (Reese, Siu and Levinson, 1950). Frente a esta visión, las LPMOs presentan

una forma única de escindir polímeros mediante oxidación del sustrato para formar ácidos aldónicos (Horn *et al.*, 2012). Este mecanismo se describió como dependiente de cobre y de un dador de electrones. Este último elemento puede encontrarse dentro del sustrato (ácido gálico o distintos componentes de la lignina), pueden ser añadidos externamente (por ejemplo, glutatión o ácido ascórbico) o pueden provenir de la acción de la enzima celobiosa deshidrogenasa (CDH), que actúa de forma sinérgica con la LPMO. Los sitios activos de las LPMOs se localizan en una superficie plana formada por bucles y contienen un ión de cobre de tipo (II), que interacciona con el oxígeno molecular (**Figura 18**). Esta reacción es seguida por la reducción de uno de los átomos de oxígeno a agua y la introducción del otro en el sustrato (MacPherson and Murphy, 2007). Este centro catalítico está coordinado por dos histidinas altamente conservadas y el amino terminal, que en el caso de las LPMOs bacterianas son una alanina y una fenilalanina coordinadas de forma ecuatorial con el ion de cobre. En los hongos estas posiciones corresponden a una tirosina y a un átomo de oxígeno de una molécula de agua.

Las LPMOs han sido reclasificadas como enzimas auxiliares AA (*Auxiliary Activity*), en la base de datos de enzimas activas sobre carbohidratos CAZy (Carbohydrate-Active enZYmes). La actividad monooxigenasa de estas enzimas puede clasificarse en seis familias, AA9, AA10, AA11, AA13, AA14 y AA15 (M *et al.*, 2018; Sabbadin *et al.*, 2018; Forsberg *et al.*, 2019). La enzima SamLPMO10C es una LPMO de *Streptomyces ambofaciens* recientemente clonada y caracterizada (Valenzuela *et al.*, 2017). SamLPMO10C, SamC de ahora en adelante, pertenece a la familia AA10. Los miembros de este grupo se conocían anteriormente como módulos de unión a carbohidratos de la familia 33 (CBM33). En él se engloban proteínas dependientes de cobre que suelen ser de pequeño peso molecular y se pueden encontrar en bacterias, virus que infectan insectos, arqueas y hongos (Cantarel *et al.*, 2009). Se ha descrito actividad de algunas enzimas de este grupo sobre celulosa y otras sobre quitina, el segundo compuesto orgánico más abundante del planeta después de la celulosa y que se encuentra en la cutícula de artrópodos y la pared celular de hongos y levaduras. Se han encontrado casi 2000 posibles LPMOs en la familia AA10, aunque menos del 5 % ha sido caracterizado. La primera AA10 aislada fue CHB1 de *Streptomyces olivaceoviridis* en 1994 , pero su capacidad de despolimerización por medio de oxidación no se demostró hasta quince años más tarde (Schnellmann *et al.*, 1994; Vaaje-Kolstad *et al.*, 2010). La estructura de las AA10 consiste en un plegamiento β-sándwich con dos laminas β antiparalelas conectadas

por bucles, sin la presencia de las clásicas ranuras de unión al sustrato (Karkehabadi *et al.*, 2008). Poseen superficies planas que contienen residuos aromáticos y polares que se adaptan a las partes cristalinas de los polímeros (Forsberg *et al.*, 2014a) y se cree que a causa de la unión a estas superficies planas, el centro metálico de la LPMO se orienta para dar el corte en C1 (Vu *et al.*, 2014).

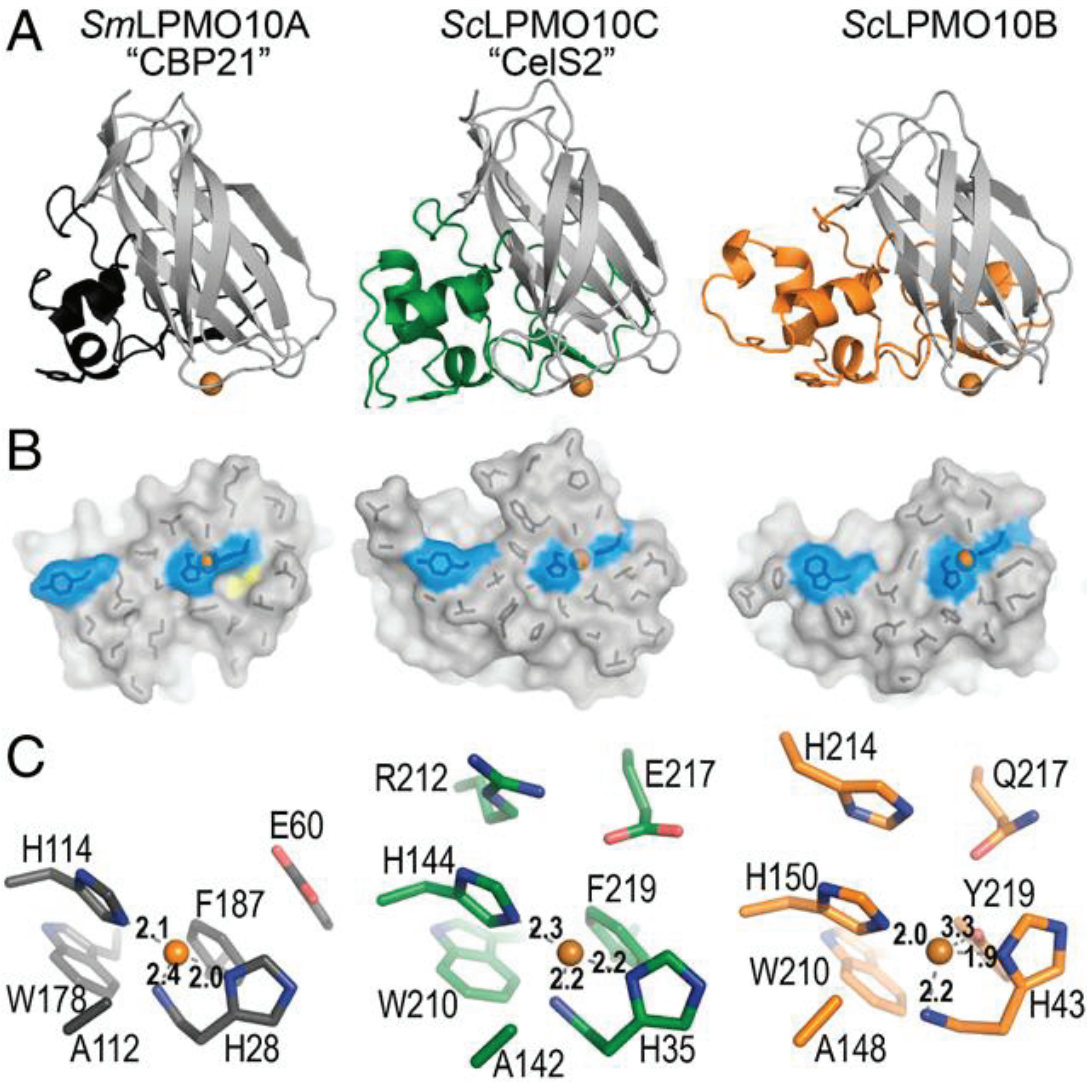

Figura 18. Estructura de tres LPMOs de la familia AA10: ***a)*** CBP21 (negro: superficie de unión a quitina, oxida en C1, PDB 2BEM), CelS2 (verde: superficie de unión a celulosa, oxida en C1) y ScLPMO10B (naranja: superficie de unión a sustratos celulósicos y quitina, oxidando en C1 y C4 y en C1, respectivamente). Las esferas naranjas corresponden a los iones de cobre tipo (II). ***b)*** Proyección de la superficie del área de unión del sustrato, supone una rotación de 90 º alrededor del eje horizontal de los planos anteriores. En azul se muestran los residuos de histidina y los residuos con anillos aromáticos. ***c)*** Centros activos de las LPMO. Modificado de Forsberg *et al.*, 2014a.

1.4.3. Funcionalización de la CB con SamC para la obtención de nanocristales

En este trabajo se explora la posibilidad de obtener NCC a partir de la CB mediante la acción de enzimas disruptoras de la celulosa. Para ello, se combinó un cóctel enzimático cuya formulación contenía una mezcla de endo y exoglucanasas y la LPMO SamC. Desde el descubrimiento de las LPMO, no han sido pocos los estudios basados en la sinergia que presentan con ciertas celulasas durante la digestión de sustratos celulósicos, y se les ha atribuido un papel relevante como pretratamiento en la obtención de NFC (Horn *et al.*, 2012; Valls *et al.*, 2019). Se cree que actúan en primer lugar, haciendo la celulosa cristalina más accesible a las glucosil hidrolasas (Johansen, 2016; Valenzuela *et al.*, 2017). La preferencia de la SamC por sustratos celulósicos de elevado índice de cristalinidad (Valenzuela *et al.*, 2019) sugería que, en combinación con las celulasas, podría jugar un papel importante en la obtención de nanocristales a partir de la celulosa bacteriana mediante un tratamiento exclusivamente enzimático.

2. OBJETIVOS

2. Objetivos

El desarrollo de la presente tesis doctoral se ha llevado a cabo en el laboratorio de investigación de enzimas microbianas de aplicación industrial, dentro de la sección de Microbiología, Virología y Biotecnología del Departamento de Genética, Microbiología, y Estadística. El grupo de investigación se dedica a la identificación y optimización de enzimas modificadoras de la biomasa para su valorización y generación de nuevos biomateriales de interés biotecnológico. Dentro de este contexto, el objetivo principal de esta tesis es la valorización de la celulosa bacteriana mediante el empleo de técnicas respetuosas con el medio ambiente. Este objetivo se ha abordado desde dos enfoques, que definen las dos líneas de investigación de esta tesis: el estudio de la CB como matriz biológicamente activa como soporte para la inmovilización de enzimas y su conversión en nanocristales a través de un tratamiento enzimático. Los objetivos específicos son los siguientes:

1. Identificación, clonación y mejora de nuevas lipasas.
    a. Comprobar si, tras una mutagénesis dirigida en los dominios de su centro catalítico y en el péptido señal la proteína LipJ adquiere actividad termófila.
    b. Modificación del punto H110 mediante la confección de una librería NNK para determinar si tiene efecto sobre la actividad termófila de LipJ.
2. Funcionalización de la celulosa bacteriana: inmovilización de enzimas.
    a. Inmovilización de una lipasa comercial y de LipJ.
    b. Inmovilización de la enzima lisozima.
3. Producción de nanocristales de celulosa bacteriana (BCNC).
    a. Optimización de la producción de BCNC mediante enzimas LPMO y celulasas.
    b. Caracterización de los BCNC obtenidos.
    c. Recubrimiento de soportes vegetales con los BCNC y determinación de las propiedades adquiridas.

3. INFORMES

3. Informes

3.1. Listado de publicaciones

Por orden de aparición en este trabajo, la presente tesis doctoral se centra en cuatro artículos publicados y uno en preparación:

1. Estupiñán, M., Buruaga, C., Pastor, F. I. J., Martínez, J., & Diaz, P. (2019). Shift in Bacillus sp. JR3 esterase LipJ activity profile after addition of essential residues from family I.5 thermophilic lipases. *Biochemical Engineering Journal*, *144*, 166–176. https://doi.org/10.1016/j.bej.2019.01.023
2. Buruaga-Ramiro, C., Valenzuela, S. V., Pastor, F. I. J., Martínez, J., & Diaz, P. (2020). Unexplored lipolytic activity of Escherichia coli: Implications for lipase cloning. *Enzyme and Microbial Technology*, *139*, 109590. https://doi.org/10.1016/j.enzmictec.2020.109590
3. Buruaga-Ramiro, C., Valenzuela, S. V., Valls, C., Roncero, M. B., Pastor, F. I. J., Díaz, P., & Martínez, J. (2020). Bacterial cellulose matrices to develop enzymatically active paper. *Cellulose*, *27*(6), 3413–3426. https://doi.org/10.1007/s10570-020-03025-9
4. Buruaga-Ramiro, C., Valenzuela, S. V., Valls, C., Roncero, M. B., Pastor, F. I. J., Díaz, P., & Martinez, J. (2020). Development of an antimicrobial bioactive paper made from bacterial cellulose. *International Journal of Biological Macromolecules*. https://doi.org/10.1016/j.ijbiomac.2020.04.234
5. Buruaga-Ramiro, C., Fernández-Gándara, N., Cabañas-Romero, V., Valenzuela, S. V., Díaz, P., & Martínez, J. Lytic polysaccharyde monooxigenases and cellulases on the production of bacterial cellulose nanocrystals. En curso.

3.2. Informe sobre el factor de impacto

Los artículos que forman parte de la memoria de la tesis doctoral presentada por Carolina Buruaga Ramiro han sido publicados o están en preparación para su publicación en revistas internacionales indexadas en el Journal Citation Reports ® tal y como se detalla a continuación:

1. Estupiñán, M., **Buruaga, C.**, Pastor, F. I. J., Martínez, J., & Diaz, P. (2019). Shift in Bacillus sp. JR3 esterase LipJ activity profile after addition of essential residues from family I.5 thermophilic lipases. BIOCHEMICAL ENGINEERING JOURNAL, *144*, 166–176. https://doi.org/10.1016/j.bej.2019.01.023

Esta revista se encuentra incluida en el primer cuartil del área temática de: biotecnología y microbiología aplicada (48/156) e ingeniería química (26/142), con un factor de impacto para el año 2019 de 3.475.

2. **Buruaga-Ramiro, C.**, Valenzuela, S. V., Pastor, F. I. J., Martínez, J., & Diaz, P. (2020). Unexplored lipolytic activity of Escherichia coli: Implications for lipase cloning. ENZYME AND MICROBIAL TECHNOLOGY, *139*, 109590. https://doi.org/10.1016/j.enzmictec.2020.109590

Esta revista se encuentra incluida en el segundo cuartil del área temática de biotecnología y microbiología aplicada (66/159) con un factor de impacto para el año 2020 de 3.493.

3. **Buruaga-Ramiro, C.**, Valenzuela, S. V., Valls, C., Roncero, M. B., Pastor, F. I. J., Díaz, P., & Martínez, J. (2020). Bacterial cellulose matrices to develop enzymatically active paper. CELLULOSE, *27*(6), 3413–3426. https://doi.org/10.1007/s10570-020-03025-9

Esta revista se encuentra incluida en el primer cuartil del área temática de: ciencias de los materiales, papel y madera agricultura (1/22), ciencia de los materiales y textil (2/25) y ciencia de los polímeros (11/88), con un factor de impacto para el año 2020 de 5.044.

4. **Buruaga-Ramiro, C.**, Valenzuela, S. V., Valls, C., Roncero, M. B., Pastor, F. I. J., Díaz, P., & Martinez, J. (2020). Development of an antimicrobial bioactive paper made from bacterial cellulose. INTERNATIONAL JOURNAL OF BIOLOGICAL MACROMOLECULES. https://doi.org/10.1016/j.ijbiomac.2020.04.234

Esta revista se encuentra incluida en el primer cuartil del área temática de: bioquímica y biología molecular (52/297), ciencias de polímeros (6/88) y química aplicada (9/74), con un factor de impacto para el año 2020 de 6.953.

5. **Buruaga-Ramiro, C**., Fernández-Gándara, N., Cabañas-Romero, V., Valenzuela, S. V., Díaz, P., & Martínez, J. Lytic polysaccharyde monooxigenases and cellulases on the production of bacterial cellulose nanocrystals.

Este trabajo ha sido enviado a la revista EUROPEAN POLYMER JOURNAL, que se encuentra incluida en el primer cuartil del área temática de ciencias de polímeros (15/88) con un factor de impacto para el año 2020 de 4.598.

Dra. Josefina Martínez Martínez
Directora de tesis

Dra. Pilar Diaz Lucea
Directora y tutora de tesis

3.3. Informe de participación en las publicaciones

La doctoranda Carolina Buruaga Ramiro ha participado en los artículos que forman parte de su tesis doctoral de la manera que se detalla a continuación:

1. Estupiñán, M., Buruaga, C., Pastor, F. I. J., Martínez, J., & Diaz, P. (2019). Shift in Bacillus sp. JR3 esterase LipJ activity profile after addition of essential residues from family I.5 thermophilic lipases. *Biochemical Engineering Journal*, *144*, 166–176. https://doi.org/10.1016/j.bej.2019.01.023

La doctoranda llevó a cabo la mayor parte del trabajo experimental y participó activamente en el diseño de los ensayos.

2. Buruaga-Ramiro, C., Valenzuela, S. V., Pastor, F. I. J., Martínez, J., & Diaz, P. (2020). Unexplored lipolytic activity of Escherichia coli: Implications for lipase cloning. *Enzyme and Microbial Technology*, *139*, 109590. https://doi.org/10.1016/j.enzmictec.2020.109590

La doctoranda llevó a cabo la parte experimental y participó activamente en el diseño experimental.

3. Buruaga-Ramiro, C., Valenzuela, S. V., Valls, C., Roncero, M. B., Pastor, F. I. J., Díaz, P., & Martínez, J. (2020). Bacterial cellulose matrices to develop enzymatically active paper. *Cellulose*, *27*(6), 3413–3426. https://doi.org/10.1007/s10570-020-03025-9

La doctoranda llevó a cabo la parte experimental, participó activamente en el diseño experimental y en la redacción del manuscrito.

4. Buruaga-Ramiro, C., Valenzuela, S. V., Valls, C., Roncero, M. B., Pastor, F. I. J., Díaz, P., & Martinez, J. (2020). Development of an antimicrobial bioactive paper made from bacterial cellulose. *International Journal of Biological Macromolecules*. https://doi.org/10.1016/j.ijbiomac.2020.04.234

La doctoranda llevó a cabo la parte experimental, participó activamente en el diseño experimental y en la redacción del manuscrito.

5. Buruaga-Ramiro, C., Fernández-Gándara, N., Cabañas-Romero, V., Valenzuela, S. V., Díaz, P., & Martínez, J. Lytic polysaccharyde monooxigenases and cellulases on the production of bacterial cellulose nanocrystals. En curso.

La doctoranda llevó a cabo la parte experimental, participó activamente en el diseño experimental y en la redacción del manuscrito.

Ninguno de los coautores de los artículos aquí expuestos ha utilizado los datos descritos en dichas publicaciones para elaborar sus tesis doctorales.

Dra. Josefina Martínez Martínez
Directora de tesis

CPISR-1 C MARIA PILAR DIAZ LUCEA
Firmado digitalmente por CPISR-1 C MARIA PILAR DIAZ LUCEA
Fecha: 2021.10.29 15:36:51 +02'00'

Dra. Pilar Diaz Lucea
Directora y tutora de tesi

4. ARTÍCULOS

4. Artículos

4.1. Capítulo 1. Caracterización de lipasas bacterianas

4.1.1. ***Artículo 1.*** *Shift in Bacillus sp. JR3 esterase LipJ activity profile after addition of essential residues from family I.5 thermophilic lipases.*

4.1.2. ***Artículo 2.*** *Unexplored lipolytic activity of Escherichia coli: Implications for lipase cloning.*

Shift in *Bacillus sp*. JR3 esterase LipJ activity profile after addition of essential residues from family I.5 thermophilic lipases

Recientemente se describió LipJ, una esterasa mesófila perteneciente al clado específico de la familia de lipasas bacterianas I.5, que posee la misma estructura aún con distintos motivos en su secuencia. En este estudio se emplearon dos aproximaciones para modificar LipJ mediante la adición de características de la familia I.5 por tal de cambiar su perfil de actividad. La mutagénesis de saturación iterativa de un residuo posiblemente involucrado en la coordinación de Zn^{2+} produjo una variante, LipJ –H110N, que mostró un cambio notable en la especificidad de sustrato, posiblemente impulsado por cambios en el número y en la distancia de las interacciones polares relevantes para la coordinación del ión Zn^{2+}. Además, las variantes E27A, G136A y M139Q obtenidas por mutagénesis dirigida como mutantes simples, dobles o triples, mostraron un cambio general en la especificidad hacia temperaturas más elevadas y sustratos de cadena más larga, exhibiendo todas ellas una mayor actividad que LipJ en sustratos C7. Los resultados obtenidos sugieren que la región N-terminal de LipJ puede contribuir a la acomodación del sustrato, mientras que las variantes que contenían la(s) mutación(ones) en el pentapéptido mostraron una actividad máxima a 50 ° C, siendo el triple mutante el único que presentó actividad a 80 ºC, potenciada por la presencia del ión Mn^{2+}. El modelo 3D y el acoplamiento molecular (*molecular docking*) indicaron una mejor acomodación de los sustratos de cadena media y para un ambiente de Zn^{2+} modificado, en concordancia con los cambios en el perfil de sustratos y de temperatura observados.

Biochemical Engineering Journal 144 (2019) 166–176

Contents lists available at ScienceDirect

Biochemical Engineering Journal

journal homepage: www.elsevier.com/locate/bej

Regular article

Shift in *Bacillus* sp. JR3 esterase LipJ activity profile after addition of essential residues from family I.5 thermophilic lipases

Mónica Estupiñán[a], Carolina Buruaga[a], F.I. Javier Pastor[a,b], Josefina Martínez[a,b], Pilar Diaz[a,b,*]

[a] Department of Genetics, Microbiology and Statistics, Faculty of Biology, University of Barcelona, Av. Diagonal 643, 08028, Barcelona, Spain
[b] Institute of Nanoscience and Nanotechnology (IN2UB), University of Barcelona, Spain

HIGHLIGHTS

- Engineering LipJ to recover essential traits of thermophilic lipases.
- Improved specificity and temperature of LipJ variants.
- Zn^{2+} coordination region important for thermophilicity.
- Mn^{2+} enhanced activity of selected LipJ mutants.
- 3D model analysis evidenced better substrate accommodation.

ARTICLE INFO

Keywords:
Protein engineering
Lipase
Pentapeptide
Thermophilicity
Evolution
Bacillus

ABSTRACT

We recently described LipJ, a mesophilic esterase clustering in a specific clade of bacterial lipase family I.5, bearing the same structure but several distinct sequence motifs. Two mutagenesis approaches were used here to modify LipJ by addition of common features of family 1.5 lipases, searching for changes on the activity profile. Iterative saturation mutagenesis of a residue possibly involved in Zn^{2+} coordination produced a LipJ variant –H110N– displaying a remarkable shift in substrate specificity, possibly boosted by changes in number and distance of relevant polar interactions for Zn^{2+} coordination. Also, variants E27 A, G136 A and M139Q were obtained by site directed mutagenesis as single, double or triple mutants, showing a general shift in specificity towards higher temperature and longer chain-length substrates, all of them displaying higher activity than LipJ on C7 substrates. The results obtained suggest that the N-terminal region of LipJ may indeed contribute to substrate accommodation, whereas mutations at the pentapeptide displayed maximum activity at 50 °C, with the triple mutant showing activity even at 80 °C, greatly enhanced by Mn^{2+}. 3D modelling and molecular docking analysis of selected mutants provided clues for a better accommodation of medium chain-length substrates, and for a modified Zn^{2+} environment, in agreement with the substrate and temperature profile shifts observed.

1. Introduction

Carboxylesterases (EC 3.1.1.-), widely distributed in nature, are a diverse group of well-known and profusely used biocatalysts performing either hydrolysis of acyl-glycerides or their synthesis through esterification, interesterification or transesterification reactions [1–4]. During the last years, lipases have increasingly been used in food, cosmetics, detergent, pharmaceutical, fuel or fine chemistry industries, where they have extensively contributed to improve economy and sustainability by substitution of previous chemically-driven processes [1,2,12,4–11]. In general, carboxylesterases are robust enzymes that can be used under mild conditions without cofactor addition, thus being economically attractive biocatalysts for industrial purposes [5,7,8,12–15]. Nevertheless, there are still certain processes requiring enzymes displaying tolerance to more extreme conditions or acting on longer chain-length substrates [16,17]. For those reactions requiring such conditions, several strategies can be followed in order to obtain the biocatalysts that fit the desired properties: either isolation of new enzymes [18–21] or, alternatively, their modification to get improved activities [16,22–29]. And of course, both approaches can be combined to produce the biocatalyst of choice for a defined process [14,15,22].

Structurally, carboxylesterases are constituted by an alternation of

* Corresponding author at: Department of Genetics, Microbiology and Statistics, Faculty of Biology, University of Barcelona. Av. Diagonal 643, 08028, Barcelona, Spain.
E-mail address: pdiaz@ub.edu (P. Diaz).

https://doi.org/10.1016/j.bej.2019.01.023
Received 15 November 2018; Received in revised form 15 January 2019; Accepted 24 January 2019
Available online 02 February 2019
1369-703X/

α-helices and β-sheets forming a characteristic α/β–fold, with a catalytic triad including a serine as the catalytic residue, and an aspartic/glutamic acid which is hydrogen bonded to a histidine, usually being the nucleophile serine embedded in the G(A)X**S**XG consensus pentapeptide, and the oxyanion hole for substrate accommodation [2,30]. Also, most so called "true lipases" bear an extra α-helix known as *lid*, responsible for the interfacial activation phenomenon [2]. Based on amino acid sequence and the presence of conserved motifs, bacterial carboxylesterases were initially classified into eight families [31]. However, considering structural features and phylogenetic analysis, at least 19 families have been described up to date [21,30,32–34].

In a previous work, we described the isolation of the mesophilic strain *Bacillus* sp. JR3 from an ancient volcanic soil of a laurel forest (Laurisilva) at El Hierro island (Canary Islands, Spain), displaying a strikingly high extracellular lipase activity at extremely high temperatures (80–100 °C) [35]. A new carboxylesterase −LipJ− was isolated from strain JR3, cloned in *E. coli* and characterized. Surprisingly, LipJ displayed maximum activity only under mild conditions, with optimum temperature at 30 °C and great loss of activity when tested at high temperatures. However, phylogenetic and structure analysis of LipJ assigned the enzyme to bacterial lipase family I.5, although positioned in a differentiated clade, similarly to *Actinibacillus thermoaerophilus* LipAT lipase (also named HZ) [33,35,36]. Moreover, superimposition of the 3D model of LipJ with the structures of the closest thermophilic lipases from *Pelosinus fermentans* (pdb: *5ah0*) [37] and *Geobacillus stearothermophilus* L1 (pdb: *1ku0*) [38] allowed prediction of putative Ca^{2+} and Zn^{2+}-binding cavities in LipJ [35], a common trait found among bacterial thermophilic lipases with lid domain [38–40]. Nevertheless, no notable thermal tolerance increase was obtained when LipJ was assayed in the presence of such ions, getting even lower activity when Zn^{2+} was added to the reaction mix [35]. The different properties of LipJ with respect to the nearest crystallized family I.5 lipases could be justified by the finding of variations in conserved and probably key residues between LipJ and family I.5 lipases at both, the signal peptide cleavage site and at the pentapeptide motif. Alternatively, amino acid H110, found to be different in LipJ and in close proximity to the Zn^{2+}-coordinating residues, could apply for this effect [35]. In fact, this hypothesis is supported by previous results showing that modification of the equivalent amino acid in *C. botulinum* esterase (pdb: *5ah1*) [41] produced a variant –F182Y– with improved thermophilicity [42].

Several authors have tried to shed light on the residues or structures responsible for the properties of thermophilic lipases [38–40,42–44]. The set of results obtained point to either a tetrahedral Zn^{2+} coordination constituted by conserved residues (D90, H110, H116 and D267 in *Geobacillus stearothermophilus* L1 lipase) [38,42], formation of salt bridges like in *Geobacillus thermodenitrificans* EstGtA2 [45], large structure rearrangements of the α5 [46] or the α6 and α7 helices, stabilized by a Zn^{2+}-binding domain [39,42,47], presence of two Trp residues (W89 and W240 in BTL2 lipase) playing a critical function in Zn^{2+} binding to the coordination site [40], dimer formation like in Pf2001 or LipAT-HZ esterases [33,36,44], or the hydrophobicity of the substrate [43] as the most significant causes for activity increase of family I.5 lipases at high temperatures and on long chain-length substrates. In order to get a deeper knowledge of LipJ, a singular family I.5 esterase, we here applied a rational mutagenesis approach to obtain improved LipJ variants by introducing common features found in crystalized thermophilic lipases from family I.5, and to study the consequences of such mutations on either temperature or substrate profile.

2. Materials and methods

2.1. Strains, plasmids and growth conditions

Strain *Bacillus* sp. JR3 (CECT 9334) was grown on Luria-Bertani medium (LB) and incubated for 24 h at 30 °C under aerobic conditions. Recombinant clones *E. coli* DH5α and BL21 Star(DE3) bearing *lipJ* in pET28a (Novagen) [35] were routinely cultured overnight at 37 °C in LB medium supplemented with kanamycin (50 μg ml^{-1}) or with IPTG (isopropyl-β-D-thiogalactopyranoside; 1 mM) and X-gal (5-bromo-4-chloro-3-indolyl-β-D-galactopyranoside; 80 μg ml^{-1}) to obtain maximum activity in the soluble fraction after overnight incubation at 21 °C. For plate activity determination, agar plates were prepared using TSA (ADSA Micro) supplemented with tributyrine (1% v/v, Sigma) and 0.0002% Rhodamine B (v/v, Sigma), as previously described [48,49]. Fast routine MUF-based paper activity tests of the grown recombinant clones obtained were performed as previously described [50,51].

2.2. DNA procedures

Plasmid DNA was purified using GeneJET Plasmid Miniprep Kit (Thermo Fisher Scientific). NZYProof DNA polymerase (NZYtech) was used for DNA amplification, and *Dpn*I restriction enzyme (Thermo Scientific) was used according to the manufacturer's specifications for QuikChange mutagenesis. All primers were purchased from Sigma-Aldrich. PCR amplifications were performed in a Gene Amp® PCR System 2400 (Perkin Elmer) and T100™ Thermal Cycler (Bio-Rad) using different cycling periods. Mutagenesis was confirmed by Sanger sequencing obtained through the analytical system CEQ™ 8000 (Beckman-Coulter) available at the Genomics Unit of the Serveis Científics i Tecnològics of the University of Barcelona (CCiTUB). DNA samples were routinely analysed by 0.8% (w/v) agarose gel electrophoresis [52], and stained with 0.004% (v/v) GreenSafe Premium (NZytech). Nucleic acid concentration and purity was measured using a Spectrophotometer ND-100 NanoDrop®.

2.3. Production of LipJ variants

Site-directed and site-specific iterative saturation mutagenesis was performed to obtain LipJ variants with improved properties. Five LipJ variants –E27 A, G136 A, M139Q, double mutant G136 A/M139Q (LipJ-DM), and triple mutant E27 A/G136 A/M139Q (LipJ-TM)– were obtained using the QuikChange site-directed mutagenesis strategy, using approximately 10 ng pET28a-LipJ DNA [35] as template for PCR amplification, and specific primers purchased from Sigma-Aldrich (Table 1). For site-specific iterative saturation mutagenesis [53], a gene library encoding all possible amino acids at position H110 of LipJ was constructed by replacing the target codon with an NNK degeneracy (N being A, T, G, or C, and K being G or T), using the appropriate primers (Table 1). For both strategies, the subsequent PCR products were incubated for 3 h at 37 °C with *Dpn*I endonuclease in order to digest the methylated parental DNA, and the resulting DNAs were transformed into *E. coli* DH5α, purified and confirmed by sequencing. For NNK-library activity screening, four sets of 30 colonies were pooled for plasmid DNA isolation and further transformation into the expression strain *E. coli* BL21Star (DE3). Selected clones carrying LipJ variants with higher activity than wild type LipJ were isolated and cultured for plasmid purification and sequencing. Clone carrying wild type BL21/pET28a-LipJ was used as a control.

2.4. Expression of LipJ variants

For LipJ variant production, exponential growth cultures (OD_{600nm} = 0.6–0.8) of recombinant *E. coli* BL21/pET28a-LipJ mutants in LB medium supplemented with kanamycin (50 μg ml^{-1}) were induced with 1 mM IPTG at 21 °C for 16 h. Cells were collected by centrifugation at 9000× rpm for 20 min (Beckman-Coulter VA-1000), 20-fold concentrated in 20 mM Tris−HCl buffer pH 7.0, and disrupted using a GEA PandaPLUS 2000 homogenizer (1200 bars). Clarified cell extracts were recovered after centrifugation at 10,000× rpm for 20 min at 4 °C (Beckman-Coulter High-Speed VA-1000) for activity determination. Bradford assays were performed for protein concentration determination using bovine serum albumin (BSA) as the standard [24,54].

Table 1
Primers.

Mutant	Primer	Sequence (5´- 3´)
LipJ-E27 A	LipJE27 A Fw	CTTACGCTG**C**AGAGAAACAACAAAATAATTAC
	LipJE27 A Rv	TTGTTTCTCT**G**CAGCGTAAGTTATTTTTG
LipJ-G136 A	LipJG136 A Fw	TTTAGTTG**C**GCATAGCATGGGTGGACAAACG
	LipJG136 A Rv	CCATGCTATGC**G**CAACTAAATGAACTTTATT
LipJ-M139Q	LipJM139Q Fw	GGCATAGC**CA**GGGTGGACAAACGATTAG
	LipJM139Q Rv	TGTCCACC**CT**GGCTATGCCCAACTAAATGAAC
LipJ-G136 A/M139Q	LipJM139Q Fw	ATTTAGTTG**C**GCATAGC**CA**GGGTGGAC
	LipJM139Q Rv	GTTGTCCACCC**TG**GCTATGC**G**CAACTAAATGAAC
LipJ library	LipJH110NNK Fw	CTGAGAAA**NNK**GGACATAATCGTTTTGG
H110/NNK	LipJH110-NNK Rv	TTATGTCC**MNN**TTTCTCAGCATGTGCGG

List of primers designed for LipJ site directed mutagenesis (LipJ-E27 A, LipJ-G136 A, LipJ-M139Q, LipJ-G136 A/M139Q) and library of iterative saturation mutagenesis (H110/NNK codon degeneracy [53]. Mutations are shown underlined in **bold**.

2.5. Activity assays

Lipolytic activity of crude cell extracts from LipJ variants was analysed by measuring the release of MUF (methylumbelliferone, Sigma-Aldrich) from MUF-derivative fatty acid (C_4, C_7 and C_{18}) substrates (Sigma-Aldrich) prepared in ethylene glycol methyl ester (EGME) at 25 mM, using a Varian Cary Eclipse spectrofluorometer (Agilent Technologies) equipped with a microplate reader, as previously reported [51,55]. One unit of activity was defined as the amount of enzyme that released 1 μmol of MUF per minute under the assay conditions used. All determinations of enzyme activity were performed after two replicas of triplicates (6 determinations per sample). Values correspond to the average ± standard deviation. Optimum temperature of LipJ variants was determined by analysis of the activity over a range from 20 to 99 °C at pH 7, using 0.5 mM MUF-derivatives as substrates [51,55]. To evaluate the effect of several ions on activity, assays were performed on MUF-heptanoate in the presence of their corresponding chlorides (Al^{+3}, Ba^{+2}, Ca^{+2}, Cu^{+2}, Fe^{+2}, Hg^{+2}, K^{+}, Li^{+2}, Mg^{+2}, Mn^{+2}, Na^{+}, NH_4^{+}, Zn^{+2}), used at 1 and 10 mM. Residual activity was measured at 50 °C and 80 °C and pH 7 using a conventional assay on MUF-heptanoate, and expressed as a percentage of activity without ions. Kinetic parameters of LipJ and selected variants (*Vmax* and *Km*) were determined at 30 °C and 50 °C on MUF-butyrate and MUF-heptanoate by fitting hyperbolic Michaelis-Menten curves with Graph Pad software.

2.6. Bioinformatics

BLAST searches were routinely performed for DNA or protein sequence analysis and to retrieve identity and similarity percentages by pairwise alignment [56]. Multiple sequence alignments were obtained using T-Coffee (http://tcoffee.crg.cat/) [57] or ClustalO (http://www.ebi.ac.uk/Tools/msa/clustalo/) [58]. BioEdit v.7.0.1 [59] was used for consensus pattern determination. Identification of putative signal peptide [60] was performed through SignalP versions 3.0 or 4.1 (http://www.cbs.dtu.dk/services/SignalP/). ExPASy proteomics server was used to analyse the physico-chemical parameters (ProtParam tool; http://web.expasy.org/protparam/), and to predict isoelectric point and molecular mass of each enzyme [61]. ProDom (http://prodom.prabi.fr/prodom/), Pfam (http://pfam.xfam.org/), and InterProScan 5.2 (http://www.ebi.ac.uk/interpro/) were used for domain identification [62], and a Hidden Markov Model was created with HMMER (http://www.ebi.ac.uk/Tools/hmmer/) for detection of conserved protein domains [63]. The 3D model and secondary structure prediction of LipJ variants was obtained from Phyre2 (http://www.sbg.bio.ic.ac.uk/˜phyre2/html/page.cgi?id=index) [64] and Swiss Model Server [65] with default settings, using the closest template proteins with available 3D structure: *Pelosinus fermentans* lipase PfL1 (pdb *5AH0*, 93% coverage, 56% identity) [37] and *Geobacillus stearothermophilus* lipase L1 (pdb *1KU0*, 92% coverage, 49% identity) [38]. Model validation was done with Phyre2 server, and Pymol Molecular Graphics System, Version 1.5.0.4, Schrödinger, LLC (http://www.pymol.org) was used for visualization, superimposition, identification of conserved amino acids or ion coordinating residues and cavities, and for flexibility analysis through the B-Putty function. Docking with MUF-derivative substrates was performed using Patch Dock tool [66]. Several binding variations were acquired for each interaction, and the final models chosen for analysis were selected taking into consideration two criteria: (*i*) the substrate should be correctly positioned inside the pocket constituted by the catalytic triad and the oxyanion hole motif, and (*ii*) a feasible interaction between catalytic serine (S^{138}) and the tested substrate should occur. From an average of ten docking models generated for each substrate on each enzyme molecule, only those covering these criteria were selected and used for further analysis. Pdbs for the substrates were obtained from PubChem (https://pubchem.ncbi.nlm.nih.gov/). Mutational sensitivity was analyzed with the tool SuSPect (www.sbg.bio.ic.ac.uk/suspect) [67], and *in silico* ligand pocket was detected in wild type and mutant variants using fpocket2 [68].

3. Results and discussion

3.1. Conserved residues in family I.5 lipases

There are some common features in terms of conserved amino acids or sequence motifs, which are shared by most family I.5 lipases. In most cases these conserved patterns include the presence of a cavity for Zn^{2+} coordination, probably involved in the stabilization of the enzyme. In fact, metal coordination, described to have a relevant role in the regulation of the lid opening of thermophilic lipases, has also been proposed as an important factor for the general thermostability of proteins [42,47,69]. This is the case for *Geobacillus stearothermophilus* L1, T1 or T6 lipases [38,39,69], *Geobacillus thermocatenulatus* BTL2 lipase [40], or *Pelosinus fermentans* [37] and *Clostridium botulinum* [41,42,47] esterases, all of them containing specific residues involved in Zn^{2+} coordination (D61, H81, H87 and D238 in *Geobacillus stearothermophilus* L1 lipase; D90, H110, H116 and D267 including the signal peptide) [38]. These ion binding traits have been described to directly participate in temperature-dependent enzyme activation [38,42], in association with large structure rearrangements of helices α-6 and α-7 [39,69] and possibly also helix α-5 [46]. Such structural dynamics of around 70 amino acids involving the concerted movement of the lid for masking or unmasking the active site [39] might drastically affect the accessibility to the active site depending on the hydrophobicity and length of the substrate [43], or by favouring enzyme dimerization, as recently suggested [36,44]. Moreover, presence of two Trp residues (W61 and W212 in BTL2 lipase; W89 and W240 including the signal peptide) flanking the Zn^{2+}-binding amino acids has also been reported to play a critical role in the Zn^{2+} tetrahedral coordination site for enhancing lipase activity at high temperatures [40].

Table 2
Comparison of LipJ with specific motifs of the closest family I.5 lipases.

DATA	Comments	LipJ *Bacillus* JR3	EstA *C. botulinum*	PfL1 *P. fermentans*	T6 *B. stearothermophilus*	T1 *G. zalihae*	L1 *B. stearothermophilus*	BTL2 *G. thermocatenulatus*
pdb		3D Model	*5ah1*	*5ah0*	*4 × 7b*	*2dsn*	*1ku0*	*2w22*
UniProt	Accession	A0A1C8Y7C2	A5I055	A0A0A0YMQ9	Q93 A71	Q842J9	O66015	Q59260
Identity/coverage (%)		100/100	46/92	53/92	46/92	48/92	49/92	48/92
Signal peptide	Putative for LipJ	(1-28)	1-30	NO	1-30	1-28	1-29	1-28
Catalytic residues	Catalytic triad	S138	S210	S114	S143	S141	S142	S142
		D341	D412	D315	D347	D345	D346	D346
		H380	H454	H357	H388	H386	H387	H387
Pentapeptide	Motif	**G**HS**M**G	**G**HS**M**G	AHS**M**G	AHSQG	AHSQG	AHSQG	AHSQG
Oxyanion hole	Predicted for LipJ	PIILVNGFAG	PIVLVHGFMG	PIVLVHGFMG	PIVLLHGFTG	PIVLLHGFTG	PIVLLHGFTG	PIVLLHGFTG
Zn^{2+} coordination site	Zn^{2+} tetrahedral coordination residues	D86	D158	D56	D91	D89	D90	D90
		H106	H178	H76	H111	H109	H110	H110
		H112	H184	H82	H117	H115	H116	H116
		D260	D330	D233	D268	D266	D267	D267
Possibly involved Trp	Hydrophobic. Restrict flexibility of the site	W85	W157	W55	W90	W88	W89	W89
		W232	W302	W205	W241	W239	W240	W240
Extra interest in Zn^{2+} cavity (related to *Clostridium* EstA)	Suggested thermal activity improvement	**H110**	**F182**	**K80**	**H115**	**H113**	**D114**	**H114**
		W232	W302	W205	W241	W239	W240	W240
		W85	W157	W55	W90	W88	W89	W89
		S155	S227	S131	S160	S158	S159	S159
		S83	S155	S53	S88	S86	S87	S87
Relevant in helix α-7 (related to *Clostridium* EstA)	Extra Zn^{2+} coordination	D260	D330	D233	D268	D266	D267	D267
		Q231	Q301	Q204	Q240	Q238	Q239	Q239
		Putative H-bond with D86	H-bond with D158					
Relevant in helix α-6 (related to *Clostridium* EstA)	Salt bridges in *Clostridium* Est1 with Q93 & R161	K228	K298	K201	K237	K235	K236	K236
		D230	D300	D203	D239	D237	D238	D238
	Suggested extra salt bridges	K54	K126	K24	K58	K56	K57	K57
		R117	R189	R87	R122	R120	R121	R121
	For putative PBAT degradation	S83	S155	S53	S88	S86	S87	S87
		Y102	Y174	Y72	Y107	Y105	Y106	Y106
Ca^{2+} binding		G315	Crystal with K^+	Crystal with K^+	G316	G314	G315	G315
		Other residues not found			E390	E388	E389	E389
					D395	D393	D394	D395
					P396	P394	P395	P396
Cap domain(s)	Predicted for LipJ	196-200	266-333	178-255	207-222		223-250	197-267
			364-408	282-328				
Helix α-6	Predicted for LipJ	201-217	263-267	167-170			204-223	205-220 (closed) 192-225 (open)
Helix α-7	Predictede for LipJ	243-250	270-285	173-190			249-258	250-264
Substrate		C4	C2	C8	C12	C12	C3-C18	C8
Temperature (ºC)		30	50	50	40	70	68	60
4D structure	Putative for LipJ	Monomer	Monomer	Dimer	Monomer	Dimer	Monomer	Monomer
Comments		No interfacial activation observed	Lid + Zn^{2+} cavity sorrounded by an extra domain	Lid + Zn^{2+} cavity sorrounded by an extra domain	Lid located at so called α-9 helix	Lid in α-6 and α-7 helices for interfacial activation coupled with temperature switch activation	Suggested Lid opening not mediated by T but by substrate	2 Lids at α-6 and α-7 helices + Zn^{2+}
References		[35] This work	[41,42]	[37]	[70]	[69,78]	[38,39]	[39,40]

Most relevant residues, structures and patterns of the closest family I.5 thermophilic bacterial lipases, compared with LipJ. For proper comparison, residue numbering of all enzymes includes the signal peptide.

Taking into consideration the previous data, we carefully analysed the sequence/structure of LipJ and tried to find differences in the most significant residues putatively involved in enzyme activation of family I.5 lipases. Table 2 shows the comparison details between LipJ and the closest crystalized family I.5 lipases in terms of significant residues for activity. Although we expected to find one or more relevant amino acid substitutions at some of these important positions in LipJ, we had to conclude that all those amino acids described to be directly involved in thermophilicity could indeed be found on LipJ sequence. Moreover, all conserved residues maintain the same position and distance in LipJ than their counterparts in the other lipases/esterases studied. The four Zn^{2+}-coordination residues D86, H106, H112, D260 plus tryptophans W85 and W232 were found in both, the amino acid sequence plus the 3D model structure of LipJ, included in an extra Zn-domain typical for members of family I.5 lipases [37,40–42,70,71]. Moreover, other residues suggested to be relevant on α-6 and α-7 helices, putatively involved in extra Zn^{2+} coordination or for the establishment of stabilizing salt bridges, were also found at the corresponding positions in LipJ except for residue H110, which was also a different amino acid in the closest *P. fermentans* and *C. botulinum* lipases (Table 2). Interestingly, the corresponding residue in *C. botulinum* EstA (F182) was recently modified, and mutant F182Y resulted in a variant with increased thermophilicity [42], suggesting that this amino acid might indeed play a role in providing improved properties.

3.2. NNK library of residue H110

Being amino acid H110 the only significantly different residue found between the closest crystalized family I.5 lipases and LipJ, and taking into consideration the effect observed after F182 modification in *C. botulinum* EstA [42], we investigated the possibility of obtaining a better LipJ variant after modification of residue H110. For this purpose we constructed an NNK codon degeneracy library, and analysed both, substrate specificity and temperature of the variants obtained. Out of more than 100 recombinant clones analysed, those showing the highest fluorescence when tested on paper assays [50,51] on MUF-butyrate or MUF-heptanoate (not shown) were selected for further sequencing and activity determination. Among the mutants analysed, those having acquired an asparagine at position 110 displayed more activity than wild type LipJ on both, MUF-butyrate and MUF-heptanoate (Fig. 1). When assayed at 30 °C on MUF-butyrate, activity of mutant H110 N was 5 times higher than that of wild type LipJ (50.3 U/g and 10 U/g, respectively), whereas a 12.7-fold increased activity was registered on MUF-heptanoate (76.2 U/g versus 6.04 U/g, respectively), indicating that asparagine contributes to a shift in substrate specificity, making the reaction more favourable for longer chain-length substrates. However, a moderate 3-fold increase of activity of mutant H110 N on MUF-heptanoate was observed when assays were performed at 60 °C (15.3 U/g versus 5 U/g, respectively), suggesting that asparagine does indeed contribute to modify the enzyme's substrate specificity but it does not have a great impact on thermophilicity, contrarily to what was expected from the previously reported results obtained for *C. botulinum* esterase [42]. However, analysis of the structural flexibility of a validated 3D model structure of mutant H110 N and wild type LipJ through the B-Putty function of PyMol (Fig. 2) revealed a more compact structure for mutant H110 N (Fig. 2A) compared to that of wild type LipJ (Fig. 2B), evidencing that the presence of an asparagine at position 110 affects the global flexibility of the enzyme and suggests that mutant H110 N is well equipped for supporting higher temperatures than wild type LipJ. On the other hand, *in silico* analysis of the 3D model structure of H110 N showed that presence of an asparagine at position 110 could produce different polar bonds or additional Zn^{2+} interactions in the tetrahedral coordination area that might be responsible for the changes in substrate specificity observed (Fig. 3). Thus, while residue H110 of wild type LipJ (Fig. 3A) establishes a single polar interaction with the neighbouring histidine H106 (distance 3.09 Å), substitution by an

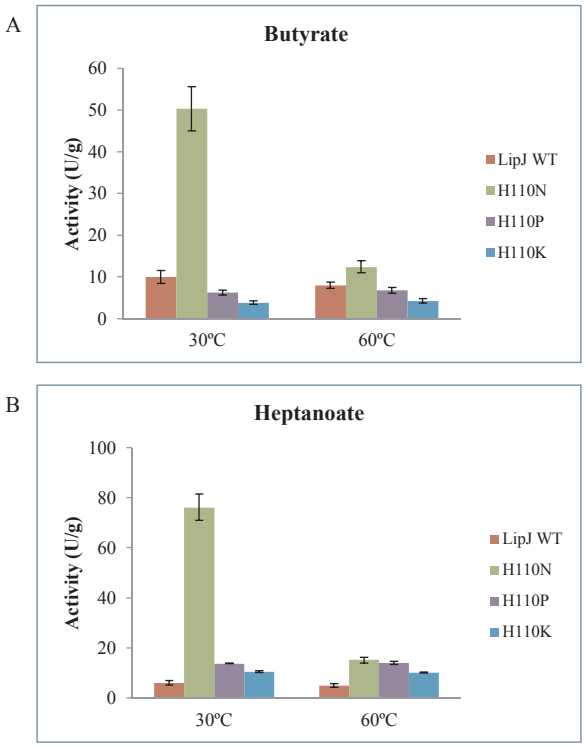

Fig. 1. Activity comparison for three selected clones bearing a different amino acid at position 110. Clone H110 N, bearing an asparagine, showed the highest activity on short and longer chain-length substrates at both, 30 and 60 °C. Clones H110 P and H110 K contain a proline and a lysine at position 110, respectively. Values are the mean of two replicas with triplicate samples.

asparagine (Fig. 3B) allows two polar contacts with amino acid H106 (distances 2.77 and 3.12 Å), maintaining the same angle. Being histidine 106 one of the major residues involved in Zn^{2+} coordination, we also measured the effect of the presence of an asparagine at position 110 on the interactions driven by H106. Interestingly, we found that whereas in wild type LipJ (Fig. 3A) amino acid H106 displayed two polar interactions with the Zn^{2+} ion (distances 3.14 and 3.29 Å), only one interaction occurs between H106 and Zn^{2+} (distance 3.12 Å) in mutant H110 N (Fig. 3B). This reduced coordination interaction might produce a relaxation of the tetrahedral Zn-binding area that could in turn cause a modification of the global enzyme structure, thus rendering an enzyme variant with a better configuration for accepting longer chain substrates, without causing a relevant effect on temperature tolerance. At this respect, molecular docking analysis confirmed a better fit of MUF-heptanoate on the catalytic cleft of mutant H110 N than in wild type LipJ (Fig. 3C). This hypothesis is in agreement with previous results showing that tightly bound Zn^{2+} appears to control the lipase activation and stabilization of the enzyme, as happens for L1 lipase [72].

3.3. Recovery of additional family I.5 lipase common traits

In a different approach, a detailed amino acid sequence analysis of LipJ was performed, evidencing that the enzyme bears two pentapeptides, a proximal motif –**G**H**S**M**G**– distinct from that of most crystalized family I.5 thermophilic lipases (**A**H**SQG**) [31] but similar to that of *Actinibacillus thermoaerophilus* LipAT [36], and an additional pentapeptide-like motif –**AA**S**F**G–, also found in other carboxylesterases and suggested not to be involved in the catalytic activity [35,55]. We also found a probably non-functional signal peptide, with an altered residue (E27) at the predicted cleavage site that might prevent the correct processing and secretion of LipJ. As the enzyme was cloned from a mesophilic bacterial strain isolated from a former volcanic soil,

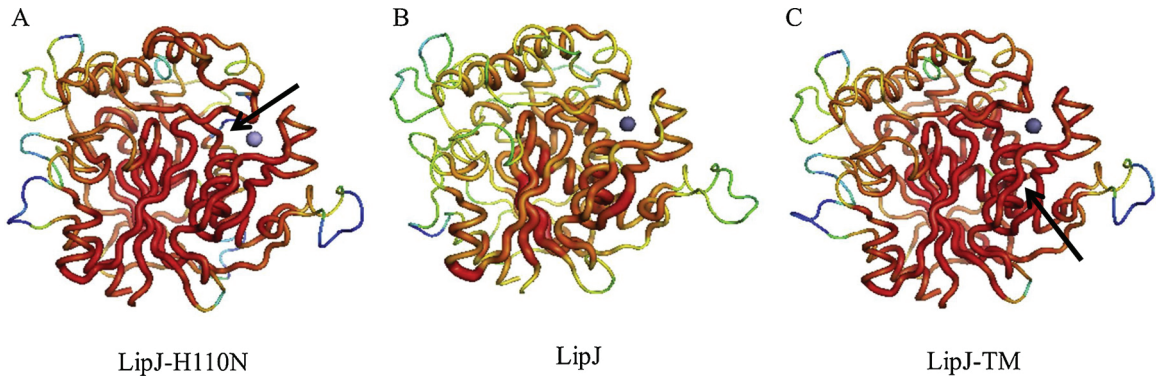

Fig. 2. B-putty flexibility analysis of the validated 3D model structures of LipJ and selected variants H110 N and LipJ-TM. Wild type LipJ (B) displays significantly higher flexibility than mutants H110 N (A) and LipJ-TM (C), both appearing as more compact structures and therefore, better equipped to tolerate higher temperatures. In agreement with the results obtained, loss of polar interactions of H106 with Zn^{2+} ion (grey sphere) in mutant H110 N generates a loosening in the Zn-binding environment (A, arrow) that could account for a better fitting of longer chain-length substrates. On the other hand, mutant LipJ-TM shows a more compact structure close to the Zn-binding region (C, arrow), in agreement with the increased thermophilicity observed (For interpretation of the references to colour in this figure legend, the reader is referred to the web version of this article).

displaying an interesting lipase activity at extremely high temperatures −80 to 100 °C−, we hypothesized that the strain and part of its catalytic machinery could have evolved towards a mesophilic mode when the harsh volcanic conditions disappeared and the environment became more benign [35]. This would justify the finding of a carboxylesterase showing many traits of thermophilic lipases but displaying a typically mesophilic behaviour, with preference for short chain-length substrates. Thus, in order to go back to the putative ancestral condition of LipJ included in family I.5 lipases, we analysed the mutational sensitivity of the described features of LipJ at both, the signal peptide region and the predicted catalytic pentapeptide motif, to avoid possible effects on activity. We then applied a directed mutagenesis approach based on producing single point mutations over those residues that might hypothetically be involved in the catalytic behaviour and secretion of LipJ; that is, changing the acidic residue E27 at the predicted cleavage site of the putative signal peptide of LipJ to facilitate enzyme processing and secretion, and substituting amino acids G136 and M139 of LipJ pentapeptide by those most frequently found in family I.5 enzymes (although some thermophilic lipases have also been reported to bear a GXSXG pentapeptide motif) [33,36].

As stated at the Materials and Methods section, three single mutants (E27 A, G136 A and M139Q), a double mutant –LipJ-DM– at the conserved pentapeptide (G136 A/M139Q), and a triple mutant –LipJ-TM– (E27 A/G136 A/M139Q) were obtained for further biochemical characterization. *In silico* analysis of these single point mutations showed no apparent impact on the protein structure and enzymatic function, and pointed to residue H137, located at the pentapeptide motif, as the amino acid most sensitive to mutation [67].

3.4. Activity determination of LipJ mutants

In order to evaluate differences in both, thermophilicity and substrate specificity of LipJ variants compared to the wild type enzyme, activity analysis were performed at 30 °C and 80 °C on three different

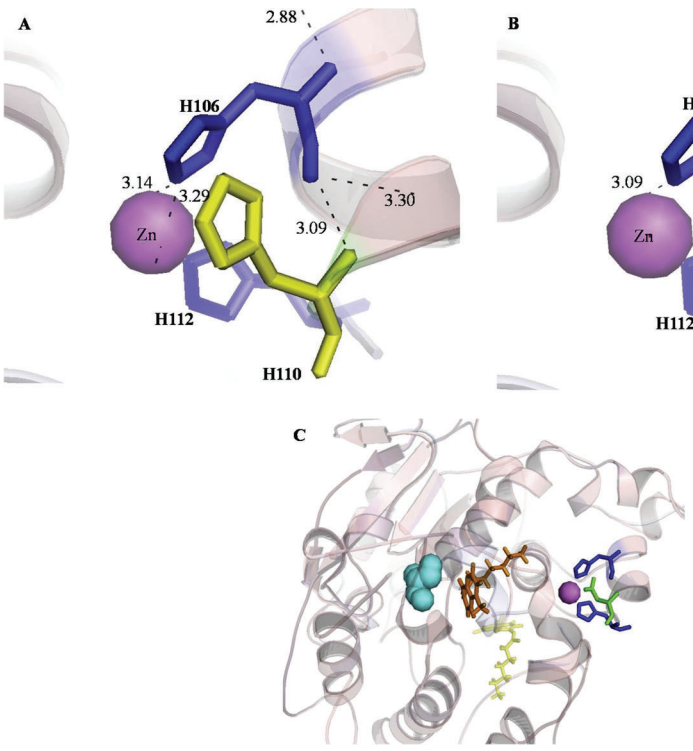

Fig. 3. 3D model structure of variant LipJ-H110 N (light pink) superimposed to LipJ (pale grey). Catalytic serine (C) and Zn^{2+} ion (A,B,C) are shown as cyan and violet spheres, respectively. Histidines 106 and 112, involved in Zn^{2+} coordination, are shown as blue sticks (A,B). Histidine 110 in wild type LipJ (A) and asparagine at position 110 in mutant H110 N (B) are depicted as yellow and green sticks, respectively. Polar interactions of histidine 106 affecting Zn^{2+} environment in wild type LipJ (A) and in mutant H110 N (B) are shown as dashed lines, with the distances indicated. (C) Docking of MUF-heptanoate with the two superimposed enzymes, where MUF-heptanoate is depicted as orange sticks for the docking with variant H110 N, and as pale yellow sticks for the docking with wild type LipJ (For interpretation of the references to colour in this figure legend, the reader is referred to the web version of this article).

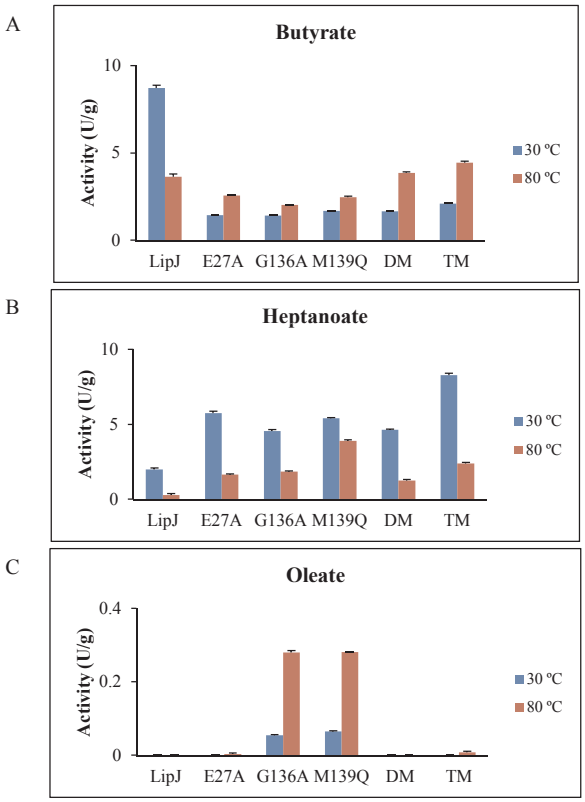

Fig. 4. Determination of activity of LipJ and the site directed mutagenesis variants obtained. Assays were performed on short, medium and long chain-length MUF-derivative substrates at 30 and 80 °C. (A) MUF-butyrate; (B) MUF-heptanoate; (C) MUF-oleate. Values are the mean of two replicas with triplicate samples.

chain-length substrates (C_4, C_7 and C_{18}) (Fig. 4). As expected from previous studies [35], wild type LipJ displayed the highest activity on MUF-butyrate at 30 °C (8.7 U/g) (Fig. 4A), showing lower or negligible activity on longer chain-length substrates (Fig. 4B, C). Interestingly, all LipJ variants displayed a remarkable shift in substrate specificity towards longer chain-length substrates, with maximum activity on MUF-heptanoate at both, 30 and 80 °C, and a remarkable 4.6-fold activity increase at 30 °C shown by the triple mutant LipJ-TM on MUF-heptanoate (8.3 U/g) (Fig. 4B).This activity improvement reflects indeed a synergistic effect of mutation E27 A over mutant LipJ-DM, as supported by the activity increase shown by LipJ-TM when compared to both, the single and double mutants.

These observations suggest that not only the catalytic serine (S^{138}) environment but also the N-terminal alpha helix constituted by residues 1–26 are directly involved in substrate accommodation or catalysis. At this respect, previous *in silico* studies ambiguously predicted a putative cleavage site for LipJ signal peptide [35], which indeed seems not being properly processed, thus allowing the N-terminal peptide to actively participate in substrate accommodation for hydrolysis (Fig. 4B). Therefore, the mesophilic behaviour of wild type LipJ might be explained by an evolutive adaptation event derived from its more recent location inside the cell, where the enzyme has not been exposed to environmental condition oscillations or temperature-related damage, and were hydrophobic, long chain-length substrates are less available due to the cell membrane barrier [73], thus losing some of its ancestral features [35].

The highest activity at 80 °C on MUF-heptanoate was achieved by single mutant M139Q (3.9 U/g) (Fig. 4B), suggesting that substitution of a Met by a Gln at this position of the pentapeptide may be determinant for temperature-dependent enzyme activation on longer chain-length substrates. This fact was confirmed when mutant M139Q was assayed on MUF-oleate at 80 °C (0.28 U/g), showing a 37-fold activity increase with respect to LipJ (0.0075 U/g), tested under the same conditions (Fig. 4C). Although Met and Gln are similar in size, their degree of hydrophobicity is different [74], a feature that could account for the improvement of activity at high temperature and on longer chain-length substrates. Moreover, this effect might be related to important changes in enzyme activity that can occur when Gln is located on a solvent-accessible surface, as previously reported [75].

In general, the overall activity of LipJ variants was very low on MUF-oleate (Fig. 4C), with LipJ and some of the mutants showing negligible activity at both temperatures. Only the single pentapeptide mutants G136 A and M139Q displayed scarce activity on this substrate, which was significantly higher at 80 °C. For mutant G136 A, both Ala and Gly are similar small amino acids in size, with Ala being a hydrophobic, aliphatic amino acid that might contribute to stabilizing the structure, whereas in non-polar Gly, the side-chain methyl group is absent, thus facilitating the accommodation of hydrophobic substrates, a fact that would explain the substrate specificity shift observed. In fact, a good correlation has been described between the relative stabilizing effects of Ala and Gly with the total change in solvent-accessible hydrophobic surface area of the folded protein on mutations of Gly to Ala [76], which could be the cause for the stabilization of the active site loop conformation in LipJ [77] as happens in *P. fermentans* lipase [37], and which could also account for an improved accessibility of longer chain, more hydrophobic substrates to the catalytic Ser^{138} residue of these LipJ variants.

In order to check the former hypothesis, we performed *in silico* molecular docking studies for LipJ-TM using MUF-butyrate, MUF-heptanoate and MUF-oleate, as representative substrates for short-, mid- and long-chain-length fatty acids (Fig. 5). For such purpose, the 3D model structure of the triple mutant was constructed and validated for comparison with wild type LipJ. In agreement with the experimental results obtained above, variant LipJ-TM would generate more space in the vicinity of the active site to accommodate MUF-heptanoate (Fig. 5D) than wild type LipJ (Fig. 5C), whereas the docking positioning with MUF-butyrate appeared similarly favourable for variant LipJ-TM (Fig. 5B) and wild type LipJ (Fig. 5A). On the contrary, MUF-oleate would neither enter nor accommodate in the active site of any of the two enzyme variants studied. In fact, the substrate binding pocket occurring in both, LipJ and LipJ-TM might be too buried (Fig. 5E, F) to tightly accommodate C18 substrates, which would abandon the molecule without being catalysed.

In addition to the previous observations, all site directed mutants obtained displayed not only a shift in substrate specificity but also an increased tolerance to higher temperatures (Fig. 4), suggesting that recovery of the canonical pentapeptide signature (AHSQG) of thermophilic lipases, and the most probable cleavage of the N-terminal signal peptide helix in the protein do indeed contribute to a significant increase in thermophilicity, coupled to a shift towards longer chain-length substrates.

3.5. Activity profile of selected LipJ variants

Among the variants obtained, double mutant LipJ-DM and the triple mutant LipJ-TM were selected for further characterization due to their increased activity at both, 30 and 80 °C on MUF-heptanoate, a longer chain-length substrate on which wild type LipJ displayed much lower activity at high temperature. Therefore, cell extracts of variants LipJ-DM and LipJ-TM plus wild type control LipJ were obtained and their kinetics and activity profile were assayed on MUF-heptanoate.

As shown in Fig. 6A, a significant activity increase was observed for LipJ-DM and LipJ-TM at 50 °C when assayed on MUF-heptanoate whereas, as expected, wild type LipJ displayed maximum activity at 30 °C, with a clear tendency to loose activity at higher temperatures. This pattern is in agreement with the previous results obtained on assays performed on MUF-heptanoate at 30 and 80 °C (Fig. 4B), and

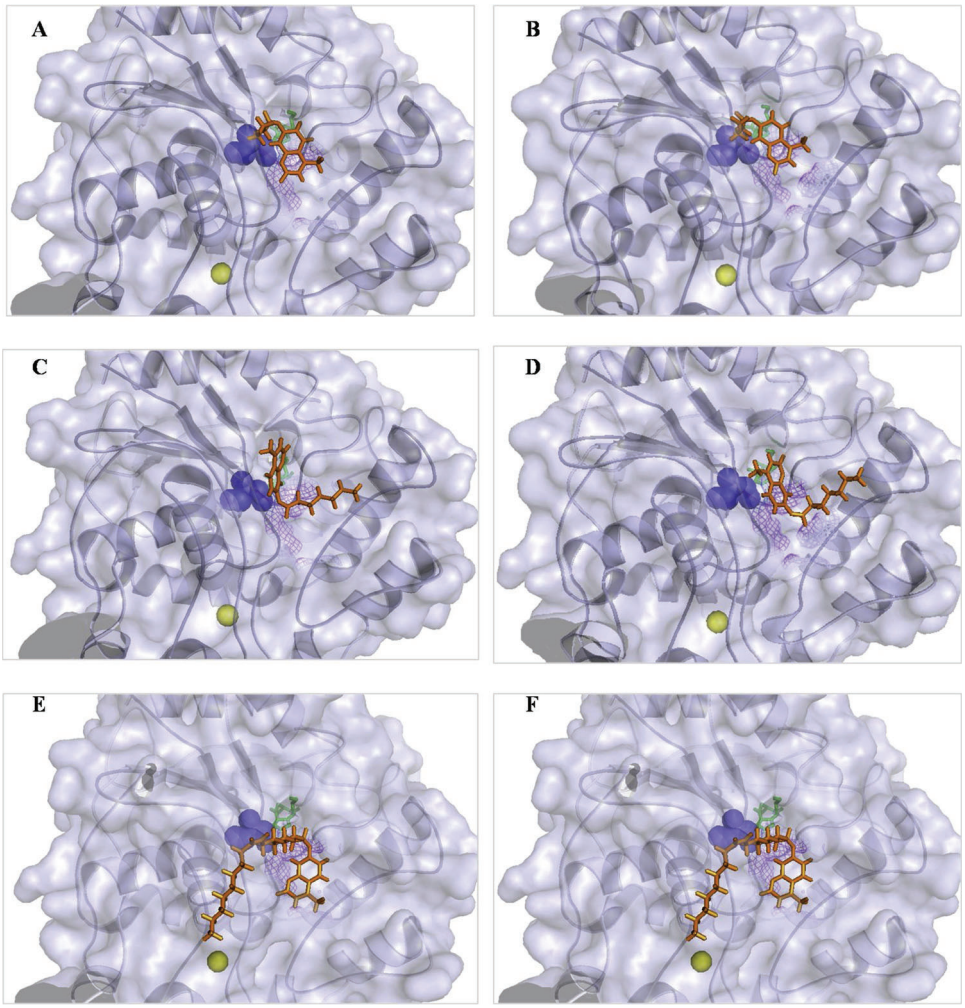

Fig. 5. Docking analysis of short (MUF-butyrate; A, B), medium (MUF-heptanoate, C, D) and long (MUF-oleate, E, F) chain-length substrates bound to the 3D validated model structures of wild type LipJ (A, C, E) and the triple mutant LipJ-TM (B, D, F). Catalytic serine and the Zn^{2+} ion are depicted as blue and yellow spheres, respectively. Other amino acids of the catalytic triad appear as green sticks, and the oxyanion hole is depicted as a purple mesh. MUF-derivative substrates are highlighted in orange (For interpretation of the references to colour in this figure legend, the reader is referred to the web version of this article).

evidences that the mutations introduced in LipJ are not only responsible for a substrate specificity shift but also for the temperature activity increase recorded. They also confirm the synergistic effect of mutation E27 A at the signal peptide, as LipJ-TM displays double specific activity compared to that of LipJ-DM, containing only two residue mutations at the pentapeptide. The increase in thermophilicity observed was confirmed for mutant LipJ-TM through B-Putty analysis of a validated 3D model structure. As shown in Fig. 2, the whole structure of wild type LipJ (Fig. 2B) appears much more flexible than that of mutant LipJ-TM (Fig. 2C), where a higher degree of compactness appears close to the Zn^{2+} environment, confirming the observed higher tolerance of the triple mutant to increased temperatures.

Analysis of the kinetics behaviour of these enzyme variants revealed that all cell extracts displayed the same Michaelis-Menten kinetics profile when assayed on MUF-derivatives, showing no interfacial activation (Fig. 6B,C). In agreement with previous results, a significant difference could be detected when the kinetics of wild-type LipJ, LipJ-DM and LipJ-TM were tested on different chain-length substrates at the optimum temperature for each enzyme variant (Fig. 6B,C). While LipJ displayed a better behaviour on short chain substrates and at moderate temperature (30 °C) (Fig. 6B), LipJ-TM showed much better activity on MUF-heptanoate at 50 °C (Fig. 6C), previously shown to be its optimum temperature (Fig. 6A). Vmax/Km values for wild type LipJ and variant LipJ-TM were 5.21/45.9 and 0.9/60.3, respectively on MUF-butyrate at 30 °C, and 114.6/141.1 and 86.4/113.9, respectively on MUF-hepatonate at 50 °C. Therefore, an overall improvement in the catalytic properties of LipJ-TM was observed with respect to those of wild-type LipJ when tested at 50 °C on MUF-heptanoate (Fig. 6C).

As reported above, most family I.5 lipases bind Zn^{2+} or other ions, which have been proposed to be involved in temperature-dependent activation or substrate accommodation [38,39,42]. From previous *in silico* analysis we reported that LipJ displays many traits of thermophilic lipases, including the conserved structure and folding, and the presence of putative cavities for accepting metal ions. A substantial gain in LipJ activity at temperatures over 60 °C was achieved in a previous work when the reaction mix was supplemented with 20 mM Ca^{2+}, but on the contrary, presence of Zn^{2+} in the reaction mix resulted in a complete loss of activity; only Ba^{2+} and Mn^{2+} contributed to increase activity of LipJ at 60 °C [35]. To further investigate if any ions could improve the thermophilic activity of selected LipJ-TM variant, activity in the presence of several ions in the reaction mix was tested at 50 and 80 °C. As shown in Fig. 7, Mn^{2+} displayed a significant 2 and 2.5-fold activity increase at 50 (Fig. 7A) and 80 °C (Fig. 7B), respectively when assayed at 10 mM. Like for wild type LipJ, presence of Zn^{2+} in the reaction mix caused inhibition of LipJ-TM, an effect that was even more dramatic when tested at 80 °C. This suggests that probably other residues different from those substituted in LipJ-TM variant would be more directly involved in Zn^{2+}-dependent enzyme temperature activation. Further

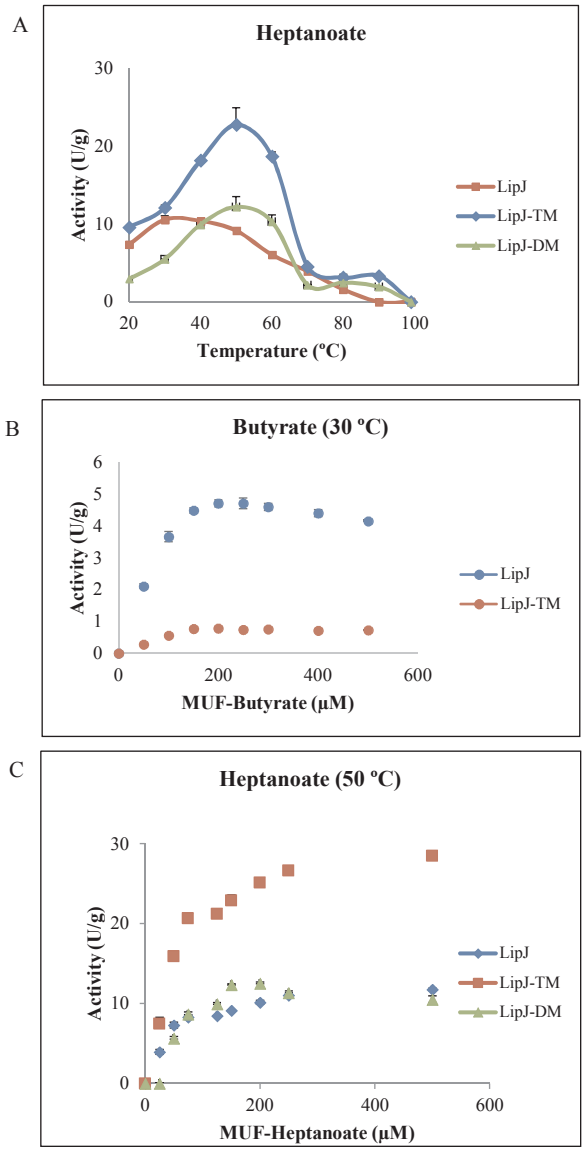

Fig. 6. Temperature (A) and kinetics (B,C) profile of wild type LipJ and variants LipJ-DM and LipJ-TM. (A) Assays for optimum temperature determination were performed on MUF-heptanoate, whereas MUF-butyrate (B) and MUF-heptanoate (C) were used for determination of the kinetic parameters on two different chain-length substrates, measured at the optimum temperature for each variant. Values are the mean of two replicas performed in triplicate.

assays, mostly based on random mutagenesis, would be required to identify such residues, as previously happened for *C. botulinum* EstA, the closest family I.5 carboxylesterase structure with a non-canonical pentapeptide studied and modified to date [41,42,47].

4. Conclusions

Mesophilic *Bacillus* sp. JR3 LipJ esterase, clustering in a differentiated clade among family I.5 lipases [35], was engineered here to recover the essential traits of bacterial family I.5 lipases. Several LipJ variants were obtained using either QuikChange site-directed mutagenesis or iterative saturation mutagenesis through an NNK degeneracy library at position H110, predicted to be putatively involved in Zn^{2+} coordination and stabilization of the lid structure [42,47]. The results obtained so far clearly demonstrate that mesophilic esterase LipJ has satisfactorily been converted into a more specific and thermophilic lipase through modification of those residues described to provide

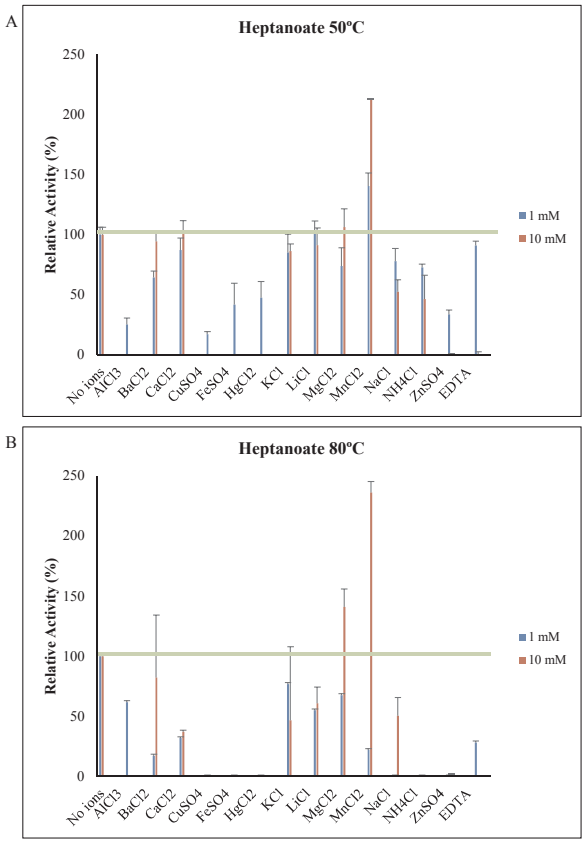

Fig. 7. Effect of several ions and EDTA on the activity of variant LipJ-TM. Assays were performed in duplicate at 50 °C (A) and 80 °C (B).

essential features from family I.5 lipases. In particular, the triple mutant with modifications at the N-terminal region and the pentapeptide, and variant at the Zn^{2+} coordination site, LipJ-H110 N, displayed an interesting shift in substrate specificity towards MUF-heptanoate and a significant increase in optimum temperature, greatly enhanced by the presence of Mn^{2+}. This positions the newly obtained variants as good candidates for further investigation and application.

Funding

This work was supported by the Scientific and Technological Research Council (MINECO, Spain), grants CTQ2017-84966-C2-2-R, CTQ2014-59632-R, Pla de Recerca de Catalunya, grant 2014SGR-534 00327, PCI-AECID projectA203563511, and Generalitat de Catalunya to the “Xarxa de Referència en Biotecnologia” (XRB).

Ethical statement

This article does not contain any studies with human participants or animals performed by any of the authors.

Conflict of interest

All authors declare that they have no conflict of interest.

Acknowledgements

We thank the Serveis Cientifico-Tècnics of the University of Barcelona for technical support in sequencing. CB acknowledges an APIF pre-doctoral grant from the University of Barcelona.

References

[1] U.T. Bornscheuer, Microbial carboxyl esterases: classification, properties and application in biocatalysis, FEMS Microbiol. Rev. 26 (2002) 73–81, https://doi.org/10.1111/j.1574-6976.2002.tb00599.x.

[2] K.E. Jaeger, B.W. Dijkstra, M.T. Reetz, Bacterial biocatalysts: molecular biology, three-dimensional structures, and biotechnological applications of lipases, Annu. Rev. Microbiol. 53 (1999) 315, https://doi.org/10.1146/annurev.micro.53.1.315.

[3] M. Ferrer, R. Bargiela, M. Martínez-Martínez, J. Mir, R. Koch, O.V. Golyshina, P.N. Golyshin, Biodiversity for biocatalysis: a review of the α/β-hydrolase fold superfamily of esterases-lipases discovered in metagenomes, Biocatal. Biotransform. 33 (2015) 235–249, https://doi.org/10.3109/10242422.2016.1151416.

[4] G. Angajala, P. Pavan, R. Subashini, Lipases: an overview of its current challenges and prospectives in the revolution of biocatalysis, Biocatal. Agric. Biotechnol. 7 (2016) 257–270, https://doi.org/10.1016/j.bcab.2016.07.001.

[5] T. Drepper, T. Eggert, W. Hummel, C. Leggewie, M. Pohl, F. Rosenau, S. Wilhelm, K.-E. Jaeger, Novel biocatalysts for white biotechnology, Biotechnol. J. 1 (2006) 777–786.

[6] K.-E. Jaeger, M.T. Reetz, Microbial lipases form versatile tools for biotechnology, Trends Biotechnol. 16 (1998) 396–403.

[7] R. Gupta, A. Kumari, P. Syal, Y. Singh, Molecular and functional diversity of yeast and fungal lipases: their role in biotechnology and cellular physiology, Prog. Lipid Res. 57 (2015) 40–54.

[8] R. Gupta, N. Gupta, P. Rathi, Bacterial lipases: an overview of production, purification and biochemical properties, Appl. Microbiol. Biotechnol. 64 (2004) 763–781.

[9] G. Antranikian, U.T. Bornscheuer, A. Liese, Highlights in biocatalysis, ChemCatChem 2 (2010) 879–880, https://doi.org/10.1002/cctc.201000228.

[10] U.T. Bornscheuer, R.J. Kazlauskas, Hydrolases in Organic Synthesis: Regio- and Stereoselective Biotransformations, Wiley-VCH, 2006.

[11] M.T. Reetz, Biocatalysis in organic chemistry and biotechnology: past, present, and future, J. Am. Chem. Soc. 135 (2013) 12480–12496, https://doi.org/10.1021/ja405051f.

[12] R. Kourist, J. González-Sabín, B. Siebers, M. Julsing, Editorial: applied microbiology for chemical syntheses, Front. Microbiol. 8 (2017) 1931, https://doi.org/10.3389/fmicb.2017.01931.

[13] M. Kapoor, M.N. Gupta, Lipase promiscuity and its biochemical applications, Process Biochem. 47 (2012) 555–569, https://doi.org/10.1016/j.procbio.2012.01.011.

[14] C.P.S. Badenhorst, U.T. Bornscheuer, Getting momentum: from biocatalysis to advanced synthetic biology, Trends Biochem. Sci. 43 (2018) 180–198, https://doi.org/10.1016/j.tibs.2018.01.003.

[15] U.T. Bornscheuer, The fourth wave of biocatalysis is approaching, Philos. Trans. R. Soc. A Math. Eng. Sci. 376 (2018) 20170063, , https://doi.org/10.1098/rsta.2017.0063.

[16] K.S. Siddiqui, Some like it hot, some like it cold: temperature dependent biotechnological applications and improvements in extremophilic enzymes, Biotechnol. Adv. 33 (2015) 1912–1922, https://doi.org/10.1016/j.biotechadv.2015.11.001.

[17] T. Narancic, R. Davis, J. Nikodinovic-Runic, K.E.O.' Connor, Recent developments in biocatalysis beyond the laboratory, Biotechnol. Lett. 37 (2015) 943–954, https://doi.org/10.1007/s10529-014-1762-4.

[18] S. Falcocchio, C. Ruiz, F.I.J. Pastor, L. Saso, P. Diaz, Identification of a carboxylesterase-producing *Rhodococcus* soil isolate, Can. J. Microbiol. 51 (2005) 753–758.

[19] N. Prim, C. Ruiz, C. Bofill, F.I.J. Pastor, P. Diaz, Isolation of lipolytic microorganisms from subtropical soils. cloning, purification and characterization of a novel esterase from strain *Pseudomonas* sp CR-611, J. Biotechnol. 118 (2005) S120.

[20] C. Ruiz, F.I.J. Pastor, P. Diaz, Isolation of lipid- and polysaccharide-degrading micro-organisms from subtropical forest soil, and analysis of lipolytic strain *Bacillus* sp CR-179, Lett. Appl. Microbiol. 40 (2005) 218–227, https://doi.org/10.1111/j.1472-765X.2005.01660.x.

[21] A. Bassegoda, F.I.J. Pastor, P. Diaz, *Rhodococcus* sp. strain CR-53 lipR, the first member of a new bacterial lipase Family (Family X) displaying an unusual Y-type oxyanion hole, similar to the *Candida antarctica* lipase clan, Appl. Environ. Microbiol. 78 (2012) 1724–1732.

[22] A. Bassegoda, S. Cesarini, P. Diaz, Lipase improvement: goals and strategies, Comput. Struct. Biotechnol. J. 2 (2012) 1–8, https://doi.org/10.5936/csbj.201209005.

[23] S. Cesarini, C. Bofill, F.I.J. Pastor, M.T. Reetz, P. Diaz, A thermostable variant of *P. aeruginosa* cold-adapted LipC obtained by rational design and saturation mutagenesis, Process Biochem. 47 (2012) 2064–2071.

[24] A. Bassegoda, G.-S.S. Nguyen, M. Schmidt, R. Kourist, P. Diaz, U.T. Bornscheuer, Rational Protein Design of *Paenibacillus barcinonensis* Esterase EstA for Kinetic Resolution of Tertiary Alcohols, ChemCatChem 2 (2010) 962–967.

[25] A. Fillat, P. Romea, F. Urpí, F.I.J. Pastor, P. Diaz, Improving enantioselectivity towards tertiary alcohols using mutants of *bacillus* sp. BP-7 esterase EstBP7 holding a rare GGG(X)-oxyanion hole, Appl. Microbiol. Biotechnol. 98 (2014) 4479–4490.

[26] A. Fillat, P. Romea, F.I.J. Pastor, F. Urpí, P. Diaz, Kinetic resolution of esters from secondary and tertiary benzylic propargylic alcohols by an improved esterase-variant from *Bacillus* sp. BP-7, Catal. Today 255 (2015) 16–20.

[27] P. Panizza, S. Cesarini, P. Diaz, S. Rodríguez Giordano, Saturation mutagenesis in selected amino acids to shift *Pseudomonas* sp. acidic Lipase Lip I.3 substrate specificity and activity, Chem. Commun. 51 (2015) 1330–1333.

[28] T. Davids, M. Schmidt, D. Böttcher, U.T. Bornscheuer, Strategies for the discovery and engineering of enzymes for biocatalysis, Curr. Opin. Chem. Biol. 17 (2013) 215–220, https://doi.org/10.1016/J.CBPA.2013.02.022.

[29] U.T. Bornscheuer, Biocatalysis: successfully crossing boundaries, Angew. Chem. Int. Ed. 55 (2016) 4372–4373, https://doi.org/10.1002/anie.201510042.

[30] K.-E.E. Jaeger, T. Eggert, Lipases for biotechnology, Curr. Opin. Biotechnol. 13 (2002) 390–397.

[31] J.L. Arpigny, K.E. Jaeger, Bacterial lipolytic enzymes: classification and properties, Biochem. J. 343 (1999) 177–183, https://doi.org/10.1042/bj3430177.

[32] A. Castilla, P. Panizza, D. Rodríguez, L. Bonino, P. Díaz, G. Irazoqui, S. Rodríguez-Giordano, A novel thermophilic and halophilic esterase from *Janibacter* sp. R02, the first member of a new lipase Family (Family XVII), Enzyme Microb. Technol. 98 (2017) 86–95, https://doi.org/10.1016/j.enzmictec.2016.12.010.

[33] M. Masomian, R. Noor Zaliha Raja Abd Rahman, A. Bakar Salleh, M. Basri, Analysis of comparative sequence and genomic data to verify phylogenetic relationship and explore a New subfamily of bacterial lipases, PLoS One 11 (2016), https://doi.org/10.1371/journal.pone.0149851.

[34] F. Kovacic, N. Babić, U. Krauss, K.-E. Jaeger, Classification of lipolytic enzymes from bacteria, in: F. Rojo (Ed.), Aerob. Util. Hydrocarb. Oils Lipids, Springer, 2019, , https://doi.org/10.1007/978-3-319-39782-5_39-1.

[35] J. Ribera, M. Estupiñán, A. Fuentes, A. Fillat, J. Martínez, P. Diaz, *Bacillus* sp. JR3 esterase LipJ: a new mesophilic enzyme showing traces of a thermophilic past, PLoS One. 12 (2017) e0181029, , https://doi.org/10.1371/journal.pone.0181029.

[36] X. Zottig, F. Meddeb-Mouelhi, D.M. Charbonneau, M. Beauregard, Characterization of a novel alkalophilic lipase from Aneurinibacillus thermoaerophilus: lid heterogeneity and assignment to family I.5, Protein J. 36 (2017) 478–488, https://doi.org/10.1007/s10930-017-9743-9.

[37] A. Biundo, A. Hromic, T. Pavkov-Keller, K. Gruber, F. Quartinello, K. Haernvall, V. Perz, M.S. Arrell, M. Zinn, D. Ribitsch, G.M. Guebitz, Characterization of a poly (butylene adipate-co-terephthalate)-hydrolyzing lipase from *Pelosinus fermentans*, Appl. Microbiol. Biotechnol. 100 (2016) 1753–1764, https://doi.org/10.1007/s00253-015-7031-1.

[38] S.-T. Jeong, H.-K. Kim, S.-J. Kim, S.-W. Chi, J.-G. Pan, T.-K. Oh, S.-E. Ryu, Novel zinc-binding center and a temperature switch in the *Bacillus stearothermophilus* L1 Lipase, J. Biol. Chem. 277 (2002) 17041–17047, https://doi.org/10.1074/jbc.M200640200.

[39] C. Carrasco-López, C. Godoy, B. de Las Rivas, G. Fernández-Lorente, J.M. Palomo, J.M. Guisán, R. Fernández-Lafuente, M. Martínez-Ripoll, J.A. Hermoso, Activation of bacterial thermoalkalophilic lipases is spurred by dramatic structural rearrangements, J. Biol. Chem. 284 (2009) 4365–4372, https://doi.org/10.1074/jbc.M808268200.

[40] E. Timucin, A. Cousido-Siah, A. Mitschler, A. Podjarny, O.U. Sezerman, Probing the roles of two tryptophans surrounding the unique zinc coordination site in lipase family I.5, Proteins. 84 (2015) 129–142 (Accessed February 5, 2018), file:///C:/Users/MICROBIOLOGIA-pdiaz/Downloads/Timucin_et_al-2016-Proteins_Structure,_Function,_and_Bioinformatics.pdf.

[41] V. Perz, A. Baumschlager, K. Bleymaier, S. Zitzenbacher, A. Hromic, G. Steinkellner, A. Pairitsch, A. Łyskowski, K. Gruber, C. Sinkel, U. Küper, D. Ribitsch, G.M. Guebitz, Hydrolysis of synthetic polyesters by *Clostridium botulinum* esterases, Biotechnol. Bioeng. 113 (2016) 1024–1034, https://doi.org/10.1002/bit.25874.

[42] A. Biundo, G. Steinkellner, K. Gruber, T. Spreitzhofer, D. Ribitsch, G.M. Guebitz, Engineering of the zinc-binding domain of an esterase from *Clostridium botulinum* towards increased activity on polyesters, Catal. Sci. Technol. 7 (2017) 1440–1447, https://doi.org/10.1039/C7CY00168A.

[43] M. Zulhilmi, A. Rahman, A.B. Salleh, R. Noor, Z. Raja, M. Basyaruddin, M. Basri, T.C. Leow, Unlocking the Mystery Behind the Activation Phenomenon of T1 Lipase: A Molecular Dynamics Simulations Approach, (2012), https://doi.org/10.1002/pro.2108.

[44] N. Varejão, R.A. De-Andrade, R.V. Almeida, C.D. Anobom, D. Foguel, D. Reverter, Structural mechanism for the temperature-dependent activation of the hyperthermophilic Pf2001 esterase, Structure 26 (2018) 199–208, https://doi.org/10.1016/j.str.2017.12.004 e3.

[45] D.M. Charbonneau, M. Beauregard, Role of key Salt Bridges in thermostability of *G. thermodenitrificans* EstGtA2: distinctive patterns within the New bacterial lipolytic enzyme family XV, PLoS One 8 (2013) e76675, , https://doi.org/10.1371/journal.pone.0076675.

[46] N. Goodarzi, A.A. Karkhane, A. Mirlohi, F. Tabandeh, I. Torktas, S. Aminzadeh, B. Yakhchali, M. Shamsara, M.A.-S. Ghafouri, Protein engineering of Bacillus thermocatenulatus lipase via deletion of the α5 helix, Appl. Biochem. Biotechnol. 174 (2014) 339–351, https://doi.org/10.1007/s12010-014-1063-3.

[47] A. Biundo, J. Reich, D. Ribitsch, G.M. Guebitz, Synergistic effect of mutagenesis and truncation to improve a polyesterase from *Clostridium botulinum* for polyester hydrolysis, Sci. Rep. 8 (2018) 3745, https://doi.org/10.1038/s41598-018-21825-9.

[48] N. Prim, A. Blanco, J. Martinez, F.I.J. Pastor, P. Diaz, estA, a gene coding for a cell-bound esterase from *Paenibacillus* sp BP-23, is a new member of the bacterial subclass of type B carboxylesterases, Res. Microbiol. 151 (2000) 303–312, https://doi.org/10.1016/s0923-2508(00)00150-9.

[49] G. Kouker, K.E. Jaeger, Specific and sensitive plate assay for bacterial lipases, Appl. Environ. Microbiol. 53 (1987) 211–213.

[50] P. Diaz, N. Prim, F.I.J. Pastor, Direct fluorescence-based lipase activity assay, Biotechniques 27 (1999) 696–699.

[51] N. Prim, M. Sánchez, C. Ruiz, F.I.J. Pastor, P. Diaz, Use of methylumbeliferyl-derivative substrates for lipase activity characterization, J. Mol. Catal. B Enzym. 22 (2003), https://doi.org/10.1016/S1381-1177(03)00048-1.

[52] J. Sambrook, D.W. Russell, Molecular Cloning: A Laboratory Manual, Cold Spring Harbor Laboratory Press {a}, 10 Skyline Drive, Plainview, NY, 11803-2500, USA, 2001.

[53] M.T. Reetz, J.D. Carballeira, Iterative saturation mutagenesis (ISM) for rapid directed evolution of functional enzymes, Nat. Protoc. 2 (2007) 891–903.
[54] M.M. Bradford, Rapid and sensitive method for quantitation of microgram quantities of protein utilizing principle of protein dye binding, Anal. Biochem. 72 (1976) 248–254.
[55] P. Panizza, N. Syfantou, F.I.J. Pastor, S. Rodríguez, P. Díaz, Acidic Lipase Lip I.3 from a *Pseudomonas* fluorescens-like strain displays unusual properties and shows activity on secondary alcohols, J. Appl. Microbiol. 114 (2013) 722–732, https://doi.org/10.1111/jam.12089.
[56] S.F. Altschul, T.L. Madden, A.A. Schäffer, J. Zhang, Z. Zhang, W. Miller, D.J. Lipman, Gapped BLAST and PSI-BLAST: a new generation of protein database search programs, Nucleic Acids Res. 25 (1997) 3389–3402, https://doi.org/10.1093/nar/25.17.3389.
[57] C. Notredame, D.G. Higgins, J. Heringa, T-Coffee: A novel method for fast and accurate multiple sequence alignment, J. Mol. Biol. 302 (2000) 205–217, https://doi.org/10.1006/jmbi.2000.4042.
[58] F. Sievers, A. Wilm, D. Dineen, T.J. Gibson, K. Karplus, W. Li, R. Lopez, H. McWilliam, M. Remmert, J. Söding, J.D. Thompson, D.G. Higgins, Fast, scalable generation of high-quality protein multiple sequence alignments using Clustal Omega, Mol. Syst. Biol. 7 (2011) 539, https://doi.org/10.1038/msb.2011.75.
[59] T. Hall, BioEdit: a user-friendly biological sequence alignment editor and analysis program for Windows 95/98/NT, Nucleic Acids Symp. Ser. 41 (1999) 95–98.
[60] T.N. Petersen, S. Brunak, G. von Heijne, H. Nielsen, SignalP 4.0: discriminating signal peptides from transmembrane regions, Nat. Methods. 8 (2011) 785–786, https://doi.org/10.1038/nmeth.1701.
[61] E. Gasteiger, C. Hoogland, A. Gattiker, S. Duvaud, M.R. Wilkins, R.D. Appel, A. Bairoch, Protein identification and analysis tools on the ExPASy server, Proteomics Protoc. Handb. Humana Press, Totowa, NJ, 2005, pp. 571–607, https://doi.org/10.1385/1-59259-890-0 571.
[62] E. Quevillon, V. Silventoinen, S. Pillai, N. Harte, N. Mulder, R. Apweiler, R. Lopez, InterProScan: protein domains identifier, Nucleic Acids Res. 33 (2005) W116–20, https://doi.org/10.1093/nar/gki442.
[63] R.D. Finn, J. Clements, S.R. Eddy, HMMER web server: interactive sequence similarity searching, Nucleic Acids Res. 39 (2011) W29–37, https://doi.org/10.1093/nar/gkr367.
[64] L.A. Kelley, S. Mezulis, C.M. Yates, M.N. Wass, M.J.E. Sternberg, The Phyre2 web portal for protein modeling, prediction and analysis, Nat. Protoc. 10 (2015), https://doi.org/10.1038/nprot.2015.053.
[65] T. Schwede, J. Kopp, N. Guex, M.C. Peitsch, SWISS-MODEL: an automated protein homology-modeling server, Nucleic Acids Res. 31 (2003) 3381–3385.
[66] D. Schneidman-Duhovny, Y. Inbar, R. Nussinov, H.J. Wolfson, PatchDock and SymmDock: servers for rigid and symmetric docking, Nucleic Acids Res. 33 (2005) W363–7.
[67] C.M. Yates, I. Filippis, L.A. Kelley, M.J.E. Sternberg, SuSPect: enhanced prediction of single amino acid variant (SAV) phenotype using network features, J. Mol. Biol. 426 (2014) 2692–2701, https://doi.org/10.1016/j.jmb.2014.04.026.
[68] V. Le Guilloux, P. Schmidtke, P. Tuffery, Fpocket: an open source platform for ligand pocket detection, BMC Bioinformatics 10 (2009) 168, https://doi.org/10.1186/1471-2105-10-168.
[69] H. Matsumura, T. Yamamoto, T.C. Leow, T. Mori, A.B. Salleh, M. Basri, T. Inoue, Y. Kai, R.N.Z.R.A. Rahman, Novel cation-π interaction revealed by crystal structure of thermoalkalophilic lipase, Proteins Struct. Funct. Bioinform. 70 (2007) 592–598, https://doi.org/10.1002/prot.21799.
[70] A. Dror, M. Kanteev, I. Kagan, S. Gihaz, A. Shahar, A. Fishman, Structural insights into methanol-stable variants of lipase T6 from *Geobacillus stearothermophilus*, Appl. Microbiol. Biotechnol. 99 (2015) 9449–9461, https://doi.org/10.1007/s00253-015-6700-4.
[71] E. Timucin, O.U. Sezerman, Zinc modulates self-assembly of *Bacillus thermocatenulatus* Lipase, Biochemistry 54 (2015) 3901–3910, https://doi.org/10.1021/acs.biochem.5b00200.
[72] W.-C. Choi, M.H. Kim, H.-S. Ro, S.R. Ryu, T.-K. Oh, J.-K. Lee, Zinc in lipase L1 from *Geobacillus stearothermophilus* L1 and structural implications on thermal stability, FEBS Lett. 579 (2005) 3461–3466, https://doi.org/10.1016/j.febslet.2005.05.016.
[73] E. Martínez, M. Estupiñán, F.I.J. Pastor, M. Busquets, P. Díaz, A. Manresa, Functional characterization of ExFadLO, an outer membrane protein required for exporting oxygenated long-chain fatty acids in *Pseudomonas aeruginosa*, Biochimie. 95 (2013) 290–298.
[74] M.J. Betts, R.B. Russell, Amino acid properties and consequences of substitutions, Bioinformatics for Geneticists, John Wiley & Sons, Ltd, Chichester, UK, 2003, pp. 289–316, https://doi.org/10.1002/0470867302.ch14.
[75] D. Chin, A.R. Means, Methionine to glutamine substitutions in the C-terminal domain of calmodulin impair the activation of three protein kinases, J. Biol. Chem. 271 (1996) 30465–30471, https://doi.org/10.1074/JBC.271.48.30465.
[76] L. Serrano, J.-L. Neira, J. Sancho, A.R. Fersht, Effect of alanine versus glycine in α-helices on protein stability, Nature 356 (1992) 453–455, https://doi.org/10.1038/356453a0.
[77] J. López-Llano, L.A. Campos, J. Sancho, α-helix stabilization by alanine relative to glycine: roles of polar and apolar solvent exposures and of backbone entropy, Proteins Struct. Funct. Bioinform. 64 (2006) 769–778, https://doi.org/10.1002/prot.21041.
[78] T.C. Leow, R.N.Z.R.A. Rahman, M. Basri, A.B. Salleh, High level expression of thermostable lipase from Geobacillus sp. strain T1, Biosci. Biotechnol. Biochem. 68 (2004) 96–103, https://doi.org/10.1271/bbb.68.96.

Unexplored lipolytic activity of *Escherichia coli*: Implications for lipase cloning

Investigaciones recientes en lipasas clonadas en *Escherichia coli* revelaron la presencia de actividad lipolítica que no era debida al gen codificante de la lipasa clonada sino a la actividad intrínseca de la cepa huésped. Para confirmar esta hipótesis, se analizó la actividad de las cepas de *E. coli* de uso más frecuente mediante pruebas rápidas en papel, zimogramas y espectrofluorometría. En los zimogramas de los extractos celulares crudos se detectó una banda de Ca. 18-20 kDa que mostraba actividad en MUF-butirato. Los ensayos espectrofluorométricos confirmaron la presencia de actividad lipolítica baja, pero significativa en *E. coli*, siendo la cepa BL21 la que poseía la actividad más elevada. Se realizó una caracterización detallada de dicha actividad lipolítica utilizando extractos de células de *E. coli* BL21, donde se encontró preferencia por sustratos C7, aunque en menor grado, también los sustratos más cortos fueron hidrolizados. Curiosamente, la actividad lipolítica de E. coli muestra rasgos de una enzima termófila, con una actividad lipolítica óptima a 50 ºC y pH 8, un rasgo nunca descrita para *E.coli*. También se realizaron ensayos de cinética y de inhibición, en que se demostró que la actividad podía verse inhibida por varios iones metálicos o por Triton X-100® y SDS, utilizados en análisis de zimogramas. Tales propiedades - baja actividad, preferencia por sustratos de longitud de cadena media y una elevada temperatura operacional - podrían justificar por qué esta actividad no se había explorado hasta, aunque se hayan clonado y expresado multitud de lipasas y esterasas en cepas de *E.coli.* Sin embargo, de ahora en adelante, las futuras investigaciones centradas en lipasas clonadas deberían tener en cuenta la presencia de tal actividad lipolítica basal.

Enzyme and Microbial Technology 139 (2020) 109590

Contents lists available at ScienceDirect

Enzyme and Microbial Technology

journal homepage: www.elsevier.com/locate/enzmictec

Unexplored lipolytic activity of *Escherichia coli*: Implications for lipase cloning

Carolina Buruaga-Ramiro, Susana V. Valenzuela, F.I.J. Pastor, Josefina Martínez, Pilar Diaz*

Department of Genetics, Microbiology and Statistics, Faculty of Biology, and Institute of Nanoscience and Nanotechnology (IN2UB), University of Barcelona, Av. Diagonal 643, 08028 Barcelona Spain

ARTICLE INFO

Keywords:
Lipase
E. coli
Lipase cloning

ABSTRACT

Recent investigations on cloned bacterial lipases performed in our laboratory revealed the presence of lipolytic activity that was not due to the cloned lipase-coding gene but was probably the result of an intrinsic activity of *Escherichia coli* itself. To confirm such a hypothesis, we assayed the activity of frequently used *E. coli* strains by fast paper tests, zymograms and spectrofluorometry. A band of Ca. 18 − 20 kDa showing activity on MUF-butyrate was detected in zymogram analysis of crude cell extracts in all *E. coli* strains assayed. Moreover, the spectrofluorometric results obtained confirmed the presence of low but significant lipolytic activity in *E. coli*, with strain BL21 showing the highest activity. Detailed characterization of such a lipolytic activity was performed using *E. coli* BL21 cell extracts, where preference for C7 substrates was found, although shorter substrates were also hydrolysed to a minor extent. Interestingly, *E. coli* lipolytic activity displays traits of a thermophilic enzyme, showing maximum activity at 50 °C and pH 8, an unexpected feature never described before. Kinetic and inhibition analysis were also performed showing that activity can be inhibited by several metal ions or by Triton X-100® and SDS, used in zymogram analysis. Such properties – low activity, preference for medium chain-length substrates, and high operational temperature – might justify why this activity had gone unexplored until now, even when many lipases and esterases have been cloned and expressed in *E. coli* strains in the past. From now on, lipase researchers should take into consideration the presence of such a basal lipolytic activity before starting their lipase cloning or expression experiments in *E.coli*.

1. Introduction

Lipolytic enzymes are mostly constituted by “true” lipases (EC 3.1.1.3, triacylaglycerol hydrolases) and esterases (EC 3.1.1.1, carboxyl ester hydrolases), both belonging to the α/β-fold group of hydrolases. They represent an enormous group of biocatalysts, widely distributed in nature, that have received great attention in the last decades due to their broad array of substrate specificity, their robustness and their versatility in catalysed reactions [1,2]. Lipolytic enzymes can perform both, the hydrolysis and synthesis of triacylglycerides depending on the water content of the reaction medium, without any requirement for added cofactors. The ability of lipolytic enzymes to perform inter- or trans- esterifications, together with their stereo- or enantio- selectivity, have set this group of enzymes as powerful biocatalysts for applications in areas such as food technology, detergent formulation, flavour and drug production, synthesis of optically pure compounds [1,3–7], or biofuel synthesis [8] among others [7,9–12]. Moreover, their versatile properties justify the presence of lipolytic enzymes in all biological groups, including archaea, virus or bacteria, where they perform functions related to lipid metabolism, transport, signalling, or carbon uptake among others [6].

Many lipolytic enzymes have been isolated, cloned and characterized in the past using *E. coli* strains as the host of preference [13–15]. However, poor attention has been paid to the intrinsic lipolytic activity of such a usual host, where although without deep characterization, the existence of putative lipolytic enzymes has already been described [16–18]. In general, in all these works, good production and activity of the cloned enzymes has been achieved for further uses and characterization [19]. However, for those enzymes showing poor activity, care must be taken with the basal activity shown by *E. coli* itself [16,18]. This was the case in our recent research when cloning a rare lipase −LipG− isolated from *Bacillus* sp. JR3 [18], showing an unprecedented architecture (unpublished results). Although bearing most of the traits of a lipase, including the conserved G(A)-X-S-X-G consensus pentapeptide and the typical catalytic triad constituted by a serine as the nucleophile residue, an aspartic acid, and a histidine as the proton

* Corresponding author.
E-mail address: pdiaz@ub.edu (P. Diaz).

https://doi.org/10.1016/j.enzmictec.2020.109590
Received 10 January 2020; Received in revised form 5 May 2020; Accepted 6 May 2020
Available online 11 May 2020

donor, LipG did not show significant lipolytic activity. Therefore, we had to conclude that the putative lipase cloned was not indeed displaying lipolytic activity (unpublished). Search for other possible activities of such an unusual enzyme is now being performed.

Taking into consideration these and previous results of our research indicating the most probable existence of a significant lipolytic background in *E. coli* strains frequently used for lipase/esterase cloning and expression, we decided to explore the intrinsic lipolytic activity of *E. coli* by performing a detailed characterization of such an activity. The lipolytic activity of the *E. coli* strains frequently used in lipase cloning or expressing was assayed here for confirmation, and *E. coli* BL21 crude cell extract activity was determined and characterized under several conditions. The information released can be of interest for those researchers involved in the cloning of heterologous lipolytic enzymes in *E. coli* strains.

2. Materials and methods

2.1. Strains, plasmids and growth conditions

E. coli DH5α (Invitrogen), BL21 star (DE3) (Invitrogen), TOP10F' (Invitrogen), and CECT 515 (Migula, 1895, Castellani & Chalmers, 1919) strains were used for intrinsic lipolytic activity determination assays. They were routinely cultured overnight at 37 °C in LB broth or on LB agar plates, and were used as host strains for cloning and expression of other lipase-encoding genes, used as a control. For plate activity detection, CeNAN (ASDA Micro) agar plates supplemented with olive oil (1% w/v, Carbonell) or tributyrine (1% w/v, Sigma) emulsified with 0.1% arabic gum (w/v, Sigma) and 0.0002% Rhodamine B (v/v, Sigma) were used [20] and incubated at 37 °C, as previously described [21]. Pure cultures of all strains were maintained at 4 °C and stored in glycerol stocks at −80 °C.

Plasmids pET28a and pLATE11 (Novagen/ThermoFisher Scientific) were used as expression vectors, producing recombinant *E. coli* clones carrying selected lipase coding genes, used as control samples in our assays. Media were supplemented with antibiotics (ampicillin 100 μg mL^{-1}; kanamycin 50 μg mL^{-1}) or IPTG (isopropyl-β-D-thiogalactopyranoside; 1 mM) when required for recombinant clone selection or gene expression [22].

Cloning of the putative lipase LipG was performed after amplification of a DNA fragment from strain *Bacillus* sp. JR3, using degenerate primers for thermophilic lipases [18]. The resulting PCR fragment was ligated to pGEM-T® Easy vector (Promega) and transformed into *E. coli* DH5α. For overexpression, pGEMT-LipG was digested with *Nco*I/*Hind*III, ligated to the doubly digested expression vector pET28a and transformed in *E. coli* BL21 star (DE3).

2.2. DNA procedures

Plasmid DNA was purified using GeneJET Plasmid Miniprep Kit (Thermo Fisher Scientific). When required, DNA polymerases and restriction enzymes (Biotools/Thermo Scientific) were used following the manufacturer's recommendations. DNA samples were routinely analysed by 0.8% (w/v) agarose gel electrophoresis [22], and stained with 0.004% GreenSafe Premium (v/v, NZytech). Nucleic acid concentration and purity were measured using a Spectrophotometer ND-100 NanoDrop®.

2.3. Cell fraction preparation

For cell extract preparation, exponential growth cultures (OD_{600nm} = 0.6 − 0.8) of wild type and recombinant *E. coli* strains in LB medium (supplemented with kanamycin; 50 μg mL^{-1} or ampicillin; 100 μg mL^{-1} when required) were induced with 1 mM IPTG at 16 °C for 24 h. Cells were collected by centrifugation at 6000 x rpm for 15 min, suspended in 20 mM Tris − HCl buffer pH 7.0, and disrupted using a GEA PandaPLUS 2000 homogenizer (1200 bars) or by sonication with a Labsonic 1510 sonicator (B. Braun; 80 W, 3 min). Clarified cell extracts were recovered after centrifugation at 10,000 × rpm for 20 min at 4 °C (Beckman-Coulter High-Speed VA-1000) for activity determination. Bradford assays were performed for protein concentration determination using bovine serum albumin (BSA) as the standard [23,24]. Concentrated (25X) cell extract samples were obtained using ultrafiltration Centricon™ devices (Amicon®) of 10 kDa cutoff, and analysed by 12% SDS-PAGE [25] after short time (0 − 5 min) treatments at 100 °C. Zymogram analysis was performed as previously described [26,27] using 100 μM MUF-butyrate prepared in Tris HCl 20 mM buffer (pH 7) at 30 and 60 °C, and visualized under UV light in a Gel Doc XR System (BioRad) before staining with BlueSafe (NZytech).

2.4. Activity assays

Lipolytic activity of supernatants or crude cell extracts of *E. coli* strains was analysed by measuring the release of *para*-nitrophenol (*p*NP) (Sigma-Aldrich) or methylumbelliferone (MUF) (Sigma-Aldrich) from *p*NP or MUF-derivative fatty acid substrates, prepared in 20 mM DMSO and 25 mM metoxiethanol, respectively, as previously reported [14,26–28]. Absorbance (for *p*NP substrates) and fluorescence (for MUF substrates) were measured using a BioRad 3550 microplate reader or a Variant Cary Eclipse spectrofluorometer (Agilent Technologies) equipped with a microplate reader, respectively. One unit of activity was defined as the amount of enzyme that released 1 μmol of *p*NP or MUF per minute under the assay conditions used. All determinations of enzyme activity were performed by two biological replicas of technical triplicates (6 determinations per sample). Paper and zymogram assays were performed on MUF-derivative substrates as previously described [26,27].

Optimum temperature of *E. coli* lipolytic activity was determined by analysis of the activity over a range from 4 to 100 °C, using 0.5 mM MUF-heptanoate as a substrate [28]. Optimum pH of cell extracts was determined by measuring activity on MUF-heptanoate and 50 mM Britton-Robinson buffer in a pH range from 3 to 9. Thermal stability was determined by incubating cell extracts at temperatures from 4 to 100 °C for 1–72 h and activity was then measured under standard assay conditions once samples reached the optimum temperature of the enzyme, determined as mentioned above. To evaluate the effect of metal ions or inhibitors on activity, assays were performed on MUF-heptanoate in the presence of several chlorides (Al^{+3}, Ba^{+2}, Ca^{+2}, Cu^{+2}, Fe^{+2}, Hg^{+2}, K^{+}, Li^{+2}, Mg^{+2}, Mn^{+2}, Na^{+}, NH_4^{+}, Zn^{+2}), used at 1 and 10 mM. Moreover, inhibition by Triton X-100® (0–40%) and SDS (0–2%) were assayed at 30 °C and 60 °C on MUF-heptanoate and *p*NP-octanoate, respectively. Residual activity was measured at optimum pH and temperature using a conventional assay on MUF-heptanoate, and expressed as a percentage of activity without ions or inhibitors, respectively. Kinetic parameters (*Vmax* and *Km*) were determined under optimal assay conditions by fitting hyperbolic Michaelis-Menten curves with GraphPad Prism® software version 6.

3. Results and discussion

3.1. E. coli lipolytic activity

Recent works performed in our laboratory for characterization of an unusual lipase-like sequence from *Bacillus* sp. JR3 [18] (*lip*G, unpublished) cloned in *E. coli* BL21 revealed that the recombinant clones assayed displayed almost the same level of activity on MUF-butyrate as that shown by the host *E. coli* strain itself. Several replicas of such an assay were performed to discard the possibility of an artefact, but very similar activity was always achieved for both, the host strain and recombinant clones. Therefore, a set of serial assays were performed to test activity on short, mid and long chain-length MUF-derivative substrates at both, 30 and 60 °C (Fig. 1). To guarantee expression of *lip*G in

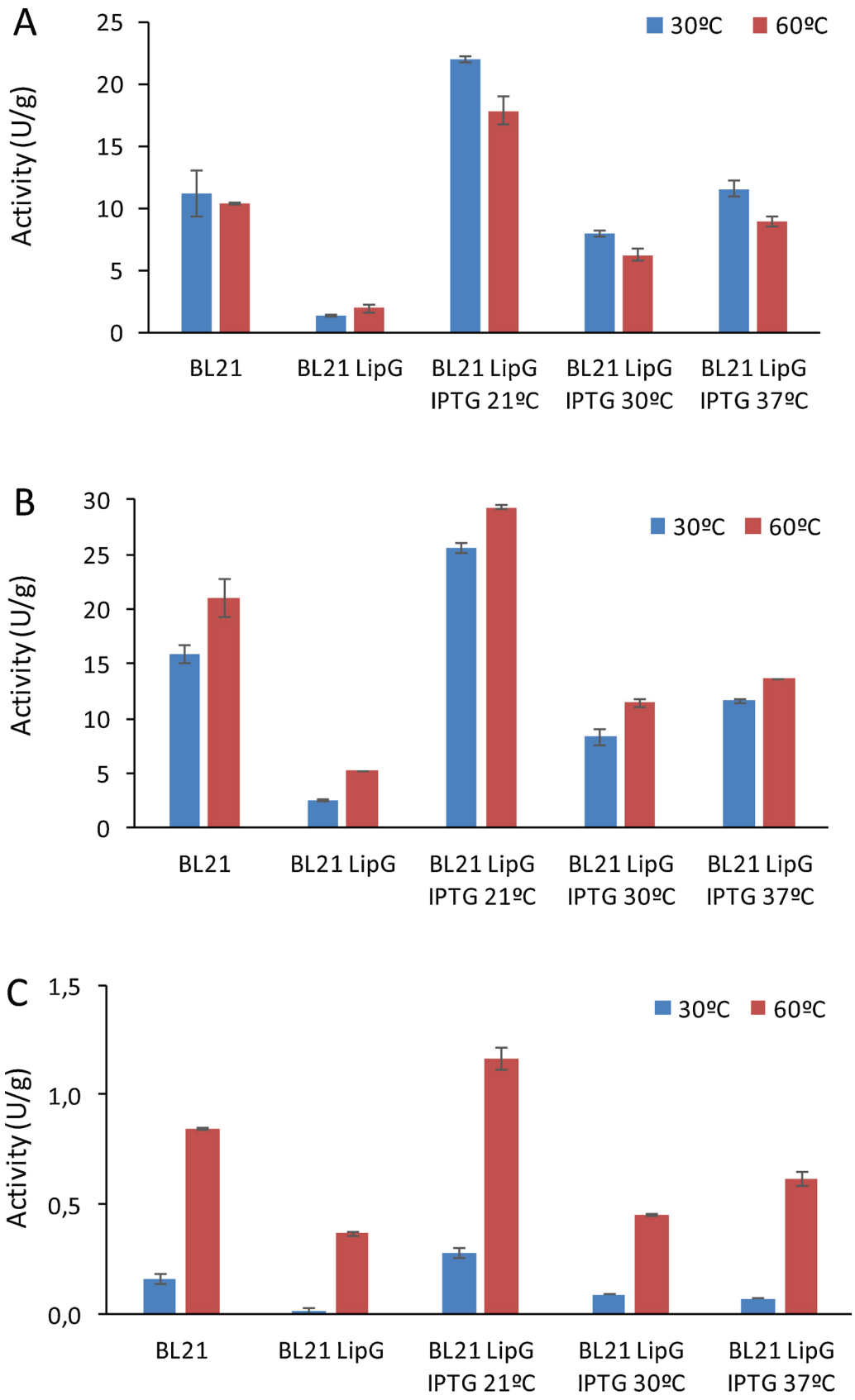

Fig. 1. Lipolytic activity of cell extracts from strain *E. coli* BL21 and a recombinant clone (BL21 LipG) carrying the unusual lipase-like sequence *lip*G. Assays were performed on MUF-butyrate (A), MUF-heptanoate (B) and MUF-oleate at 30 and 60 ˚C. Recombinant clone carrying *lip*G gene was induced with IPTG at 21 ˚C, 30 ˚C and 37 ˚C.

recombinant clone *E. coli* BL21 LipG, IPTG induction at different temperatures (21 °C, 30 °C and 37 °C) was assayed, and activity of crude cell extracts was analysed. For all substrates tested, the highest activity was observed in cell extracts of *E. coli* BL21 LipG induced at 21 °C with 1 mM IPTG (Fig. 1), showing slightly higher activity on MUF-heptanoate at 60 °C (29.34 U/g). However, the activity values shown by this induced recombinant clone were very low on all substrates (21.99 U/g, MUF-butyrate at 30 °C; 29.34 U/g, MUF-heptanoate at 60 °C; 1.16 U/g, MUF-oleate at 60 °C), and similar to those of the host strain *E. coli* BL21 (11.22 U/g, MUF-butyrate at 30 °C; 21.06 U/g, MUF-heptanoate at 60 °C; 0.85 U/g MUF-oleate at 60 °C), suggesting that LipG was hardly displaying a basal activity. Activity of uninduced recombinant clone LipG was even lower than that of strain *E. coli* BL21, a fact that might be justified by the plasmid and growth in the presence of antibiotic. These results were confirmed after zymogram analysis in both, SDS and native gels, where no extra activity bands appeared for LipG recombinant clone. To investigate the possibility that the low activity shown by LipG could be due to aggregation or to the binding of the enzyme to particulated cell components, the insoluble fraction (cell debris) of cell extracts was also tested on MUF-heptanoate at 30 and 60 °C and through zymogram analysis. The results (not shown) proved that the insoluble fraction of both, *E. coli* BL21 and recombinant *E. coli* BL21 LipG displayed similar but very low activity, with the highest values found at 60 °C (5.68 U/g and 3.46 U/g, respectively). In all cases, most activity was found in soluble cell extracts and MUF-heptanoate was the substrate of preference for both, recombinant LipG clone and strain BL21 (Fig. 1).

3.2. Paper and zymogram activity analysis

Similar results were obtained when crude cell extracts from recombinant clone *E. coli* BL21 LipG induced with IPTG at different temperatures were analysed by fast paper assays [27] on MUF-butyrate or MUF-heptanoate (Fig. 2A), thus suggesting that most of the activity observed was indeed derived from the host *E. coli* BL21 strain itself. Once confirmed that induced cell extracts of *E. coli* BL21 LipG did not display any significant increase of activity over that of the host strain, we concluded that most probably we were detecting an intrinsic activity of *E. coli.* Presence of such an activity had already been detected in former results obtained in our research with lipases [15,29] and previously revealed by other authors [16,17]. To prove it, we performed paper and zymogram analysis of cell extracts from four *E. coli* strains frequently used for enzyme cloning, using also cell extracts of recombinant clone *E. coli* BL21 LipJ [18,30] coding for a mesophilic 43 kDa esterase, and supernatants from the highly lipolytic strain *Bacillus* sp. JR3 [18] as positive controls. As suspected, all *E. coli* strains tested on paper assays (Fig. 2B) and zymograms (Fig. 3) displayed lipolytic activity, showing fluorescence emission and a band of Ca. 20 kDa with activity towards MUF-butyrate and MUF-heptanoate at both, 30 and 60 °C. As shown in Fig. 2B, all tested *E. coli* strains displayed similar activity on the assayed substrates, being MUF-heptanoate the substrate of preference and *E. coli* BL21 the strain showing the highest fluorescence emission. As expected from previous results, activity on MUF-oleate was very poor for all samples, including the supernatnat of *Bacillus* JR3, and could not be detected in strain CECT 515. Zymogram analysis (Fig. 3), revealed that all *E. coli* cell extratcs display a band of 18 − 20 kDa with activity on both substrates and at the two temperatures assayed. In general, activity on MUF-butyrate was higher at 30 °C than at 60 °C, whereas all *E. coli* strains, and specially BL21, displayed better fluorescence emission when assayed on MUF-heptanoate at 60 °C. As previously described [18], LipJ appeared as a band of Ca. 43 kDa only when assayed on MUF-butyrate at 30 °C but not at 60 °C or on MUF-heptanoate (Fig. 3, samples 5). The results obtained here unambiguously demonstrate the presence of a basal but significant lipolityc activity in *E. coli* strains frequently used for lipase cloning procedures, and suggest that such an activity shows thermophilic traits (higher fluorescence emission at 60 °C) with preference for medium chain-length substrates, thus deserving further characterization.

3.3. Specific characterization of E. coli lipolytic activity

Although such an intrinsic *E. coli* lipolytic activity has been known for a long time by researchers working on cloned lipases and the possible existence of four putative esterases has been described before [16,17], to our knowledge the properties of such an activity have never been deeply studied, neither such an enzyme or enzymes have been cloned. Therefore, we decided to perform the specific characterization of *E. coli* lipolytic activity by determining substrate specificity, kinetic parameters, optimum pH and temperature, thermal stability, or the ability of defined ions or substances for activity inhibition or activation. For such purpose, we used crude cell extracts from *E. coli* BL21, one of the most frequently used strains for expression of lipase/esterase-coding genes [15,31,32].

As mentioned above, *E. coli* BL21 lipolytic activity displays preference for medium chain-length substrates like MUF-heptanoate, showing better performance at 60 °C (Fig. 1). Initially, a growth curve of *E. coli* BL21 was obtained to find out the moment of maximum lipolyitc activity production. Crude cell extracts of samples taken at different growth times were assayed on MUF-heptanoate at 60 °C, revealing that the lipolytic activity of *E. coli* is produced soon during growth, reaching maximum after 7 h incubation and maintaining this activity up to 30 h, still retaining 50% activity after 72 h growth (Fig. 4A). The parallelism found between growth and lipolytic activity production might suggest that such an activity is probably involved in important tasks of the central cell metabolism.

The previous observation that *E. coli* lipolytic activity could indeed be thermophilic (Figs. 1 and 3) led us to assay crude cells extracts of strain BL21 on MUF-heptanoate at different temperatures. As shown in Fig. 4B, maximum temperature on this substrate was attained at 50 °C, confirming the thermophilic nature of *E. coli* lipolytic activity. Moreover, thermal stability was also assayed at 50 °C after 1 h incubation of crude cell extracts in the temperature range from 4 to 80 °C, resulting in a thermotolerant enzyme that maintained 100% activity up to 50 °C, keeping more than 80% residual activity after 1 h incubation at 60 °C (Fig. 4D). When thermal stability was measured after long time incubation (48 h) at 30, 50 and 60 °C, the activity was only reduced in a 30% and a 40% when incubated at 30 and 50 °C, respectively, showing a half life time of 3 h when incubated at 60 °C (Fig. 4E). From these results we can thus conclude that *E. coli* BL21 bears an intracellular lipolytic activity showing traits of a thermophilic and thermostable enzyme.

Optimum pH was assayed on MUF-heptanoate at 50 °C using crude cell extracts of *E. coli* BL21. The range of pH from 3 to 9 was acquired using Britton-Robinson buffer, as stated at the Materials and Methods section. In agreement with Nantel's previous report [16], maximum activity was achieved at pH 8, confirming the alkalophilic nature of the enzyme, a trait that is more commonly found in lipases from Gram-positive bacteria [33,34] and which appears frequently associated to thermophilic enzymes [35–37].

Taking into consideration the results obtained above, the kinetics parameters of *E. coli* BL21 lipolytic activity were determined at 50 °C pH 8, using MUF-heptanoate as a substrate in the range of concentrations from 0 to 500 μM. The activity of strain BL21 displayed a Km of 150 μM and a Vmax of 30.2 Units g^{-1}, suggesting that such an activity does not indeed belong to an efficient enzyme, as confirmed by the results stated above (Fig. 1). Analysis of the kinetics behaviour of the activity revealed that it displayed a typical Michaelis-Menten kinetics profile when assayed on MUF-heptanoate, (not shown), a result that would be in agreement with the enzyme being an intracellular esterase [1].

According to previously reported data, most thermophilic lipases can bind Zn^{2+} or other ions like Ca^{2+} at defined cavities or coordinated

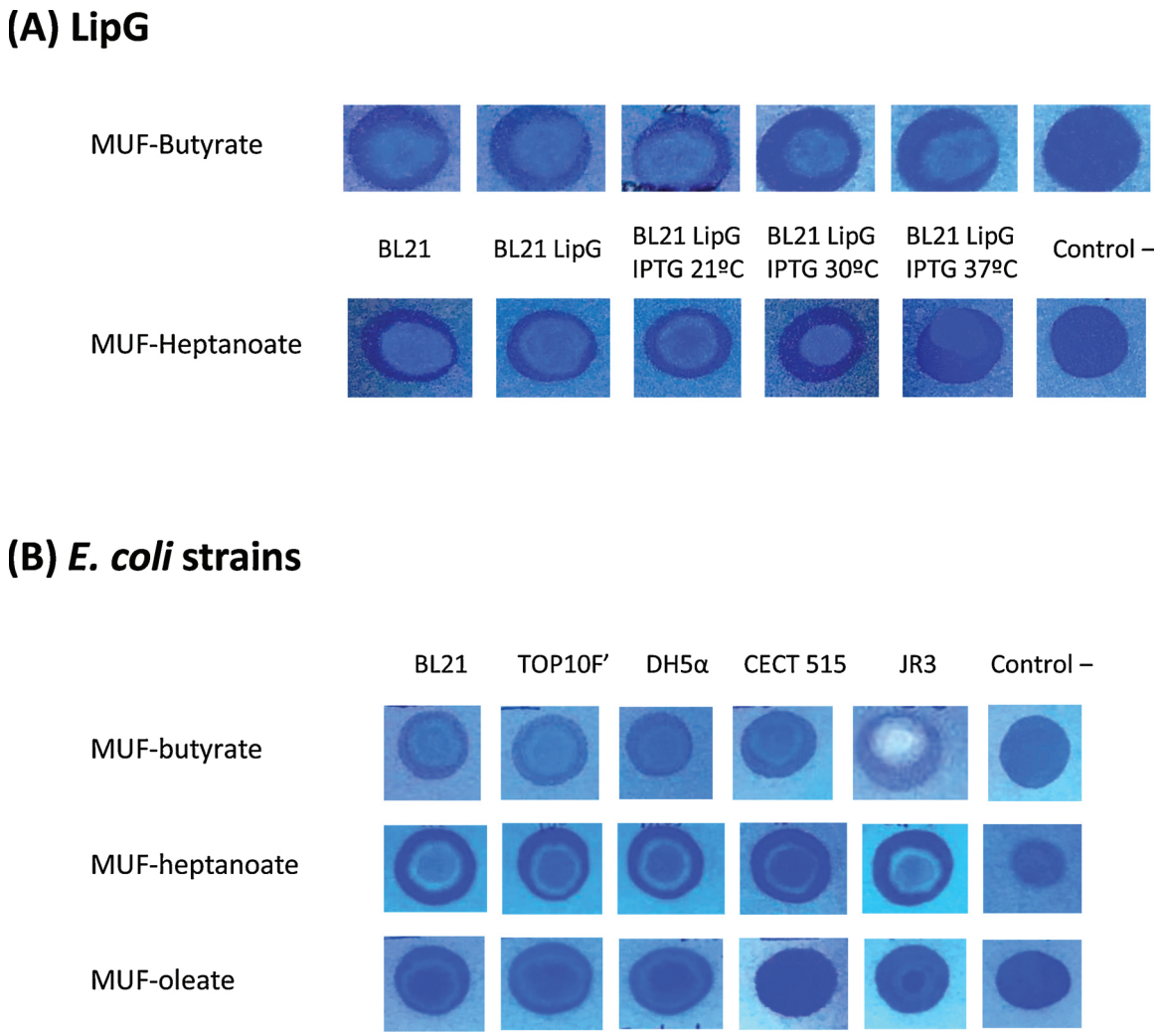

Fig. 2. Paper activity assays performed on different MUF-derivative substrates at 30 °C, as previously described [27]. (A) Cell extracts from *E. coli* BL21 and the recombinant clone carrying LipG, induced with IPTG at different temperatures, assayed for activity on MUF-butyrate or MUF-heptanoate. (B) Crude cell extracts from different *E. coli* strains (BL21, TOP10F', DH5α, and CECT515), assayed on MUF-butyrate, MUF-heptanoate or MUF-oleate. JR3 corresponds to a supernatant sample of the highly lipolytic strain *Bacillus* sp. JR3 [18], used as a positive control. Negative controls were prepared with the corresponding substrate but without any biological sample.

tetrahedral structures. Apparently such ions contribute to make the enzyme activity more efficient at high temperatures [35–39]. Being *E. coli* BL21 lipolytic activity due to a thermophilic enzyme, we assayed crude cell extracts of the strain in the presence of several ions to investigate their ability to cause activation or inhibition of such an activity. Fig. 5 shows the results obtained from assays performed at 50 °C on MUF-heptanoate in the presence of 1 and 10 mM concentrations of different metal ions. On the contrary to what happens for most thermophilic lipases described and in clear contradiction with the results described by Nantel in 1973 [16], no activation was observed in the presence of Zn^{2+} or Ca^{2+}. In fact, Ca^{2+} did not produce any significant effect on *E. coli* lipolytic activity, whereas Zn^{2+} caused a pronounced inhibition of the enzyme, that retained only a 15% residual activity when assayed at 1 mM, and negligible activity was detected at 10 mM.

Other ions like Cu^{2+}, Fe^{2+}, Hg^{2+} and Al^{3+} completely inhibited the activity at 10 mM and maintained very low activity values at 1 mM, being Fe^{2+} the only one showing 40% residual activity when assayed at this concentration. Among the ions assayed, no significant enzyme activation could be detected except for Mg^{2+}, which produced an activity increase close to 120%, far from the values obtained when thermophilic lipases are assayed in the presence of Zn^{2+} or Ca^{2+} [18,30,35,38].

In addition to the inhibition/activation assays performed in the presence of different metal ions, activity assays were also performed in the presence of different concentrations of SDS and Triton X-100®, two of the compounds routinely used in SDS-PAGE and zymogram (Fig. 3) analysis [26,27]. Fig. 5 shows how SDS is responsible for a strong inhibition of *E. coli* lipolytic activity, showing lack of activity when assayed at 0.4% or higher concentrations (Fig. 5). This result is also in contradiction with the previous description of *E. coli* lipolytic activity, that suggested a strict requirement for high concentrations of SDS [16]. Nevertheless, such a discrepancy might be attributed to the low SDS concentrations tested in our work, far from the 250 mM values suggested to have an activation effect [16]. However, it is important to highlight the interest of this result because it indicates that no activity would be recovered from an electrophoresis gel by means of extracting the corresponding band. Therefore, recovery of activity will necessarily involve the renaturing/refolding of the enzyme. For such purpose we usually wash the gels with 2.5% Triton X-100®, a concentration that, in general, allows for a convenient refolding of the enzyme for activity recovery. However, when assays were performed in the presence of several concentrations of Triton X-100®, a significant decrease of activity was observed for increasing concentrations of Triton X-100®. At the typical concentration for refolding (2.5%) used for zymogram analysis, the activity was not completely recovered, showing a 20% loss

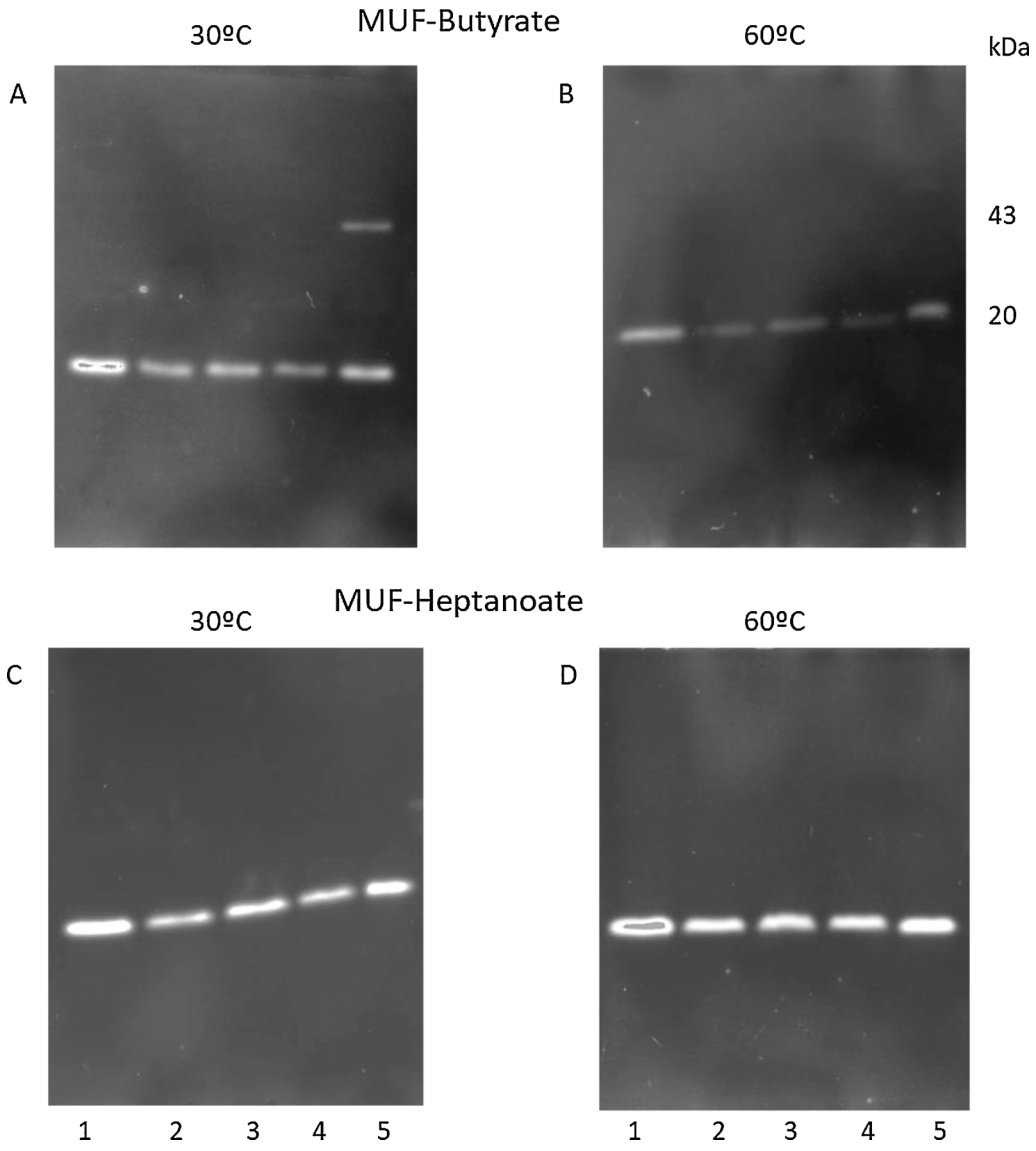

Fig. 3. Zymogram analysis of crude cell extracts from *E. coli* strains BL21 (samples 1), TOP10F' (samples 2), DH5α (samples 3) and CECT 515 (samples 4), analysed on MUF-butyrate (A,B) or MUF-heptanoate (C, D) at 30 °C (A, C) and 60 °C (B, D). Sample 5 in all gels corresponds to crude cell extracts from recombinant clone *E. coli* BL21-LipJ, carrying a mesophilic 43 kDa esterase previously described [18,30], used as a control. All samples, including that of control *E. coli* BL21-LipJ, display a band of Ca. 20 kDa with activity on both substrates at the two temperatures assayed. As expected, a band of 43 kDa with activity on MUF-butyrate only at 30 °C, corresponding to control mesophilic LipJ esterase, can be observed in lane 5 (A). The anomalous alignment of bands in B and C were due to curved running of the gels.

of activity. This is a significant information to keep in mind when performing zymogram analysis of *E. coli* lipolytic activity, as not all real activity (only 80%) will be detected in zymograms.

Although the existence of *E. coli* lipolytic activity is well known [18] and has previously been described [16], including the finding of four putative esterases [17], such an activity has never been cloned, purified or assayed in detail. Therefore, new bioinformatic prospections of *E. coli* genome are being carried out by means of genome mining in order to identify the gene or genes responsible for such an activity and to clone them in a heterologous host like a lipase activity-depleted *Pseudomonas* strain previously used in our laboratory for lipase expression [40,41]. Isolation and cloning of the gene or genes responsible for *E. coli* lipolytic activity is now under progress.

From the above results, we conclude that although *E. coli* lipolytic activity is not really efficient, its existence and properties must be taken into consideration when cloning lipases or esterases in *E. coli* host strains, even more if the cloned enzymes do not bear a strong activity by themselves or if they are thermophilic. Most probably, the reason why until now many researchers have used *E. coli* strains as the host for lipase cloning without any interference caused by the intrinsic lipolytic activity of *E. coli* may be justified by the properties of the enzyme described here. First of all, the low activity shown, which in general allows for a good activity determination of the cloned heterologous enzyme without any significant effect of the basal *E. coli* activity. Also the substrate profile of *E. coli* activity, showing preference for medium chain-length substrates, a fact that has probably avoided interferences of such an activity in assays performed using short chain-length substrates. And of course, the optimum pH and temperature of *E. coli* activity, which make a significant difference with respect to most of the cloned lipases characterized, which usually display milder working conditions. And finally, it has become familiar for some authors to report in their zymograms the presence of a 18 − 20 kDa band corresponding the host strain without need for extra explanations because the existence of this activity was already known from 1973 [16] but in fact consciously ignored. We here wanted to reveal the most important features of such a frequent but poorly explored lipolytic activity.

Author agreement

All authors have read and approved the manuscript, which has not previously been submitted to any journal, and declare that they have no conflict of interest.

Funding

This work was supported by the Scientific and Technological

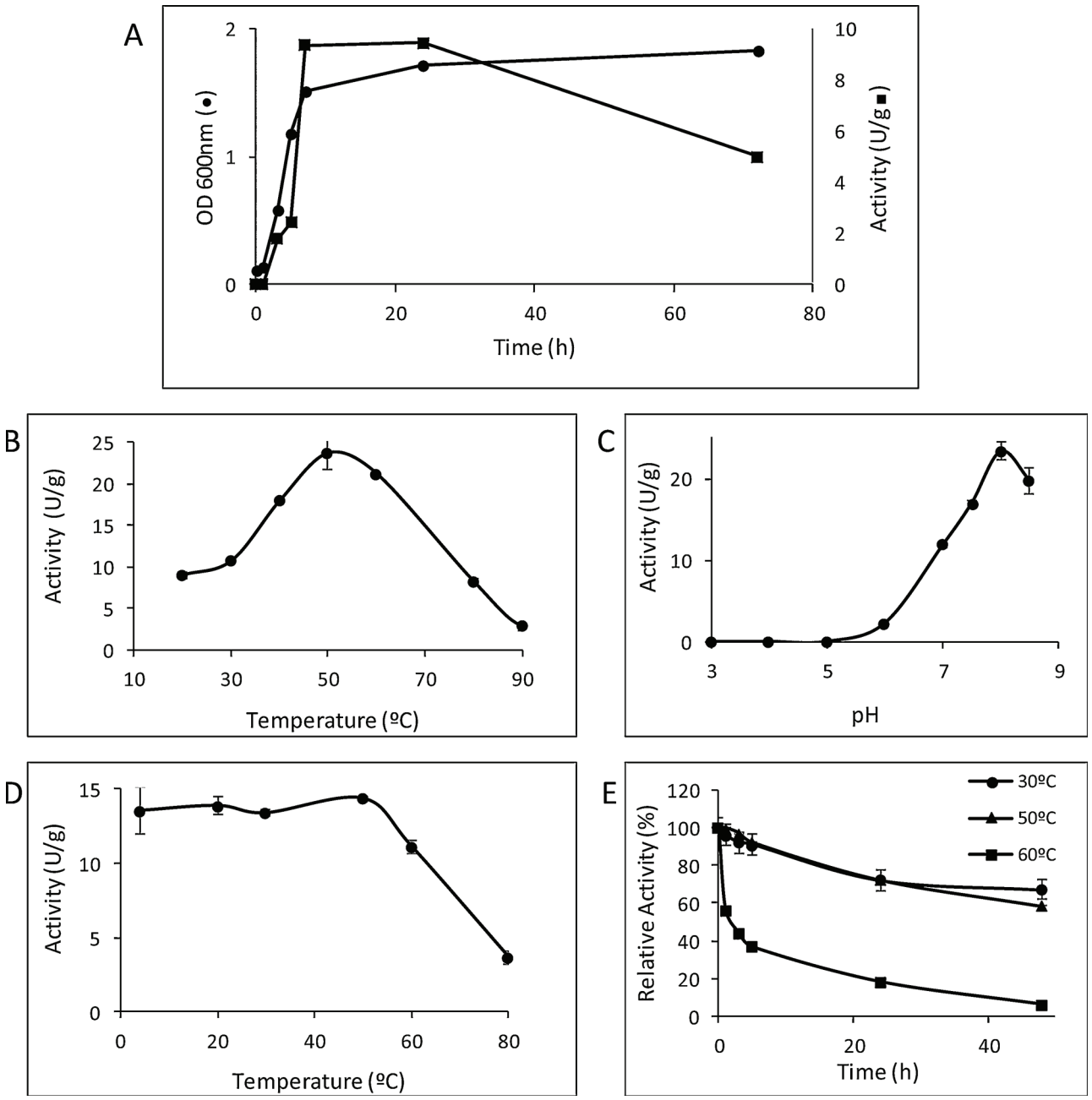

Fig. 4. Analysis of the properties of *E. coli* lipolytic activity, assayed on MUF-heptanoate from crude cell extracts. (A) Lipolytic activity production (■) during growth (●). (B) Optimum temperature. (C) Optimum pH. (D) 1 h thermal stability assayed at 50 °C after incubation at different temperatures. (E) Long term thermal stability measured at 50 °C after incubation at 30 °C (●), 50 °C (▲) and 60 °C (■).

Research Council (MINECO, Spain), grant BIOFABCEL CTQ2017-84966-C2-2-R, by Pla de Recerca de Catalunya, grant 2017SGR-30, and Generalitat de Catalunya to the Xarxa de Referència en Biotecnologia" (XRB).

Ethical Statement

This article does not contain any studies with human participants or animals performed by any of the authors.

CRediT authorship contribution statement

Carolina Buruaga-Ramiro: Conceptualization, Data curation, Investigation, Validation. **Susana V. Valenzuela:** Data curation, Methodology, Software. **F.I.J. Pastor:** Funding acquisition, Project administration. **Josefina Martínez:** Formal analysis, Methodology, Resources, Supervision, Validation, Writing - original draft. **Pilar Diaz:** Conceptualization, Funding acquisition, Funding acquisition, Project administration, Resources, Supervision, Writing - original draft, Writing - review & editing.

Declaration of Competing Interest

All authors declare that they have no conflict of interest.

Acknowledgements

We thank the Serveis Cientifico-Tècnics of the University of Barcelona for technical support in sequencing and A. Calbet is

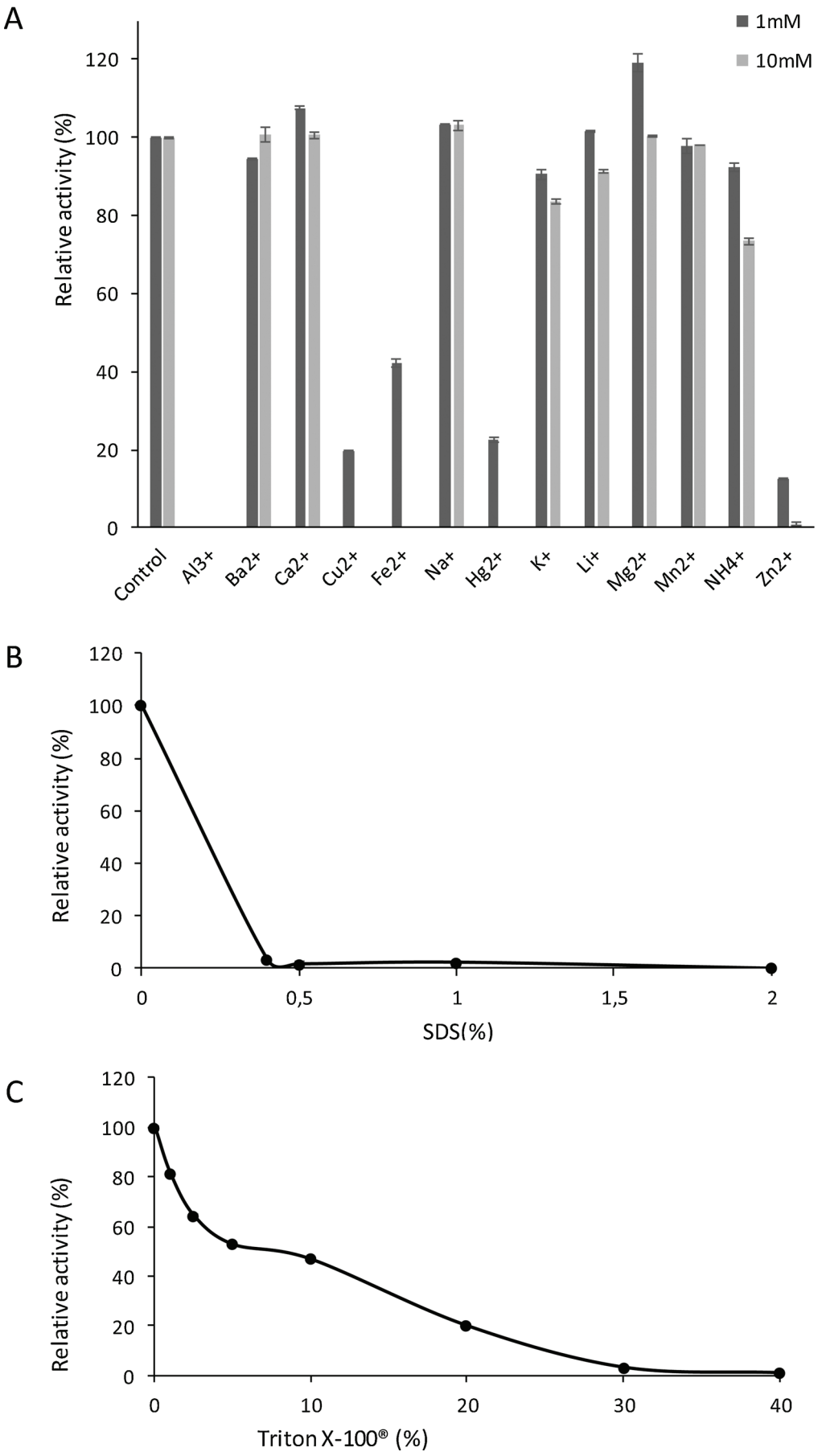

(caption on next page)

Fig. 5. Inhibition/activation assays of *E. coli* lipolytic activity, measured on MUF-heptanoate (A) or *p*NP-octanoate (B, C) at 50 °C. Effect of different metal ions assayed at 1 and 10 mM (A), SDS (B) and Triton X-100® (C) on activity. Although SDS caused complete activity inhibition at 0.4% concentration (used in SDS-PAGE analysis), 80% activity recovery can be achieved after the renaturing/refolding tratment with 2.5% Triton X-100®, as described previously [26,27].

acknowledged for technical assistance. C. Buruaga-Ramiro acknowledges an APIF pre-doctoral grant from the University of Barcelona.

Appendix A. Supplementary data

Supplementary material related to this article can be found, in the online version, at doi:https://doi.org/10.1016/j.enzmictec.2020.109590.

References

[1] K.E. Jaeger, B.W. Dijkstra, M.T. Reetz, Bacterial biocatalysts: molecular biology, three-dimensional structures, and biotechnological applications of lipases, Annu. Rev. Microbiol. 53 (1999) 315, https://doi.org/10.1146/annurev.micro.53.1.315.

[2] U.T. Bornscheuer, C. Bessler, R. Srinivas, S.H. Krishna, S. Hari Krishna, Optimizing lipases and related enzymes for efficient application, Trends Biotechnol. 20 (2002) 433–437.

[3] T. Drepper, T. Eggert, W. Hummel, C. Leggewie, M. Pohl, F. Rosenau, S. Wilhelm, K.-E. Jaeger, Novel biocatalysts for white biotechnology, Biotechnol. J. 1 (2006) 777–786.

[4] K.-E. Jaeger, M.T. Reetz, Microbial lipases form versatile tools for biotechnology, Trends Biotechnol. 16 (1998) 396–403.

[5] R. Gupta, A. Kumari, P. Syal, Y. Singh, Molecular and functional diversity of yeast and fungal lipases: their role in biotechnology and cellular physiology, Prog. Lipid Res. 57 (2015) 40–54.

[6] R. Gupta, N. Gupta, P. Rathi, Bacterial lipases: an overview of production, purification and biochemical properties, Appl. Microbiol. Biotechnol. 64 (2004) 763–781.

[7] G. Angajala, P. Pavan, R. Subashini, Lipases: an overview of its current challenges and prospectives in the revolution of biocatalysis, Biocatal. Agric. Biotechnol. 7 (2016) 257–270, https://doi.org/10.1016/j.bcab.2016.07.001.

[8] S. Cesarini, R.F. Haller, P. Diaz, P.M. Nielsen, Combining phospholipases and a liquid lipase for one-step biodiesel production using crude oils, Biotechnol. Biofuels 7 (2014) 29.

[9] U.T. Bornscheuer, Microbial carboxyl esterases: classification, properties and application in biocatalysis, FEMS Microbiol. Rev. 26 (2002) 73–81, https://doi.org/10.1111/j.1574-6976.2002.tb00599.x.

[10] G. Antranikian, U.T. Bornscheuer, A. Liese, Highlights in biocatalysis, ChemCatChem. 2 (2010) 879–880, https://doi.org/10.1002/cctc.201000228.

[11] U.T. Bornscheuer, R.J. Kazlauskas, Hydrolases in Organic Synthesis: Regio- and Stereoselective Biotransformations, Wiley-VCH, 2006.

[12] U.T. Bornscheuer, Biocatalysis: successfully crossing boundaries, Angew. Chemie Int. Ed. 55 (2016) 4372–4373, https://doi.org/10.1002/anie.201510042.

[13] A. Bassegoda, A. Fillat, F.I.J. Pastor, P. Diaz, Special Rhodococcus sp. CR-53 esterase Est4 contains a GGG(A)X-oxyanion hole conferring activity for the kinetic resolution of tertiary alcohols, Appl. Microbiol. Biotechnol. 97 (2013) 8559–8568, https://doi.org/10.1007/s00253-012-4676-x.

[14] C. Bofill, N. Prim, M. Mormeneo, A. Manresa, F.I. Javier Pastor, P. Diaz, F.I.J. Pastor, P. Diaz, Differential behaviour of *Pseudomonas* sp. 42A2 LipC, a lipase showing greater versatility than its counterpart LipA, Biochimie 92 (2010) 307–316.

[15] B. Infanzón, S.V. Valenzuela, A. Fillat, F.I.J. Pastor, P. Diaz, Unusual carboxylesterase bearing a GGG(A)X-type oxyanion hole discovered in Paenibacillus barcinonensis BP-23, Biochimie. 104 (2014) 108–116, https://doi.org/10.1016/j.biochi.2014.06.003.

[16] G. Nantel, P. Proulx, Lipase activity in *E. coli.* Biochim. Biophys. Acta 316 (1973) 156–161, https://doi.org/10.1016/0005-2760(73)90005-2.

[17] E. Kuznetsova, M. Proudfoot, S.A. Sanders, J. Reinking, A. Savchenko, C.H. Arrowsmith, A.M. Edwards, A.F. Yakunin, Enzyme genomics: application of general enzymatic screens to discover new enzymes, FEMS Microbiol. Rev. 29 (2005) 263–279, https://doi.org/10.1016/j.femsre.2004.12.006.

[18] J. Ribera, M. Estupiñán, A. Fuentes, A. Fillat, J. Martínez, P. Diaz, *Bacillus* sp. JR3 esterase LipJ: a new mesophilic enzyme showing traces of a thermophilic past, PLoS One 12 (2017) e0181029, , https://doi.org/10.1371/journal.pone.0181029.

[19] A. Bassegoda, F.I.J. Pastor, P. Diaz, *Rhodococcus* sp. Strain CR-53 lipR, the first member of a new bacterial lipase family (Family X) displaying an unusual Y-type oxyanion hole, similar to the Candida antarctica lipase clan, Appl. Environ. Microbiol. 78 (2012) 1724–1732.

[20] G. Kouker, K.E. Jaeger, Specific and sensitive plate assay for bacterial lipases, Appl. Environ. Microbiol. 53 (1987) 211–213.

[21] C. Ruiz, F.I.J. Pastor, P. Diaz, Isolation of lipid- and polysaccharide-degrading micro-organisms from subtropical forest soil, and analysis of lipolytic strain *Bacillus* sp. CR-179, Lett. Appl. Microbiol. 40 (2005) 218–227, https://doi.org/10.1111/j.1472-765X.2005.01660.x.

[22] J. Sambrook, D.W. Russell, Molecular Cloning: a Laboratory Manual, Cold Spring Harbor Laboratory Press, Plainview, NY, USA, 2001, pp. 11803–12500.

[23] M.M. Bradford, Rapid and sensitive method for quantitation of microgram quantities of protein utilizing principle of protein dye binding, Anal. Biochem. 72 (1976) 248–254.

[24] A. Bassegoda, G.-S.S. Nguyen, M. Schmidt, R. Kourist, P. Diaz, U.T. Bornscheuer, Rational protein design of Paenibacillus barcinonensis esterase EstA for kinetic resolution of tertiary alcohols, ChemCatChem. 2 (2010) 962–967.

[25] U.K. Laemmli, Cleavage of structural proteins during assembly of head of bacteriophage-T4, Nature. 227 (1970) 680-.

[26] N. Prim, M. Sánchez, C. Ruiz, F.I.J. Pastor, P. Diaz, Use of methylumbeliferyl-derivative substrates for lipase activity characterization, J. Mol. Catal. B Enzym. (2003), https://doi.org/10.1016/S1381-1177(03)00048-1.

[27] P. Diaz, N. Prim, F.I.J. Pastor, Direct fluorescence-based lipase activity assay, Biotechniques. 27 (1999) 696–699.

[28] C. Ruiz, S. Falcocchio, E. Xoxi, F.I. Javier Pastor, P. Diaz, L. Saso, F.I.J. Pastor, Activation and inhibition of *Candida rugosa* and *Bacillus*-related lipases by saturated fatty acids, evaluated by a new colorimetric microassay, Biochim. Biophys. Acta – General Subj. 1672 (2004) 184–191.

[29] B. Infanzón, P.H. Sotelo, J. Martínez, P. Diaz, Rational evolution of the unusual Y-type oxyanion hole of Rhodococcus sp. CR53 lipase LipR, Enzyme Microb. Technol. 108 (2018) 26–33, https://doi.org/10.1016/j.enzmictec.2017.09.001.

[30] M. Estupiñán, C. Buruaga, F.I.J. Pastor, J. Martínez, P. Diaz, Shift in *Bacillus* sp. JR3 esterase LipJ activity profile after addition of essential residues from family I.5 thermophilic lipases, Biochem. Eng. J. 144 (2019) 166–176, https://doi.org/10.1016/j.bej.2019.01.023.

[31] A. Bassegoda, F.I.J. Pastor, P. Diaz, Rhodococcus sp. Strain CR-53 LipR, the first member of a new bacterial lipase family (Family X) Displaying an unusual Y-Type oxyanion hole, similar to the Candida antarctica lipase clan, Appl. Environ. Microbiol. 78 (2012) 1724–1732, https://doi.org/10.1128/AEM.06332-11.

[32] C. Ruiz, S. Falcocchio, F.I.J. Pastor, L. Saso, P. Diaz, Helicobacter pylori EstV: identification, cloning, and characterization of the first lipase isolated from an epsilon-proteobacterium, Appl. Environ. Microbiol. 73 (2007) 2423–2431, https://doi.org/10.1128/aem.02215-06.

[33] N. Prim, A. Blanco, J. Martinez, F.I.J. Pastor, P. Diaz, estA, a gene coding for a cell-bound esterase from Paenibacillus sp BP-23, is a new member of the bacterial subclass of type B carboxylesterases, Res. Microbiol. 151 (2000) 303–312, https://doi.org/10.1016/s0923-2508(00)00150-9.

[34] N. Prim, F.I.J. Pastor, P. Diaz, Cloning and Characterization of a Bacterial Cell-Bound Type B Carboxylesterase from *Bacillus* sp. BP-7, Curr. Microbiol. 42 (2001) 237–240, https://doi.org/10.1007/s002840110210.

[35] A. Biundo, G. Steinkellner, K. Gruber, T. Spreitzhofer, D. Ribitsch, G.M. Guebitz, Engineering of the zinc-binding domain of an esterase from Clostridium botulinum towards increased activity on polyesters, Catal. Sci. Technol. 7 (2017) 1440–1447, https://doi.org/10.1039/C7CY00168A.

[36] E. Timucin, A. Cousido-Siah, A. Mitschler, A. Podjarny, O.U. Sezerman, Probing the roles of two tryptophans surrounding the unique zinc coordination site in lipase family I.5, Proteins 84 (2015) 129–142.

[37] N. Varejão, R.A. De-Andrade, R.V. Almeida, C.D. Anobom, D. Foguel, D. Reverter, Structural mechanism for the temperature-dependent activation of the hyperthermophilic Pf2001 esterase, Structure. 26 (2018) 199–208, https://doi.org/10.1016/j.str.2017.12.004 e3.

[38] S.-T. Jeong, H.-K. Kim, S.-J. Kim, S.-W. Chi, J.-G. Pan, T.-K. Oh, S.-E. Ryu, Novel zinc-binding center and a temperature switch in theBacillus stearothermophilus L1 lipase, J. Biol. Chem. 277 (2002) 17041–17047, https://doi.org/10.1074/jbc.M200640200.

[39] C. Carrasco-López, C. Godoy, B. de las Rivas, G. Fernández-Lorente, J.M. Palomo, J.M. Guisán, R. Fernández-Lafuente, M. Martínez-Ripoll, J.A. Hermoso, Activation of bacterial thermo alkalophilic lipases is spurred by dramatic structural rearrangements, J. Biol. Chem. 284 (2009) 4365–4372, https://doi.org/10.1074/jbc.M808268200.

[40] P. Panizza, S. Cesarini, P. Diaz, S. Rodríguez Giordano, Saturation mutagenesis in selected amino acids to shift Pseudomonas sp. Acidic lipase Lip I.3 substrate specificity and activity, Chem. Commun. 51 (2015) 1330–1333, https://doi.org/10.1039/C4CC08477B.

[41] S. Cesarini, C. Bofill, F.I.J. Pastor, M.T. Reetz, P. Diaz, A thermostable variant of P. Aeruginosa cold-adapted LipC obtained by rational design and saturation mutagenesis, Process Biochem. 47 (2012) 2064–2071, https://doi.org/10.1016/j.procbio.2012.07.023.

4.2. Capítulo 2. Funcionalización de la celulosa bacteriana: inmovilización de enzimas

4.2.1. ***Artículo 3.*** *Bacterial cellulose matrices to develop enzymatically active paper.*

4.2.2. ***Artículo 4.*** *Development of an antimicrobial bioactive paper made from bacterial cellulose.*

Bacterial cellulose matrices to develop enzymatically active paper

Este trabajo estudia la idoneidad de diferentes matrices de celulosa bacteriana para preparar nanocomposites enzimáticamente activos, siempre dentro de un marco de tecnologías más amigables con el medio ambiente. Después de la producción y la purificación de la CB, se obtuvieron dos matrices: CB en suspensión acuosa (BCS, por sus siglas en inglés *Bacterial Cellulose Suspesion*) y papel de CB (BCP por sus siglas en inglés *Bacterial Cellulose Paper*). A continuación, se inmovilizó una lipasa en ambas por adsorción física, obteniendo los nanocomposites de Lipasa/CB. Una vez constatado que ni la morfología ni la cristalinidad, analizadas mediante microscopía electrónica de barrido y difracción de rayos-X, respectivamente, se vieron afectadas por la unión de la enzima, se midió la actividad específica en diferentes condiciones y se procedió a la evaluación de las propiedades operacionales. En comparación a la enzima libre, se observó un desplazamiento hacia temperaturas más elevadas, actividades en rangos de pH más amplios y un leve cambio de tendencia en la especificidad de sustrato. Aunque la actividad específica del nanocomposite Lipasa/BCS era ligeramente más elevada que la del nanocomposite Lipasa/BCP, éste último mostró una gran estabilidad térmica, reusabilidad y durabilidad: retuvo un 60 % de la actividad después de 48 h a 60 ºC, mantuvo el 100 % de actividad después de reciclar el nanocomposite diez veces a pH 7 y a 60 ºC y siguió siendo activo después de ser almacenado durante más de un mes a temperatura ambiente. Los resultados, pues, sugirieron que los nanocomposites Lipasa/CB son materiales prometedores para el desarrollo de estrategias biotecnológicas verdes con potencial aplicación tanto en procesos industriales, como la industria de detergentes y alimentaria, como en biomedicina. En concreto, el nanocomposite Lipasa/BCP podría ser un elemento clave en la elaboración de papeles bioactivos de dispositivos simples, portátiles y desechables.

Cellulose
https://doi.org/10.1007/s10570-020-03025-9

ORIGINAL RESEARCH

Bacterial cellulose matrices to develop enzymatically active paper

Carolina Buruaga-Ramiro · Susana V. Valenzuela · Cristina Valls · M. Blanca Roncero · F. I. Javier Pastor · Pilar Díaz · Josefina Martínez

Received: 18 November 2019 / Accepted: 26 January 2020

Abstract This work studies the suitability of bacterial cellulose (BC) matrices to prepare enzymatically active nanocomposites, in a framework of more environmentally friendly methodologies. After BC production and purification, two kind of matrices were obtained: BC in aqueous suspension and BC paper. A lipase was immobilised onto the BC matrices by physical adsorption, obtaining Lipase/BC nanocomposites. Neither morphology nor crystallinity, measured by scanning electron microscopy and X-ray diffractometry respectively, of the BC were affected by the binding of the protein. The activity of Lipase/BC suspension and Lipase/BC paper was tested under different conditions, and the operational properties of the enzyme were evaluated. A shift towards higher temperatures, a broader pH activity range, and slight differences in the substrate preference were observed in the immobilised lipase, compared with the free enzyme. Specific activity was higher for Lipase/BC suspension (4.2 U/mg) than for Lipase/BC paper (1.7 U/mg) nanocomposites. However, Lipase/BC paper nanocomposites showed improved thermal stability, reusability, and durability. Enzyme immobilised onto BC paper retained 60% of its activity after 48 h at 60 °C. It maintained 100% of the original activity after being recycled 10 times at pH 7 at 60 °C and it remained active after being stored for more than a month at room temperature. The results suggested that lipase/BC nanocomposites are promising biomaterials for the development of green biotechnological devices with potential application in industrials bioprocesses of detergents and food industry and biomedicine. Lipase/BC paper nanocomposite might be a key component of bioactive paper for developing simple, handheld, and disposable devices.

C. Buruaga-Ramiro · S. V. Valenzuela · F. I. J. Pastor · P. Díaz · J. Martínez (✉)
Department of Genetics, Microbiology and Statistics, Faculty of Biology, University of Barcelona, Av. Diagonal 643, 08028 Barcelona, Spain
e-mail: jmartinez@ub.edu

C. Buruaga-Ramiro
e-mail: buruaga.cbr@ub.edu

S. V. Valenzuela
e-mail: susanavalenzuela@ub.edu

F. I. J. Pastor
e-mail: fpastor@ub.edu

P. Díaz
e-mail: pdiaz@ub.edu

C. Buruaga-Ramiro · S. V. Valenzuela · F. I. J. Pastor · P. Díaz · J. Martínez
Institute of Nanoscience and Nanotechnology (IN2UB), Universitat de Barcelona, Barcelona, Spain

C. Valls · M. B. Roncero
CELBIOTECH_Paper Engineering Research Group, EGE Department, Universitat Politècnica de Catalunya, Barcelona Tech, 08222 Terrassa, Spain
e-mail: cristina.valls@upc.edu

M. B. Roncero
e-mail: blanca.roncero@upc.edu

Published online: 31 January 2020

Graphic abstract

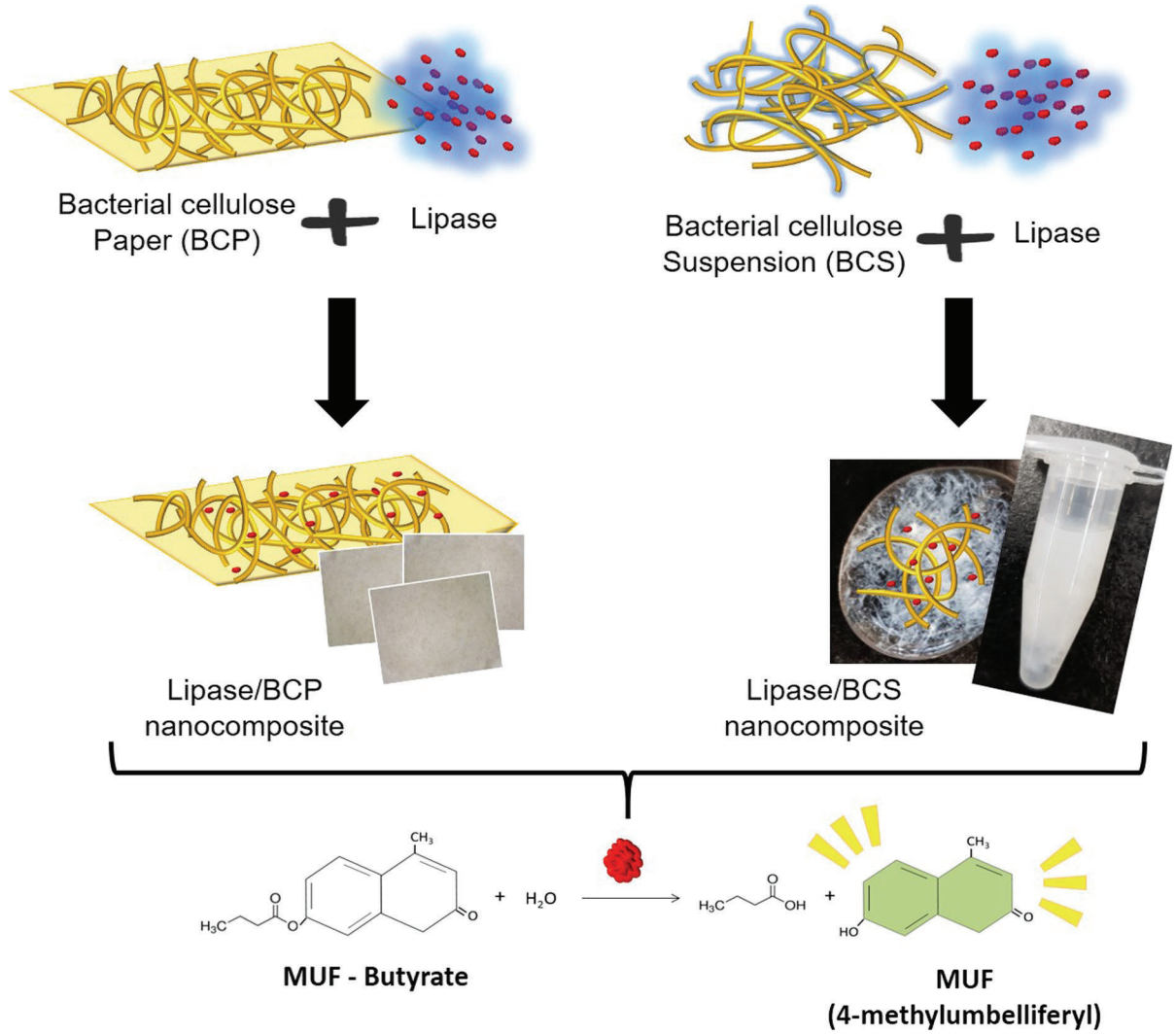

Keywords Bacterial cellulose · Lipase immobilization · Physical adsorption · Nanocomposite · Bacterial cellulose biopaper

Introduction

In recent years has been increasing interest in the design of functional nanocomposites for advanced biotechnological applications. Nanocomposites consist of the combination of two types of individual materials, the matrix and the material imbedded on it, being at least one of the two of nano size dimension. Often, the matrix acts as a scaffold and supports an organic molecule with biological activity (Mohamad et al. 2015). The matrix provides the physic-chemical characteristics to the composite, while the molecule in it imparts biological properties to the matrix. Over the last two decades, the study of cellulosic nanofibres as the supporting matrix in nanocomposites has become an increasingly topical subject (Ferreira et al. 2018).

Cellulose is very abundant in nature and the biopolymer of choice in many applications. Traditionally plants have been the main source of cellulose. However, plant-derived cellulose is always bound to hemicelluloses and lignin and, before further used, it needs to be purified by enzymatic, chemical and/or

mechanical treatments that have a high economic and environmental impact (Abdul Khalil et al. 2012). Cellulose synthesized by bacteria is referred to as bacterial cellulose (BC), an extracellular polymer produced by some microorganisms, especially from the genera *Komagateibacter* (Bielecki et al. 2005). Apart from being chemically pure (Chawla et al. 2009), BC displays a higher degree of crystallinity, a higher tensile strength, a higher water-holding capacity and a finer three-dimensional nanofibre network, being all these features of relevant importance for practical applications (Yano et al. 2005; Lee et al. 2014). Its three-dimensional open porous network structure of nanofibres, with a large surface area, is suitable to hold a large amount of inorganic and organic molecules. Moreover, cellulose contains available hydroxyl groups in its surface that provide the possibility of molecular adsorption by the formation of hydrogen bonds and electrostatic interactions (Pahlevan et al. 2018). In fact, BC has been used in the preparation of several composite materials for various applications, such as in electrical devices, batteries, biosensors, electromagnetic shielding, biomedical applications or electrochromic devices (Evans et al. 2003; Kim et al. 2011; Shi et al. 2012; Ul-Islam et al. 2012a, b; Hänninen et al. 2015; Zhou et al. 2019).

Immobilization of enzymes has several advantages, such as easy separation of enzyme from products in the reaction mix, reusability of the enzyme and increased stability (Wang 2006; Omagari et al. 2009; Kadokawa 2012). These characteristics have promoted the widely utilization of enzyme immobilization in industry (Klemm et al. 1998; Božič et al. 2012). In biotechnology, immobilized enzyme-based biosensors have huge applications in various fields as biomedicine, the detection of environmental pollutants or the monitoring of food safety and industrial bioprocesses (Monosik et al. 2012; Nigam and Shukla 2015; Rocchitta et al. 2016). The use of nanomaterials as enzyme supports have expanded its applicability (Molinero-Abad et al. 2014). However, the development of new nanomaterials that are cheap, highly pure and non-toxic is needed (Kim et al. 2015).

BC is an attractive biocompatible candidate as a carrier for the immobilization of enzymes. Its porous ultrafine network allows for high accessibility onto the active site, through low diffusion resistance and easy recoverability as well as potential applicability for continuous operations (Sulaiman et al. 2015). In addition, BC is considered not only safer but more environmentally friendly than other nanomaterials (Lu et al. 2013). An effective enzyme immobilization on BC can be achieved using methods such as covalent binding or cross linking (Yao et al. 2013; Lin and Dufresne 2014). However, these methods often require chemical modifications of the matrix and/or the use of chemical linkers that complicate the procedure limiting the functionality of the composite generating residues that are harmful for the environment (Castro et al. 2014). Physical methods for the immobilization of enzymes imply the attachment of the biomolecule to the matrix through physical forces such as van der Waals, electrostatic or hydrophobic interactions, and hydrogen bounding (Credou and Berthelot 2014). They do not need chemical modification of either the matrix or the enzyme, allowing minimal configuration change of the enzyme (Choi 2004). Enzyme immobilization by physical adsorption has been described for lysozyme onto BC fibres in suspension (Bayazidi et al. 2018), for lipase onto BC nanocrystals (Kim et al. 2015) and for nisin, laccase and lipase onto BC membranes (Wu et al. 2017; Yuan et al. 2018; dos Santos et al. 2018). Nevertheless, obtaining an enzymatically active BC nanocomposite that had the physical characteristics and the handiness of the paper would be of great interest.

The aim of this paper was to prepare Enzyme/BC nanocomposites to evaluate the suitability of BC matrices as supports for enzyme immobilization by physical adsorption. Among the great variety of enzymes, lipases (EC 3.1.1.3, triacylaglycerol hydrolases) have gained much attention as the most powerful biocatalyst for applications in areas such as food technology, detergent formulation, flavour and drug production and biofuel synthesis, among others (Angajala et al. 2016). Therefore, a lipase was chosen due to its enormous relevance in the development of bioassays and biosensors (Pohanka 2019). Protein loading, hydrolytic activity and enzymatic stability of lipases immobilized on BC matrices were evaluated at different conditions of pH and temperature and compared to free lipase. Matrices of both BC suspension (BCS) and BC paper (BCP) were compared. To the best of our knowledge, this is the first description of enzyme immobilization in BC paper, a matrix that combine the high surface-to-volume ratio of the BC nanofibres with the stiffness and the mechanical

properties of paper, and that could lead to the design of devices for high performance applications.

Experimental section

Materials

Komagataeibacter intermedius JF2, a bacterial cellulose producer, was previously isolated in the laboratory (Fernández et al. 2019). Callera™ Trans L, a commercial liquid formulation of *Thermomyces lanuginosus* lipase (Nordblad et al. 2014) was supplied by Novozymes. Lipase (37 kDa, pI 4.4) was purified (elution buffer: 20 mM TrisHCl pH 7, 500 mM NaCl and 0.02% sodium azide) from the commercial preparation by ionic exchange chromatography using HiTrap™ Q HP (GE Healthcare) columns in an AKTA™ FPLC protein purification system.

Preparation of bacterial cellulose matrices

To produce BC, *K. intermedius* JF2 was grown on the Hestrin and Schramm (HS) medium, containing 20 g/L glucose, 20 g/L peptone, 10 g/L yeast extract, 1.15 g/L citric acid, 6.8 g/L Na_2HPO_4, pH 6. The cultures were statically incubated at 25–28 °C for 7 days. After incubation, bacterial cellulose membranes generated in the air/liquid interface of the culture media were harvested, rinsed with water and incubated in 1% NaOH at 70 °C overnight. Finally, the BC membranes were thoroughly washed in deionized water until the pH reached neutrality. Membranes were mechanically disrupted with a blender and homogenized (Homogenizing System UNIDRIVE X1000) to obtain a BC paste containing a suspension of BC fibres. The amount of BC in the suspension was determinate by drying samples of known weight at 60 °C until constant weight was reached. The bacterial cellulose paste was used to produce BC paper sheets using a Rapid–Köthen laboratory former (Frank–PTI) following the ISO-5269:2004 standard method, obtaining a bacterial cellulose paper (BCP) matrix of a weight of 70 g/m^2. The BC in aqueous suspension (BCS) matrix was obtained diluting the BC paste at to 7 mg/mL. Procedures for the generation of CB matrices are schematized in Fig. 1.

Preparation of lipase/bacterial cellulose nanocomposites

Adsorption of lipase to BC matrices was conducted as follows: for BCP matrices, pieces of 1 cm^2 (7 mg ± 0.2) were immersed into the lipase binding solution (10 µg/mL, 20 mM TrisHCl pH 7), and incubated at 22 °C with slight shaking for 18 h. Then, samples were removed, washed twice by dipping in buffer solution (20 mM TrisHCl, pH 7), air-dried and stored at room temperature. For adsorption of lipase in BCS matrices, a volume containing 7 mg of dry BC was centrifuged 5 min at 4000 rpm in an Allegra™ X-22R benchtop centrifuge (Beckman Coulter) to remove excess of water and resuspended in the same volume of lipase binding solution. After incubation at 22 °C with slight shaking for 18 h, the solids were separated by centrifugation and washed twice with the buffer solution to remove the unbound enzyme. Finally, pellet was resuspended in the same buffer and stored at 4 °C before used.

Protein determination

The content of protein in the composites was determined comparing initial and final concentrations of protein in the lipase binding solution according to the Bradford's protein assay (Bradford 1976). The residual protein in the washing solutions was considered. Protein loading was calculated using Eq. (1) (Chen et al. 2015).

$$\begin{aligned} &Protein\ loading\left(\frac{\mu g}{g\ BC}\right) \\ &= [Total\ protein\ of\ free\ lipase\ (\mu g) \\ &\quad - Total\ residual\ protein\ of\ free\ lipase\ after\ immobilization\ (\mu g)]/[Total\ mass\ of\ BC\ matrix\ (g)] \end{aligned} \tag{1}$$

Scanning electron microscopy (SEM)

Dried samples of Lipase/BC nanocomposites were analysed by SEM (JSM 7100 F) using a LED filter. Samples were graphite coated using a Vacuum Evaporator EMITECH K950X221. The diameter of the fibres was measured using the ImageJ software.

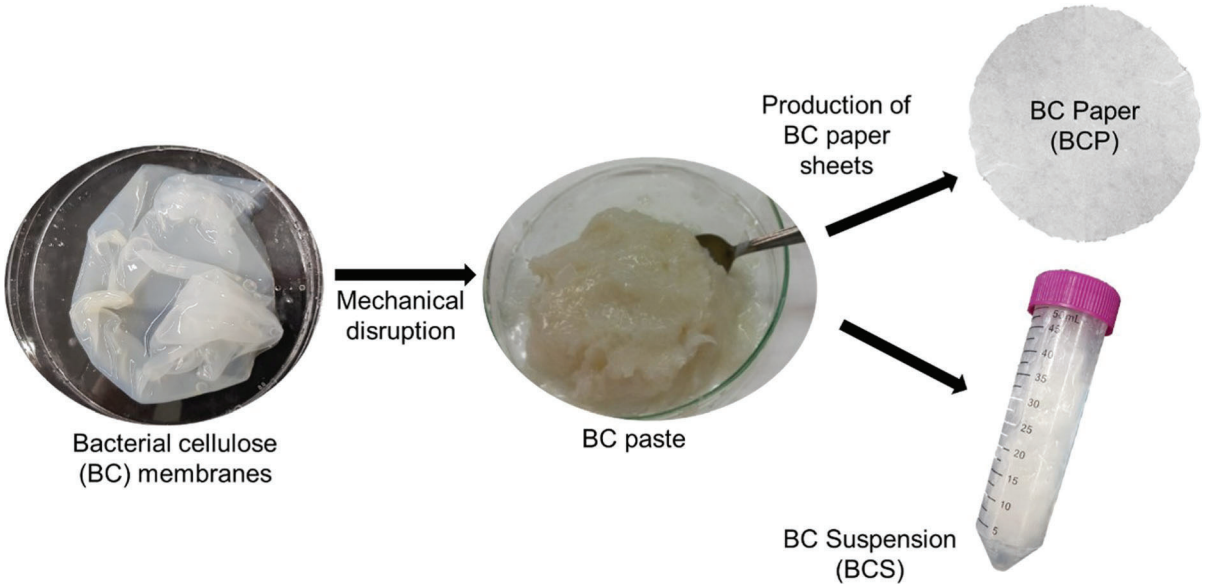

Fig. 1 Schematic representation of the process to obtain bacterial cellulose matrices

X-ray diffractometry (XRD)

Dried samples of Lipase/BC nanocomposites were subjected to XRD analysis (PANalytical X'Pert PRO MPD Alpha1 powder diffractometer). The samples were analysed at the radiation wavelength of 1.5406 Å. Samples were scanned from 2° to 50°, 2θ range. Samples were fixed over a zero background Silicon single crystal sample holder (PW1817/32), and the ensembles were mounted in a PW1813/32 sample holder. All the replicates of each sample were measured with the same Silicon holder. The crystallinity index (CI) of produced bacterial cellulose was calculated based on Eq. (2) (Segal et al. 1959):

$$\mathrm{CI}(\%) = \frac{\mathrm{I_c} - \mathrm{I_{am}}}{\mathrm{I_c}} \times 100 \quad (2)$$

where I_c is the maximum intensity of the lattice diffraction and I_{am} is the intensity of the peak at 2θ = 18°, which corresponds to the amorphous part of cellulose. The intensity of the peaks was measured as the maximum value obtained for the peak considering a baseline.

Water absorption capacity

To assess the water absorption capacity of the BC paper, samples were weighted and immersed in deionized water for 24 h. After 24 h, excess of water was removed, and the weight was measured. The WAC was expressed according Eq. (3):

$$\mathrm{WAC} = \frac{\mathrm{W_{wet}} - \mathrm{W_{dry}}}{\mathrm{W_{dry}}} \quad (3)$$

where W_{wet} is the weight of wet BC paper and W_{dry} is the initial weight of the dried BC paper.

Operational properties of the immobilized lipase

Lipase hydrolytic activity was analysed by measuring the release of MUF (methylumbelliferone) from MUF-derivate fatty acid (C4, C7, and C18) substrates (Sigma-Aldrich). Stock solutions of MUF-substrates were prepared at 25 mM in ethylene glycol methyl ester (EGME). The working solution contained 250 µM of MUF-substrates in 20 mM TrisHCl pH 7. MUF was measured using a Varian Cary Eclipse spectrofluorometer (Agilent Technologies) equipped with a microplate reader, as previously reported (Panizza et al. 2013). One unit of activity was defined as the amount of enzyme that released one mmol of MUF per minute under the assay conditions. The specific activity and the recovery of lipase activity were calculated using Eqs. (4) and (5).

$$\text{Specific activity of immobilized lipase}\left(\frac{\text{U}}{\text{mg protein}}\right) = \frac{\text{Activity of immobilized enzyme}\left(\frac{\text{U/mL}}{\text{g BC}}\right)}{\text{Protein loading}\left(\frac{\text{mg protein/mL}}{\text{g BC}}\right)} \quad (4)$$

$$\text{Recovery of lipase activity}\ (\%) = \frac{\text{Specific activity of immobilized lipase}}{\text{Specific activity of free lipase}} \times 100 \quad (5)$$

The determination of the operational characterization and properties of Lipase/BC nanocomposites was carried out with samples containing 7 mg BC (dry weigh)/mL. For Lipase/BCP, the nanocomposites were immersed into the appropriated buffer at the conditions being analysed. For Lipase/BCS nanocomposites, samples were centrifuged, and solids were suspended into the appropriated buffer, at the conditions being analysed. Assays of free lipase activity were run in parallel.

Influence of temperature and thermal stability

Optimum temperature of free and absorbed lipase was determined by the analysis of the activity over a range from 30 to 90 °C at pH 7. Long-term thermal stability was analysed based on the residual activity of lipase measured after incubation at 60 °C in 20 mM TrisHCl pH 7 for a determinate period of time.

Influence of pH

Optimum pH of free and absorbed lipase was determined by analysis of the activity at various pH values with the appropriate buffers 20 mM: acetate buffer (pH 4 and 5), phosphate buffer (pH 6) and TrisHCl (pH 7, 8 and 9).

Determination of kinetics constants

The determination of the Michaelis–Menten constant (K_m) and the maximum reaction rate (V_{max}) of both free and immobilized lipase were carried out using MUF-butyrate as substrate, with initial concentrations varying from 50 to 1000 μM. The kinetic parameters were calculated by fitting hyperbolic Michaelis–Menten curves with GraphPad Prism 6 software (San Diego, California).

Statistical analysis

All determinations of enzyme activity were performed after two replicas of triplicates (6 determinations per sample). Experimental data were expressed as means ± standard deviations and were analysed statistically by the paired Student's t test method and analysis of variance (ANOVA) in STATGRAPHICS Centurion XVIII software (Statgraphics.Net, Madrid) among more than two groups. Scheffe's multiple range test was used to detect differences among mean values. A value of $p \leq 0.05$ was considered statistically significant. Bartlett's test was used to test homogeneity of variance for all samples. Assumption that the residuals were normally distributed was tested with the Shapiro–Wilk test.

Results and discussion

Adsorption of lipase in BC matrices and activity of the BC nanocomposites

pH plays a key role in the immobilization process by physical adsorption of proteins onto cellulose (Lin et al. 2015). The optimal pH for lipase immobilization into BC paper was tested in acetate buffer at pH 3 and 5, and TrisHCl buffer pH 7. Buffers concentration of the lipase binding solution was 20 mM, as it is described that lower ionic strength can enhance the formation of the protein/polysaccharide composites (Chai et al. 2014). The amount of protein adsorbed into BC paper at the different pHs is shown in Table 1. Results indicated that the highest efficiency of lipase adsorption was at pH 3, suggesting electrostatic bounding between the positive charged protein and the overall negative charge cellulose due to hydroxyl groups and molecular dipole. However, when enzymatic activity of the obtained Lipase/BC paper nanocomposites was measured under standard conditions, at pH 7, the enzyme immobilized at pH 3 showed less specific activity than the immobilized at pH 5 and at pH 7 (Table 1). These results suggested that the buffer at pH 3 used for the immobilization process, while favouring its binding, inactivated the enzyme. Therefore, and to maintain the same working

Table 1 Effect of the pH on the adsorption of the lipase onto BC paper and enzymatic activity of the adsorbed lipase

pH	Lipase adsorbed (μg/cm^2)	Specific activity (U/mg protein)
pH 3	5.29 ± 0.4	0.89 ± 0.03
pH 5	2.90 ± 0.36	1.99 ± 0.02
pH 7	2.65 ± 0.11	1.69 ± 0.11

conditions as in the determinations of enzymatic activity, further adsorption experiments were conducted with 20 mM Tris at pH 7, conditions that allowed both good adsorption and specific activity.

Lipase was physically adsorbed onto BC cellulose fibres, both in aqueous suspension (BCS) and in paper (BCP) obtaining Lipase/BCS and Lipase/BCP nanocomposites, respectively (Table 2). BCS showed higher capacity to adsorb protein than BCP, which could be attributed to the difference in the density of their nanofibrils' network that influences the accessibility of the protein to the matrix of cellulose. Moreover, during the process of paper production to obtain BCP matrices, the fibres of cellulose undergo dehydration through evaporation of water. The loss of the molecules of water produce irreversible formation of new hydrogen bounds between the hydroxyl groups of adjacent glucan chains that would hinder the diffusion of the protein (Seves et al. 2001). To test if this structural modification would affect the adsorption properties of the BC matrix, its water absorption capacity (WAC) was measured (Eq. 3). BCP showed a WAC of 263 ± 28%, around 37 times its dry weight. As expected, WAC of BC paper was lower than that reported for never dried native BC membranes (Meftahi et al. 2010). However, Fernandez et al. (Fernández et al. 2019) reported values of WAC of only 10–20% for dry films of BC membranes. The results obtained indicated that the dry BC paper matrices maintained enough WAC to carry out adsorption assays by immersing the paper matrix in the aqueous solution of the enzyme for its immobilization. Nevertheless, in BCP, probably most of the protein binding is taking place only in the most superficial layers of fibres of the matrix.

The obtained nanocomposites were enzymatically active, although specific activity of the immobilized enzyme decreased with respect to that of the free enzyme (Table 2). This is a common phenomenon described previously for a variety of enzymes and immobilizer supports (Lian et al. 2012). However, differences in the specific activity between the two types of Lipase/nanocomposites were observed. Enzyme bounded to BCS maintained about 68% of activity respect to the free enzyme, while enzyme bounded to BCP maintained only 28%, approximately (Table 2). The decrease of lipase activity after immobilization may be due to the changes in structural conformation of lipase and lower accessibility of substrate to its active sites (Kim et al. 2015). After the enzyme is entrapped and immobilized in the porous network of BC, more mass transfer resistance forms compared to the free enzyme, impairing the binding efficiency between the enzyme and the substrate (Chen et al. 2015). This effect is more accused for the lipase adsorbed onto BCP, which is a less porous matrix than BCS owing to its higher fibre density after water evaporation. Consequently, the lipase has less diffusional mechanisms, influencing the activity of the enzyme (Estevinho et al. 2014).

Table 2 Characteristics of lipase immobilized onto BCP and BCS matrices

Matrix	Adsorbed protein (μg/g BC)	Specific activity (U/mg protein)	Recovered activity (%)
Free enzyme	–	6.13 ± 0.4	–
Lipase/BCP nanocomposite	416.37 ± 85	1.69 ± 0.11	27.6
Lipase/BCS nanocomposite	737.35 ± 106	4.15 ± 0.14	67.7

Physical characterization of lipase/BC nanocomposites

Lipase/BC nanocomposites were characterized in terms of morphology and chemical structure and crystallinity by SEM and XRD, respectively.

Morphology observation by SEM

SEM images of BCP and BCS matrices are shown in Fig. 2. In both of them, it could be observed a connected structure consisting of ultrafine cellulose fibrils with a diameter of about 50–70 nm, which results in large surface area. This high surface area and porous features of BC would provide microchannels to entrap enzyme and would improve the contact area exposed to protein molecules (Chen et al. 2015). BCP fibres disposition was more flawless than in BCS fibres, where the fibres displayed a higher density. No changes were observed in the morphology or in the arrangement of the nanofibers after immobilization of the lipase.

Crystallinity

XRD patterns of Lipase/BC nanocomposites were measured. Figure 3 shows diffraction peaks at 2θ angles around 18.4° and 22.7°; the presence of which were ascribed to the typical profile of cellulose I (natural cellulose) in crystalline form (Chen et al. 2015) for BCP and BCS matrices and their Lipase/nanocomposites. Even though immobilization of lipase caused a slight broadening of all peaks, intensities were not dramatically changed. The estimated degree of crystallinity index (Eq. 2) of the pure BC was 94% for BCP and 93% for BCS. With the introduction of lipase, the crystallinity index did not change (94% for both nanocomposites). These results indicated that no changes in the crystalline structure within the cellulose fibres did occur during the incorporation of lipase by physical adsorption, suggesting that characteristics as mechanical strength and interfacial properties of the cellulose fiber were not modified (Huang et al. 2014).

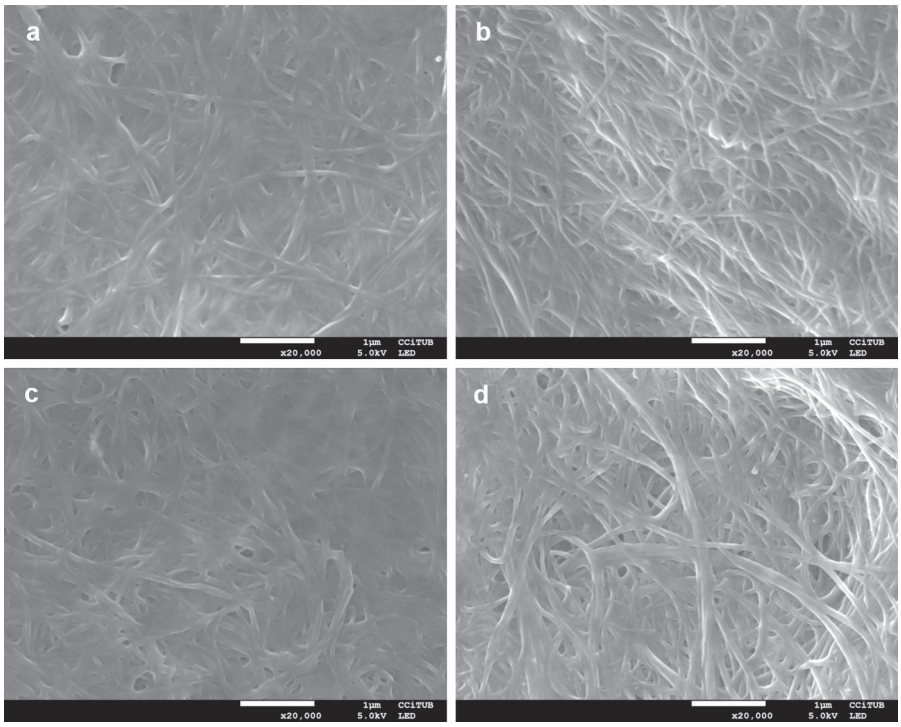

Fig. 2 Scanning electron microscopic (SEM) images of BCP (**a**), BCS (**b**), Lipase/BCP nanocomposite (**c**) and Lipase/BCS nanocomposite (**d**)

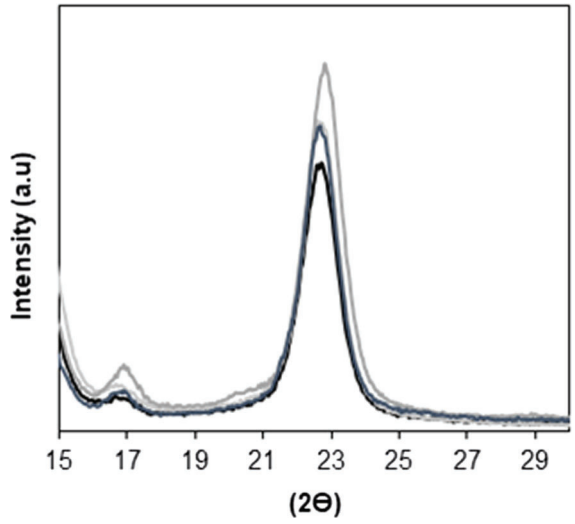

Fig. 3 XRD patterns of BCP (black line), BCS (grey line), Lipase/BCP nanocomposite (light grey line) and Lipase/BCS nanocomposite (dark grey line)

Operational properties of lipase BC/nanocomposites

Effect of the temperature and thermal stability

The effect of temperature on the activity of free and immobilized lipase was studied in the temperature range of 30–90 °C (Fig. 4a). Free enzyme had its optimum temperature activity between 40 and 50 °C, while Lipase/BCS nanocomposite retained its maxim activity at 50 °C. Remarkably, Lipase/BCP nanocomposite shifted its optimal temperature to 60–70 °C and, in addition, it broadened the range of temperature where the enzyme can be active. This shift of the optimum temperature suggested an increase in the thermal stability of the immobilized lipase, and it could be related to the change of structural stabilisation of the immobilized enzyme (Chen et al. 2015). In fact, the thermal stability of lipase at 60 °C was highly enhanced by the adsorption of lipase onto BCP (Fig. 4b). After 2 h of incubation, the residual activity of free lipase and Lipase/BCS nanocomposite was about 50% whereas the lipase immobilized onto BCP retained more than 60% of enzymatic activity after 48 h. These results highlight that the BCP matrix provided a framework of great stability for the activity of the lipase at elevated temperatures. This enhanced stability could be attributed to the restricted conformational mobility of the entrapped lipase molecules after immobilization (Frazão et al. 2014) onto cellulose matrix, delaying the rate of inactivation (Yuan et al. 2018), and it has been reported by other authors for other BC supports as BC membranes (Yuan et al. 2018) and BC nanocrystals (Kim et al. 2015).

Effect of pH

The effect of pH on the activity of free and immobilized lipase was tested under various pH (Fig. 5). The general profiles of the pH dependency were very similar; pH 8 was optimal for free enzyme and Lipase/BCP nanocomposites. Nevertheless, the higher activity of Lipase/BCS nanocomposites was preserved at a wider range of pH, showing the highest activity

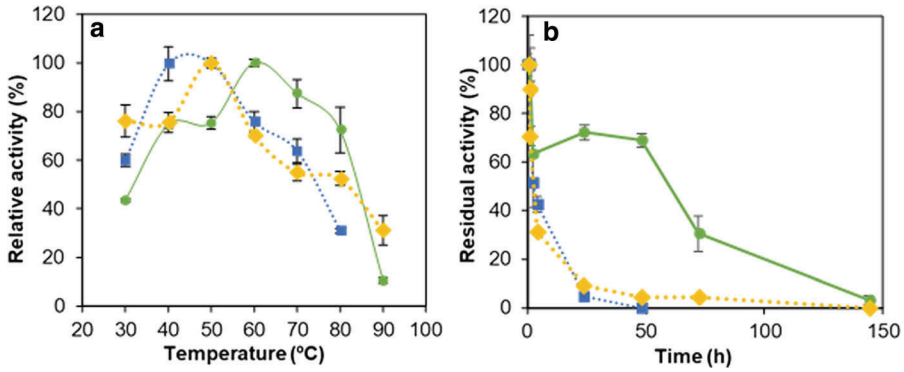

Fig. 4 Lipase activity at different temperatures (**a**). Activity was expressed in relative values, with the highest activity denoting 100%. **b** Thermal stability at 60 °C under different times of incubation, where residual activity was expressed as percentage of the initial activity at time zero. Squares line = free lipase, dots line = Lipase/BCP nanocomposite, rhombus line = Lipase/BCS nanocomposite

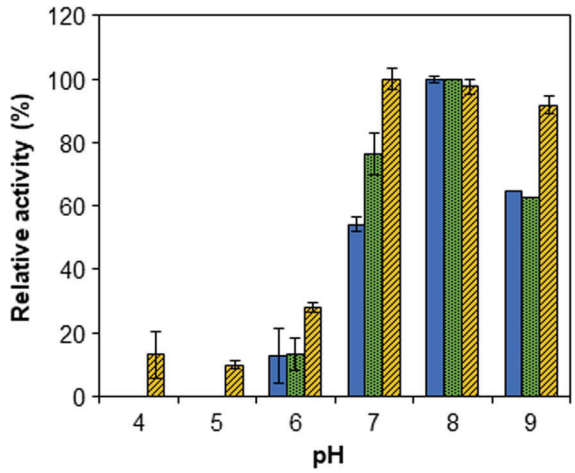

Fig. 5 Effect of pH on free lipase and the Lipase/BC nanocomposites. Activity was expressed in relative values, with the highest activity denoting 100%. Solid bars = free lipase, dot bars = Lipase/BCP, line bars = Lipase/BCS

between pH 7 and 9. Very low activity was detected at pH lower than 6.

Specificity of substrate length

Specificity of substrate length of Lipase/BCS and lipase/BCP nanocomposites was tested on MUF-derivative fatty acid of different chain-length and compared with that of the free lipase. The free enzyme and the enzyme immobilized onto BCS and BCP nanocomposites showed activity on butyrate (C4) heptanoate (C7) and oleate (C18) (Fig. 6). Butyrate was the optimum substrate, with significant differences regarding the other two assayed substrates. However, even if all of them demonstrated the same profile of relative activity, the most striking result to emerge from the data was that with oleate. Interestingly, Lipase/BCP nanocomposite showed higher activity with oleate than Lipase/BCS nanocomposite and free lipase, suggesting that the lowest water content matrix could better accommodate more hydrophobic substrates.

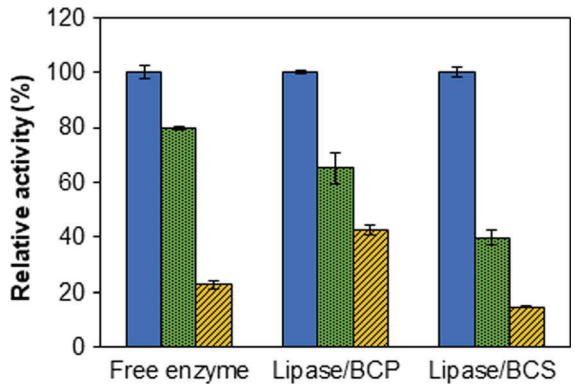

Fig. 6 Specificity of substrate for the free lipase and the Lipase/BC nanocomposites: butyrate (solid bars), heptanoate (dot bars) and oleate (line bars). Activity was expressed in relative values, with the highest activity denoting 100%

Kinetic constants

Enzyme activity was measured at different substrate concentrations (50–1000 μM) with free and immobilized lipases. The kinetic data was fitted to the Michaelis–Menten equation and parameters were calculated. The kinetic parameters are summarized in Table 3. Both K_m and V_{max} were affected by immobilization process. K_m has higher values in immobilized enzyme than the in the free one: in Lipase/BCP nanocomposite it was almost the double, whereas in Lipase/BCS nanocomposite an approximately fourfold increase was observed, indicating a weaker attachment of substrate to enzyme. Diffusional limitations due to the immobilization of the enzyme would cause a lower affinity for the substrate.

During the process of immobilization by physical adsorption, the orientation of the immobilized lipase on the matrix was not a controlled process. Therefore, an improper fixation could hinder the active site for binding of substrates to the immobilized enzyme (Yang et al. 2010). The increasing of kinetic parameters correlates favourably with previous studies on enzyme immobilization (Bayazidi et al. 2018).

Leaching of the lipase from the nanocomposites

The stability of immobilized lipase onto BC matrices was determinated. Lipase/BC nanocomposites were incubated in buffer solution (20 mM TrisHCl pH 7) at room temperature and enzymatic activity was measured in the solution at several times. Lipase activity was not detected at times 0, 24 and 48 h. After 72 h, only about 4% of the lipase activity was released from the Lipase/BCP nanocomposites, whereas for Lipase/BCS nanocomposites no leaching of activity was detected (Table 4). At this time, the activity that remained in the nanocomposites was measured. The results indicated that Lipase/BCP nanocomposites

Table 3 Kinetic constants of free and immobilized lipase

	K_m (μM)	V_{max} (U/mg protein)
Free lipase	169.9 ± 25.75	3.03 ± 0.18
Lipase/BCP nanocomposite	276.9 ± 53.02	3.31 ± 0.32
Lipase/BCS nanocomposite	659.0 ± 264.3	6.44 ± 1.7

Table 4 Activity and leaching of lipase from BC nanocomposites

	t = 0 h	t = 72 h		
	mU/mL	mU/mL	% leaching	% remaining activity
Lipase/BCP	5.6 ± 0.03	5.74 ± 0.90	3.9	100
Lipase/BCS	20.8 ± 0.4	6.93 ± 0.62	0	33

maintained 100% of the activity, in accordance with the results obtained from the leaching of the activity. However, Lipase/BCS nanocomposites retained only 33% of the activity, suggesting that the enzyme lost activity during the 72 h incubation at room temperature (Table 4).

It has been described that the interactions by physical adsorption between enzymes and plant cellulose supports would be not strong enough to ensure permanent immobilization and to prevent, consequently, the leaking of the biomolecules (Credou and Berthelot 2014). Nevertheless, in this study, the lipase adsorbed onto BCP matrices seemed to be strongly entrapped. Probably, the high density and specific surface area provided by BC nanofibers resulted in more available hydroxyl groups where the lipase can be adsorbed (Skočaj 2019). Moreover, the porous three-dimensional structure of nanofibers would help to retain the enzyme.

Reusability of lipase/BC nanocomposites

To determine the reusability of the Lipase/BC nanocomposites activity was measured. Then, Lipase/BCP nanocomposites were rinsed twice by immersion in 20 mM TrisHCl pH 7 and allowed to air-dry before the following activity assay. Lipase/BCS nanocomposites were rinsed by centrifugation and resuspension of the pellet in 20 mM TrisHCl pH 7. A third centrifugation allowed the resuspension of the pellet in the reaction buffer for subsequent lipase activity assay. These operational cycles were repeated 10 consecutive times. Results are shown in Fig. 7. The

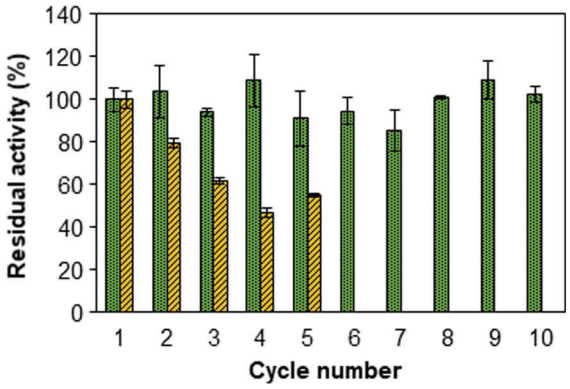

Fig. 7 Reusability of the Lipase/BCP nanocomposites (dot bars) and the Lipase/BCS nanocomposites (line bars). The reusability was expressed as the percent of remaining activity where activity from the first run was taken as 100%

activity of the BCS nanocomposites gradually decreased with the subsequent cycles, retaining 55% of the original activity after five recycling times, although significant differences were already detected in the second round of recycling. As for the Lipase/BCP nanocomposites, the activity did no decrease along the reusing cycles, without any significant difference. In comparison to other supports, as green coconut fibre, where a laccase was immobilized by physical adsorption, the composite lost 30% of its initial activity in the second cycle (Cristóvão et al. 2011). Therefore, BCP would stand out as a matrix that allows a notable operational stability. Moreover, the efficiency of reusability of lipase on BC paper was higher of that described for a crosslinking-immobilized laccase on BC membrane, which showed 69% of

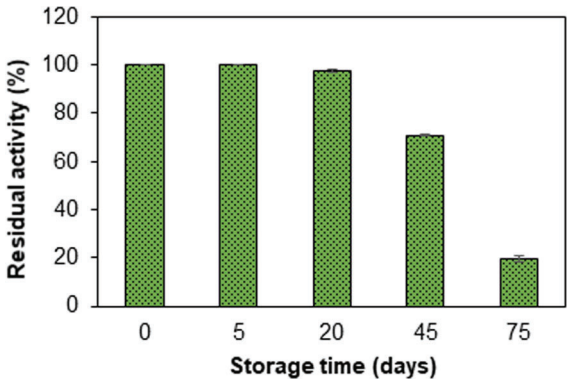

Fig. 8 Stability of Lipase/BCP nanocomposite during a 75-days storage at room temperature. Residual activity was expressed as percentage of the initial activity at time zero

its original activity after seven recycling times (Chen et al. 2015). Good reusability of enzyme can lead to significant reduction of operational cost which is of utmost relevance for the industry (Silva et al. 2006) and for practical applications as biosensors (Nigam and Shukla 2015).

Storage stability of the lipase/BCP nanocomposites

The effect of storing time on the functionality of Lipase/BCP nanocomposite was studied during 75 days period. Results showed that nanocomposites with immobilized enzyme could be stored at room temperature during at least 20 days without any significant loss of activity, retaining 71% after 45 days (Fig. 8). These results indicated that neither the enzyme activity nor the cellulose-attachment of the enzyme were compromised under these conditions during several weeks. The biocompatibility and the three-dimensional network of nanofibers of the BC in conjunction with the water-free environment of BCP allowed the preservation of the activity of the enzyme without the need for special storage. Those are essential properties to be found in biopaper based devices (Crini 2005).

Conclusions

In the present work, the immobilization of lipase by physical adsorption, a cost-effective and environmentally friendly method, generated functional bacterial cellulose-based nanocomposites. BCS matrices showed higher protein adsorption capacity than BCP matrices. Likewise, Lipase/BCS presented higher specific activity than Lipase/BCP nanocomposites. However, enzyme immobilized onto BCP was able to operate at higher temperatures and showed greater thermal stability. Moreover, Lipase/BCP nanocomposites maintained their enzymatic activity after several weeks of storage at room temperature and for, at least, 10 reusing cycles. This study could be the first step in establishing a process to obtain bioactive BC paper, considering "BC paper" as the material obtained from bacterial cellulose paste in the form of thin sheets that combine the characteristics of BC nanofibers with the stiffness and physical properties of paper. It is foreseeable that nanocomposites of BC paper with other enzymes could be obtained. Enzyme/BCP nanocomposites are of particular interest because they could be used as part of biosensors devices with applications in many fields including clinical diagnosis, environmental monitoring, and food quality control. Due to their operational properties, they could be suitable for point-of-use testing devices.

Acknowledgments We thank Novozymes (Denmark) for kindly providing soluble lipase Callera Trans L and X. Andrés for technical assistance. This work was financed by the Spanish Ministry of Economy, Industry and Competitiveness, Grants CTQ2017-84966-C2-2-R, FILMBIOCEL CTQ2016-77936-R (funding also from FEDER) and MICROBIOCEL (CTQ2017-84966-C2-1-R), and by the Pla de Recerca de Catalunya, Grant 2017SGR-30, and by the Generalitat de Catalunya, "Xarxa de Referència en Biotecnologia" (XRB). C. Buruaga-Ramiro acknowledges an APIF predoctoral Grant from the University of Barcelona. Special thanks are due to the Serra Húnter Fellow to Cristina Valls.

Compliance with ethical standards

Conflict of interest The authors declare that they have no conflict of interest.

References

Abdul Khalil HPS, Bhat AH, Ireana Yusra AF (2012) Green composites from sustainable cellulose nanofibrils: a review. Carbohydr Polym 87:963–979. https://doi.org/10.1016/j.carbpol.2011.08.078

Angajala G, Pavan P, Subashini R (2016) Lipases: an overview of its current challenges and prospectives in the revolution

of biocatalysis. Biocatal Agric Biotechnol 7:257–270. https://doi.org/10.1016/j.bcab.2016.07.001

Bayazidi P, Almasi H, Asl AK (2018) Immobilization of lysozyme on bacterial cellulose nanofibers: characteristics, antimicrobial activity and morphological properties. Int J Biol Macromol 107:2544–2551. https://doi.org/10.1016/j.ijbiomac.2017.10.137

Bielecki S, Krystynowicz A, Turkiewicz M, Kalinowska H (2005) Bacterial cellulose. In: Vandamme EJ, De Baets S, Steinbüchel A (eds) Biopolymers online. Wiley, Weinheim

Božič M, Gorgieva S, Kokol V (2012) Laccase-mediated functionalization of chitosan by caffeic and gallic acids for modulating antioxidant and antimicrobial properties. Carbohydr Polym 87:2388–2398. https://doi.org/10.1016/j.carbpol.2011.11.006

Bradford MM (1976) A rapid and sensitive method for the quantitation of microgram quantities of protein utilizing the principle of protein-dye binding. Anal Biochem 72:248–254. https://doi.org/10.1016/0003-2697(76)90527-3

Castro C, Vesterinen A, Zuluaga R et al (2014) In situ production of nanocomposites of poly(vinyl alcohol) and cellulose nanofibrils from Gluconacetobacter bacteria: effect of chemical crosslinking. Cellulose 21:1745–1756. https://doi.org/10.1007/s10570-014-0170-1

Chai C, Lee J, Huang Q (2014) The effect of ionic strength on the rheology of pH-induced bovine serum albumin/κ-carrageenan coacervates. LWT Food Sci Technol 59:356–360. https://doi.org/10.1016/j.lwt.2014.05.024

Chawla PR, Bajaj IB, Survase SA, Singhal RS (2009) Microbial cellulose: fermentative production and applications. Food Technol Biotechnol 47:107–124

Chen L, Zou M, Hong FF (2015) Evaluation of fungal laccase immobilized on natural nanostructured bacterial cellulose. Front Microbiol. https://doi.org/10.3389/fmicb.2015.01245

Choi MMF (2004) Progress in enzyme-based biosensors using optical transducers. Microchim Acta 148:107–132. https://doi.org/10.1007/s00604-004-0273-8

Credou J, Berthelot T (2014) Cellulose: from biocompatible to bioactive material. J Mater Chem B 2:4767–4788. https://doi.org/10.1039/C4TB00431K

Crini G (2005) Recent developments in polysaccharide-based materials used as adsorbents in wastewater treatment. Prog Polym Sci 30:38–70. https://doi.org/10.1016/j.progpolymsci.2004.11.002

Cristóvão RO, Tavares APM, Brígida AI et al (2011) Immobilization of commercial laccase onto green coconut fiber by adsorption and its application for reactive textile dyes degradation. J Mol Catal B Enzym 72:6–12. https://doi.org/10.1016/j.molcatb.2011.04.014

dos Santos CA, dos Santos GR, Soeiro VS et al (2018) Bacterial nanocellulose membranes combined with nisin: a strategy to prevent microbial growth. Cellulose 25:6681–6689. https://doi.org/10.1007/s10570-018-2010-1

Estevinho BN, Damas AM, Martins P, Rocha F (2014) Microencapsulation of β-galactosidase with different biopolymers by a spray-drying process. Food Res Int 64:134–140. https://doi.org/10.1016/j.foodres.2014.05.057

Evans BR, O'Neill HM, Malyvanh VP et al (2003) Palladium-bacterial cellulose membranes for fuel cells. Biosens Bioelectron 18:917–923. https://doi.org/10.1016/S0956-5663(02)00212-9

Fernández J, Morena AG, Valenzuela SV et al (2019) Microbial cellulose from a komagataeibacter intermedius strain isolated from commercial wine vinegar. J Polym Environ 27:956–967. https://doi.org/10.1007/s10924-019-01403-4

Ferreira FV, Dufresne A, Pinheiro IF et al (2018) How do cellulose nanocrystals affect the overall properties of biodegradable polymer nanocomposites: a comprehensive review. Eur Polym J 108:274–285. https://doi.org/10.1016/j.eurpolymj.2018.08.045

Frazão CJR, Silva NHC, Freire CSR et al (2014) Bacterial cellulose as carrier for immobilization of laccase: optimization and characterization. Eng Life Sci 14:500–508. https://doi.org/10.1002/elsc.201400054

Hänninen T, Orelma H, Laine J (2015) TEMPO oxidized cellulose thin films analysed by QCM-D and AFM. Cellulose 22:165–171. https://doi.org/10.1007/s10570-014-0530-x

Huang Y, Zhu C, Yang J et al (2014) Recent advances in bacterial cellulose. Cellulose 21:1–30. https://doi.org/10.1007/s10570-013-0088-z

Kadokawa J (2012) Preparation and applications of amylose supramolecules by means of phosphorylase-catalyzed enzymatic polymerization. Polymers (Basel) 4:116–133. https://doi.org/10.3390/polym4010116

Kim J, Cai Z, Lee HS et al (2011) Preparation and characterization of a Bacterial cellulose/chitosan composite for potential biomedical application. J Polym Res 18:739–744. https://doi.org/10.1007/s10965-010-9470-9

Kim HJ, Park S, Kim SH et al (2015) Biocompatible cellulose nanocrystals as supports to immobilize lipase. J Mol Catal B Enzym 122:170–178. https://doi.org/10.1016/j.molcatb.2015.09.007

Klemm D, Philipp B, Heinze T et al (1998) Comprehensive cellulose chemistry: volume I: fundamentals and analytical methods. Wiley. https://onlinelibrary.wiley.com/doi/book/10.1002/3527601929

Lee K-Y, Buldum G, Mantalaris A, Bismarck A (2014) More than meets the eye in bacterial cellulose: biosynthesis, bioprocessing, and applications in advanced fiber composites. Macromol Biosci 14:10–32. https://doi.org/10.1002/mabi.201300298

Lian Z-X, Ma Z-S, Wei J, Liu H (2012) Preparation and characterization of immobilized lysozyme and evaluation of its application in edible coatings. Process Biochem 47:201–208. https://doi.org/10.1016/j.procbio.2011.10.031

Lin N, Dufresne A (2014) Nanocellulose in biomedicine: current status and future prospect. Eur Polym J 59:302–325. https://doi.org/10.1016/j.eurpolymj.2014.07.025

Lin Q, Zheng Y, Wang G et al (2015) Protein adsorption behaviors of carboxymethylated bacterial cellulose membranes. Int J Biol Macromol 73:264–269. https://doi.org/10.1016/j.ijbiomac.2014.11.011

Lu H, Gui Y, Zheng L, Liu X (2013) Morphological, crystalline, thermal and physicochemical properties of cellulose nanocrystals obtained from sweet potato residue. Food Res Int 50:121–128. https://doi.org/10.1016/j.foodres.2012.10.013

Meftahi A, Khajavi R, Rashidi A et al (2010) The effects of cotton gauze coating with microbial cellulose. Cellulose 17:199–204. https://doi.org/10.1007/s10570-009-9377-y

Mohamad NR, Marzuki NHC, Buang NA et al (2015) An overview of technologies for immobilization of enzymes and surface analysis techniques for immobilized enzymes. Biotechnol Biotechnol Equip 29:205–220. https://doi.org/10.1080/13102818.2015.1008192

Molinero-Abad B, Alonso-Lomillo MA, Domínguez-Renedo O, Arcos-Martínez MJ (2014) Malate quinone oxidoreductase biosensors based on tetrathiafulvalene and gold nanoparticles modified screen-printed carbon electrodes for malic acid determination in wine. Sens Actuators B Chem 202:971–975. https://doi.org/10.1016/j.snb.2014.06.057

Monosik R, Stredansky M, Tkac J, Sturdik E (2012) Application of enzyme biosensors in analysis of food and beverages. Food Anal Methods 5:40–53. https://doi.org/10.1007/s12161-011-9222-4

Nigam VK, Shukla P (2015) Enzyme based biosensors for detection of environmental pollutants—a review. J Microbiol Biotechnol 25:1773–1781. https://doi.org/10.4014/jmb.1504.04010

Nordblad M, Silva VTL, Nielsen PM, Woodley JM (2014) Identification of critical parameters in liquid enzyme-catalyzed biodiesel production. Biotechnol Bioeng 111:2446–2453. https://doi.org/10.1002/bit.25305

Omagari Y, Matsuda S, Kaneko Y, Kadokawa J (2009) Chemoenzymatic synthesis of amylose-grafted cellulose. Macromol Biosci 9:450–455. https://doi.org/10.1002/mabi.200800237

Pahlevan M, Toivakka M, Alam P (2018) Mechanical properties of TEMPO-oxidised bacterial cellulose-amino acid biomaterials. Eur Polym J 101:29–36. https://doi.org/10.1016/j.eurpolymj.2018.02.013

Panizza P, Syfantou N, Pastor FIJ et al (2013) Acidic lipase Lip I.3 from a *Pseudomonas fluorescens*-like strain displays unusual properties and shows activity on secondary alcohols. J Appl Microbiol 114:722–732. https://doi.org/10.1111/jam.12089

Pohanka M (2019) Biosensors and bioassays based on lipases, principles and applications: a review. Molecules 24:616. https://doi.org/10.3390/molecules24030616

Rocchitta G, Spanu A, Babudieri S et al (2016) Enzyme biosensors for biomedical applications: strategies for safeguarding analytical performances in biological fluids. Sensors 16:780. https://doi.org/10.3390/s16060780

Segal L, Creely JJ, Martin AE, Conrad CM (1959) An empirical method for estimating the degree of crystallinity of native cellulose using the X-ray diffractometer. Text Res J 29:786–794. https://doi.org/10.1177/004051755902901003

Seves A, Testa G, Bonfatti AM et al (2001) Characterization of native cellulose/poly(ethylene glycol) films. Macromol Mater Eng 286:524–528. https://doi.org/10.1002/1439-2054(20010901)286:9%3c524:AID-MAME524%3e3.0.CO;2-B

Shi Z, Zang S, Jiang F et al (2012) In situ nano-assembly of bacterial cellulose–polyaniline composites. RSC Adv 2:1040–1046. https://doi.org/10.1039/C1RA00719J

Silva CJSM, Zhang Q, Shen J, Cavaco-Paulo A (2006) Immobilization of proteases with a water soluble–insoluble reversible polymer for treatment of wool. Enzyme Microb Technol 39:634–640. https://doi.org/10.1016/j.enzmictec.2005.11.016

Skočaj M (2019) Bacterial nanocellulose in papermaking. Cellulose 26:6477–6488. https://doi.org/10.1007/s10570-019-02566-y

Sulaiman S, Mokhtar MN, Naim MN et al (2015) A review: potential usage of cellulose nanofibers (CNF) for enzyme immobilization via covalent interactions. Appl Biochem Biotechnol 175:1817–1842. https://doi.org/10.1007/s12010-014-1417-x

Ul-Islam M, Khan T, Park JK (2012a) Water holding and release properties of bacterial cellulose obtained by in situ and ex situ modification. Carbohydr Polym 88:596–603. https://doi.org/10.1016/j.carbpol.2012.01.006

Ul-Islam M, Khan T, Park JK (2012b) Nanoreinforced bacterial cellulose–montmorillonite composites for biomedical applications. Carbohydr Polym 89:1189–1197. https://doi.org/10.1016/j.carbpol.2012.03.093

Wang P (2006) Nanoscale biocatalyst systems. Curr Opin Biotechnol 17:574–579. https://doi.org/10.1016/j.copbio.2006.10.009

Wu S-C, Wu S-M, Su F-M (2017) Novel process for immobilizing an enzyme on a bacterial cellulose membrane through repeated absorption. J Chem Technol Biotechnol 92:109–114. https://doi.org/10.1002/jctb.4994

Yang J, Ma X, Zhang Z et al (2010) Lipase immobilized by modification-coupled and adsorption–cross-linking methods: a comparative study. Biotechnol Adv 28:644–650. https://doi.org/10.1016/j.biotechadv.2010.05.014

Yano H, Sugiyama J, Nakagaito AN et al (2005) Optically transparent composites reinforced with networks of bacterial nanofibers. Adv Mater 17:153–155. https://doi.org/10.1002/adma.200400597

Yao W, Wu X, Zhu J et al (2013) In vitro enzymatic conversion of γ-aminobutyric acid immobilization of glutamate decarboxylase with bacterial cellulose membrane (BCM) and non-linear model establishment. Enzyme Microb Technol 52:258–264. https://doi.org/10.1016/j.enzmictec.2013.01.008

Yuan H, Chen L, Hong FF, Zhu M (2018) Evaluation of nanocellulose carriers produced by four different bacterial strains for laccase immobilization. Carbohydr Polym 196:457–464. https://doi.org/10.1016/j.carbpol.2018.05.055

Zhou D, Sun Y, Bao Z et al (2019) Improved cell viability and biocompatibility of bacterial cellulose through in situ carboxymethylation. Macromol Biosci 19:1800395. https://doi.org/10.1002/mabi.201800395

Development of an antimicrobial bioactive paper made from bacterial cellulose.

La celulosa bacteriana (CB) ha sido erigido como un atractivo material con capacidad de adsorción de agentes antimicrobianos gracias al entramado tridimensional que forman las fibras y sus elevadas área superficial y porosidad. En el presente estudió se generó un papel de CB en el que se inmovilizó la enzima lisozima por adsorción física, obteniendo el composite Lisozima – papel de CB. La morfología y la estructura cristalina del composite eran similares a las de la CB, tal y como indicaron los análisis de microscopía electrónica de barrido y de difracción de rayos X, respectivamente. Respecto a las propiedades operacionales, las actividades específicas de la enzima inmovilizada y la lisozima libre eran similares. Además, la lisozima inmovilizada era operativa en un rango más amplio de temperaturas y mostró una estabilidad térmica más elevada. Los composites mantuvieron su actividad al menos 80 días sin ningún requerimiento especial de conservación. El papel Lisozima-BC mostró actividad antimicrobiana contra bacterias grampositivas y gramnegativas, inhibiendo su crecimiento en un 82 % y un 68 %, respectivamente. Adicionalmente, la presencia de lisozima incrementó un 30 % la actividad antioxidante del papel de CB. Estos resultados indicaron que la CB es un material apto para la elaboración de papeles bioactivos al ofrecer un ambiente biocompatible sin comprometer la actividad de la proteína inmovilizada. El papel de CB con propiedades antimicrobianas y antioxidantes podría tener una aplicación en el campo del empaquetamiento activo.

International Journal of Biological Macromolecules 158 (2020) 587–594

Contents lists available at ScienceDirect

International Journal of Biological Macromolecules

journal homepage: http://www.elsevier.com/locate/ijbiomac

Development of an antimicrobial bioactive paper made from bacterial cellulose

Carolina Buruaga-Ramiro [a,b], Susana V. Valenzuela [a,b], Cristina Valls [c], M. Blanca Roncero [c], F.I. Javier Pastor [a,b], Pilar Díaz [a,b], Josefina Martinez [a,b,*]

[a] Department of Genetics, Microbiology and Statistics, Faculty of Biology, University of Barcelona, Av. Diagonal 643, 08028 Barcelona, Spain
[b] Institute of Nanoscience and Nanotechnology (IN2UB), Universitat de Barcelona, Av. Diagonal 645, 08028 Barcelona, Spain
[c] CELBIOTECH_Paper Engineering Research Group, EGE Department, Universitat Politècnica de Catalunya, Barcelona Tech, 08222 Terrassa, Spain

ARTICLE INFO

Article history:
Received 10 March 2020
Received in revised form 16 April 2020
Accepted 27 April 2020
Available online 1 May 2020

Keywords:
Bacterial cellulose paper
Enzyme immobilization
Active packaging

ABSTRACT

Bacterial cellulose (BC) has emerged as an attractive adsorptive material for antimicrobial agents due to its fine network structure, its large surface area, and its high porosity. In the present study, BC paper was first produced and then lysozyme was immobilized onto it by physical adsorption, obtaining a composite of lysozyme-BC paper. The morphology and the crystalline structure of the composite were similar to that of BC paper as examined by scanning electron microscopy and X-ray diffraction, respectively. Regarding operational properties, specific activities of immobilized and free lysozyme were similar. Moreover, immobilized enzyme showed a broader working temperature and higher thermal stability. The composites maintained its activity for at least 80 days without any special storage. Lysozyme-BC paper displayed antimicrobial activity against Gram-positive and Gram-negative bacteria, inhibiting their growth by 82% and 68%, respectively. Additionally, the presence of lysozyme increased the antioxidant activity of BC paper by 30%. The results indicated that BC is a suitable material to produce bioactive paper as it provides a biocompatible environment without compromising the activity of the immobilized protein. BC paper with antimicrobial and antioxidant properties may have application in the field of active packaging.

1. Introduction

Food packaging is one of the most critical steps in terms of food safety. Packaging which, apart from offering a barrier to the outside environment, performs some other role, is defined as active packaging [1]. An active food-packaging can provide antioxidant and antimicrobial properties through the direct interaction of compounds with the food as well as help to remove some negative factors, such as oxygen or water vapor [2], thus improving food stability [3]. Loading of natural antimicrobial substances is receiving considerable attention as a means of inactivating bacterial cells, slowing the growth rate of microorganisms, and maintaining food quality and safety [4,5]. Lysozyme is an enzyme with antimicrobial activity that can be abundantly found in nature and is produced by plants, fungus, bacteria, birds and mammals [6]. Because of its selective activity against the cell walls of a wide variety of Gram-positive and Gram-negative bacteria [7,8], lysozyme is extensively used in the food industry and classified as GRAS [9–12]. Lysozyme has been shown to be effective as a preservative of cheeses, cow's milk, beer [13], fresh fruits and vegetables, fish and meat [14], and wine. However, direct addition of free lysozyme to food may lead to some loss of its activity because of its high sensitivity and quick inactivation under different environmental conditions [15,16]. Enzymes immobilized into a polymeric matrix usually gain stability against pH, temperature, and other environmental factors [17]. A usual way to prepare antimicrobial packaging is through chemical immobilization of antimicrobial agents to the packaging material [18]. Even though an effective enzyme immobilization can be achieved by covalent binding or cross linking [19,20], these methods often require chemical modifications of the matrix and/or the use of chemical linkers that complicate the procedure, limit the functionality of the resulting composite, and generate residues harmful for the environment [21]. On the contrary, physical methods as direct adsorption are the most simple, cost-effective, and environmentally friendly techniques for enzyme immobilization [22,23].

Among the available packaging materials, cellulose-based matrices have attracted increasing interest as good carriers for a wide range of antimicrobial agents [9,24]. Bacterial cellulose (BC) – also called

* Corresponding author at: Department of Genetics, Microbiology and Statistics, Faculty of Biology, Universitat de Barcelona, Av. Diagonal 643, 08028 Barcelona, Spain.
E-mail addresses: buruaga.cbr@ub.edu (C. Buruaga-Ramiro), susanavalenzuela@ub.edu (S.V. Valenzuela), cristina.valls@upc.edu (C. Valls), blanca.roncero@upc.edu (M.B. Roncero), fpastor@ub.edu (F.I.J. Pastor), pdiaz@ub.edu (P. Díaz), jmartinez@ub.edu (J. Martinez).

https://doi.org/10.1016/j.ijbiomac.2020.04.234
0141-8130/

bacterial nanocellulose - is synthetized as an exopolysaccharide by aerobic bacteria, such as acetic acid bacteria of the genus *Komagataeibacter* [25]. Compared to plant cellulose, BC displays superior structural and mechanical properties [26,27] and has become a new basic material for advanced applications, including artificial skin, wound dressings, and scaffold for tissue engineering [28–33]. Additionally, BC is inert and biocompatible under a wide range of conditions. Owing to its large surface area, high porosity and fine network structure, BC is able to easily entrap different types of molecules [20,34,35]. Moreover, from the original produced BC, diverse matrices can be obtained showing different physical and mechanical properties that allow different applications [36–38]. Enzyme immobilization by physical adsorption onto BC has been already described for lipase onto BC nanocrystals [39] and for nisin, laccase and lipase onto BC membranes [40–42]. Lysozyme has been successfully immobilized onto BC nanofibres in suspension [16] and onto other polymeric supports as plant cellulose materials and chitosan [43–45].

Recently, it has been described the production of paper from bacterial cellulose pulp in the form of thin sheets that combine the characteristics of BC nanofibres with the stiffness and physical properties of paper [46,47]. Moreover, this material is a suitable matrix to immobilized biologically active molecules by physical adsorption [48]. Composites of metals and BC paper with antimicrobial activity have been successfully obtained [46,49]. However, to our knowledge, this is the first description regarding the combination of BC paper and the antimicrobial enzyme lysozyme. The main goal of this work was to produce a Lysozyme/BC bioactive paper and evaluate its antimicrobial properties and operational characteristics under different conditions. This study could lead to the design of a new active packaging material.

2. Material and methods

2.1. Materials

Bacterial cellulose was produced by *Komagataeibacter intermedius* JF2, a strain previously isolated in the laboratory [50]. Antimicrobial activity was tested against *Staphylococcus aureus* CECT 234, and *Escherichia coli* CECT 515. Strains were obtained from the Spanish Type Culture Collection (CECT). Lysozyme from chicken egg white (L6876) was purchased from Merck.

2.2. Production of lysozyme/bacterial cellulose paper (Lys-BCP)

K. intermedius JF2 was grown on the Hestrin and Schramm (HS) medium, containing 20 g/L glucose, 20 g/L peptone, 10 g/L yeast extract, 1,15 g/L citric acid, 6,8 g/L Na_2HPO_4, pH 6. After 7 days of static incubation, bacterial cellulose membranes generated in the air/liquid interface of the culture media were harvested, rinsed with water and incubated in 1% NaOH at 70 °C overnight to remove the bacteria. Then, the BC membranes were thoroughly washed in deionized water until the pH reached neutrality. Finally, membranes were mechanically disrupted with a blender and homogenized (Homogenizing System UNIDRIVE X1000) to obtain a BC pulp containing a suspension of BC fibres. The amount of BC was determinate by drying samples at 60 °C until constant weight was reached. This pulp was used to produce BC paper sheets using a Rapid–Köthen laboratory former (Frank–PTI) following the ISO–5269:2004 standard method, obtaining a bacterial cellulose paper (BCP) of a grammage of 70 g/m^2. Adsorption of lysozyme to BCP was conducted immersing pieces of 1 cm^2 into a lysozyme binding solution (10 g/L in 20 mM KH_2PO_4, pH 6), and incubated at room temperature with slight shaking for 18 h. Then, samples were washed twice in buffer solution (20 mM KH_2PO_4, pH 6), air-dried and stored at room temperature.

2.3. Protein determination

Initial and final concentrations of protein in the lysozyme binding solution were measured according to the Bradford's protein assay [51] to determinate the content of protein in the Lys-BCP biopaper, taking into account also the residual protein in the washing solutions. Protein loading was calculated using Eq. (1) [35].

$$\textit{Protein loading}\left(\frac{\mu g}{gBC}\right) = [\textit{Total protein of free lipase}\ (\mu g) - \textit{Total residual protein of free lipase after immobilization}\ (\mu g)]/[\textit{Total mass of BC matrix}\ (g)] \quad (1)$$

2.4. Scanning electron microscopy (SEM)

Dried samples of Lys-BCP were analysed by SEM (JSM 7100 F) using a LED filter. Samples were graphite coated using a Vacuum Evaporator EMITECH K950X221. The diameter of the fibres was measured using the ImageJ software.

2.5. X-ray diffractometry (XRD)

Dried samples of Lys-BCP were subjected to XRD analysis (PANalytical X'Pert PRO MPD Alpha1 powder diffractometer). The samples were analysed at the radiation wavelength of 1.5418 Å. Samples were scanned from 2° to 50°, 2Θ range. Samples were fixed over a zero background Silicon single crystal sample holder (pw1817/32), and the ensembles were mounted in a PW1813/32 sample holder. All the replicates of each sample were measured with the same Silicon holder. The crystallinity index (CI) of bacterial cellulose was calculated based on Eq. (2) [52]:

$$\mathrm{CI}(\%) = \frac{I_c - I_{am}}{I_c} \times 100 \quad (2)$$

where I_c is the maximum intensity of the lattice diffraction and I_{am} is the height of the intensity at the minimum at 2Θ between 18° and 19°, which corresponds to the amorphous part of cellulose.

2.6. Operational properties of the immobilized lysozyme

Lysozyme hydrolytic activity was analysed by measuring the release of MUF (methylumbelliferone) from MUF-derivate β-D-*N*,*N*′,*N*′-triacetylchitotrioside hydrate substrate (Merck). Stock solution of MUF-substrate was prepared at 12,5 mM in dimethyl formamide (DMF): water (1:1). The working solution contained 250 μM of MUF-substrate in 20 mM KH_2PO_4, pH 6. MUF was measured using a Varian Cary Eclipse spectrofluorometer (Agilent Technologies) equipped with a microplate reader (λex = 360 nm, λem = 465 nm). One unit of activity was defined as the amount of enzyme that released one μmol of MUF per minute under the assay conditions. The specific activity and the recovery of lysozyme activity were calculated using Eqs. (3) and (4).

$$\text{Specific activity of immobilized lysozyme}\left(\frac{\text{mU}}{\text{mg protein}}\right) = \frac{\text{Activity of immobilized enzyme}\left(\frac{\text{mU/ml}}{\text{g BC}}\right)}{\text{Protein loading}\left(\frac{\text{mg protein/ml}}{\text{g BC}}\right)} \quad (3)$$

$$\text{Recovery of lysozyme activity}\ (\%) = \frac{\text{Specific activity of immobilized lysozyme}}{\text{Specific activity of free lysozyme}} \times 100 \quad (4)$$

The determination of the operational properties of Lys/BCP biopaper was carried out immersing pieces of 1 cm^2 into 1 mL of the appropriated buffer at the conditions being analysed. Assays of free lysozyme activity were run at the same time. Optimum temperature of free and absorbed lysozyme was determined by the analysis of the activity over a range from 30 °C to 90 °C at pH 6. Long-term thermal stability was based on the residual activity of lysozyme measured after incubation at room temperature in 20 mM KH_2PO_4 pH 6 for a determinate period of time. Optimum pH of free and absorbed lysozyme was determined by analysis of the activity at various pH values with the appropriate buffers 20 mM: acetate buffer (pH 4 and 5), phosphate buffer (pH 6) and TrisHCl (pH 7, 8 and 9).

2.7. Antimicrobial activity

The antimicrobial properties of Lys-BCP biopaper were tested against the Gram-positive bacteria *Staphylococcus aureus* and the Gram-negative *Escherichia coli* using the dynamic contact conditions test, adapted from ASTM E2149–01 (*Standard test Method for determining the antimicrobial activity agents under dynamic contact conditions*). To obtain the inoculum, the strains were grown overnight in TSB at 37 °C in shaking conditions. The overnight cultures were centrifuged for 4 min at 14,000 rpm in an Eppendorf® 52424 centrifuge, and the pellet suspended in 20 mM KH_2PO_4. Pieces of 1 cm^2 were immersed in 1 mL of a suspension of a known concentration of the microorganism and incubated at room temperature while slightly stirred. A control was run with samples of BCP under the same conditions. The viable cells on the suspension were determined at different times, and the percentage of reduction was calculated by Eq. (5).

$$\%\text{cell viability reduction} = \frac{\text{viable CFU at } t_0 - \text{viable CFU at } t_x}{\text{viable CFU at } t_0} \text{ x } 100 \quad (5)$$

where t_0 is the time 0 h and t_x is the time at which the percentage of reduction is calculated.

2.8. Antioxidant activity

The antioxidant activity was assessed by a procedure consisting in the determination of the antioxidant capacity of insoluble components by quantification of the inhibition of 2,2′-Azino-bis(3-ethylbenzothiazoline-6-sulphonic acid radical ($ABTS^+$) [53–55]. Firstly, the ABTS* radical was pre-formed adding 140 mM potassium persulfate to 7 mM ABTS. Then, samples of 1 cm^2 of Lys-BCP and BCP were placed in microcentrifuge tubes and 1 mL of $ABTS^+$ was added. After that, the tubes were centrifuged at 14000 rpm in an Eppendorf® 52424 centrifuge and incubated in the darkness for 30 min. Finally, 900 μL of the liquid was pipetted in a cuvette and the final absorbance at 730 nm was measured in a T92+ UV Spectrophotometer (PG Instruments). A tube without sample was used as the blank. The percentage of inhibition, corresponding the percentage of antioxidant activity, was calculated according to Eq. (6).

$$ABTS^* \text{inhibition } (\%) = \frac{A_i - A_f}{A_i} \times 100 \quad (6)$$

where A_i is the ABTS* absorbance value of the blank, and A_f is the ABTS* absorbance value after contact with the antioxidant compound.

2.9. Statistical analysis

All determinations of enzyme activity were performed after two replicas of triplicates (6 determinations per sample). Experimental data were expressed as means ± standard deviations and were analysed statistically by one-way single factor or more analysis of variance (ANOVA) in STATGRAPHICS Centurion XVIII software (Statgraphics.Net, Madrid), considering a value of $p \leq 0.05$ statistically significant. Scheffe's multiple range test was used to detect differences among mean values. Bartlett's test was used to test homogeneity of variance for all samples. Assumption that the residuals were normally distributed was tested with the Shapiro-Wilk test.

3. Results and discussion

3.1. Adsorption of lysozyme and specific activity of the biopaper

Factors as the ionic strength and the charge density play an important role in the formation of complexes between proteins and polysaccharides [56]. Lysozyme adsorption was performed with a 20 mM KH_2PO_4 binding solution at pH 6. The lysozyme has an isoelectric point of 11.5 [57], therefore, at pH 6 the protein is positively charged and adsorbs on the BCP anionic surface [58]. Moreover, 6 is the optimum pH for lysozyme activity [13] which allowed maintaining the same working conditions in the determinations of enzymatic activity. In addition, it has been described that low ionic strength enhances the formation of the protein/polysaccharide composites [59]. In these conditions, lysozyme was blended by physically adsorption onto BCP at a rate of 80.39 μg/mg of BC fibres, equivalent to 0.5 mg/cm^2 of paper sheet, obtaining a Lysozyme/BCP composite (Lys-BCP) (Table 1).

The content of lysozyme bounded to BC was higher than previously reported for lysozyme immobilized onto chitosan supports [43,60]. Furthermore, the lysozyme absorbed in the paper made from BC showed enzymatic activity indicating that the Lys-BCP composite was biologically active (Table 1). Regarding specific activity, the immobilized enzyme retained over 92% of the activity of the free enzyme, even though a decrease of specific activity is a common phenomenon described for immobilized enzymes due to a lower accessibility of substrate to active sites [61]. However, BC large surface area results in more available hydroxyl groups [62], which highly enhances protein loading onto its fibres, displaying a higher absorption capacity when compared with wood pulp cellulose [39,63]. In addition, three-dimensional structure provided by BC nanofibres would help to retain the enzyme [48]. The results indicated that BCP is a suitable support for lysozyme binding, leading to the maintenance of a specific activity very similar to the free enzyme.

3.2. Characterization of the Lys-BCP biopaper

The morphological structure of BCP and Lys-BCP was investigated by SEM analysis (Fig. 1). SEM images of the BCP surface (Fig. 1A) showed a dense and homogeneous matrix of nanofibres with a diameter of 50–70 nm. Pores randomly distributed through the matrix would provide microchannels to entrap protein molecules [35]. The structure of Lys-BCP was very similar (Fig. 1B). However, even though the nanofibres arrangement barely changed by the immobilization of lysozyme, a smooth layer could be observed on the surface, perhaps due to the coating of BCP by the enzyme. In the literature, other authors

Table 1
Characteristics of lysozyme immobilized onto BCP.

	Adsorbed lysozyme		Specific activity	Recovered activity
	(mg/cm^2 BCP)	(μg/mg BC)	(μU/mg protein)	(%)
Free lysozyme	–	–	153 ± 5	–
Lys-BCP	0.5 ± 0.13	80.39 ± 21	141 ± 16	91.9

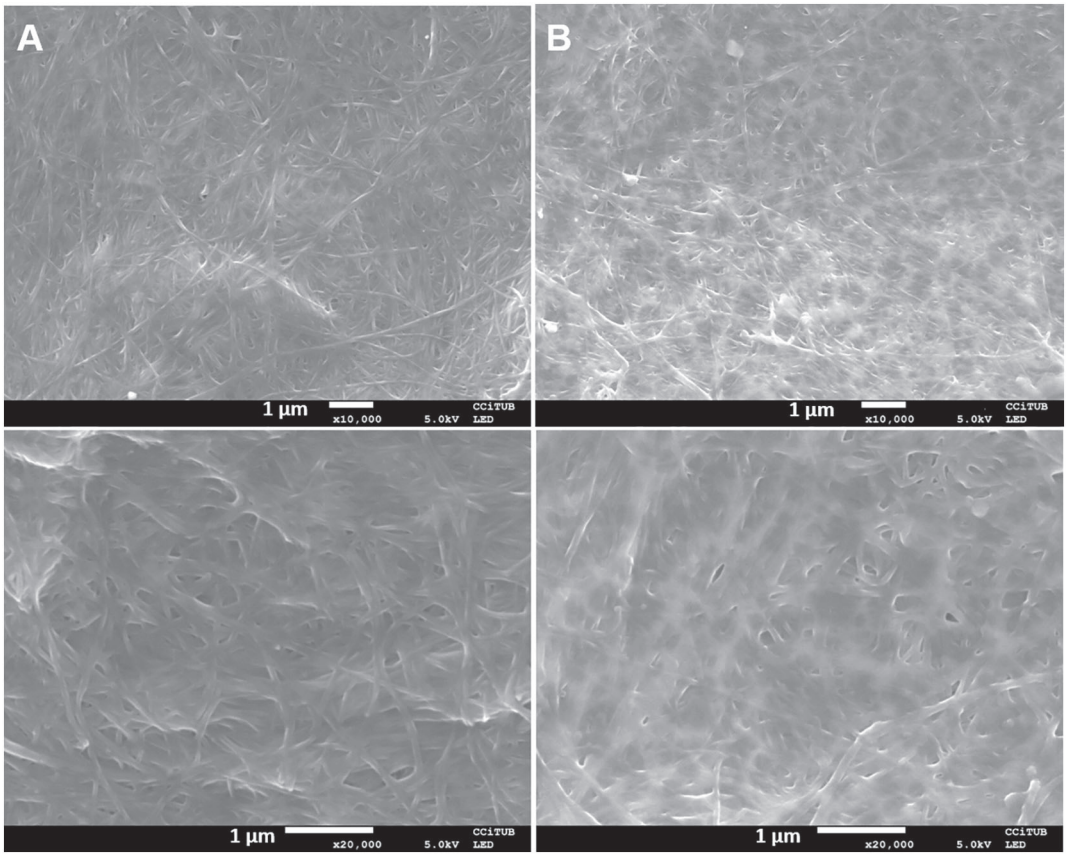

Fig. 1. Scanning electron microscopic (SEM) images of BCP (A) and Lys-BCP (B) at two different magnifications (up 10.000 x; down 20.000 x).

had also reported weak irregularities after protein immobilization, as Zhijiang et al. [64], who detected the same type of layer on the surface of a collagen/BC composite.

XRD patterns were measured to analyse microstructural changes on the BC due to the immobilization of lysozyme. Fig. 2 shows diffraction peaks at 2Θ angles around 18,4° and 22,7°, the main diffraction peaks of the typical profile of cellulose in crystalline form [65]. With the introduction of lysozyme, the profile did not change. Moreover, the estimated degree of crystallinity index (Eq. (2)) was 93% for both of them, suggesting that crystallinity is not affected during the process of adsorption. These findings contrast with those of Bayazidi et al. [16], who registered a dramatic decrease of the degree of crystallinity after

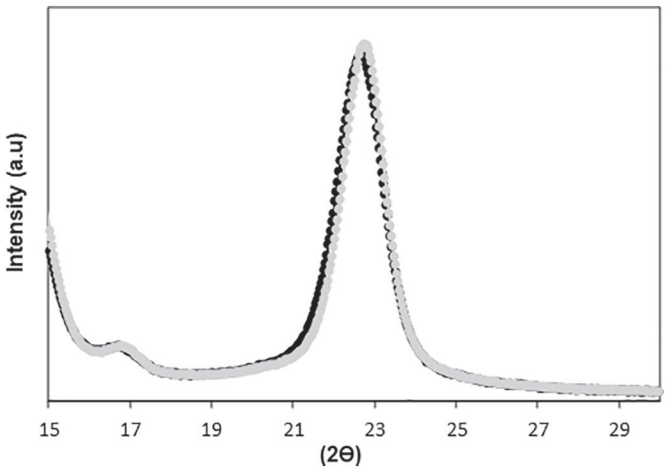

Fig. 2. XRD patterns of BCP (black line) and Lys-BCP biopaper (grey line).

immobilizing lysozyme on BC nanofibres suspension. However, BC nanofibres suspended in aqueous medium and BCP are matrices with different fibre density and porous structure. During the process of papermaking, the fibres of cellulose undergo dehydration through evaporation of water. This loss of water molecules produces irreversible formation of new hydrogen bounds between the hydroxyl groups of adjacent glucan chains holding the structure strongly [66]. Results indicated that no changes in the crystalline structure within the cellulose fibres did occur during the incorporation of lysozyme by physical adsorption, suggesting that characteristics as mechanical strength and interfacial properties of the cellulose fibre were not modified [67].

3.3. Operational characterization the Lys-BCP biopaper

The effect of temperature, thermal stability and pH on the enzymatic activity is reported in Fig. 3. The optimal catalytic temperature of Lys-BCP was higher than that of free form (Fig. 3A): free enzyme had its optimum temperature at 37 °C while Lys-BCP nanocomposite retained its maxim activity between 50 and 60 °C with statistically significant differences. Changes of physical and chemical properties of the immobilized enzyme could be related with this increase of thermal stability [35]. However, food storing is usually performed at room temperature or at 4 °C [11,18,60]. For this reason, and for taking into account for foreseeable applications, it should be pointed out that Lys-BCP had not only more relative activity but a higher specific activity than the free enzyme in the range 20–30 °C. Moreover, as can be seen in Fig. 3B, room temperature stability was highly enhanced by the adsorption of lysozyme onto BCP: Lys-BCP residual activity was about 70% after 2 h of incubation up to 24 h, as corroborated by the statistical analysis, whereas for the same time, free lysozyme conserved over 40% of the activity. At 72 h, inactivation of free enzyme took place, while Lys-BCP was still active, retaining 10% of initial activity. Lysozyme immobilized onto BCP is more stable as

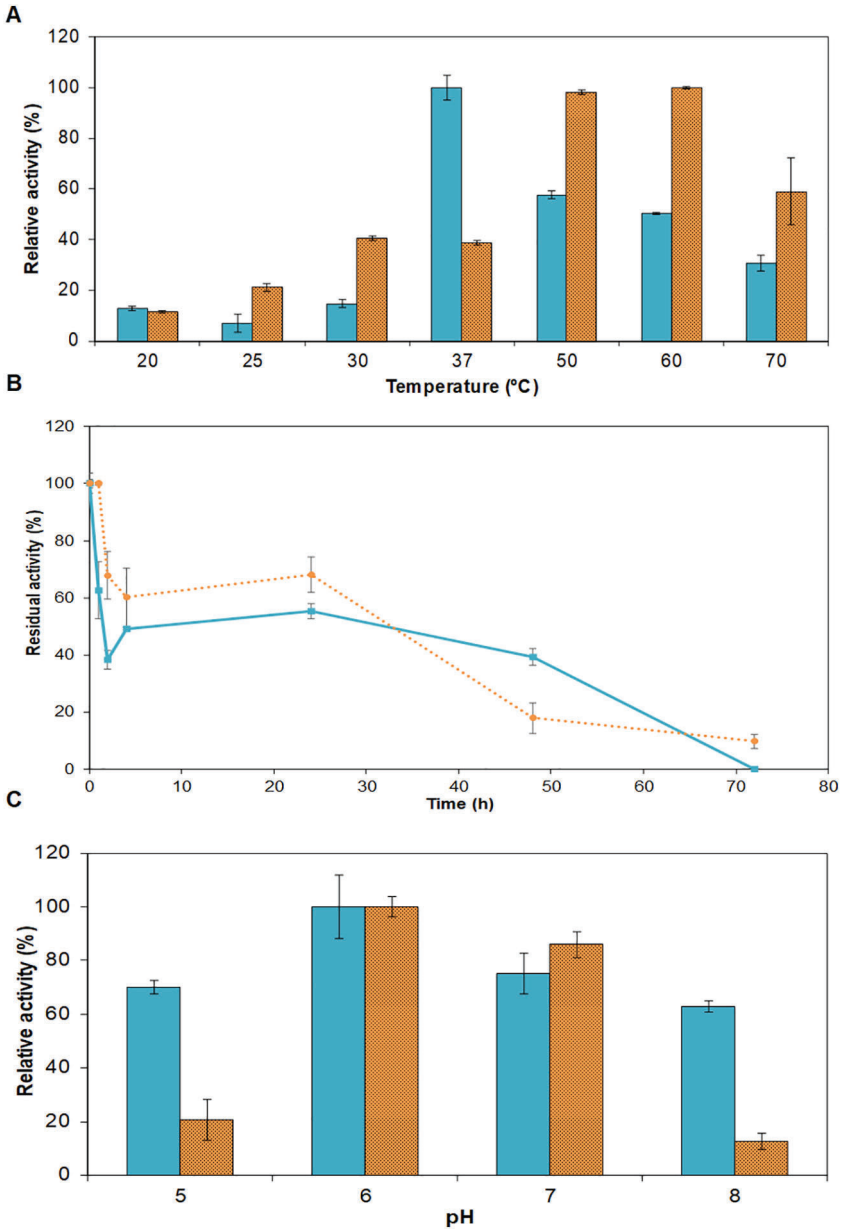

Fig. 3. Operational characteristics of the Lys-BCP biopaper. Data are presented as average ± standard deviation and were statistically analysed by analysis of variance (ANOVA, considering a value of $p \leq 0.05$ statistically significant. (A) Lysozyme activity at different temperatures. Activity was expressed in relative values, with the highest activity denoting 100%. Solid bars = free lysozyme, dot bars = Lys – BCP. (B) Thermal stability at room temperature under different times of incubation, where residual activity was expressed as percentage of the initial activity at time zero. Solid line = free lysozyme, dot line = Lys – BCP. (C) Effect of pH. Activity was expressed in relative values, with the highest activity denoting 100%. Solid bars = free lysozyme, dot bars = Lys – BCP.

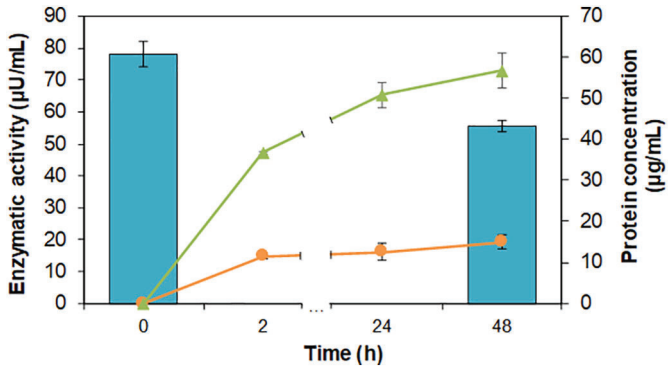

Fig. 4. Leaching of lysozyme from Lys-BC biopaper. Bars = Lys – BCP enzymatic activity; dots line = medium enzymatic activity; triangle line = medium protein concentration.

the restricted conformational mobility of the molecule embedded in the BCP matrix would delay the rate of inactivation [41,68].These results suggested that lysozyme would be more effective as a food preservative in an immobilization state than in a soluble bulk state. Free and immobilized lysozyme showed similar activity at pH 6 and 7, being

Table 2
Viable cell counts (CFU/mL) and cell viability reduction (%) of microorganisms in contact with Lys-BCP.

		CFU/mL	% reduction
Staphylococcus aureus	t_0	$2.52 \cdot 10^3$	0
	t_4	$1.46 \cdot 10^3$	46
	t_{24}	$4.50 \cdot 10^2$	82
Escherichia coli	t_0	$1.10 \cdot 10^3$	0
	t_4	$5.70 \cdot 10^2$	48
	t_{24}	$3.50 \cdot 10^2$	68

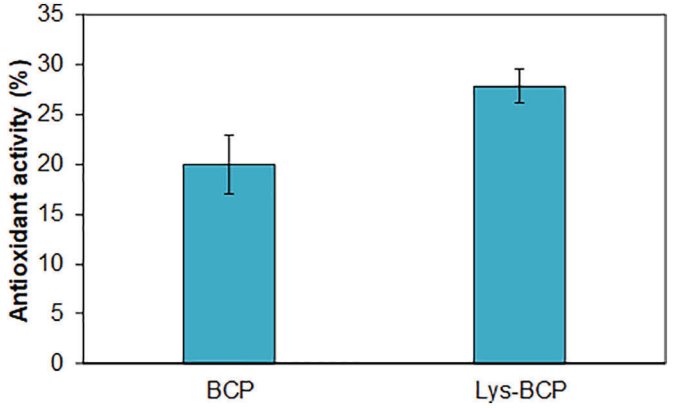

Fig. 5. Antioxidant activity of BCP and Lys-BCP supports. Data are presented as average ± standard deviation and were statistically analysed by analysis of variance (ANOVA, considering a value of $p \leq 0.05$ statistically significant.

pH 6 the optimum. However, the immobilized enzyme was less active at pH 5 and 8 than the free enzyme (Fig. 3C). The stability of some enzymes at different pH can be coupled to conformational changes in the molecule [69]. Results suggested that the binding to BC nanofibres would restrict the conformational mobility of lysozyme, decreasing its activity when was not operating at optimum pH. It is worth noting that no disintegration or erosion of the biopapers was observed after 72 h in the aqueous medium at pH 6 and room temperature.

3.4. Leaching of lysozyme from the Lys-BCP biopaper

To determinate the stability of immobilized lysozyme onto BCP, samples of the biopaper were incubated in buffer solution at room temperature. Enzymatic activity in the Lys-BCP biopaper, and enzymatic activity and protein contain in the surrounding aqueous medium, were measured at different times (Fig. 4). After 2 h of incubation, 20% of the initial Lys-BCP activity was found in the medium. This value remained nearly constant up to 48 h. The protein content in the medium also increases during the first 2 h of incubation, corroborating activity values, and continues to increase slightly until 48 h. At that time, the amount of protein released to the medium was about 8% of the total protein absorbed in the paper. Most of the release of enzyme took place during the first 2 h in contact with the aqueous solution and could be attributed to the molecules that were loosely attached to the BC nanofibres. On the other hand, Lys-BCP biopaper retained 70% of its original activity after 48 h of incubation in aqueous medium. Although physical adsorption is the simplest method of immobilization, it is not always feasible. Often, as in the case of cellulose of plant origin, the interactions between the enzyme and the support are not strong enough for immobilization and prevention of leakage of the attached biomolecules [22]. In this study, only a small fraction of the lysozyme migrated from the biopaper, suggesting that the high concentration of hydroxyl groups and the nanofibre network of the bacterial cellulose matrix was able to stabilize and retain the enzyme.

3.5. Antimicrobial activity

Lys-BCP was tested for its antimicrobial activity against Gram-positive and Gram-negative bacteria. As Sjollema et al. [70] suggested, in the evaluation of antimicrobial surface designs, a challenge concentration in line with the intended application should be applied. Considering that Lys-BCP design is most intended for prophylactic use, antimicrobial activity was evaluated at maximum challenge numbers of 1000 CFU per cm^2. In Table 2, is clearly shown the antimicrobial effect of Lys-BCP biopaper on the viability of *S. aureus* and *E. coli*, which showed about 82% and 68% reduction, respectively, after 24 h. *S. aureus* was more sensitive to lysozyme than *E. coli*, probably due to the well-known differences in structure and composition of the Gram-positive and Gram-negative bacteria cell wall. Biopaper's capability to kill microorganisms in aqueous surroundings is a relevant characteristic for applications, such as food packaging design to avoid microbial spoilage [71].

3.6. Antioxidant activity

Antioxidant activity of BC paper and Lys-BCP bioactive paper was assessed. BCP showed some antioxidant activity (Fig. 5). Previous studies have reported the presence of aldehyde groups in BC [46] and its antioxidant capability [72]. Moreover, when lysozyme is immobilized onto BCP, the antioxidant activity of the bioactive paper increased about 30%, being statistically significant. Lysozyme antioxidant activity could be attributed to NH_2 residues which have the capacity to scavenge radicals [73]. This is an interesting property in materials used for active packaging applications. Antioxidant agents in coatings and packaging preserve the nutritional value and extend the shelf-life of packaged food [74].

3.7. Storage and durability

The functionality of the Lys-BCP active paper was tested over a period of 80 days of storage (Fig. 6). Results indicated that the biopaper

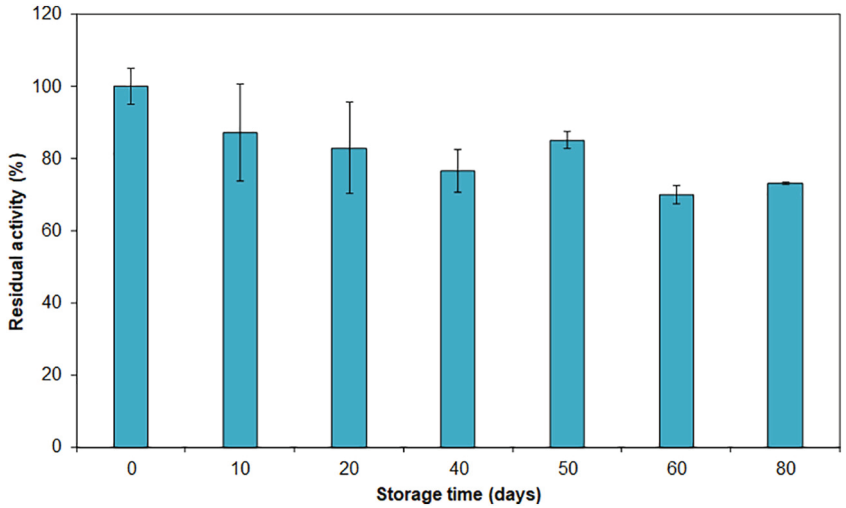

Fig. 6. Stability of Lys-BCP active paper stored at room temperature. Residual activity was expressed as percentage of the initial activity at time zero. Data are presented as average ± standard deviation and were statistically analysed by analysis of variance (ANOVA, considering a value of $p \leq 0.05$ statistically significant.

could be stored at room temperature for several weeks without any statistically significant loss of enzymatic activity, and retained over 70% of residual activity after 80 days. This high storage stability can be related to the biocompatibility and nano network structure of BC which, in a water-free environment, allowed the preservation of lysozyme without the need of special storage, such as low temperature.

4. Conclusions

In this work, a functional active paper made from BC with antimicrobial activity against Gram-positive and Gram-negative bacteria, and oxidative scavenging capacity was generated. The immobilization by physical adsorption of lysozyme onto BC paper had no negative effect on the specific activity of lysozyme or on the morphology and crystallinity of the paper. Lysozyme was stabilized and well retained in the matrix of nanofibres. Lys-BCP biopaper was active in a wide range of temperatures, showing higher stability than the free enzyme at room temperature. Additionally, it was easily stored at room temperature without any decrease in enzymatic activity for several weeks. Moreover, owning the intrinsically nature of its components, Lys-BCP active paper is biodegradable and biocompatible. Lys-BCP biopaper presents attractive features to be part of the design of new active packaging materials. It is foreseeable that other biomolecules can be physically absorbed into paper made from bacterial cellulose to obtain active papers with different functionalities.

Acknowledgments

This work was financed by the Spanish Ministry of Economy, Industry and Competitiveness, grants CTQ2017-84966-C2-2-R, FILMBIOCEL (CTQ2016-77936-R) (funding also from FEDER) and MICROBIOCEL (CTQ2017-84966-C2-1-R), and by the Pla de Recerca de Catalunya, grant 2017SGR-30, and by the Generalitat de Catalunya, "Xarxa de Referència en Biotecnologia" (XRB). C. Buruaga-Ramiro acknowledges an APIF predoctoral grant from the University of Barcelona. Special thanks are due to the Serra Húnter Fellow to Cristina Valls.

Declaration of competing interest

Authors have no conflict of interest to declare.

References

[1] L. Vermeiren, F. Devlieghere, M. van Beest, N. de Kruijf, J. Debevere, Developments in the active packaging of foods, Trends Food Sci. Technol. 10 (1999) 77–86, https://doi.org/10.1016/S0924-2244(99)00032-1.
[2] V.K. Bajpai, M. Kamle, S. Shukla, D.K. Mahato, P. Chandra, S.K. Hwang, P. Kumar, Y.S. Huh, Y.-K. Han, Prospects of using nanotechnology for food preservation, safety, and security, J. Food Drug Anal. 26 (2018) 1201–1214, https://doi.org/10.1016/j.jfda.2018.06.011.
[3] N. Dasgupta, S. Ranjan, D. Mundekkad, C. Ramalingam, R. Shanker, A. Kumar, Nanotechnology in agro-food: from field to plate, Food Res. Int. 69 (2015) 381–400, https://doi.org/10.1016/j.foodres.2015.01.005.
[4] C.O. Gill, Active packaging in practice: meat, Nov. Food Packag. Tech, 2003https://doi.org/10.1016/B978-1-85573-675-7.50021-3.
[5] N.P. Guerra, C.L. Macias, A.T. Agrasar, L.P. Castro, Development of a bioactive packaging cellophane using NisaplinR as biopreservative agent, Lett. Appl. Microbiol. 40 (2005) 106–110, https://doi.org/10.1111/j.1472-765X.2004.01649.x.
[6] J.K. Branen, P.M. Davidson, Enhancement of nisin, lysozyme, and monolaurin antimicrobial activities by ethylenediaminetetraacetic acid and lactoferrin, Int. J. Food Microbiol. 90 (2004) 63–74, https://doi.org/10.1016/S0168-1605(03)00172-7.
[7] H.R. Ibrahim, U. Thomas, A. Pellegrini, A helix-loop-helix peptide at the upper lip of the active site cleft of lysozyme confers potent antimicrobial activity with membrane permeabilization action, J. Biol. Chem. (2001)https://doi.org/10.1074/jbc.M106317200.
[8] J.S. Rudra, K. Dave, D.T. Haynie, Antimicrobial polypeptide multilayer nanocoatings, J. Biomater. Sci. Polym. Ed. 17 (2006) 1301–1315, https://doi.org/10.1163/156856206778667433.
[9] A. Cagri, Z. Ustunol, E.T. Ryser, Antimicrobial edible films and coatings, J. Food Prot. 67 (2004) 833–848, https://doi.org/10.4315/0362-028X-67.4.833.
[10] K. Hanušová, L. Vápenka, J. Dobiáš, L. Mišková, Development of antimicrobial packaging materials with immobilized glucose oxidase and lysozyme, Open Chem. 11 (2013)https://doi.org/10.2478/s11532-013-0241-4.
[11] S. Mangalassary, I. Han, J. Rieck, J. Acton, P. Dawson, Effect of combining nisin and/or lysozyme with in-package pasteurization for control of Listeria monocytogenes in ready-to-eat turkey bologna during refrigerated storage, Food Microbiol. 25 (2008) 866–870, https://doi.org/10.1016/j.fm.2008.05.002.
[12] K. Sung, S.A. Khan, M.S. Nawaz, C.E. Cerniglia, M.L. Tamplin, R.W. Phillips, L.C. Kelley, Lysozyme as a barrier to growth of Bacillus anthracis strain Sterne in liquid egg white, milk and beef, Food Microbiol. 28 (2011) 1231–1234, https://doi.org/10.1016/j.fm.2011.03.002.
[13] F. Makki, T.D. Durance, Thermal inactivation of lysozyme as influenced by pH, sucrose and sodium chloride and inactivation and preservative effect in beer, Food Res. Int. 29 (1996) 635–645, https://doi.org/10.1016/S0963-9969(96)00074-9.
[14] A.O. Gill, R.A. Holley, Surface application of lysozyme, nisin, and EDTA to inhibit spoilage and pathogenic bacteria on ham and bologna, J. Food Prot. 63 (2000) 1338–1346, https://doi.org/10.4315/0362-028X-63.10.1338.
[15] N.L. Rose, P. Sporns, M.E. Stiles, L.M. McMullen, Inactivation of nisin by glutathione in fresh meat, J. Food Sci. 64 (1999) 759–762, https://doi.org/10.1111/j.1365-2621.1999.tb15906.x.
[16] P. Bayazidi, H. Almasi, A.K. Asl, Immobilization of lysozyme on bacterial cellulose nanofibers: characteristics, antimicrobial activity and morphological properties, Int. J. Biol. Macromol. 107 (2018) 2544–2551, https://doi.org/10.1016/j.ijbiomac.2017.10.137.
[17] Y. Fang, X.-J. Huang, P.-C. Chen, Z.-K. Xu, Polymer materials for enzyme immobilization and their application in bioreactors, BMB Rep. 44 (2011) 87–95, https://doi.org/10.5483/BMBRep.2011.44.2.87.
[18] D. Ercolini, I. Ferrocino, A. La Storia, G. Mauriello, S. Gigli, P. Masi, F. Villani, Development of spoilage microbiota in beef stored in nisin activated packaging, Food Microbiol. 27 (2010) 137–143, https://doi.org/10.1016/j.fm.2009.09.006.
[19] N. Lin, A. Dufresne, Nanocellulose in biomedicine: current status and future prospect, Eur. Polym. J. 59 (2014) 302–325, https://doi.org/10.1016/j.eurpolymj.2014.07.025.
[20] W. Yao, X. Wu, J. Zhu, B. Sun, C. Miller, In vitro enzymatic conversion of γ-aminobutyric acid immobilization of glutamate decarboxylase with bacterial cellulose membrane (BCM) and non-linear model establishment, Enzym. Microb. Technol. 52 (2013) 258–264, https://doi.org/10.1016/j.enzmictec.2013.01.008.
[21] C. Castro, A. Vesterinen, R. Zuluaga, G. Caro, I. Filpponen, O.J. Rojas, G. Kortaberria, P. Gañán, In situ production of nanocomposites of poly(vinyl alcohol) and cellulose nanofibrils from Gluconacetobacter bacteria: effect of chemical crosslinking, Cellulose 21 (2014) 1745–1756, https://doi.org/10.1007/s10570-014-0170-1.
[22] J. Credou, T. Berthelot, Cellulose: from biocompatible to bioactive material, J. Mater. Chem. B 2 (2014) 4767–4788, https://doi.org/10.1039/C4TB00431K.
[23] B.N. Estevinho, N. Samaniego, D. Talens-Perales, M.J. Fabra, A. López-Rubio, J. Polaina, J. Marín-Navarro, Development of enzymatically-active bacterial cellulose membranes through stable immobilization of an engineered β-galactosidase, Int. J. Biol. Macromol. 115 (2018) 476–482, https://doi.org/10.1016/j.ijbiomac.2018.04.081.
[24] V.T. Nguyen, M.J. Gidley, G.A. Dykes, Potential of a nisin-containing bacterial cellulose film to inhibit Listeria monocytogenes on processed meats, Food Microbiol. 25 (2008) 471–478, https://doi.org/10.1016/j.fm.2008.01.004.
[25] S. Bielecki, A. Krystynowicz, M. Turkiewicz, H. Kalinowska, Bacterial cellulose, in: E.J. Vandamme, S. De Baets, A. Steinbüchel (Eds.), Biopolym. Online, Wiley-VCH Verlag GmbH & Co. KGaA, Weinheim, Germany, 2005https://doi.org/10.1002/3527600035.bpol5003.
[26] D. Klemm, F. Kramer, S. Moritz, T. Lindström, M. Ankerfors, D. Gray, A. Dorris, Nanocelluloses: a new family of nature-based materials, Angew. Chemie Int. Ed. 50 (2011) 5438–5466, https://doi.org/10.1002/anie.201001273.
[27] A. Fillat, J. Martínez, C. Valls, O. Cusola, M.B. Roncero, T. Vidal, S.V. Valenzuela, P. Diaz, F.I.J. Pastor, Bacterial cellulose for increasing barrier properties of paper products, Cellulose (2018)https://doi.org/10.1007/s10570-018-1967-0.
[28] B.R. Evans, H.M. O'Neill, V.P. Malyvanh, I. Lee, J. Woodward, Palladium-bacterial cellulose membranes for fuel cells, Biosens. Bioelectron. 18 (2003) 917–923, https://doi.org/10.1016/S0956-5663(02)00212-9.
[29] Z. Shi, S. Zang, F. Jiang, L. Huang, D. Lu, Y. Ma, G. Yang, In situ nano-assembly of bacterial cellulose–polyaniline composites, RSC Adv. 2 (2012) 1040–1046, https://doi.org/10.1039/C1RA00719J.
[30] T. Hänninen, H. Orelma, J. Laine, TEMPO oxidized cellulose thin films analysed by QCM-D and AFM, Cellulose 22 (2015) 165–171, https://doi.org/10.1007/s10570-014-0530-x.
[31] J. Kim, Z. Cai, H.S. Lee, G.S. Choi, D.H. Lee, C. Jo, Preparation and characterization of a Bacterial cellulose/Chitosan composite for potential biomedical application, J. Polym. Res. 18 (2011) 739–744, https://doi.org/10.1007/s10965-010-9470-9.
[32] M. Ul-Islam, T. Khan, J.K. Park, Water holding and release properties of bacterial cellulose obtained by in situ and ex situ modification, Carbohydr. Polym. 88 (2012) 596–603, https://doi.org/10.1016/j.carbpol.2012.01.006.
[33] N. Klinthoopthamrong, D. Chaikiawkeaw, W. Phoolcharoen, K. Rattanapisit, P. Kaewpungsup, P. Pavasant, V.P. Hoven, Bacterial cellulose membrane conjugated with plant-derived osteopontin: preparation and its potential for bone tissue regeneration, Int. J. Biol. Macromol. (2020)https://doi.org/10.1016/j.ijbiomac.2020.01.158.
[34] B. Yu, H. Cheng, W. Zhuang, C. Zhu, J. Wu, H. Niu, D. Liu, Y. Chen, H. Ying, Stability and repeatability improvement of horseradish peroxidase by immobilization on amino-functionalized bacterial cellulose, Process Biochem. 79 (2019) 40–48, https://doi.org/10.1016/j.procbio.2018.12.024.
[35] L. Chen, M. Zou, F.F. Hong, Evaluation of fungal laccase immobilized on natural nanostructured bacterial cellulose, Front. Microbiol. 6 (2015)https://doi.org/10.3389/fmicb.2015.01245.

[36] G. D'Ayala, M. Malinconico, P. Laurienzo, Marine derived polysaccharides for biomedical applications: chemical modification approaches, Molecules. 13 (2008) 2069–2106, https://doi.org/10.3390/molecules13092069.
[37] G.A. Vikhoreva, I.N. Gorbacheva, L.S. Gal'braikh, Chemical modification of aquatic polysaccharides. A review, Fibre Chem. 26 (1994) 326–334, https://doi.org/10.1007/BF02396600.
[38] N. Karaki, A. Aljawish, C. Humeau, L. Muniglia, J. Jasniewski, Enzymatic modification of polysaccharides: mechanisms, properties, and potential applications: a review, Enzym. Microb. Technol. 90 (2016) 1–18, https://doi.org/10.1016/j.enzmictec.2016.04.004.
[39] H.J. Kim, S. Park, S.H. Kim, J.H. Kim, H. Yu, H.J. Kim, Y.-H. Yang, E. Kan, Y.H. Kim, S.H. Lee, Biocompatible cellulose nanocrystals as supports to immobilize lipase, J. Mol. Catal. B Enzym. 122 (2015) 170–178, https://doi.org/10.1016/j.molcatb.2015.09.007.
[40] C.A. dos Santos, G.R. dos Santos, V.S. Soeiro, J.R. dos Santos, M. de A. Rebelo, M.V. Chaud, M. Gerenutti, D. Grotto, R. Pandit, M. Rai, A.F. Jozala, Bacterial nanocellulose membranes combined with nisin: a strategy to prevent microbial growth, Cellulose 25 (2018) 6681–6689, https://doi.org/10.1007/s10570-018-2010-1.
[41] H. Yuan, L. Chen, F.F. Hong, M. Zhu, Evaluation of nanocellulose carriers produced by four different bacterial strains for laccase immobilization, Carbohydr. Polym. 196 (2018) 457–464, https://doi.org/10.1016/j.carbpol.2018.05.055.
[42] S.-C. Wu, S.-M. Wu, F.-M. Su, Novel process for immobilizing an enzyme on a bacterial cellulose membrane through repeated absorption, J. Chem. Technol. Biotechnol. 92 (2017) 109–114, https://doi.org/10.1002/jctb.4994.
[43] Z.-X. Lian, Z.-S. Ma, J. Wei, H. Liu, Preparation and characterization of immobilized lysozyme and evaluation of its application in edible coatings, Process Biochem. 47 (2012) 201–208, https://doi.org/10.1016/j.procbio.2011.10.031.
[44] J.-M. Park, M. Kim, H.-S. Park, A. Jang, J. Min, Y.-H. Kim, Immobilization of lysozyme-CLEA onto electrospun chitosan nanofiber for effective antibacterial applications, Int. J. Biol. Macromol. 54 (2013) 37–43, https://doi.org/10.1016/j.ijbiomac.2012.11.025.
[45] S. Ranote, P. Jamwal, D. Kumar, B. Ram, S. Jamwal, G.S. Chauhan, Stabilization of lysozyme via covalent immobilization onto two cellulosic materials: cotton bandage and lawn cloth, Trends Carbohydr. Res. 10 (2018) 54–63.
[46] A.G. Morena, M.B. Roncero, S.V. Valenzuela, C. Valls, T. Vidal, F.I.J. Pastor, P. Diaz, J. Martínez, Laccase/TEMPO-mediated bacterial cellulose functionalization: production of paper-silver nanoparticles composite with antimicrobial activity, Cellulose 26 (2019) 8655–8668, https://doi.org/10.1007/s10570-019-02678-5.
[47] L.V. Cabañas-Romero, C. Valls, S.V. Valenzuela, M.B. Roncero, F.I.J. Pastor, P. Diaz, J. Martínez, Bacterial cellulose–chitosan paper with antimicrobial and antioxidant activities, Biomacromolecules 21 (2020) 1568–1577, https://doi.org/10.1021/acs.biomac.0c00127.
[48] C. Buruaga-Ramiro, S.V. Valenzuela, C. Valls, M.B. Roncero, F.I.J. Pastor, P. Díaz, J. Martínez, Bacterial cellulose matrices to develop enzymatically active paper, Cellulose (2020)https://doi.org/10.1007/s10570-020-03025-9.
[49] N. Phutanon, K. Motina, Y.-H. Chang, S. Ummartyotin, Development of CuO particles onto bacterial cellulose sheets by forced hydrolysis: a synergistic approach for generating sheets with photocatalytic and antibiofouling properties, Int. J. Biol. Macromol. 136 (2019) 1142–1152, https://doi.org/10.1016/j.ijbiomac.2019.06.168.
[50] J. Fernández, A.G. Morena, S.V. Valenzuela, F.I.J. Pastor, P. Díaz, J. Martínez, Microbial cellulose from a Komagataeibacter intermedius strain isolated from commercial wine vinegar, J. Polym. Environ. 27 (2019) 956–967, https://doi.org/10.1007/s10924-019-01403-4.
[51] M.M. Bradford, A rapid and sensitive method for the quantitation of microgram quantities of protein utilizing the principle of protein-dye binding, Anal. Biochem. 72 (1976) 248–254, https://doi.org/10.1016/0003-2697(76)90527-3.
[52] L. Segal, J.J. Creely, A.E. Martin, C.M. Conrad, An empirical method for estimating the degree of crystallinity of native cellulose using the X-ray diffractometer, Text. Res. J. 29 (1959) 786–794, https://doi.org/10.1177/004051755902901003.
[53] A. Serpen, E. Capuano, V. Fogliano, V. Gökmen, A new procedure to measure the antioxidant activity of insoluble food components, J. Agric. Food Chem. 55 (2007) 7676–7681, https://doi.org/10.1021/jf071291z.
[54] C. Valls, M.B. Roncero, Antioxidant property of TCF pulp with a high hexenuronic acid (HexA) content, Holzforschung 67 (2013) 257–263, https://doi.org/10.1515/hf-2012-0114.
[55] O. Cusola, C. Valls, T. Vidal, M.B. Roncero, Conferring antioxidant capacity to cellulose based materials by using enzymatically-modified products, Cellulose 22 (2015) 2375–2390, https://doi.org/10.1007/s10570-015-0668-1.
[56] D. Dong, X. Li, Y. Hua, Y. Chen, X. Kong, C. Zhang, Q. Wang, Mutual titration of soy proteins and gum arabic and the complexing behavior studied by isothermal titration calorimetry, turbidity and ternary phase boundaries, Food Hydrocoll. 46 (2015) 28–36, https://doi.org/10.1016/j.foodhyd.2014.11.019.
[57] T. Oshima, S. Taguchi, K. Ohe, Y. Baba, Phosphorylated bacterial cellulose for adsorption of proteins, Carbohydr. Polym. 83 (2011) 953–958, https://doi.org/10.1016/j.carbpol.2010.09.005.
[58] Q. Lin, Y. Zheng, G. Wang, X. Shi, T. Zhang, J. Yu, J. Sun, Protein adsorption behaviors of carboxymethylated bacterial cellulose membranes, Int. J. Biol. Macromol. 73 (2015) 264–269, https://doi.org/10.1016/j.ijbiomac.2014.11.011.
[59] C. Chai, J. Lee, Q. Huang, The effect of ionic strength on the rheology of pH-induced bovine serum albumin/κ-carrageenan coacervates, LWT – Food Sci. Technol. 59 (2014) 356–360, https://doi.org/10.1016/j.lwt.2014.05.024.
[60] E. Cappannella, I. Benucci, C. Lombardelli, K. Liburdi, T. Bavaro, M. Esti, Immobilized lysozyme for the continuous lysis of lactic bacteria in wine: bench-scale fluidized-bed reactor study, Food Chem. 210 (2016) 49–55, https://doi.org/10.1016/j.foodchem.2016.04.089.
[61] T. Haider, Q. Husain, Concanavalin A layered calcium alginate–starch beads immobilized β galactosidase as a therapeutic agent for lactose intolerant patients, Int. J. Pharm. 359 (2008) 1–6, https://doi.org/10.1016/j.ijpharm.2008.03.013.
[62] M. Skočaj, Bacterial nanocellulose in papermaking, Cellulose 26 (2019) 6477–6488, https://doi.org/10.1007/s10570-019-02566-y.
[63] H. Ougiya, N. Hioki, K. Watanabe, Y. Morinaga, F. Yoshinaga, M. Samejima, Relationship between the physical properties and surface area of cellulose derived from adsorbates of various molecular sizes, Biosci. Biotechnol. Biochem. 62 (1998) 1880–1884, https://doi.org/10.1271/bbb.62.1880.
[64] C. Zhijiang, Y. Guang, Bacterial cellulose/collagen composite: characterization and first evaluation of cytocompatibility, J. Appl. Polym. Sci. 120 (2011) 2938–2944, https://doi.org/10.1002/app.33318.
[65] H. Almasi, B. Ghanbarzadeh, J. Dehghannya, A.A. Entezami, A.K. Asl, Novel nanocomposites based on fatty acid modified cellulose nanofibers/poly(lactic acid): morphological and physical properties, Food Packag. Shelf Life 5 (2015) 21–31, https://doi.org/10.1016/j.fpsl.2015.04.003.
[66] A. Seves, G. Testa, A.M. Bonfatti, E. Dubini Paglia, E. Selli, B. Marcandalli, Characterization of native cellulose/poly(ethylene glycol) films, Macromol. Mater. Eng. 286 (2001) 524–528, https://doi.org/10.1002/1439-2054(20010901)286:9<524::AID-MAME524>3.0.CO;2-B.
[67] Y. Huang, C. Zhu, J. Yang, Y. Nie, C. Chen, D. Sun, Recent advances in bacterial cellulose, Cellulose 21 (2014) 1–30, https://doi.org/10.1007/s10570-013-0088-z.
[68] C.J.R. Frazão, N.H.C. Silva, C.S.R. Freire, A.J.D. Silvestre, A.M.R.B. Xavier, A.P.M. Tavares, Bacterial cellulose as carrier for immobilization of laccase: optimization and characterization, Eng. Life Sci. 14 (2014) 500–508, https://doi.org/10.1002/elsc.201400054.
[69] L. Mazzei, M. Cianci, S. Benini, S. Ciurli, The impact of pH on catalytically critical protein conformational changes: the case of the urease, a nickel enzyme, Chem. A Eur. J. (2019)https://doi.org/10.1002/chem.201902320.
[70] J. Sjollema, S.A.J. Zaat, V. Fontaine, M. Ramstedt, R. Luginbuehl, K. Thevissen, J. Li, H.C. van der Mei, H.J. Busscher, In vitro methods for the evaluation of antimicrobial surface designs, Acta Biomater. 70 (2018) 12–24, https://doi.org/10.1016/j.actbio.2018.02.001.
[71] A. Barbiroli, F. Bonomi, G. Capretti, S. Iametti, M. Manzoni, L. Piergiovanni, M. Rollini, Antimicrobial activity of lysozyme and lactoferrin incorporated in cellulose-based food packaging, Food Control 26 (2012) 387–392, https://doi.org/10.1016/j.foodcont.2012.01.046.
[72] L. Zhang, H. Ge, M. Xu, J. Cao, Y. Dai, Physicochemical properties, antioxidant and antibacterial activities of dialdehyde microcrystalline cellulose, Cellulose 24 (2017) 2287–2298, https://doi.org/10.1007/s10570-017-1255-4.
[73] K. Crouvisier-Urion, P.R. Bodart, P. Winckler, J. Raya, R.D. Gougeon, P. Cayot, S. Domenek, F. Debeaufort, T. Karbowiak, Biobased composite films from chitosan and lignin: antioxidant activity related to structure and moisture, ACS Sustain. Chem. Eng. 4 (2016) 6371–6381, https://doi.org/10.1021/acssuschemeng.6b00956.
[74] J.M. Lorenzo, R. Batlle, M. Gómez, Extension of the shelf-life of foal meat with two antioxidant active packaging systems, LWT – Food Sci. Technol. 59 (2014) 181–188, https://doi.org/10.1016/j.lwt.2014.04.061.

4.3. Capítulo 3. Funcionalización de la celulosa bacteriana: obtención de nanocristales con un tratamiento enzimático

4.3.1. ***Artículo 5.*** *Lytic polysaccharyde monooxigenases and cellulases on the production of bacterial cellulose nanocrystals.*

Lytic polysaccharyde monooxigenases and cellulases on the production of bacterial cellulose nanocrystals

Los materiales obtenidos de recursos naturales como la celulosa están atrayendo una gran atención debido al uso excesivo de derivados fósiles del petróleo. Los nanocristales de celulosa son un nanomaterial renovable con propiedades de la nanoescala que no están presentes en la dimensión macroscópica, además de las ventajas de la propia celulosa. En este estudio se realizó un tratamiento enzimático para la obtención de nanocristales de celulosa bacteriana (BCNC), una aproximación mucho más amigable con el medio ambiente que la tradicional hidrólisis ácida. La combinación de una oxidación de una monooxigenasa lítica de polisacáridos (LPMO), seguida de una digestión de una mezcla de glucosil hidrolasas fue suficiente para producir BCNC. Una vez obtenidos, se caracterizaron en cuanto a morfología y tamaño se refiere mediante microscopía electrónica y difracción láser, respectivamente. Además, la carga negativa generada por la LPMO proporcionó a los nanocristales una buena dispersión uniforme en solución acuosa, como demostró la determinación del potencial zeta. De acuerdo con la curva de termogravimentría, la estabilidad térmica fue más elevada respecto a la celulosa bacteriana nativa. Además, la alta relación de aspecto de los BCNC permitió su uso como agente de recubrimiento de materiales celulósicos preexistentes. Los nanomateriales obtenidos mostraron propiedades mecánicas mejoradas, una elevada capacidad de retención de agua e impermeabilidad a las grasas. Estas atractivas características podrían llevar a que los nanocompuestos poliméricos que contienen BCNC tengan un impacto en el campo de los materiales de envasado biocompatibles y biodegradables.

UNIVERSITAT DE BARCELONA

JOSEFINA MARTÍNEZ

Tel +34 934 034 627
E-mail: jmartinez@ub.edu http://www.ub.edu/enzimsmicrobians

Department of Genetics, Microbiology & Statistics
Microbiology, Virology and Biotechnology Section
Faculty of Biology

Avinguda Diagonal 643
08028 Barcelona

Tel. +34 934 021 488
Tel. +34 934 021 489
Fax +34 934 034 629
dept-microbiologia-biol@ub.edu
www.ub.edu

Editor
European Polymer Journal

September 22, 2021

Dear Editor,

Please find enclosed our manuscript entitled *Lytic polysaccharide monooxigenases and cellulases on the production of bacterial cellulose nanocrystals* signed by Carolina Buruaga-Ramiro, Noelia Fernández-Gándara, L. Verónica Cabañas-Romero, Susana V. Valenzuela, F.I. Javier Pastor, Pilar Diaz and Josefina Martínez. All authors have approved the manuscript and mutually agree to submit it for publication in *European Polymer Journal*. Authors have no conflict of interest to declare. We confirm that this manuscript has not been published elsewhere in whole or in part and is not under consideration by another journal. If accepted, it will not be published elsewhere in the same form, in English or in any other language, including electronically without the written consent of the copyright-holder.

Looking forward to hearing from you, yours sincerely,

Josefina Martínez
Professor

Lytic polysaccharide monooxygenases and cellulases on the production of bacterial cellulose nanocrystals

Carolina Buruaga-Ramiro[1,2], Noelia Fernández-Gándara[1], L. Verónica Cabañas-Romero[1,2], Susana V. Valenzuela[1,2], F.I. Javier Pastor[1,2], Pilar Diaz[1,2], Josefina Martínez[1,2]*

[1] Department of Genetics, Microbiology and Statistics, Faculty of Biology, University of Barcelona, Av. Diagonal 643, 08028, Barcelona, Spain
[2] Institute of Nanoscience and Nanotechnology (IN2UB), Universitat de Barcelona, Spain

C. Buruaga-Ramiro: buruaga.cbr@ub.edu; Noelia Fernández-Gándara: noeliafdzgandara@gmail.com; L. Verónica Cabañas-Romero veronica.cabanas@ub.edu; F.I. Javier Pastor: fpastor@ub.edu; Susana V. Valenzuela: susanavalenzuela@ub.edu; Pilar Diaz: pdiaz@ub.edu; Josefina Martínez: jmartinez@ub.edu

*Corresponding author: Josefina Martínez. Department of Genetics, Microbiology and Statistics, Faculty of Biology, Universitat de Barcelona, Av. Diagonal 643, 08028 Barcelona, Spain. e-mail: jmartinez@ub.edu. Phone: +34 934034625.

Highlights

- Bacterial cellulose nanocrystals were obtained with an enzymatic treatment.
- Lytic polysaccharide monooxygenases was used as a pretreatment for the obtention of cellulose nanocrystals.
- The obtained bacterial cellulose nanocrystals displayed a high aspect ratio, a good suspension stability and good thermostability.
- The Nanocrystals/Eucalyptus composites showed improved barrier properties and mechanical resistance.

Abstract

Cellulose nanocrystals are a renewable biomaterial with nanoscale properties which have useful applications. In this study, an enzymatic treatment, an approach much more environmentally friendly than the traditional harsh acid hydrolysis, was performed to obtain bacterial cellulose nanocrystals (BCNC). The combination of an oxidation by a lytic polysaccharide monooxygenase (LPMO) and a hydrolysis with a mixture of glycosyl hydrolases was effective to produce nanocrystals from bacteria cellulose. Morphology and size were confirmed by electron microscopy and laser diffraction, respectively. Thermal stability was also measured and determined to be higher relative to native bacterial cellulose. Additionally, it was found that the negative charges generated by the LPMO increased the dispersion of the nanocrystals in aqueous solution, measured by the zeta potential. The BCNC were used to coat pre-existing cellulosic materials. The obtained composites displayed improved mechanical properties, an elevated water retention capacity, and impermeability to oil. These attractive features could lead BCNC-containing polymer nanocomposites to make an impact in the field of biocompatible and biodegradable packaging materials.

Keywords: bacterial cellulose; bacterial cellulose nanocrystals; nanocomposites, cellulose enzymatic hydrolysis; lytic polysaccharide monooxygenases

1. Introduction

There is a need to create a sustainable material that could replace traditional plastic packaging. In order to reduce packaging waste created by non-degradable petroleum based packaging materials, in the last decades, there has been a rising effort to produce various biodegradable polymers for the development of edible films [1]. However, these biopolymer edible films have some limitations regarding their mechanical properties and water sensitivity. An alternative to overcome them is the use of nanomaterials, which can reinforce biopolymers by the formation of nanocomposites [2]. Nanocomposites are defined as the combination of two types of individual materials: the matrix and the material imbedded on it, being at least one of the two of nanometre-sized dimension [3]. The reinforcement provided by the nanomaterial provides improved mechanical, thermal, optical, and physicochemical properties in comparison to the polymer alone [2,4], even at very low fractions [5]. Thus, the nanometric size and the increased surface area of the reinforcing material provides this new nanocomposite unique properties [6].

From the wide range of natural resources, cellulose is the most abundant macromolecule on Earth, and it is seen as an exciting alternative to fossil-fuel plastics. In fact, cellulose nanocrystals (CNC) obtained from plant sources are commonly used as nanomaterials [7]. These CNC are highly crystalline and exhibit excellent properties like high tensile strength [8]. The conversion of cellulose fibres into nanocrystals results in the formation of the well-known whiskers, rod-like or ribbon-like shape with large aspect ratio, mainly due to their nanoscale dimensions. When compared to cellulose fibres, CNC possess many advantages apart from their appealing intrinsic nanoscale dimension such as high surface area, unique morphology, low density, renewability, biodegradability and high mechanical strength [9–11]. According to their structure, CNC have an abundance of hydroxyl groups on the active surface, which allows both, the hydrogen bonding with the fibres [12] and further functionalization [13]. The applications of CNC can be of two types. One the one hand, they suppose a suitable material for a wide range of applications such as synthesis of antimicrobial materials, enzyme immobilization, green catalysis, biosensing and drug delivery [14,15]. On the other hand, CNC can act as a reinforcing agent [5], with potential uses ranging from barrier films to pH sensors [16–19]. Nevertheless, bacterial cellulose (BC) is more preferred over plant cellulose for CNC obtention as it is available in relatively pure form and has better physic-chemical properties than plant cellulose [20]. BC is produced mainly by bacteria from the genera *Komagataeibacter* as an exopolysaccharide. Even though in terms of chemical structure BC is identical to the vegetal one, it is synthetized chemically pure as it does not present hemicelluloses or lignin [21]. Consequently, it does not need to be purified, reducing the

economic and the environmental impact. In addition, BC displays a higher degree of crystallinity, a higher tensile strength, a higher water-holding capacity and a finer three-dimensional nanofibre network [22,23]. Besides, its addition to other celluloses is well known to decreases porosity, improving barrier properties, which is interesting in packaging applications [24]. Nanocrystals derived from bacterial cellulose (BCNC) can be physically incorporated into various polymer matrices to form polymer nanocomposites.

CNC suspensions can be obtained by submitting native cellulose to a harsh sulfuric acid hydrolysis, often followed by ultrasound treatments, as Rånby et al. described [25]. Under this acid treatment, the amorphous regions that interconnect the crystalline regions are removed and finally, the rod-like cellulose nanocrystals are isolated [26,27]. Even if the acid hydrolysis has been improved in terms of time of hydrolysis, choice of acid and its concentration, the principle of existing technologies for conversion of cellulosic biomass into CNC has barely changed until the date. It should be noted that this method requires many hazardous chemicals, which give alarming negative impacts to the environment. Furthermore, the final properties of the NCC are also endangered [28]. Thus, it is necessary to search for new processes to produce high quality CNC, with low environmental impact and without compromising their technological or health applications. In this direction, enzymatic hydrolysis offers the potential for higher selectivity, lower energy costs and milder operating conditions than chemical processes [29]. For instance, the use of enzymes for NCC isolation is a feasible approach, at least from kraft pulp, as Lopez-Rubio et al. [30] and Svagan et al. [31] confirmed. In the enzymatic hydrolysis of cellulose, the main involved enzymes are the cellobiohydrolases (CBH) or cellulases. To digest efficiently crystalline cellulose at least three types of CBH are known to cooperate: (1) endoglucanases (EC 3.2.1.4) that cut cellulose chains in random locations; (2) exoglucanases (EC 3.2.1.91) which peel cellulose in a processive manner on the reducing or non-reducing ends of cellulose polysaccharide chains and (3) beta - glucosidases (bGLs) (EC 3.2.2.21) which hydrolyse cellobiose and various soluble cellodextrins into glucose [28,32]. Synergistic phenomena are widely observed in cellulose hydrolysis, with many forms reported and proposed [29,33,34]. However, the accessibility of the cellobiohydrolases to the crystalline regions was difficult to understand, and authors hypothesized for decades about a “a non-hydrolytic component” that, in nature, could disrupt the cellulosic substrate, increasing its accessibility for the hydrolytic enzymes [35]. It was not until 2010 that the oxidative cleavage of cellulose glycosidic bonds was described, performed by a new type of enzyme, the lytic polysaccharide monooxygenases (LPMO) [36]. LPMOs cleave

cellulose leading to the formation of aldonic acids when the C1 is oxidized and/or 4-ketoaldoses at the C4 position [37]. Since then, they have extensively been reported to promote the efficiency of cellulases during cellulose digestion [36,38,39]. They are thought to act in first place, making crystalline cellulose accessible to glycosyl hydrolases [40,41].

In this study BCNC were obtained by an environmentally friendly technique based on an exclusively enzymatic treatment of native BC. First, BC paste was treated with the enzyme SamLPMO10C, a LPMO identified and cloned in the research group [41]. Then, it was digested with a commercially available preparation of cellobiohydrolases. The obtained BCNC were characterized in terms of morphology and chemical structure by electron microscopy and X-ray diffraction, respectively, and their dispersive and thermal properties measured. Finally, BCNC were used as reinforcing agent onto pre-existing eucalyptus sheets, and the mechanical and barrier properties of the obtained composites were evaluated.

2. Methods

2.1. BC synthesis/Preparation of BC

Komagataeibacter intermedius JF2, a bacterial cellulose producer previously isolated in the laboratory [42], was grown on the Hestrin and Schramm (HS) medium, containing 20 g/L glucose, 20 g/L peptone, 10 g/L yeast extract, 1.15 g/L citric acid, 6.8 g/L Na_2HPO_4, pH 6. The cultures were statically incubated at 25 – 28 °C for 7 days. After that time, bacterial cellulose membranes generated in the air/liquid interface of the culture media were harvested, rinsed with water and incubated in 1 % (w/v) NaOH at 70 °C 18 h. Then, the BC membranes were thoroughly washed in deionized water until neutrality was reached. Membranes were mechanically disrupted with a blender and homogenized (Homogenizing System UNIDRIVE X1000) to obtain a BC paste containing a suspension of BC fibres. The amount of BC was determinated by drying samples of known weight at 60 ºC until constant weight.

2.2. Expression and purification of SamLPMO10C

Escherichia coli BL21 star (DE3) harvesting pET11/SamLPMO10C [41] was cultured in LB medium supplemented with 50 µ/mL kanamycin at 37 °C, and induced by 0,5 mM isopropyl β-D-1-thiogalactopyranoside (IPTG) at O.D. 600nm = 0.8. After cultivation at 21 °C for 18 h, cell pellets were collected by centrifugation and resuspended in 50mM Tris-HCl pH 7. Cells were lysed using PANDA GEA 2000 homogenizer at 800 bar. Soluble fraction of the cleared cell extracts were mixed with 5 % (w/v) Avicel® PH-101 (Fluka) with gentle rotary shaking for 1 h at 4 °C. Following, samples of SamLPMO10C

were purified by polysaccharide-binding as described previously [41], with some modifications: to collect bound proteins, a centrifugation of 5 min at 14,000 × g was used to separate the pellet of insoluble polysaccharides with adsorbed enzymes. The pellets were sequentially washed 3 times with fresh buffer and centrifuged to remove non-specific protein binding. Pellets were washed with 3 volumes of 1 M glucose, for 30 min each, at 4 °C with gentle rotary shaking in order to elute adsorbed enzymes. Then, samples were centrifuged at 14,000 × g for 5 min to separate supernatants (with eluted SamLPMO10C) from pellet. Homogeneity of samples were analysed by sodium dodecyl sulphate polyacrylamide gel electrophoresis (SDS-PAGE).

2.2.1. Copper saturation

Purified SamLPMO10C (Uniprot, A3KKC4) was saturated with copper by incubation with a 4-fold molar excess of $CuSO_4$ for 30 min at room temperature as described elsewhere [37]. Excess copper and glucose were removed by desalting the proteins using a PD-10 desalting columns (GE Healthcare) equilibrated with 20 mM MES buffer, pH 5.5. The concentration of desalted $Cu2^+$ - saturated SamLPMO10C was measured with NanoDrop® ND-1000 (NanoDrop Technologies, Inc), using an extinction coefficient (ε) at 280 nm of 75.775 M_1 cm_1. The enzyme solution was stored at -20 °C before used.

2.2.2. LPMO activity

Standard reactions were carried out by mixing 1 % (dry weight) of substrate with 5 µM of Cu^{2+} - saturated SamLPMO10C, 2 mM ascorbic acid and 20 µM of H_2O_2. Reactions were performed with PASC (Phosphoric Acid Swollen Cellulose) and BC in 50 mM of ammonium acetate pH 5.5 and incubated at 50 ºC with shaking for 72 h and 24 h, respectively. PASC was obtained from crystalline cellulose Avicel ® PH-101 (Fluka) treated with 70 % of H_3PO_4 according to Wood [43], using centrifugation for the sedimentation of the cellulose instead of decantation during the washing process. Control reactions without LPMO were run in the same way. All reactions were performed in duplicates at least three times. Soluble fractions generated in the degradation reactions were analysed by matrix-assisted laser desorption/ionization time of flight mass spectrometry (MALDI-TOF MS) for the analysis of oxidized products. Reaction samples (3 µl) were mixed with 7 µl of acetonitrile. 1 µl of this solution was mixed with 1 µl of matrix solution (10 mg/ml of 2,5-dihydroxybenzoic acid dissolved in acetonitrile-water [1:1, vol/vol], 0.1% [wt/vol] trifluoroacetic acid).1 µl of the mixture was spotted in duplicated onto the MALDI-TOF MS plate and allowed to dry before the analysis. Positive mass spectra were collected with a 4800 Plus MALDI TOF/TOF (ABSciex 2010) spectrometer with an Nd:YAG 200-Hz laser operated at 355 nm.

2.3. Cellulase cocktail activity

Cellulase cocktail C2 was kindly supplied by (we are awaiting authorization to disclose the source). Reducing sugars resulting from glycosil hydrolase activity were quantified by the DNS reagent method [44]. Standard assays were performed at 50 ºC in 50 mM potassium acetate buffer at pH 5. Solid material was removed by centrifugation at 12.000 x g for 5 min and cleared supernatant was analysed. One unit of enzymatic activity was defined as the amount of enzyme that release 1 µmol of reducing sugar equivalent per min. A standard curve of glucose was used to calculate activity units. All determinations were made in triplicate at least two times.

2.4. Enzymatic preparation of bacterial cellulose nanocrystals (BCNC)

Enzymatic hydrolysis of the BC paste was run using the enzymes SamLPMO10C and the cellulose cocktail Cel-02. Bacterial cellulose paste (1 % dry weight) was mixed with SamLPMO10C in 20 mM MES buffer pH 5.5 and the mixture was kept in 50 ºC for 24 h. Then, 12.5 U g^{-1} odp (oven-dried pulp) of C2 was added and the mixture was incubated at 60 ºC for 18 h. For control reaction, the same dried weight of bacterial cellulose paste was incubated in all the buffer components at the same conditions. All reactions were incubated with shaking in a water bath. Hydrolysis was stopped by heating up the reaction to 100 ºC for 10 min. The obtained suspensions were homogenized by ultrasonication (80W, 0.8s) in a Labsonic 1510 sonicator (B.Braun) for 5 min and kept at 4 ºC.

2.5. Characterization of NCBC

2.5.1. Scanning electron microscopy (SEM)

BCNC suspensions were analysed by SEM (JSM 7100 F) using a LED filter. Samples were graphite coated using a Vacuum Evaporator EMITECH K950X221. EDS analysis was carried out to verify their chemical composition. The diameter of the fibres was measured using the ImageJ software.

2.5.2. Transmission electron microscopy (TEM)

Suspensions of BCNC were negatively stained with 2 % uranyl acetate, after dropping them on a Cu grid covered with formvar and a thin carbon film and allowed to dry at room temperature. The diameter and length of BCNC were obtained using a transmission electron microscope (TEM) model JEOL 1010. Images were taken at an accelerated voltage of 80 kV.The length (L) and width (D) were determined from at least 100 measurements using the ImageJ software.

2.5.3. X-ray diffraction

X-ray diffraction patterns of dried samples of BCNC were obtained with a PANalytical X'Pert PRO MPD Alpha1 powder diffractometer.The samples were analysed at the radiation wavelength of 1.5418 Å and scanned from 2 º to 50 °, 2Θ range. Samples were fixed over a zero background Silicon single crystal sample holder (pw1817/32), and the ensembles were mounted in a PW1813/32 sample holder. The same Silicon holder was used to measure all the replicates of each sample. **Equation (1)** [45] was used to calculate the crystallinity index (CI) of bacterial cellulose:

$$\mathrm{CI}(\%) = \frac{\mathrm{I_c} - \mathrm{I_{am}}}{\mathrm{I_c}} \times 100 \quad \textbf{(1)}$$

where I_c is the maximum intensity of the lattice diffraction and I_{am} is the height of the intensity at the minimum at 2Θ between 18 º and 19 º, which corresponds to the amorphous part of cellulose.

2.6. Zeta potential

BCNC suspensions and BC were previously diluted in distilled water to a 1:5 and 1:10 sample:water ratio (v/v), respectively. Zeta potential was then measured in a Zetasier NanoZS (Malvern Instruments, UK), in triplicate.

2.7. Particle size determination

2.7.1. Light scattering (LS)

The particle size of BCNC was measured by laser diffraction in the range of 0.375-20000 µm in a Particle Size Analyzer (Beckman Coulter LS 13320), using the Micro Liquid Module in aqueous suspension and Fraunhofer optical model.

2.7.2. Filtration

After the enzymatic hydrolysis was complete, the final reaction containing the BCNC was filtered by several filters with a decreasing diameter pore size (50 µm, 6 µm, 3 µm, 0.4 µm and 0.2 µm, Nangtong FilterBio Membrane Co., Ltd). Then, the filters were left to dry at 80 ºC for 24 h and the retained biomass was weight.

2.8. Thermogravity analysis (TGA)

The thermal stability of BCNC was measured by TGA on TGA/SDTA851^e (Mettler Toledo). The experimental conditions were as follows: the test sample was heated at a

rate of 10 ºC / min to a maximum of 700 ºC in nitrogen inert medium at a flow rate of 50 mL/min. The weight of the dry sample was about 1 mg.

2.9. Composites formation and characterization

Eucalyptus/BCNC nanocomposites were obtained by a modification of the solving casting technique [46,47]. BCNC were added at different concentrations to preformed 10 % (w/v) eucalyptus sheets on a 0.2 µm pore size filter while applying vacuum. Finally, they were left to dry at room temperature for 72 h under pressure. Water permeability was measured by the water drop test (WDT) according to TAPPI standard T835 om-08. The WDT involved placing a drop of deionized water on the surface of paper and recording the time needed for complete absorption, which was signalled by vanishing of the drop specular gloss. Ten measurements per sample were made and averaged. Grease resistance was determined by the standard UNE 5707174, where silica sand was placed on the composite before dyed turpentine was added, and the time needed to penetrate it was counted. Atomic force microscopy () – Peak Force (PF) Quantitative Nanomechanical Mapping (QNM) mode – was used to determine the tensile properties. Measurements were done with an Antimony (n) doped Si from Bruker, model RTESPA-525 with the characteristics: nominal tip radius 8 nm, cantilever length of 25 µm, resonant frequency 375 - 675 kHz.

2.10. Statistical analysis

All determinations were performed after two replicas. In the case of enzyme activity, two replicas of triplicates (six determinations per sample) were measured. Experimental data were expressed as means ± standard deviations and were analysed statistically by the paired Student's *t*-test method and analysis of variance (ANOVA) if there were more than two groups in STATGRAPHICS Centurion XVIII software (Statgraphics.Net, Madrid). Scheffe's multiple range test was used to detect differences among mean values. A value of $p \leq 0.05$ was considered statistically significant. Homogeneity of variance for all samples was tested with Bartlett's test. Residues normal distribution was assumed after performing the Shapiro-Wilk test.

3. Results and Discussion

3.1. SamLPMO10C and cellulase activity onto bacterial cellulose

Prior to bacterial cellulose nanocrystals obtention by enzymatic hydrolysis, the activities of purified SamLPMO10C, hereinafter SamC, and cellulsase cocktail C2 activities were tested. SamC standard reactions were performed with PASC, routinely considered as the preferred substrate of cellulose active LPMOs [41], and BC. MALDI-TOF MS

detection of the soluble oxidized products from SamC activity is shown in **Figure 1**. The analysis of the reaction products revealed that SamC was active in both substrates, generating oxidized cellooligosaccharides with different degrees of polymerization (DP), of 4 - 7 in the case of PASC, and 4 - 6 for BC, in accordance with preovious results from the research group [41,48]. In all cases, the peak assignment was in agreement to the size of C1-oxidized from released aldonic acid oligosaccharides.

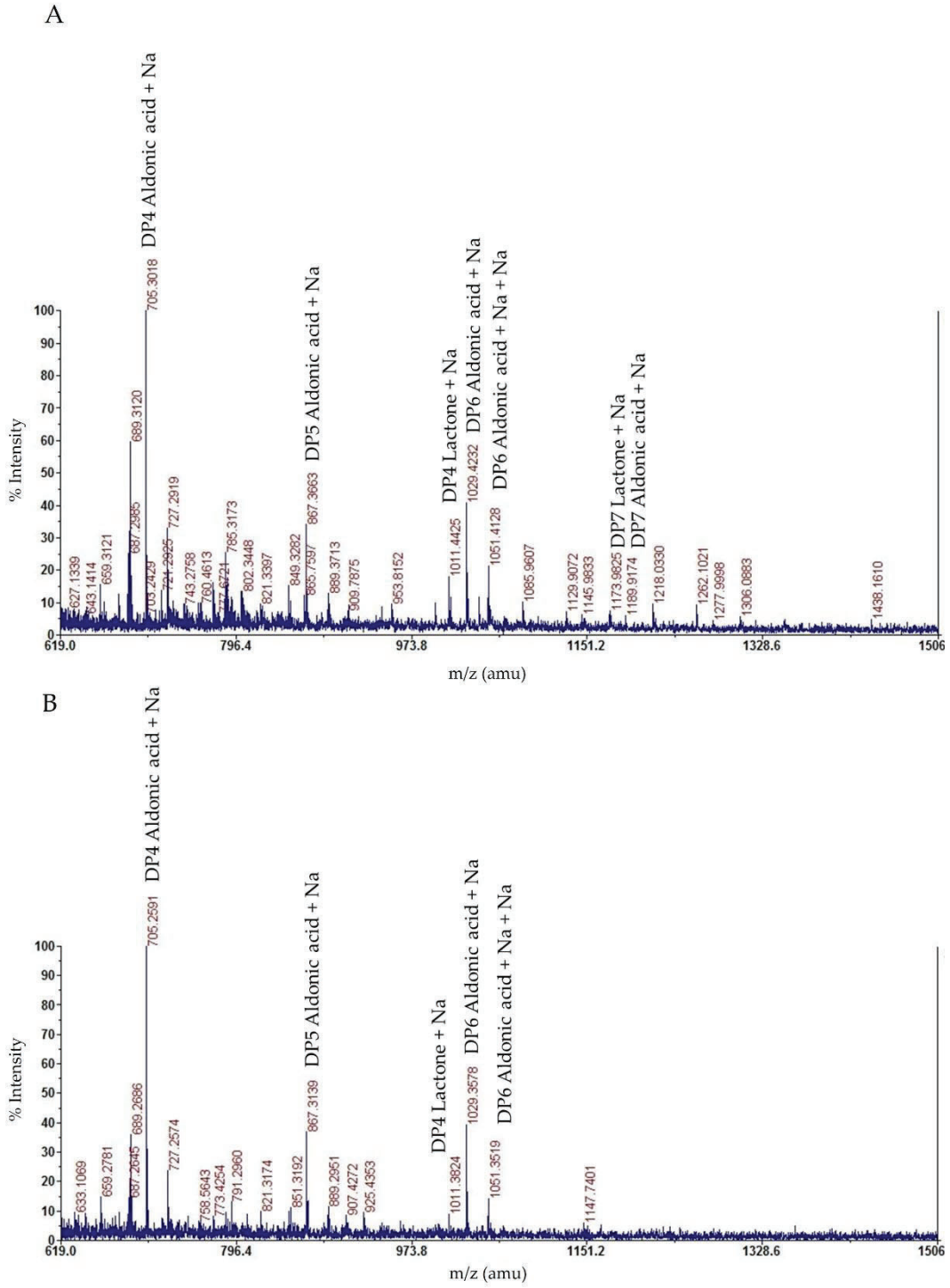

Figure 1. MALDI-TOF MS analysis of soluble oxidized products from **(A)** PASC and **(B)** BC.

Glycosyl hydrolase activity of C2 was measured by the reducing sugars method on three crystalline cellulosic substrates: soluble cellulose (CMC, carboxymethyl cellulose), insoluble microcrystalline cellulose (Avicel) and BC, the most crystalline among them. As shown in **Figure 2**, the amount of reducing sugars increased over time until a threshold was reached after 2 h of incubation, indicating, cellobiohydrolase activity. However, the activity for BC was notably higher indicating that, likewise SamC, C2 had preference for crystalline substrates as BC, the source of nanocrystals of this work.

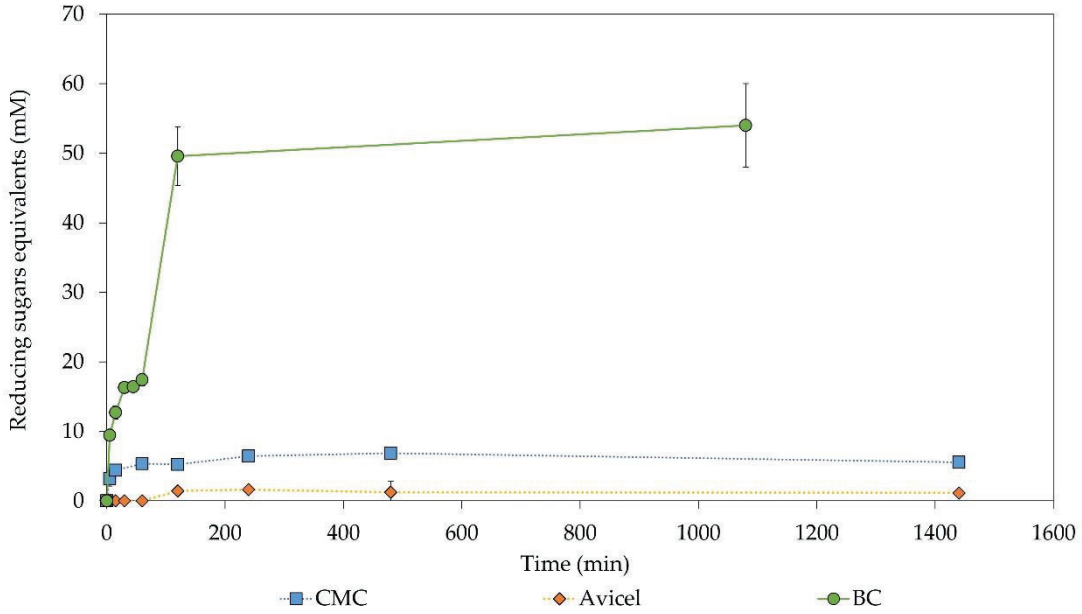

Figure 2. Activity per mM reducing sugars equivalents of the industrial cellulolytic cocktail over time on different substrates: CMC (squares line), Avicel (rhombus line) and BC (dots line).

3.2. Bacterial cellulose nanocrystals obtention and size distribution

To obtain BCNC, the BC paste was first treated with SamC and then with cellulases C2. Reactions with only SamC or C2 were also run in parallel. Mass spectrometry analysis were performed to detect soluble oxidized products from SamC activity onto BC, as well as to discard LPMO activity from the commercial cocktail C2 (**Figure A1**). The particle size distribution of the enzymatically treated samples was attempted by filtering them through a series of membranes of decreasing pore diameter. As can be seen in **Figure 3A**, there was a significant shift towards lower fibre sizes after cellulase hydrolysis of BC, in both cases, with and without prior action of SamC. However, more than 80 % of the biomass of CB treated only with SamC is retained by 50 microns, while only 37 % of the biomass subjected to the action of celluloses exceeds that size, corroborating that cellulases are the main responsible for the digestion of BC. Interestingly, with the combined SamC-C2 treatment, more particles between 3 µm and 400 nm were obtained

than with only C2 digestion [58]. These results would suggest that with LPMOs the obtained BCNC would have a larger length than those obtained with cellulases alone, which is in disagreement with the generally accepted role of auxiliary activity of LPMO [40,41,49]. This enzyme is thought to make crystalline cellulosic substrates, as BC, more accessible to the glycoside hydrolases, boosting their activity [41]. However, this pattern was repeated after measuring the reducing sugars of the filtrates < 50 µm and 200 nm of each treatment (**Figure 3B**). The value of reducing sugars after the combined SamC-C2 treatment was higher than those presented by the samples treated only with SamC, indicating that cellulase digestion has been effective. When comparing the two filtrates (< 50 µm and 200 nm) after C2 treatment, there are no apparent differences between them, which could mean that the obtained particles are of small size, with a low degree of polymerization. Nevertheless, for SamC-C2 treatment, the value of reducing sugars is more elevated in the < 50 µm filtration than in the < 200 nm one, reinforcing the prior hypothesis that a previous treatment with SamC before the cellulases digestion resulted in larger particles. Moreover, recent studies have reported severe impeding effects of C1-oxidizing LPMOs on the activity of reducing-end cellobiohydrolases [50]. Even though not knowing the underlying mechanism of this impeding effect, we justify the use of SamLPMO10C for the size and the dispersive properties of the obtained BCNC.

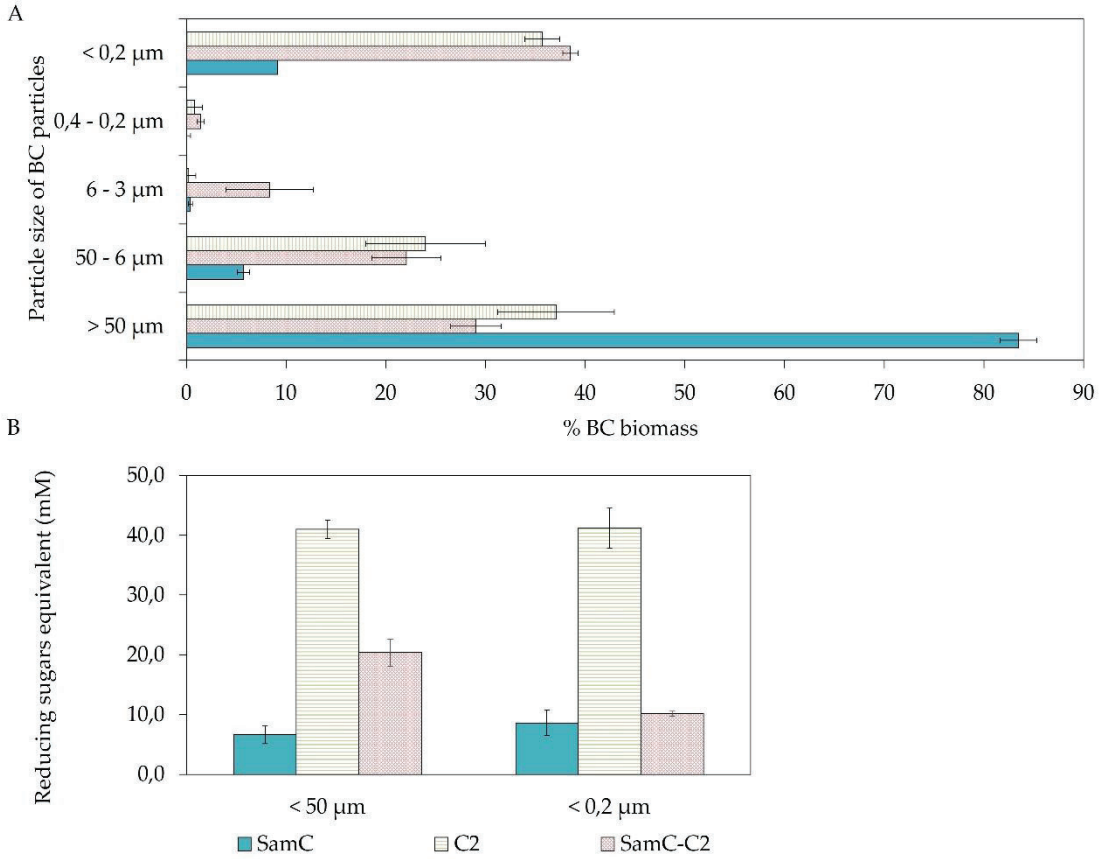

Figure 3. BCNC length distribution by filtration **(A)** and reducing sugars content **(B)** after the enzymatic treatment.

Figure 4 shows the results of laser diffraction (LS) technique by light scattering, which enabled determination of particle size, based on the diffraction of incident light on a sample. Again, it is clearly visible the effect of C2 onto the BC. In both treatments, SamC-C2 and C2, a shift towards smaller sizes particles could be observed. However, it can be noticed that particles obtained after SamC-C2 treatment had higher percentages of higher diameters than those obtained without previous SamC treatment. The high amount of particles of size > 2 µm observed in Figure 4 could be easily attributed to agglomeration [51]. Similar results were observed by other authors who explain this tendency to agglomerate with presence of strong OH^- intermolecular bonds occurring in cellulose [52]. It should be noted that this technique assumes that the analysed particles are spheres [53], and cellulose nanocrystals are rod-like particles, not spherical. Nevertheless, these results corroborated the effect of the combination of SamC and cellulases treatment on the size of BCNC found by the filtration method.

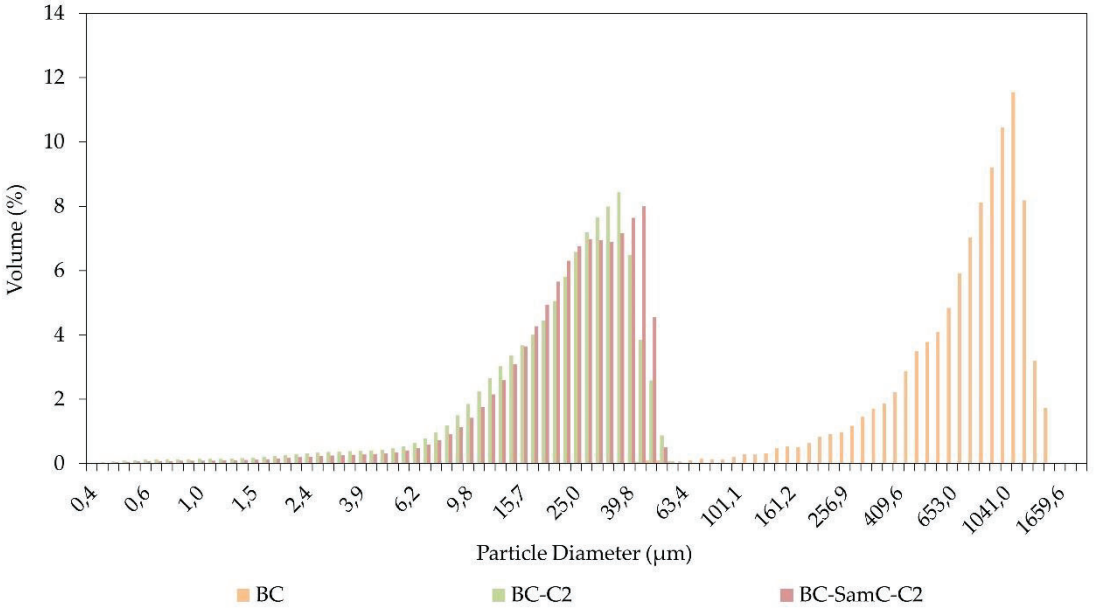

Figure 4. Particle size distribution of native BC and after enzymatic treatments.

3.3. BCNC characterization

3.3.1. Morphology

Electron microscopy images of BCNC are shown in **Figure 5** and **Figure 6**. Scanning electron microscopy (SEM) pictures of the native BC and oxidized BC by SamC (**Figure 5A**, **B**) show the typical reticulated structure consisting of ultrafine cellulose fibrils with a diameter of about 50 – 70 nm and a length exceeding 20 µm, consistent with previous results [3,54]. Treatment with SamC did not noticeably change the cellulose structure, in agreement with other authors who oxidized BC with SamLPMO10C [48] or TEMPO [55]. In images of samples of BC enzymatically treated (**Figure 5C-F**), rod-like structures compatible with BCNC were observed, with a length (L) in the range 80 nm – 2 µm.

Energy Dispersive X-ray spectroscopy (EDS) confirmed that these structures were composed of cellulose.

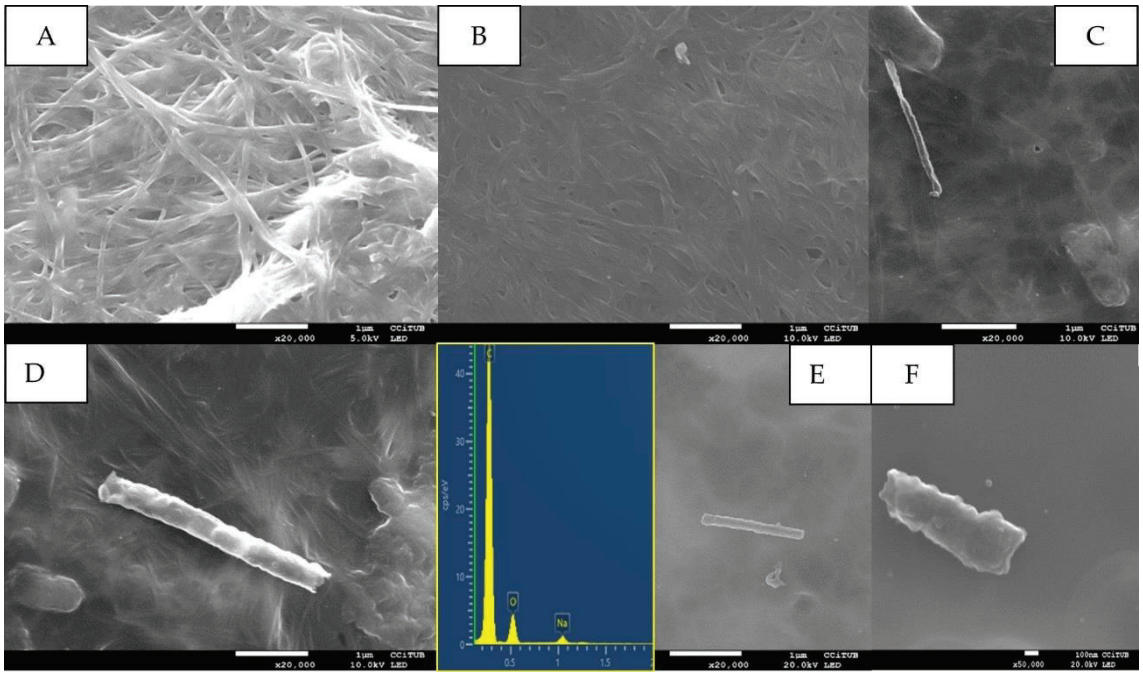

Figure 5. Electron microscopy images obtained by SEM: BC **(A)**, BC-SamC **(B)**, BCNC **(C-F)**. The insert in (E) represents the energy dispersive X-ray spectrometer (EDS) spectrum of BCNC.

Transmission electron microscopy (TEM) micrographs of BCNC allowed a more detail analysis (**Figure 6A**). The observed flat, rod-like particles had a small number of laterally associated elementary crystallites, usually from 3 to 5, as it has been previously described [25,56]. In TEM negatively stained preparations (**Figure 6B-G**), the accumulation of stain around the narrower parts of the nanocrystals suggested an alternation of narrow and wide parts along the BCNC, indicating that they have a ribbon-like shape and that a homogeneous twist occur [57]. This twist (**Figure 6H-I**), which is rarely directly observed [57], is especially clearly observed in well-dispersed ribbon-shaped bacterial cellulose [58], even if it is not clear its origin. It could be attributed to a rotational movement of bacteria or enzyme complexes or to the chiral nature of cellulose, or a combination of both [57]. BCNC had a length ranging from 80 to 2000 nm and a width ranging from 3 to 12 nm, which represented an average length (L) and width (D) of 711 ± 154 nm and 9 ± 5 nm, respectively. These sizes are in line with those reported for BCNC obtained by acid hydrolysis by others. [59–63]. BCNC are usually larger in dimension compared to those obtained from vegetal cellulose as wood and cotton [64,65], hence there are lower fractions of amorphous regions that need to be cleaved resulting in the production of larger nanocrystals [11]. Moreover, these dimensions lead to a higher ratio of length to diameter (L/D). The aspect ratio L/D of the BCNC here

obtained was 80.1. The geometrical aspect ratio of cellulose nanocrystals is very important in defining their reinforcing capability in polymer matrices. Generally, nanocrystals exhibiting a ratio L/D greater than 13 results in improved reinforcement properties of the final polymer nanocomposites [11,66].

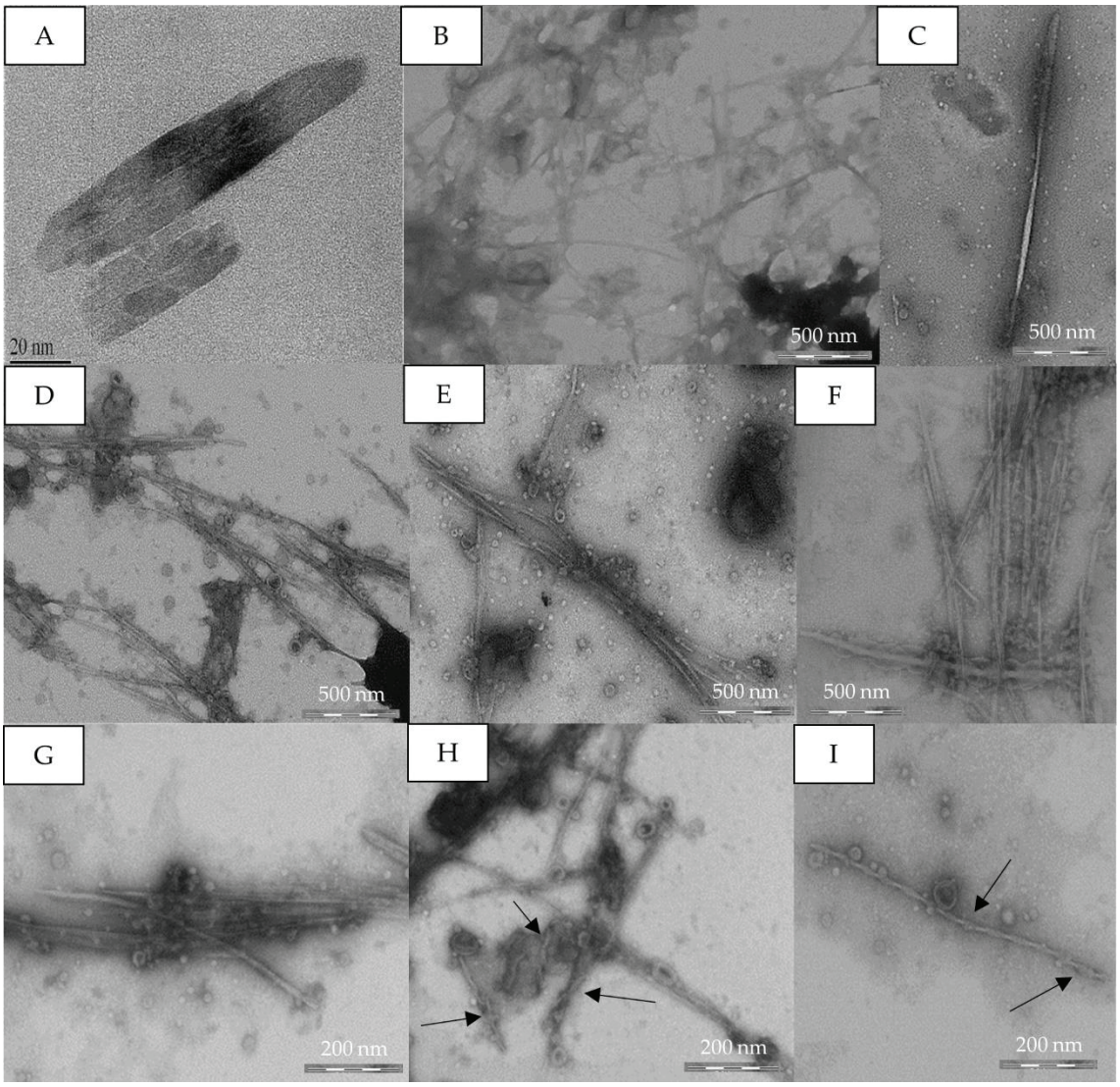

Figure 6. Electron microscopy images of BCNC obtained by TEM **(A)** and negative stain TEM **(B-I)**. The arrows in (H) and (I) highlight the twist.

3.3.2. Crystallinity

Regarding chemical structure, XRD patterns were measured. **Figure 7** showed diffraction peaks at 2Θ angles around 18.4 Θ and 22.7 Θ, corresponding to the typical profile of cellulose I (natural cellulose) in crystalline form [67]. The estimated degree of crystallinity index (Eq. 1) of the native BC was 97 % and 95 % for oxidized BC. For BCNC, obtained by SamC-C2 treatment, or only by C2 treatment, the crystallinity index barely changed, with a value of 85 %. It should be noted that BC is one of the most crystalline cellulosic substrates [48], and in this work an enzymatic digestion has been

performed. Consequently, some of the BC could have been completely hydrolysed, reflected in this slight decrease in crystallinity. In fact, it has been described that severe hydrolysis conditions can result in a likely change in the orientation of the cellulose chains [68]. However, the obtained BCNC displayed high crystallinity, even higher than BCNC obtained by acid hydrolysis [68–70], suggesting that the enzymatic treatment did not modify characteristics as mechanical strength and interfacial properties of the cellulose fibre [71].

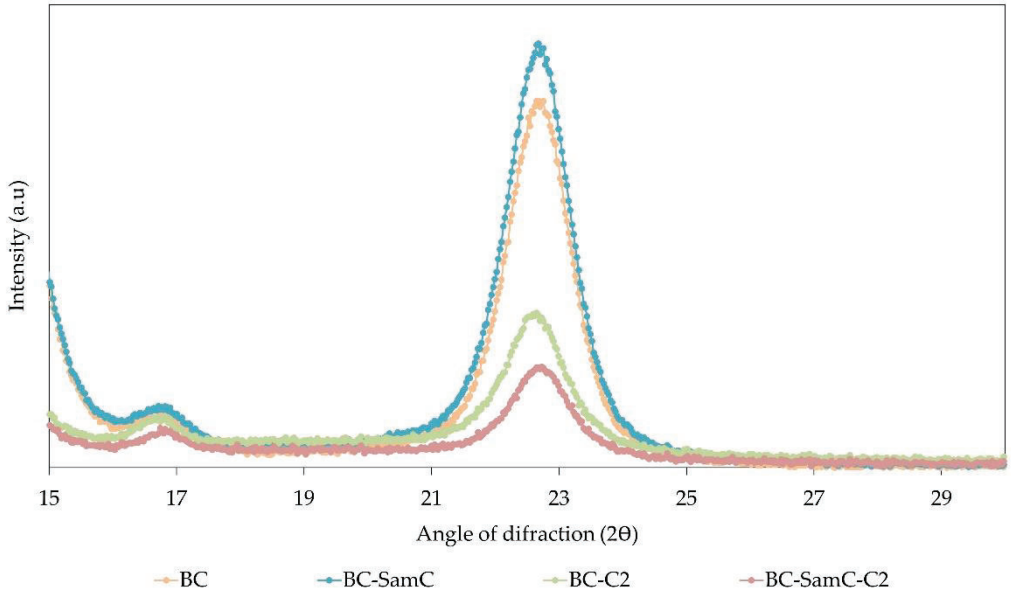

Figure 7. XRD pattern of BC, BC-SamC and BCNC (BC-C2 and BC-SamC-C2).

3.3.3. Dispersion stability

The zeta potential was measured to evaluate the dispersion stability of BCNC suspensions in water (**Figure 7)**, where less negative the values are, better is the stability [72]. Interestingly, suspensions of BCNC where SamC was applied presented a zeta potential modulus much higher than suspensions of BCNC obtained without SamC treatment (-6.5 mV and -21.4 mV, respectively), indicating that SamC treatment was necessary for their stability. These results suggested that after SamC mediated oxidation, the negatively charged carboxylic groups would promote electrostatic repulsion and prevent the aggregation of the nanocrystals. CNC obtained by sulphuric acid hydrolysis often acquire a negatively charged surface which promotes uniform dispersion in aqueous solution due to electrostatic repulsions [73]. However, even if this sulfonation results in a highly stable colloidal suspension, the obtained CNC are prone to have a lower thermal stability as compared to the native cellulose [74]. On the other hand, without these negative charges, CNC are prone to aggregate because of their strong hydrogen bonding between surface hydroxyl groups [62]. Consequently, this

uniform dispersion provided by sulphate groups is a challenge when more environmentally friendly treatments, as the enzymatic ones, are applied. One of the more efficient pretreatments to cellulose is the oxidation mediated by 2,2,6,6-tetramethyl-1-piperidinoxyl (TEMPO), as some authors have reported in the case of the obtention of oxidized nanofibrillated bacterial cellulose [55]. Alternatively, LPMOs have proved to contribute to a more sustainable production of cellulose nanofibrils [38,48], and they could also have a key role, as oxidative enzymes, in giving dispersion stability to BCNC obtained exclusively by enzymatic treatment.

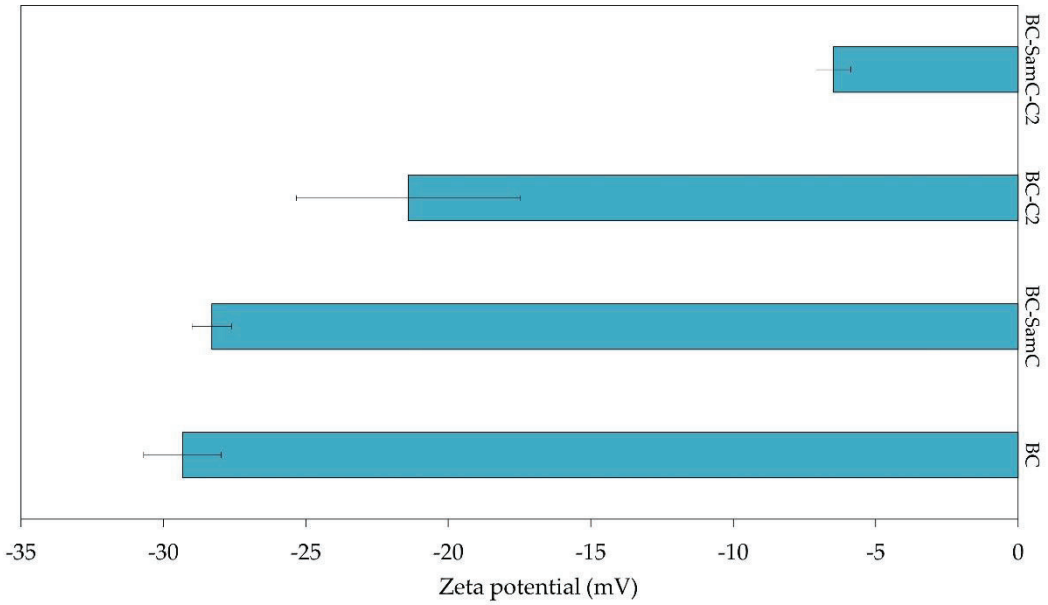

Figure 8. Results from zeta potential of suspensions of BC, BC treated with SamC (BC-SamC) and with C2 cellulases (BC-C2 and BC-SamC-C2).

3.4. Thermostability

Thermal stability of cellulose often is drastically changed due to acid hydrolysis during the process of cellulose nanocrystals obtention [74]. Therefore, it is important to establish whether the enzymatic treatments have a similar effect. For this purpose, the thermal degradation profiles of BC and BCNC were assessed by thermogravimetric analysis **(**TGA). **Figure 9** represents the three mass loss events that can be observed during TGA: the first event corresponds to the evaporation of residual water, while the second is characterized by a series of reactions degradation of cellulose, including dehydration, decomposition, and depolymerization of the glycoside units [68,75]. This major degradation step is, though, associated with a high loss of mass of cellulosic material, which is characterized by the onset temperature (T_O). The third thermal event (not shown) is related to the unburnable residue. As stated in **Table 1,** a maximum decomposition point was observed for BC and BC-SamC around 130 ºC, even if they had slightly different onset temperatures. Interestingly, enhanced thermal stability was

noticed for BCNC: the degradation process started later (around 145 ºC) and the maximum degradation rate was registered at a higher temperature (200 ºC). These differences could be related to the different defibrillation conditions [76,77]: BC, in its native form or oxidized, has a more compact structure for the same weight, leading to a better heat transference and therefore to a higher degradation rates. BCNC with high thermal stability can be used, for instance, for nanocomposites preparation where the polymers blending process requires high temperature.

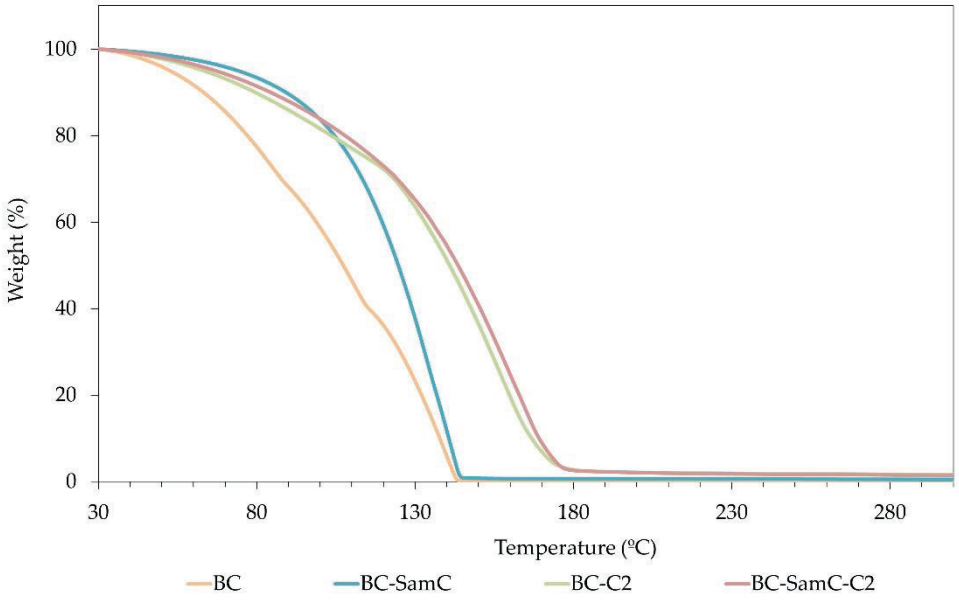

Figure 9. Thermogravimetric curve of native BC, BC-SamC and after enzymatic treatments with cellulases (BC-C2) and SamC and cellulases (BC-SamC-C2).

Table 1. TGA results for BC, BC-SamC and BCNC after enzymatic treatments with cellulases (BC-C2) and SamC and cellulases (BC-SamC-C2).

	Onset temperature degradation (T_o) (º C)	**Maximum degradation temperature (Td) (º C)**
BC	106,8	134,2
BC-SamC	124,5	131
BC-C2	140,4	195,3
BC-SamC-C2	143	199,1

3.5. Eucalyptus /BCNC nanocomposites

When a polymer is reinforced with a nanomaterial, a polymer nanocomposite is obtained. The nanometric size and the increased surface area of the reinforcing material provides this new nanocomposite unique properties. Their incorporation in many polymers, even at very low volume fractions, can significantly improve the mechanical performance, thermal stability, and barrier and optical properties due to its elevated crystallinity and better interfacial interactions [5,78]. In this study, BCNC were physically incorporated in

different doses to prepared 10 % (w/v) eucalyptus sheets by coating and water evaporation, one of the most common techniques to produce nanocomposite films [11]. As described by other authors, CNC obtained without sulphuric acid often reaggregate [62]. For this reason, CNC are usually chemically modified to improve their dispersion [12]. Nevertheless, the BCNC obtained in this study were negatively charged due to SamC treatment, and as stated by the determination of z potential, they were well dispersed. Overmore, their ratio L/D indicated a high reinforcing capability. Consequently, the obtained composites were homogeneous, no holes or big agglomerates were present in comparison to those coated with BCNC obtained without oxidation. According to literature, Xiang et al. [79] and Yuan et al. [80] proved that getting a homogeneous distribution of BCNC matrix is a key for successfully reinforcing paper in the paper industry. In further studies, these BCNC could serve as a matrix for active compounds immobilization, and the resultant nanocomposites could have special properties, as antimicrobial, antioxidant or catalytic ones [81–84]. They could also provide functionality to biodegradable packages and ability to control microbial population in the food, in the industry of food packaging [53].

3.5.1. Water permeability

All the nanocomposites showed an increased water permeability in comparison to the eucalyptus sheet (**Figure 10**). Interestingly, water retention time reached a threshold over 7 minutes at 4 % BCNC addition. This effect can be easily attributed to the low hygroscopicity of highly crystalline BCNC [62]. The water transmission preferentially occurs through the amorphous areas of cellulose and their absence leads in an increase of the time that the water drop is retained on the surface of the nanocomposite. Overmore, the negative charged BCNC contribute to this decrease in water permeability.

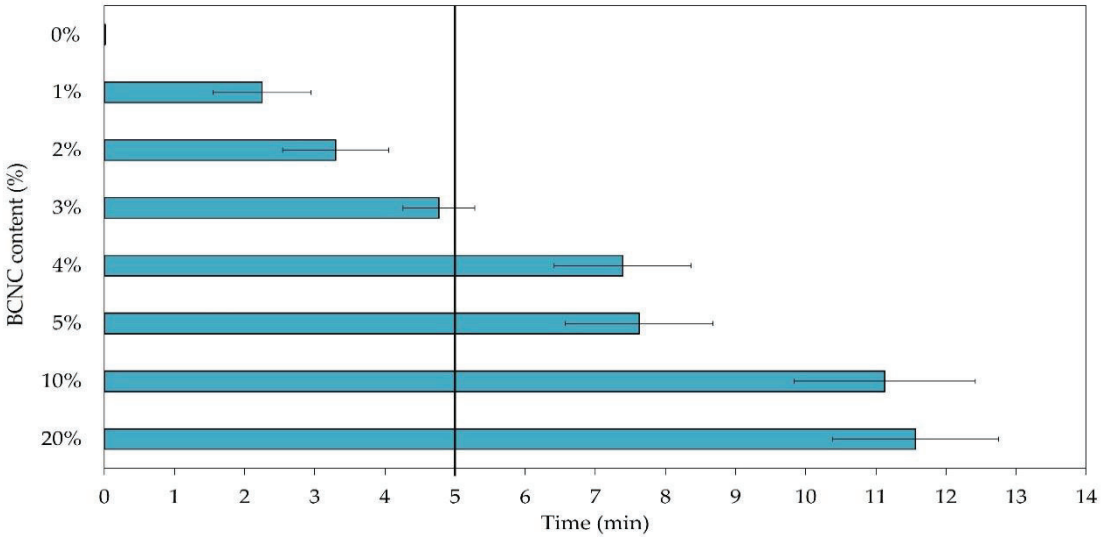

Figure 10. Water drop test values of the BCNC-eucalyptus composites with different loadings of BCNC. The black line represents the 5 min threshold.

3.5.2. Barrier properties

Regarding barrier properties, a threshold was reached again at 4 % of BCNC addition. As shown in **Figure 11**, from this concentration the nanocomposite was able to hold the trementine solution for more than 30 minutes, indicating that it was grease resistant. This enhancement in barrier properties is probably due to the reduction of eucalyptus sheets porosity [53]. According to other authors, the high aspect ratio aspect of BCNC would give this reinforcing effect, ensuring percolation, event at low loadings [78,85]. Materials with low permeability to moisture and oil are very much needed in food and biomedical packaging areas [86].

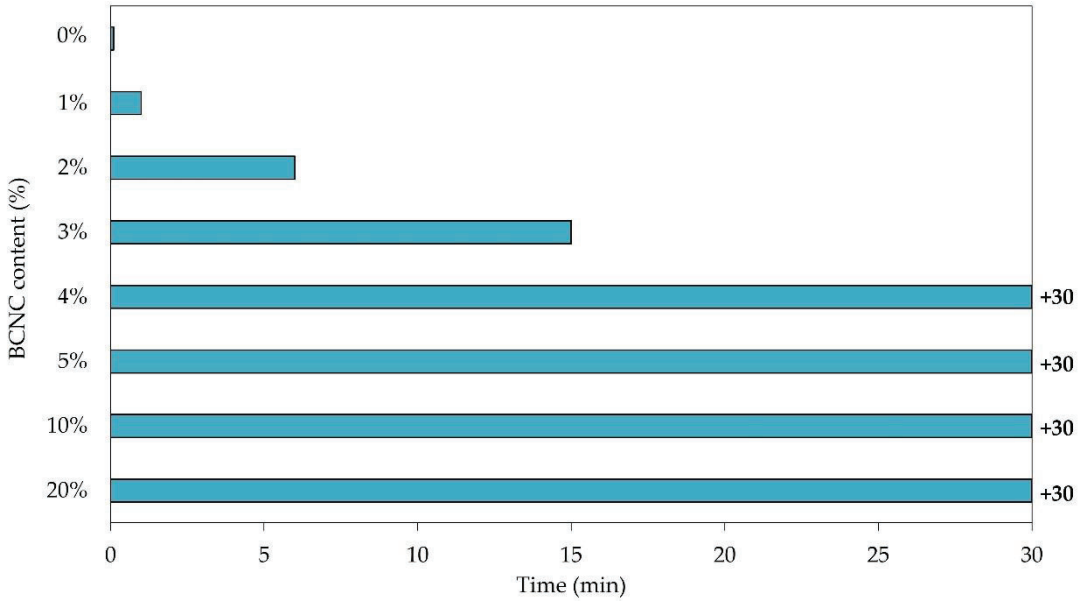

Figure 11. Barrier properties to oil of the BCNC-eucalyptus composites with different loadings of BCNC.

3.5.3. Mechanical properties

Loading of BCNC resulted in improved mechanical resistance. The highest values of Young's modulus (YM) were observed for composites with 20 % loading of BCNC (**Figure 12**). Regarding eucalyptus without BCNC, the yield strength increased almost 15 times, from 246.42 ± 190.1 MPa to 15.15 ± 4.1 GPa. However, in the literature is very often reported that composites with the smallest amount of filler are characterized by the highest values of strength parameters, resulting from their better dispersion [87–89]. Surprisingly, in our study, further increase of BCNC resulted in improvement of YM parameters, as it has been also recently described elsewhere [51,90].

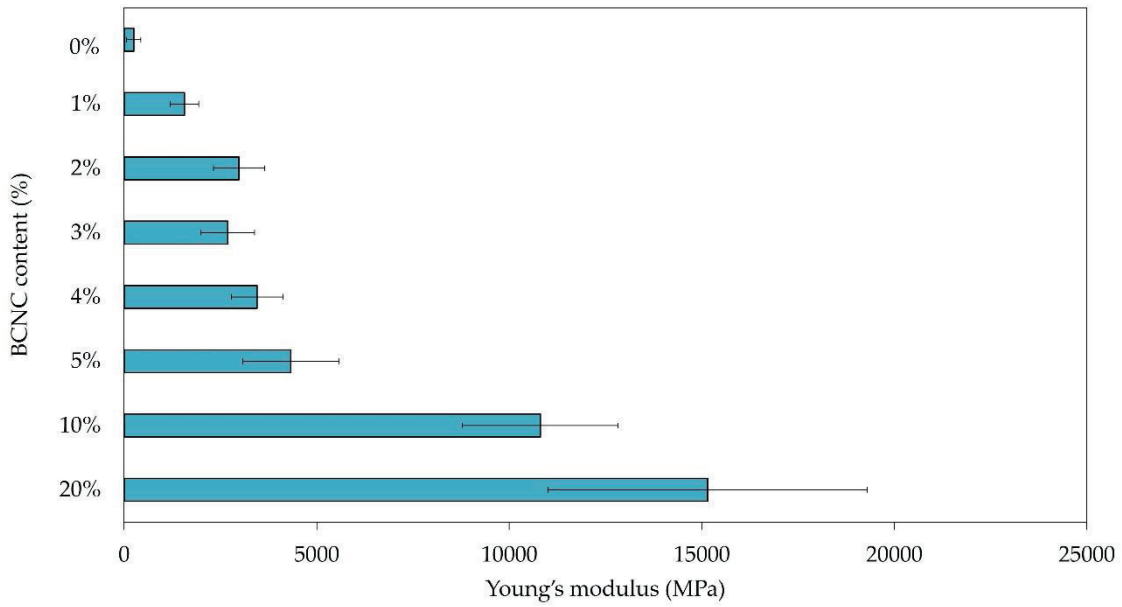

Figure 12. Young's modulus parameters obtained for the tested composites with different BCNC loadings onto eucalyptus sheets.

4. Conclusions

In this work, nanocrystals of bacterial cellulose have been obtained using a green procedure. A pretreatment with the enzyme SamLPMO10C, followed by digestion with a mixture of cellulases, led to the obtaining of nanocrystals with high aspect ratio, high crystallinity index and excellent thermal properties. The oxidative action of LPMO generated negative charges on the cellulose chains on the surface of the nanocrystals that prevented aggregation and allowed good stability in an aqueous environment. Eucalyptus cellulose sheets coated with a low percentage of bacterial cellulose nanocrystals acquired water and oil impermeability and improved mechanical properties. The properties of the nanocrystals obtained by this enzymatic process make predictable a wide range of applications.

Declaration of interest

Authors declare no conflict of interest

Funding

This work was financed by the Spanish Ministry of Economy, Industry and Competitiveness, grant CTQ2017-84966-C2-2-R, by the Pla de Recerca de Catalunya, grant 2017SGR-30, and by the Generalitat de Catalunya, "Xarxa de Referència en Biotecnologia" (XRB). C. Buruaga-Ramiro acknowledges an APIF predoctoral grant from the University of Barcelona.

Acknowledgements

We thank the Serveis Cientifico-Tècnics of the University of Barcelona (CCiTUB) for technical support in: electron microscopy; X-ray diffraction; laser diffraction; TGA analysis and AFM, and Institut de Ciències de Materials de Barcelona (ICMAB-CSIC) for z potential measure. M. Vieiros is acknowledged for technical assistance.

Data availability

The raw/processed data required to reproduce these findings cannot be shared at this time due to technical or time limitations.

Appendix

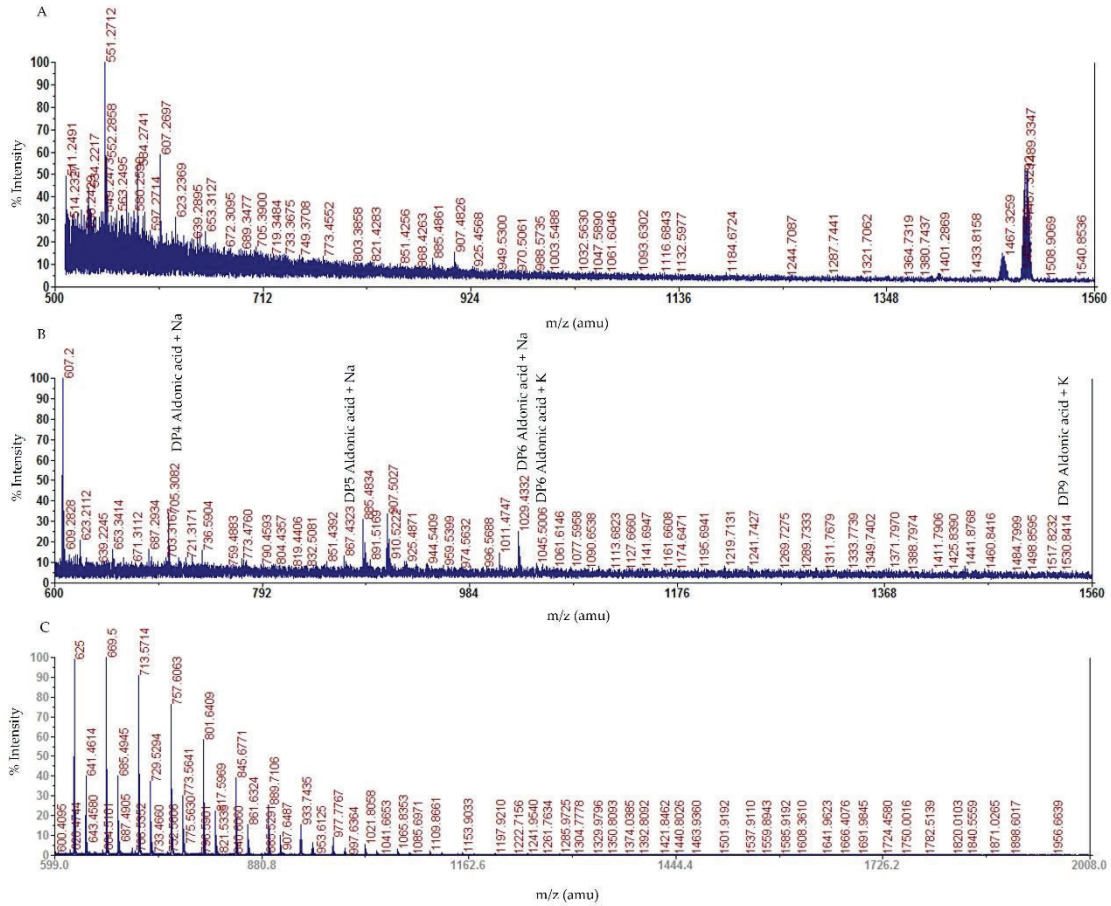

Figure A1. MALDI-TOF MS analysis of soluble oxidized products from **(A)** BC negative control, **(B)** BC-SamC and **(C)**, BC-SamC-C2.

References

[1] R.N. Tharanathan, Biodegradable films and composite coatings: Past, present and future, Trends Food Sci. Technol. 14 (2003) 71–78. https://doi.org/10.1016/S0924-2244(02)00280-7.

[2] A. Dufresne, Comparing the mechanical properties of high performances polymer nanocomposites from biological sources, J. Nanosci. Nanotechnol. 6 (2006) 322–330. https://doi.org/10.1166/jnn.2006.906.

[3] C. Buruaga-Ramiro, S. V. Valenzuela, C. Valls, M.B. Roncero, F.I.J. Pastor, P. Díaz, J. Martínez, Bacterial cellulose matrices to develop enzymatically active paper, Cellulose. 27 (2020) 3413–3426. https://doi.org/10.1007/s10570-020-03025-9.
[4] C. Zinge, B. Kandasubramanian, Nanocellulose based biodegradable polymers, Eur. Polym. J. 133 (2020) 109758. https://doi.org/10.1016/j.eurpolymj.2020.109758.
[5] J. George, S.N. Sabapathi, Cellulose nanocrystals: Synthesis, functional properties, and applications, Nanotechnol. Sci. Appl. 8 (2015) 45–54. https://doi.org/10.2147/NSA.S64386.
[6] M. Ghorbani, L. Roshangar, J. Soleimani Rad, Development of reinforced chitosan/pectin scaffold by using the cellulose nanocrystals as nanofillers: An injectable hydrogel for tissue engineering, Eur. Polym. J. 130 (2020) 109697. https://doi.org/10.1016/J.eurpolymj.2020.109697.
[7] S.J. Eichhorn, A. Dufresne, M. Aranguren, N.E. Marcovich, J.R. Capadona, S.J. Rowan, C. Weder, W. Thielemans, M. Roman, S. Renneckar, W. Gindl, S. Veigel, J. Keckes, H. Yano, K. Abe, M. Nogi, A.N. Nakagaito, A. Mangalam, J. Simonsen, A.S. Benight, A. Bismarck, L.A. Berglund, T. Peijs, Review: current international research into cellulose nanofibres and nanocomposites, J. Mater. Sci. 45 (2010) 1–33. https://doi.org/10.1007/s10853-009-3874-0.
[8] A.J. Uddin, J. Araki, Y. Gotoh, Toward “Strong” sreen nanocomposites: Polyvinyl alcohol reinforced with extremely oriented cellulose whiskers, Biomacromolecules. 12 (2011) 617–624. https://doi.org/10.1021/bm101280f.
[9] N. Dogan, T.H. McHugh, Effects of microcrystalline cellulose on functional properties of hydroxy propyl methyl cellulose microcomposite films, J. Food Sci. 72 (2007) E016–E022. https://doi.org/10.1111/j.1750-3841.2006.00237.x.
[10] C.M.O. Müller, J.B. Laurindo, F. Yamashita, Effect of cellulose fibers addition on the mechanical properties and water vapor barrier of starch-based films, Food Hydrocoll. 23 (2009) 1328–1333. https://doi.org/10.1016/j.foodhyd.2008.09.002.
[11] B.L. Peng, N. Dhar, H.L. Liu, K.C. Tam, Chemistry and applications of nanocrystalline cellulose and its derivatives: A nanotechnology perspective, Can. J. Chem. Eng. 89 (2011) 1191–1206. https://doi.org/10.1002/cjce.20554.
[12] A. Balea, E. Fuente, M. Concepcion Monte, N. Merayo, C. Campano, C. Negro, A. Blanco, Industrial application of nanocelluloses in papermaking: A review of challenges, technical solutions, and market perspectives, Molecules. 25 (2020) 526. https://doi.org/10.3390/molecules25030526.
[13] D. Roy, M. Semsarilar, J.T. Guthrie, S. Perrier, Cellulose modification by polymer grafting: A review, Chem. Soc. Rev. 38 (2009) 2046–2064. https://doi.org/10.1039/b808639g.
[14] M. Roman, S. Dong, A. Hirani, Y.W. Lee, Cellulose nanocrystals for drug delivery, ACS Symp. Ser. 1017 (2009) 81–91. https://doi.org/10.1021/bk-2009-1017.ch004.
[15] E. Lam, K.B. Male, J.H. Chong, A.C.W. Leung, J.H.T. Luong, Applications of functionalized and nanoparticle-modified nanocrystalline cellulose, Trends Biotechnol. 30 (2012) 283–290. https://doi.org/10.1016/j.tibtech.2012.02.001.
[16] M. Nogi, S. Iwamoto, A.N. Nakagaito, H. Yano, Optically Transparent Nanofiber Paper, Adv. Mater. 21 (2009) 1595–1598. https://doi.org/10.1002/adma.200803174.
[17] S. Belbekhouche, J. Bras, G. Siqueira, C. Chappey, L. Lebrun, B. Khelifi, S. Marais, A. Dufresne, Water sorption behavior and gas barrier properties of cellulose whiskers and microfibrils films, Carbohydr. Polym. 4 (2011) 1740–1748. https://doi.org/10.1016/j.carbpol.2010.10.036.
[18] L.J. Nielsen, S. Eyley, W. Thielemans, J.W. Aylott, Dual fluorescent labelling of cellulose nanocrystals for pH sensing, Chem. Commun. 46 (2010) 8929–8931. https://doi.org/10.1039/c0cc03470c.

[19] I. Kalashnikova, H. Bizot, B. Cathala, I. Capron, Modulation of cellulose nanocrystals amphiphilic properties to stabilize oil/water interface, Biomacromolecules. 13 (2012) 267–275. https://doi.org/10.1021/bm201599j.
[20] K.W. Lin, H.Y. Lin, Quality characteristics of chinese-style meatball containing bacterial cellulose (nata), J. Food Sci. 69 (2004) snq107–snq111. https://doi.org/10.1111/j.1365-2621.2004.tb13378.x.
[21] P.R. Chawla, I.B. Bajaj, S.A. Survase, R.S. Singhal, Microbial cellulose: Fermentative production and applications, Food Technol. Biotechnol. 47 (2009) 107–124.
[22] K.-Y. Lee, G. Buldum, A. Mantalaris, A. Bismarck, More Than Meets the Eye in Bacterial Cellulose: Biosynthesis, Bioprocessing, and Applications in Advanced Fiber Composites, Macromol. Biosci. 14 (2014) 10–32. https://doi.org/10.1002/mabi.201300298.
[23] H. Yano, J. Sugiyama, A.N. Nakagaito, M. Nogi, T. Matsuura, M. Hikita, K. Handa, Optically Transparent Composites Reinforced with Networks of Bacterial Nanofibers, Adv. Mater. 17 (2005) 153–155. https://doi.org/10.1002/adma.200400597.
[24] S.M. Mazhari Mousavi, E. Afra, M. Tajvidi, D.W. Bousfield, M. Dehghani-Firouzabadi, Cellulose nanofiber/carboxymethyl cellulose blends as an efficient coating to improve the structure and barrier properties of paperboard, Cellulose. 24 (2017) 3001–3014. https://doi.org/10.1007/s10570-017-1299-5.
[25] B.G. Rånby, III. Fibrous macromolecular systems. Cellulose and muscle. The colloidal properties of cellulose micelles, Discuss. Faraday Soc. 11 (1951) 158–164. https://doi.org/10.1039/DF9511100158.
[26] Y. Habibi, L.A. Lucia, O.J. Rojas, Cellulose nanocrystals: Chemistry, self-assembly, and applications, Chem. Rev. 110 (2010) 3479–3500. https://doi.org/10.1021/cr900339w.
[27] M.A.S. Azizi Samir, F. Alloin, A. Dufresne, Review of recent research into cellulosic whiskers, their properties and their application in nanocomposite field, Biomacromolecules. 6 (2005) 612–626. https://doi.org/10.1021/bm0493685.
[28] Z. Karim, S. Afrin, Q. Husain, R. Danish, Necessity of enzymatic hydrolysis for production and functionalization of nanocelluloses, Crit. Rev. Biotechnol. 37 (2017) 355–370. https://doi.org/10.3109/07388551.2016.1163322.
[29] B. Yang, Z. Dai, S.Y. Ding, C.E. Wyman, Enzymatic hydrolysis of cellulosic biomass, Biofuels. 2 (2011) 421–449. https://doi.org/10.4155/bfs.11.116.
[30] A. López-Rubio, J.M. Lagaron, M. Ankerfors, T. Lindström, D. Nordqvist, A. Mattozzi, M.S. Hedenqvist, Enhanced film forming and film properties of amylopectin using micro-fibrillated cellulose, Carbohydr. Polym. 68 (2007) 718–727. https://doi.org/10.1016/j.carbpol.2006.08.008.
[31] A.J. Svagan, M.A.S. Azizi Samir, L.A. Berglund, Biomimetic polysaccharide nanocomposites of high cellulose content and high toughness, Biomacromolecules. 8 (2007) 2556–2563. https://doi.org/10.1021/bm0703160.
[32] C. Boisset, C. Fraschini, M. Schülein, B. Henrissat, H. Chanzy, Imaging the enzymatic digestion of bacterial cellulose ribbons reveals the endo character of the cellobiohydrolase Cel6A from Humicola insolens and its mode of synergy with cellobiohydrolase Cel7A, Appl. Environ. Microbiol. 66 (2000) 1444–1452. https://doi.org/10.1128/AEM.66.4.1444-1452.2000.
[33] N.R. Gilkes, E. Jervis, B. Henrissat, B. Tekant, R.C. Miller, R.A.J. Warren, D.G. Kilburn, The adsorption of a bacterial cellulase and its two isolated domains to crystalline cellulose, J. Biol. Chem. 267 (1992) 6743–6749. https://doi.org/10.1016/s0021-9258(19)50488-4.
[34] M. Kostylev, D. Wilson, A distinct model of synergism between a processive endocellulase (TfCel9A) and an exocellulase (TfCel9A) from thermobifida fusca, Appl. Environ. Microbiol. 80 (2014) 339–344. https://doi.org/10.1128/aem.02706-13.

[35] E.T. Reese, R.G.H. Siu, H.S. Levinson, The biological degradation of soluble cellulose derivatives and its relationship to the mechanism of cellulose hydrolysis, J. Bacteriol. 59 (1950) 485–497. https://doi.org/10.1128/JB.59.4.485-497.1950.
[36] S.J. Horn, G. Vaaje-Kolstad, B. Westereng, V.G.H. Eijsink, Novel enzymes for the degradation of cellulose, Biotechnol. Biofuels. 5 (2012) 45. https://doi.org/10.1186/1754-6834-5-45.
[37] Z. Forsberg, A.K. Mackenzie, M. Sørlie, Å.K. Røhr, R. Helland, A.S. Arvai, G. Vaaje-Kolstad, V.G.H. Eijsink, Structural and functional characterization of a conserved pair of bacterial cellulose-oxidizing lytic polysaccharide monooxygenases, Proc. Natl. Acad. Sci. U. S. A. 111 (2014) 8446–8451. https://doi.org/10.1073/pnas.1402771111.
[38] C. Valls, F.I. Javier Pastor, M. Blanca Roncero, T. Vidal, P. Diaz, J. Martínez, S. V. Valenzuela, Assessing the enzymatic effects of cellulases and LPMO in improving mechanical fibrillation of cotton linters, Biotechnol. Biofuels. 12 (2019) 161. https://doi.org/10.1186/s13068-019-1502-z.
[39] B. Bissaro, A. Várnai, Å.K. Røhr, V.G.H. Eijsink, Oxidoreductases and Reactive Oxygen Species in Conversion of Lignocellulosic Biomass, Microbiol. Mol. Biol. Rev. 82 (2018). https://doi.org/10.1128/mmbr.00029-18.
[40] K.S. Johansen, Lytic Polysaccharide Monooxygenases: The Microbial Power Tool for Lignocellulose Degradation, Trends Plant Sci. 21 (2016) 926–936. https://doi.org/10.1016/j.tplants.2016.07.012.
[41] S. V. Valenzuela, G. Ferreres, G. Margalef, F.I.J. Pastor, Fast purification method of functional LPMOs from Streptomyces ambofaciens by affinity adsorption, Carbohydr. Res. 448 (2017) 205–211. https://doi.org/10.1016/j.carres.2017.02.004.
[42] J. Fernández, A.G. Morena, S. V. Valenzuela, F.I.J. Pastor, P. Díaz, J. Martínez, Microbial Cellulose from a Komagataeibacter intermedius Strain Isolated from Commercial Wine Vinegar, J. Polym. Environ. 27 (2019) 956–967. https://doi.org/10.1007/s10924-019-01403-4.
[43] T.M. Wood, Preparation of Crystalline, Amorphous, and Dyed Cellulase Substrates, Methods Enzymol. 160 (1988) 19–25. https://doi.org/10.1016/0076-6879(88)60103-0.
[44] G.L. Miller, Use of Dinitrosalicylic Acid Reagent for Determination of Reducing Sugar, Anal. Chem. 31 (1959) 426–428. https://doi.org/10.1021/ac60147a030.
[45] L. Segal, J.J. Creely, A.E. Martin, C.M. Conrad, An Empirical Method for Estimating the Degree of Crystallinity of Native Cellulose Using the X-Ray Diffractometer, Text. Res. J. 29 (1959) 786–794. https://doi.org/10.1177/004051755902901003.
[46] P. Falamarzpour, T. Behzad, A. Zamani, Preparation of nanocellulose reinforced chitosan films, cross-linked by adipic acid, Int. J. Mol. Sci. 18 (2017) 396. https://doi.org/10.3390/ijms18020396.
[47] A. Dufresne, Nanocellulose: A new ageless bionanomaterial, Mater. Today. 16 (2013) 220–227. https://doi.org/10.1016/j.mattod.2013.06.004.
[48] S. V. Valenzuela, C. Valls, V. Schink, D. Sánchez, M.B. Roncero, P. Diaz, J. Martínez, F.I.J. Pastor, Differential activity of lytic polysaccharide monooxygenases on celluloses of different crystallinity. Effectiveness in the sustainable production of cellulose nanofibrils, Carbohydr. Polym. 207 (2019) 59–67. https://doi.org/10.1016/j.carbpol.2018.11.076.
[49] O.A. Ogunyewo, A. Randhawa, M. Gupta, V.C. Kaladhar, P.K. Verma, S.S. Yazdani, Synergistic Action of a Lytic Polysaccharide Monooxygenase and a Cellobiohydrolase from Penicillium funiculosum in Cellulose Saccharification under High-Level Substrate Loading, Appl. Environ. Microbiol. 86 (2020) 1–21. https://doi.org/10.1128/AEM.01769-20.
[50] M.B. Keller, S.F. Badino, N. Røjel, T.H. Sørensen, J. Kari, B. McBrayer, K. Borch, B.M. Blossom, P. Westh, A comparative biochemical investigation of the impeding

effect of C1-oxidizing LPMOs on cellobiohydrolases, J. Biol. Chem. 296 (2021). https://doi.org/10.1016/j.jbc.2021.100504.
[51] A. Grząbka-Zasadzińska, A. Skrzypczak, S. Borysiak, The influence of the cation type of ionic liquid on the production of nanocrystalline cellulose and mechanical properties of chitosan-based biocomposites, Cellulose. 26 (2019) 4827–4840. https://doi.org/10.1007/s10570-019-02412-1.
[52] A. Dufresne, Nanocellulose: A new ageless bionanomaterial, Mater. Today. 16 (2013) 220–227. https://doi.org/10.1016/j.mattod.2013.06.004.
[53] A. Balea, E. Fuente, M. Concepcion Monte, N. Merayo, C. Campano, C. Negro, A. Blanco, Industrial application of nanocelluloses in papermaking: A review of challenges, technical solutions, and market perspectives, Molecules. 25 (2020) 526. https://doi.org/10.3390/molecules25030526.
[54] C. Buruaga-Ramiro, S. V. Valenzuela, C. Valls, M.B. Roncero, F.I.J. Pastor, P. Díaz, J. Martinez, Development of an antimicrobial bioactive paper made from bacterial cellulose, Int. J. Biol. Macromol. 158 (2020) 587–594. https://doi.org/10.1016/j.ijbiomac.2020.04.234.
[55] E.S. do Nascimento, A.L.S. Pereira, M. de O. Barros, M.K. de A. Barroso, H.L.S. Lima, M. de F. Borges, J.P. de A. Feitosa, H.M.C. de Azeredo, M. de F. Rosa, TEMPO oxidation and high-speed blending as a combined approach to disassemble bacterial cellulose, Cellulose. 26 (2019) 2291–2302. https://doi.org/10.1007/s10570-018-2208-2.
[56] R.H. Marchessault, F.F. Morehead, M.J. Koch, Some hydrodynamic properties of neutral suspensions of cellulose crystallites as related to size and shape, J. Colloid Sci. 16 (1961) 327–344. https://doi.org/10.1016/0095-8522(61)90033-2.
[57] S. Elazzouzi-Hafraoui, Y. Nishiyama, J.L. Putaux, L. Heux, F. Dubreuil, C. Rochas, The shape and size distribution of crystalline nanoparticles prepared by acid hydrolysis of native cellulose, Biomacromolecules. 9 (2008) 57–65. https://doi.org/10.1021/bm700769p.
[58] Y. Van Daele, J.F. Revol, F. Gaill, G. Goffinet, Characterization and supramolecular architecture of the cellulose-protein fibrils in the tunic of the sea peach (Halocynthia papillosa, Ascidiacea, Urochordata), Biol. Cell. 76 (1992) 87–96. https://doi.org/10.1016/0248-4900(92)90198-A.
[59] A.B. Perumal, P.S. Sellamuthu, R.B. Nambiar, E.R. Sadiku, Development of polyvinyl alcohol/chitosan bio-nanocomposite films reinforced with cellulose nanocrystals isolated from rice straw, Appl. Surf. Sci. 449 (2018) 591–602. https://doi.org/10.1016/j.apsusc.2018.01.022.
[60] M. Salari, M. Sowti Khiabani, R. Rezaei Mokarram, B. Ghanbarzadeh, H. Samadi Kafil, Preparation and characterization of cellulose nanocrystals from bacterial cellulose produced in sugar beet molasses and cheese whey media, Int. J. Biol. Macromol. 122 (2019) 280–288. https://doi.org/10.1016/j.ijbiomac.2018.10.136.
[61] J. George, A.S. Bawa, Siddaramaiah, Synthesis and characterization of bacterial cellulose nanocrystals and their PVA nanocomposites, in: Adv. Mater. Res., Trans Tech Publications Ltd, 2010: pp. 383–386. https://doi.org/10.4028/www.scientific.net/amr.123-125.383.
[62] J. George, Siddaramaiah, High performance edible nanocomposite films containing bacterial cellulose nanocrystals, Carbohydr. Polym. 87 (2012) 2031–2037. https://doi.org/10.1016/j.carbpol.2011.10.019.
[63] D. Klemm, F. Kramer, S. Moritz, T. Lindström, M. Ankerfors, D. Gray, A. Dorris, Nanocelluloses: A New Family of Nature-Based Materials, Angew. Chemie Int. Ed. 50 (2011) 5438–5466. https://doi.org/10.1002/anie.201001273.
[64] L. Heux, G. Chauve, C. Bonini, Nonflocculating and chiral-nematic self-ordering of cellulose microcrystals suspensions in nonpolar solvents, Langmuir. 16 (2000) 8210–8212. https://doi.org/10.1021/la9913957.
[65] M.M. De Souza Lima, J.T. Wong, M. Paillet, R. Borsali, R. Pecora, Translational and rotational dynamics of rodlike cellulose whiskers, Langmuir. 19 (2003) 24–29.

https://doi.org/10.1021/la020475z.
[66] A. Dufresne, Nanocellulose, De gruyter, 2012. https://doi.org/10.1515/9783110254600.
[67] L. Chen, M. Zou, F.F. Hong, Evaluation of Fungal Laccase Immobilized on Natural Nanostructured Bacterial Cellulose, Front. Microbiol. 6 (2015). https://doi.org/10.3389/fmicb.2015.01245.
[68] N.F. Vasconcelos, J.P.A. Feitosa, F.M.P. da Gama, J.P.S. Morais, F.K. Andrade, M. de S.M. de Souza Filho, M. de F. Rosa, Bacterial cellulose nanocrystals produced under different hydrolysis conditions: Properties and morphological features, Carbohydr. Polym. 155 (2017) 425–431. https://doi.org/10.1016/j.carbpol.2016.08.090.
[69] P. Singhsa, R. Narain, H. Manuspiya, Bacterial Cellulose Nanocrystals (BCNC) Preparation and Characterization from Three Bacterial Cellulose Sources and Development of Functionalized BCNCs as Nucleic Acid Delivery Systems, ACS Appl. Nano Mater. 1 (2017) 209–221. https://doi.org/10.1021/ACSANM.7B00105.
[70] C.L. Pirich, R.A. de Freitas, M.A. Woehl, G.F. Picheth, D.F.S. Petri, M.R. Sierakowski, Bacterial cellulose nanocrystals: impact of the sulfate content on the interaction with xyloglucan, Cellulose. 22 (2015) 1773–1787. https://doi.org/10.1007/S10570-015-0626-Y.
[71] Y. Huang, C. Zhu, J. Yang, Y. Nie, C. Chen, D. Sun, Recent advances in bacterial cellulose, Cellulose. 21 (2014) 1–30. https://doi.org/10.1007/s10570-013-0088-z.
[72] H. Mirhosseini, C.P. Tan, N.S.A. Hamid, S. Yusof, Effect of Arabic gum, xanthan gum and orange oil contents on ζ-potential, conductivity, stability, size index and pH of orange beverage emulsion, Colloids Surfaces A Physicochem. Eng. Asp. 315 (2008) 47–56. https://doi.org/10.1016/J.colsurfa.2007.07.007.
[73] J.F. Revol, H. Bradford, J. Giasson, R.H. Marchessault, D.G. Gray, Helicoidal self-ordering of cellulose microfibrils in aqueous suspension, Int. J. Biol. Macromol. 14 (1992) 170–172. https://doi.org/10.1016/S0141-8130(05)80008-X.
[74] M. Roman, W.T. Winter, Effect of sulfate groups from sulfuric acid hydrolysis on the thermal degradation behavior of bacterial cellulose, Biomacromolecules. 5 (2004) 1671–1677. https://doi.org/10.1021/bm034519+.
[75] M.C.I.M. Amin, A.G. Abadi, H. Katas, Purification, characterization and comparative studies of spray-dried bacterial cellulose microparticles, Carbohydr. Polym. 99 (2014) 180–189. https://doi.org/10.1016/j.carbpol.2013.08.041.
[76] D.M. Panaitescu, A.N. Frone, I. Chiulan, A. Casarica, C.A. Nicolae, M. Ghiurea, R. Trusca, C.M. Damian, Structural and morphological characterization of bacterial cellulose nano-reinforcements prepared by mechanical route, Mater. Des. 110 (2016) 790–801. https://doi.org/10.1016/j.matdes.2016.08.052.
[77] P. Rämänen, P.A. Penttilä, K. Svedström, S.L. Maunu, R. Serimaa, The effect of drying method on the properties and nanoscale structure of cellulose whiskers, Cellulose. 19 (2012) 901–912. https://doi.org/10.1007/s10570-012-9695-3.
[78] F.V. Ferreira, A. Dufresne, I.F. Pinheiro, D.H.S. Souza, R.F. Gouveia, L.H.I. Mei, L.M.F. Lona, How do cellulose nanocrystals affect the overall properties of biodegradable polymer nanocomposites: A comprehensive review, Eur. Polym. J. 108 (2018) 274–285. https://doi.org/10.1016/j.eurpolymj.2018.08.045.
[79] Z. Xiang, X. Jin, Q. Liu, Y. Chen, J. Li, F. Lu, The reinforcement mechanism of bacterial cellulose on paper made from woody and non-woody fiber sources, Cellulose. 24 (2017) 5147–5156. https://doi.org/10.1007/s10570-017-1468-6.
[80] J. Yuan, T. Wang, X. Huang, W. Wei, Dispersion and Beating of Bacterial Cellulose and their Influence on Paper Properties, BioResources. 11 (2016) 9290–9301. https://doi.org/10.15376/biores.11.4.9290-9301.
[81] C. Aulin, G. Salazar-Alvarez, T. Lindström, High strength, flexible and transparent nanofibrillated cellulose-nanoclay biohybrid films with tunable oxygen and water vapor permeability, Nanoscale. 4 (2012) 6622–6628. https://doi.org/10.1039/c2nr31726e.

[82] C.J. Ridgway, P.A.C. Gane, Constructing NFC-pigment composite surface treatment for enhanced paper stiffness and surface properties, Cellulose. 19 (2012) 547–560. https://doi.org/10.1007/s10570-011-9634-8.
[83] S.S. Nair, J. Zhu, Y. Deng, A.J. Ragauskas, High performance green barriers based on nanocellulose, Sustain. Chem. Process. 2 (2014). https://doi.org/10.1186/s40508-014-0023-0.
[84] F. Hoeng, A. Denneulin, J. Bras, Use of nanocellulose in printed electronics: A review, Nanoscale. 8 (2016) 13131–13154. https://doi.org/10.1039/c6nr03054h.
[85] N.L. Garcia de Rodriguez, W. Thielemans, A. Dufresne, Sisal cellulose whiskers reinforced polyvinyl acetate nanocomposites, Cellulose. 13 (2006) 261–270. https://doi.org/10.1007/s10570-005-9039-7.
[86] J. Lange, Y. Wyser, Recent Innovations in Barrier Technologies for Plastic Packaging - A Review, Packag. Technol. Sci. 16 (2003) 149–158. https://doi.org/10.1002/pts.621.
[87] M.K.M. Haafiz, A. Hassan, Z. Zakaria, I.M. Inuwa, M.S. Islam, M. Jawaid, Properties of polylactic acid composites reinforced with oil palm biomass microcrystalline cellulose, Carbohydr. Polym. 98 (2013) 139–145. https://doi.org/10.1016/j.carbpol.2013.05.069.
[88] J. Ambrosio-Martín, A. Lopez-Rubio, M.J. Fabra, G. Gorrasi, R. Pantani, J.M. Lagaron, Assessment of ball milling methodology to develop polylactide-bacterial cellulose nanocrystals nanocomposites, J. Appl. Polym. Sci. 132 (2015). https://doi.org/10.1002/app.41605.
[89] M. Martínez-Sanz, M.A. Abdelwahab, A. Lopez-Rubio, J.M. Lagaron, E. Chiellini, T.G. Williams, D.F. Wood, W.J. Orts, S.H. Imam, Incorporation of poly(glycidylmethacrylate) grafted bacterial cellulose nanowhiskers in poly(lactic acid) nanocomposites: Improved barrier and mechanical properties, Eur. Polym. J. 49 (2013) 2062–2072. https://doi.org/10.1016/j.eurpolymj.2013.04.035.
[90] R. Kumar, S. Kumari, B. Rai, R. Das, G. Kumar, Effect of nano-cellulosic fiber on mechanical and barrier properties of polylactic acid (PLA) green nanocomposite film, Mater. Res. Express. 6 (2019) 125108. https://doi.org/10.1088/2053-1591/AB5755.

5. DISCUSIÓN GENERAL

5. Discusión general

La concienciación sobre la necesidad de encontrar nuevos biomateriales que puedan sustituir procesos químicos agresivos con el medio ambiente es cada vez más patente. En este contexto, las enzimas y la celulosa bacteriana tienen mucho que ofrecer.

El primer capítulo se centró en la mejora, mediante técnicas de ingeniería genética, de lipasas de la cepa identificada y caracterizada en trabajos anteriores del grupo de investigación *Bacillus cereus* JR3 (Ribera *et al.*, 2017). Esta cepa fue aislada a partir de muestras de suelo volcánico de la isla de El Hierro, en las Islas Canarias. Su sobrenadante mostró una actividad lipasa termófila cuya temperatura óptima de actividad se encontraba entre 80 y 100 ºC, indicando la existencia de un sistema lipolítico extracelular, formado por una o varias lipasas, termófilo. Las lipasas se encuentran entre las principales enzimas empleadas a nivel industrial dada la gran versatilidad que presentan, más aún si su naturaleza es termófila, ya que muchas de las reacciones que se llevan a cabo en la industria de los detergentes, por ejemplo, son llevadas a cabo a elevadas temperaturas.
En el primer artículo se abordó la modificación genética de una de estas lipasas, LipJ. LipJ, a pesar de haber sido clonada con iniciadores basados en los dominios conservados de secuencias lipasas termófilas ya conocidas, y próximas a los géneros *Bacillus* y *Geobacillus*, presenta su máxima actividad a 30 ºC, sin ningún rasgo de termofilia y con una estabilidad térmica muy pobre, tal y como se ha indicado con anterioridad. De hecho, LipJ es una una enzima mesófila e intracelular. Sin embargo, su similitud de secuencia, tanto en el péptido señal como en el pentapéptido catalítico con otras lipasas termófilas bacterianas, sugiere que quizás su origen hubiera sido el de una enzima termófila que hubiera adquirido características mesófilas. Con todos estos antecedentes, los objetivos fueron dos: comprobar, si, tras una mutagénesis dirigida en los dominios de su centro catalítico y en el péptido señal la proteína LipJ adquiría actividad termófila, y la modificación del punto H110 mediante la confección de una librería NNK para determinar si tiene efecto sobre la actividad termófila. Así pues, la esterasa mesófila LipJ, de *Bacillus* sp. JR3, perteneciente a un clúster bien diferenciado de la familia de las I.5 lipasas, fue modificada genéticamente en este trabajo por tal de recuperar los rasgos característicos de la familia I.5 de lipasas bacterianas. Se obtuvieron diferentes variantes, tanto con el empleo de una mutagénesis dirigida en los dominios de su centro catalítico y en el péptido señal, como con la mutagénesis iterativa mediante la creación de una librería

de degeneración NNK en la posición H110, en que la histidina puede ser sustituida por cualquier aminoácido.

De la mutagénesis saturada de un posible residuo implicado en la coordinación del ión Zn^{2+} se obtuvo una variante de la proteína LipJ con mayor actividad a altas temperaturas con la modificación del residuo H110, la variante LipJ-H110N. Entre los mutantes analizados, el mutante H110N, con una asparagina en vez de una histidina, mostró más actividad a 30ºC con MUF-Heptanoato, multiplicando la actividad cuatro veces. A la luz de estos resultados, la asparagina sería responsable de un cambio en la especificidad de sustrato, pero no en la termoficilidad, contrariamente a lo esperado de acuerdo a la bibliografía (Biundo *et al.*, 2017, 2018). El análisis de la estructura 3D del mutante H110N, superpuesta a la de LipJ, mostró que la presencia de una asparagina en la posición 110 sería la responsable de la formación de uniones polares o de interacciones adicionales con el zinc, lo que daría explicación a los cambios en la especificidad de sustrato, tal y como también describieron otros autores para la lipasa L1 de *Bacillus stearothermophilus* (Choi *et al.*, 2005). En cuanto a la mutagénesis dirigida, los cambios introducidos fueron tres, creando un clon para cada uno (**Tabla 2**).

Tabla 2. Cambios de aminoácidos realizados en las variantes de LipJ obtenidas mediante mutagénesis dirigida.

Mutante	**Mutación**	**Posición en la secuencia de LipJ**	**Sustituciones**	**Localización en la estructura primaria**
G136A	G136A	136	Glicina (G) → Alanina (A)	Centro catalítico
M139Q	M139Q	139	Metionina (M) → Glutamina (Q)	Centro catalítico
E27A	E27A	27	Glutamato (E) → Alanina (A)	Péptido señal
DM (Doble Mutante)	G136A	136	Glicina (G) → Alanina (A)	Centro catalítico
	M139Q	139	Metionina (M) → Glutamina (Q)	
TM (Triple Mutante)	G136A	136	Glicina (G) → Alanina (A)	Centro catalítico
	M139Q	139	Metionina (M) → Glutamina (Q)	
	E27A	27	Glutamato (E) → Alanina (A)	Péptido señal

El primer cambio fue en la posición 27, el punto de corte del péptido señal, cambiando un glutamato por una alanina (variante LipJ-E27A), con la intención de facilitar el procesamiento y la secreción de la enzima. Los otros dos cambios fueron en el centro

catalítico, en la posición 136 cambiando una glicina por una alanina, y en la posición 139 sustituyendo una metionina por una glutamina (variantes LipJ-G136A y LipJ-M139Q, respectivamente), para generar un pentapéptido catalítico más parecido al de la subfamilia I.5 de lipasas bacterianas (Arpigny and Jaeger, 1999). También se obtuvieron un doble mutante para el centro catalítico (DM) y un triple mutante (TM). Se compararon la actividad relativa a 30 y 80 ºC con varios sustratos para comprobar si alguna de las mutaciones provocaba un aumento de la actividad termófila, equiparable a la descrita en el sobrenadante de *Bacillus* sp. JR3. Con su sustrato óptimo, butirato, LipJ es la proteína que muestra más actividad. Únicamente el DM y el TM mostraron más actividad a 80 ºC, sugiriendo que la modificación del pentapéptido catalítico contribuye a un incremento de la termoficidad. Cuando se midió la actividad con heptanoato, todas las variantes enzimáticas mostraron mayor actividad que la proteína original, tanto a 30 ºC como a 80 ºC, con un incremento de 4,6 veces del TM a 30 ºC, sugiriendo que la sustitución de una metionina por una glutamina podría ser determinante para la activación de la enzima dependiente de temperatura con sustratos de cadena más larga, lo que se corroboró cuando el mismo ensayo se repitió con oleato a 80 ºC, con un incremento de 37 veces la actividad de la LipJ. Estos resultados indican que, a parte de una mejora en la actividad termófila, hay un cambio en la especificidad de sustrato en todos los mutantes obtenidos. Entre ellos el DM y el TM fueron seleccionados para su posterior caracterización debido a la actividad mostrada tanto a 30 ºC como a 80 ºC con heptanoato. Para determinar la curva de temperatura óptima se evaluó la actividad presente los extractos celulares crudos sobre MUF-Heptanoato, igual que el perfil cinético. Para el TM, se observó un incremento significativo de la actividad a 50 ºC, el mismo perfil que se observó para el DM, mientras que para la proteína original, tal y como se esperaba, tiene su actividad óptima a 30 ºC, con una clara tendencia a perder actividad a temperaturas superiores.

En conjunto, los resultados obtenidos en este primer artículo demostraron que LipJ, una esterasa mesófila, fue satisfactoriamente convertida en una con una mayor actividad específica, además de más termófila mediante la modificación de los residuos descritos como esenciales para la familia I.5. En particular, el triple mutante con modificaciones en la región N-terminal y en el pentapéptido catalítico, y la variante en la coordinación del ión Zn^{2+}, LipJ-H110N, mostraron un desplazamiento interesante en la especificidad de sustrato hacia el MUF-heptanoato, acentuado también con la presencia de Mn^{2+}.

Para el segundo y último artículo de este capítulo, inicialmente se clonó otra lipasa de la misma cepa a partir de unos iniciadores diseñados a partir de los extremos del gen BCE2219 de *Bacillus cereus*, ya que las secuencias correspondientes a los aminoácidos de la región N y C terminal de las lipasas termófilas se encuentran altamente conservadas. La enzima obtenida, llamada LipG, tenía una longitud de 1602 pb, 533 aminoácidos y un peso de 56 kDa (datos no publicados). Analizando la secuencia, se detectó la presencia de un dominio α/β-hidrolasa en los primeros 256 residuos, con una región C-terminal sin ninguna homología estructural con otras familias de lipasas. Al generar un modelo 3D sólo de esta región se obtuvo una estructura de *β-sándwich,* parecido al de las inmunoglobulinas, por lo que se dedujo que LipG estaría formada por dos dominios estructurales diferentes. Sorprendentemente, sólo se conocían hasta la fecha dos precedentes de la presencia de un dominio Ig-*like* en la estructura de una enzima lipolítica (M *et al.*, 2009; Okano *et al.*, 2015), y sería la primera vez para una lipasa del género de *Bacillus*. De acuerdo a la literatura, la presencia de este dominio podría estar implicado en la formación de multímeros proteicos necesarios para la actividad enzimática, así como para la estabilidad a elevadas temperaturas (M *et al.*, 2009), algo que sería muy interesante de confirmarse conociendo el origen volcánico de la cepa *Bacillus* sp. JR3 (Ribera *et al.*, 2017). En cuanto a la caracterización de la actividad lipolítica, mostró preferencia por sustratos cortos, siendo su óptimo el acetato, aunque para los estudios posteriores se estableció el butirato como su óptimo, para mayor facilidad de los ensayos realizados. LipG mostró ser más activa en el rango de temperaturas entre 50 ºC y 60 ºC, teniendo su máximo a 60ºC, siendo una enzima termófila. Además, se constató que conservaba alrededor del 80 % de su actividad residual después de 25 h de incubación a 60 ºC y 80 ºC. Mostró un comportamiento claramente alcalófilo, exhibiendo su actividad óptima a pH 8, mientras que presentó una cinética con un perfil de Michaelis-Menten, sin mostrar activación interfacial (datos sin publicar). Sin embargo, a lo largo de todos estos ensayos, se apreció que los valores absolutos de actividad específica se situaban cerca del ruido de fondo de la técnica. Sumado a la imposibilidad de visualizar ninguna banda de esta lipasa a través de zimogramas, se especuló que la caracterización realizada hasta el momento correspondía a la actividad intrínseca de la cepa hospedadora, *Escherichia coli*.

Por tal de confirmar esta hipótesis, se evaluó esta actividad en las cepas de *E.*coli comúnmente empleadas en el laboratorio mediante ensayos cualitativos y cuantitativos. Entre ellas, se seleccionó a *E.coli* BL21 para proseguir con las determinaciones

posteriores por su amplio uso en la expresión heteróloga de esterasas y lipasas (Ruiz *et al.*, 2007; Arnau Bassegoda, Pastor and Diaz, 2012; Infanzón *et al.*, 2014). Los zimogramas revelaron una banda de Ca. 18 - 20 kDa activa con MUF-Butirato en los extractos celulares crudos, actividad que pudo ser cuantificada por espectrofluorimetría. Una caracterización más profunda permitió establecer que esta cepa tenía preferencia por sustratos de cadena media, C7, si bien también era capaz de hidrolizar sustratos de cadena corta, estableciendo sus condiciones óptimas de actividad a 50 ºC y a pH 8. Estos rasgos, más típicos de enzimas termófilas, nunca habían sido descritos en la literatura para *E.coli*. Los ensayos de cinética y de inhibición mostraron que esta actividad hidrolítica podía verse afectada por diversos iones, Triton X-100® y SDS. Todas estas propiedades – baja actividad, preferencia por sustratos de cadena media y una elevada temperatura operacional – podría justificar por qué esta actividad no había sido investigada hasta ahora, a pesar de que numerosas esterasas y lipasas han sido clonadas en *E.coli*. Y es que, en efecto, los datos reportados para los extractos celulares de *E.coli* son muy parecidos a los obtenidos de la caracterización inicial de LipG, que sería una lipasa con secuencia termófila y ubicua en *Bacillus cereus* pero sin actividad que pueda ser cuantificada. A raíz de los resultados aportados en este estudio, las futuras investigaciones basadas en la expresión de lipasas clonadas en células huésped de *E.coli* tendrán que tener en cuenta esta actividad lipolítica basal antes de proceder a la caracterización de la lipasa de interés.

El siguiente capítulo, que trata sobre la inmovilización de enzimas sobre CB, tenía como uno de los objetivos establecer un modelo con enzimas lipasas. Concretamente, se pretendía inmovilizar una lipasa comercial, por su facilidad de manipulación, y LipJ o LipG, o ambas. En el caso de LipJ, a través de las diversas mutagénesis a las que fue sometida, no se consiguió ninguna variante más termófila, aunque sí con diferencias respecto a la preferencia de sustrato. Si LipJ y LipG tienen un denominador común, además de proceder de la misma cepa, es que tienen una actividad específica muy baja, lo que las convierte en enzimas con una actividad muy difícil de cuantificar. La hipotética actividad lipolítica de LipG directamente no puede discernirse de la intrínseca de *E.coli*, mientras que la de LipJ y la de las variantes obtenidas, aunque puede discriminarse de esta actividad basal, siguen presentando unos valores muy bajos. En la inmovilización de enzimas por adsorción física, la técnica empleada a lo largo de esta tesis, siempre se asume que no se adsorbe la totalidad de la proteína presente en la solución inicial. Por

esto mismo, en una posible inmovilización de LipJ, éste sería un proceso muy costoso por la cantidad de enzima que se necesitaría producir, por tal de que quedara retenida una fracción cuya actividad fuera posible detectar. Por estas razones, la inmovilización de lipasas sobre CB se llevó a cabo sólo con la lipasa comercial.

En el primer trabajo de este segundo capítulo se estudió la idoneidad de diferentes matrices de CB para preparar nanocomposites enzimáticamente activos, siempre dentro de un marco de tecnologías más amigables con el medio ambiente. Después de la producción y la purificación de la CB, se obtuvieron dos matrices: CB en suspensión acuosa (BCS, por sus siglas en inglés *Bacterial Cellulose Suspesion*) y papel de CB (BCP por sus siglas en inglés *Bacterial Cellulose Paper*). A continuación, se inmovilizó la lipasa en ambas por adsorción física, obteniendo los nanocomposites de Lipasa/CB. Para la impregnación se pusieron en contacto las matrices BCS y BCP con una solución de enzima de concentración conocida durante 12 h a temperatura ambiente y en agitación. Posteriormente, tanto los papeles como la suspensión fueron sometidos a dos lavados progresivos en la misma solución de trabajo para quitar el excedente de proteína. Para dilucidar la cantidad de enzima adsorbida, se midió, la cantidad de proteína presente en la solución de lipasa antes y después de la impregnación. La diferencia permite obtener la cantidad de enzima, en µg, que hay por cm^2. Paralelamente, también se cuantificó la actividad lipasa de todas estas soluciones. En este último paso, si se hubiera inmovilizado LipJ o LipG, la actividad no sería detectable, y no sería posible discriminar entre una unión no eficaz o en una pérdida de actividad.

Una vez constatado que ni la morfología ni la cristalinidad, analizadas mediante microscopía electrónica de barrido y difracción de rayos X, respectivamente, se vieron afectadas por la unión de la enzima, se midió la actividad específica en diferentes condiciones y se procedió a la evaluación de las propiedades operacionales. En comparación a la enzima libre, se observó un desplazamiento hacia temperaturas más elevadas, actividades en rangos de pH más amplios y un leve cambio de tendencia en la especificidad de sustrato, un comportamiento observado por otros autores que emplearon CB como soporte, en forma de membranas (Yuan *et al.*, 2018) y nanocristales (H. J. Kim *et al.*, 2015). En la matriz BCS, que presenta un mayor contenido acuoso que la matriz BCP, la enzima tiene una mayor difusión y accede mejor al sustrato, ya que se encuentra en unas condiciones más parecidas que las de la lipasa libre (Estevinho *et al.*, 2014; Chen, Zou and Hong, 2015). Por ello, la actividad específica del nanocomposite Lipasa/BCS

era ligeramente más elevada que la del nanocomposite Lipasa/BCP. Además, la cantidad de proteína unida también era superior, lo que se atribuyó a que en suspensión la enzima tiene más facilidad para acomodarse en las fibras y puede difundir más libremente que en el papel de CB (Seves *et al.*, 2001). Aun así, el nanocomposite Lipasa/BCP mostró una gran estabilidad térmica, reusabilidad y durabilidad: retuvo un 60 % de la actividad después de 48 h a 60 ºC, mantuvo el 100 % de actividad después de reciclar el nanocomposite diez veces a pH 7 y a 60 ºC y siguió siendo activo después de ser almacenado durante más de un mes a temperatura ambiente, lo que podría explicarse por la restringida movilidad que presentaría la enzima una vez acomodada entre las fibras de CB (Frazão *et al.*, 2014), lo que a su vez retrasaría su inactivación (Yuan *et al.*, 2018). Una enzima inmovilizada tan estable y con una buena reusabilidad son condiciones esenciales para una reducción significativa de los costes de producción en la fabricación de biosensores (Chen, Zou and Hong, 2015; Nigam and Shukla, 2015; Nguyen *et al.*, 2019). Por otro lado, apenas se detectó migración a temperatura ambiente de la enzima en solución acuosa del soporte BCP, un 4 % a las 72 h. Probablemente la elevada densidad fibrilar y la elevada relación superficie/volumen del papel de CB ofrecería más grupos hidroxilo disponibles para la adsorción de la lipasa (Skočaj, 2019). Los resultados, pues, sugirieron que los nanocomposites Lipasa/CB son materiales prometedores para el desarrollo de estrategias biotecnológicas verdes con potencial aplicación tanto en procesos industriales, como la industria de detergentes y alimentaria, como en biomedicina. En concreto, el nanocomposite Lipasa/BCP podría ser un elemento clave en la elaboración de papeles bioactivos de dispositivos simples, portátiles y desechables.

En vista de los resultados anteriores, se demostró que la CB es un material con capacidad de adsorción de enzimas, probablemente gracias al entramado tridimensional que forman sus fibras, a su elevada área superficial y a su porosidad. En concreto, la matriz BCP combina el soporte resistente que ofrece un papel con todas las características propias de la CB. Es, pues, un papel que se puede mojar, además de ser biodegradable y biocompatible. Una de las aplicaciones más conocidas de la CB es en la industria alimentaria, como material de embalaje o "*food packaging*". De hecho, ya existen films de CB para este efecto. En términos de seguridad alimentaria, sin embargo, no sólo el tema del embalaje es importante, sino que lo que se conoce como embalaje activo, o "*active packaging*" está ganado mucho interés. Por *active packaging* se hace referencia a envoltorios que además de ofrecer una barrera entre el alimento y el medio exterior, ofrece

otras propiedades. Una de estas propiedades puede ser las antimicrobianas, mediante la incorporación de agentes antimicrobianos, ya que pueden inhibir o ralentizar el crecimiento de patógenos en los alimentos sin alterar la calidad del producto. Las enzimas se han convertido actualmente en los preservativos naturales más utilizados. Entre ellas, la lisozima es la más conocida a la vez que empleada, que actúa inhibiendo la síntesis de la pared bacteriana durante la replicación bacteriana. Como su adición directa sobre los alimentos puede llevar a una pérdida de su actividad debido a su elevada sensibilidad y rápida inactivación bajo diferentes condiciones ambientales (Rose *et al.*, 1999; Bayazidi, Almasi and Asl, 2018), se opta por la inmovilización de la enzima en el material de embalaje. Siguiendo esta línea, en el cuarto estudio de esta tesis, se decidió inmovilizar un agente antimicrobiano sobre la CB. Concretamente, se inmovilizó la enzima lisozima sobre la matriz BCP por adsorción física, siguiendo la metodología puesta a punto para la lipasa.

El nanocomposite Lys - BCP resultante tenía una morfología similar a la de papel de CB, ya que no se constataron modificaciones ni en la forma ni la disposición de las fibras. Tampoco se observaron cambios en su estructura química por XRD. Respecto a las propiedades operacionales, la actividad específica entre la lisozima libre y la inmovilizada eran muy similares en cuanto al valor absoluto, si bien esta última operaba en un rango más amplio de temperaturas y presentaba una mayor estabilidad térmica, indicando que proteína se mantenía estable y bien retenida entre las nanofibras. Igual que con la lipasa inmovilizada, los cambios en las propiedades físicas y químicas de la lisozima inmovilizada estarían detrás del incremento de su estabilidad (Chen, Zou and Hong, 2015). Interesantemente, Lys – BCP tenía una actividad específica más elevada entre 20 ºC y 30 ºC que la lisozima libre, de gran utilidad en la preservación de los alimentos. Los nanocomposites, que mantuvieron su actividad por lo menos 80 días sin ninguna condición especial de almacenamiento, mostraron tener actividad antimicrobiana contra la bacteria grampositiva *Staphylococcus aureus* y la gramnegativa *Escherichia coli*, inhibiendo su crecimiento un 82 % y un 68 %, respectivamente. Además, la presencia de lisozima representó un incremento de la actividad antioxidante del papel de CB del 30 %. El papel de BC por sí mismo ya mostró algo de actividad antioxidante por la presencia de grupos aldehídos (Morena *et al.*, 2019), actividad que se vio potenciada por la unión de lisozima, atribuida a los grupos amino y OH secundarios. Cabe destacar que la adición de antioxidantes en la industria alimentaria se emplea con regularidad, ya que impide o

retrasa las reacciones de oxidación que alteran los alimentos a la vez que preserva sus valores nutricionales (Lorenzo, Batlle and Gómez, 2014).

Los hallazgos descritos en este último artículo indicaron de nuevo que la CB es un material prometedor para la producción de papeles bioactivos al ofrecer un soporte biocompatible sin comprometer la actividad de la enzima inmovilizada. Un papel bioactivo con propiedades antimicrobianas y antioxidantes puede tener un papel relevante en el campo del empaquetamiento activo. Debido a la naturaleza intrínseca de sus componentes, el papel Lisozima-BCP es biodegradable y biocompatible, lo que lo convierte en candidato ideal para el diseño de nuevos materiales de envasado. Es probable que otras biomoléculas puedan ser adsorbidas en la matriz BCP para obtener más papeles biológicamente activos con diferentes funcionalidades.

Finalmente, el último capítulo de la tesis se centra en la obtención de nanocristales de CB, BCNC, mediante un tratamiento exclusivamente enzimático. Los nanocristales de celulosa se han aislado previamente de diferentes fuentes de tipo vegetal, pero éstas contienen celulosa junto con hemicelulosa, lignina y otros componentes que no se encuentran presentes en la CB. Consecuentemente, la obtención de nanocristales a partir de CB es más simple gracias a su composición pura. Actualmente, la estrategia principal para obtener NCC de fibras celulósicas todavía depende de la hidrólisis ácida, que consiste en la eliminación la celulosa amorfa para obtener celulosa altamente cristalina, además de la reducción de su tamaño (Rånby, 1951; Perumal *et al.*, 2018; Salari *et al.*, 2019). La contrapartida es que esta metodología es energéticamente costosa y genera una gran cantidad de residuos contaminantes. Además, en el caso de emplear ácido sulfúrico, los nanocristales resultantes contienen grupos sulfato que comprometen su biocompatibilidad y hacen que muestren una menor estabilidad térmica en comparación con la celulosa nativa (Roman and Winter, 2004), un parámetro importante para su uso como materiales de refuerzo. Sin embargo, estos grupos sulfatos facilitan la estabilidad de los nanocristales en medio acuoso (Revol *et al.*, 1992).

En el trabajo aquí presentado se explora la posibilidad de obtener NCC a partir de la CB con una alternativa más amigable con el medioambiente mediante la utilización de enzimas modificadoras de celulosa. De esta manera, se generarían menos residuos y se obtendrían nanocristales inalterados, mejorando su alcance en aplicaciones biomédicas y farmacéuticas. Para ello, se empleó un cóctel industrial de endo y exoglucanasas en

combinación con la monooxigenasa lítica de polisacáridos SamC, procedente de *Streptomyces ambofaciens* y clonada en el grupo de investigación (Valenzuela *et al.*, 2017). SamLPMO10C presenta un mecanismo de ruptura del enlace glucosídico mediante la oxidación del C1 de la glucosa, escindiendo enlaces que son inaccesibles para las glucosil hidrolasas, aumentando su accesibilidad al sustrato.

Una vez obtenidos, los BCNC fueron caracterizados tanto en morfología como en tamaño por microscopía electrónica de transmisión. Los BCNC tenían entre 80 nm y 2 μm de longitud y 9 nm de ancho. Como se observa en la **Tabla 3**, no existe un consenso en lo que se refiere a las dimensiones de los nanocristales, ya que dependen del origen y del procedimiento de obtención. Las medidas de los BCNC aquí obtenidos se encuentran dentro del rango de tamaños aceptados cuando se emplea la hidrólisis ácida (Klemm *et al.*, 2011; Moon *et al.*, 2011; George and Sabapathi, 2015; Nascimento *et al.*, 2021), pero con la particularidad de que se ha seguido una hidrólisis enzimática. De esta manera, con un método menos agresivo que el uso de ácido sulfúrico, se generaron unos BCNC inalterados y con una elevada relación de aspecto, de 80.1. Esta relación de aspecto geométrico consiste en la ratio longitud/ancho, y es de gran importancia para determinar su aplicabilidad en mezclas con otros polímeros. Valores más elevados de 13 indican mayor resistencia mecánica (Peng *et al.*, 2011; Dufresne, 2012).

Tabla 3. Dimensiones más comunes de los nanocristales en función del origen de la celulosa de partida y del tipo de hidrólisis ácida empleada. Modificado de George & Sabapathi, 2015.

Fuente de la celulosa	**Ácido**	**Longitud (nm)**	**Ancho (nm)**	**Ratio longitud/ancho**
Madera	H_2SO_4	100 - 300	3 – 5	20 – 100
Algodón	HCl	100 – 150	5 - 10	10 – 30
Ramio (*Boehmeria nivea)*	H_2SO_4	70 - 200	5 -15	-12
Sisal (*Agave sisalana)*	H_2SO_4	100 - 300	3 - 5	-60
Alga burbuja (*Valonia ventricosa*)	H_2SO_4	1000 - 2000	10 – 20	50 – 200
Tunicados	H_2SO_4	> 1000	10 – 20	-100
Bacteriana	H_2SO_4	100 - 1500	10 – 50	2 – 100
Bacteriana	HCl	160 - 420	15 - 25	7 - 23

La CB nativa tenía una cristalinidad del 95 %, y los BCNC mantuvieron unos valores similares, indicando que los BCNC mantendrían la fuerza mecánica y las propiedades interfaciales del material de partida (Huang *et al.*, 2014). Además, la carga negativa aportada por los grupos carboxilo, fruto de la oxidación de SamC, proporcionó buenas propiedades dispersivas a estos nanocristales debido a las repulsiones electroestáticas (Mirhosseini *et al.*, 2008), un efecto similar al producido por los grupos sulfato en la hidrólisis ácida (Roman and Winter, 2004). Esta estabilidad en suspensión acuosa, medida por el potencial z, resultó ser más elevada que la reportada por otros autores que obtuvieron BCNC con ácido sulfúrico (Pirich *et al.*, 2015; Singhsa, Narain and Manuspiya, 2018), pero sin comprometer la termoestabilidad ni su futura aplicabilidad (Martínez-Sanz, Lopez-Rubio and Lagaron, 2012). De hecho, los BCNC mostraron una estabilidad térmica superior a la CB nativa, de acuerdo con la curva de termogravimetría. En comparación, para el mismo peso, la CB presenta una estructura más compacta que los BCNC que transfiere mejor el calor, por lo que su degradación térmica se produce a menor temperatura (Rämänen *et al.*, 2012; Panaitescu *et al.*, 2016).

A mayores, el uso de enzimas permitió simplificar el protocolo de obtención de los BCNC ya que no fueron necesarios los procedimientos para la eliminación del ácido, consiguiendo que el proceso de producción sea más seguro, con menos contaminantes y con menor consumo de energía. Cabe destacar, además, que SamC parecía cambiar el patrón de actuación del cóctel de celulasas empleado. En un principio se hipotetizó que la acción oxidativa de esta enzima generaría más puntos de corte para las posibles exocelulasas, al facilitar la disgregación de las fibras, tal y como otros estudios previos de sinergia habían descrito (Johansen, 2016; Valenzuela *et al.*, 2017; Ogunyewo *et al.*, 2020). Consecuentemente, las celulasas podrían empezar la digestión en diferentes puntos de manera simultánea. Sin la acción de la LPMO, las exocelulasas deben de actuar de manera procesiva hasta degradar las fibras hasta glucosa. De esta manera es como se justificaba que con el empleo de la LPMO se generaban productos de la digestión de mayor tamaño, en comparación con los BCNC obtenidos únicamente con celulasas, tal y como indicaba la cuantificación de los azúcares reductores y la distribución de tamaños de las partículas obtenidas. Alternativamente, que el tratamiento con SamC, seguido de la digestión con celulasas, genere BCNC de mayor tamaño, podría explicarse, según investigaciones recientes, porque la oxidación en C1 impediría el posterior acomodamiento del centro activo de las celulasas (Keller *et al.*, 2021). En todo caso, la

generación de grupos carboxilo mediada por la acción oxidativa de la LPMO promueve la repulsión electrostática entre los BCNC obtenidos, que resulta en una dispersión coloidal estable.

Todas las propiedades que estos BCNC exhibieron, junto a su elevada relación de aspecto longitud/ancho, indicaban su idoneidad como agentes reforzantes en otros materiales. Es por ello que se investigó su uso como agentes de recubrimiento sobre soportes de celulosa vegetal de eucalipto, aportándoles diferentes propiedades. De hecho, en el grupo ya se había comprobado con anterioridad que la adición de CB sobre soportes de origen vegetal aporta propiedades hidrofóbicas. Por otro lado, atendiendo a que con la simple disrupción mecánica de la CB se obtiene mucha heterogeneidad de fibras, este es un proceso de difícil estandarización (Choi and Shin, 2020). Por esa razón la transformación de la pasta de CB en nanocristales es una forma de facilitar este proceso, además de permitir un abanico más amplio de aplicaciones. Con un porcentaje relativamente bajo de recubrimiento de BCNC, los nuevos biomateriales obtenidos resultaron ser impermeables al agua, al retener las gotas de agua por más de 12 minutos. Estos soportes también resultaron ser impermeables al paso de las grasas y poseían mejores propiedades mecánicas. Todas estas nuevas características que aportan los BCNC sobre otros soportes poliméricos preexistentes podrían conducir a la generación de nuevos biomateriales de alto rendimiento que podrían reemplazar productos basados en combustibles fósiles. Además de su faceta como material de recubrimiento, estos BCNC también podrían actuar como portadores de otros componentes activos, como enzimas, ya que en función de los trabajos presentados previamente en esta tesis, ha quedado patente que la CB es una excelente matriz para la inmovilización de proteínas.

6. CONCLUSIONES

6. Conclusiones

- Se han obtenido las variantes enzimáticas E27A, G136A, M139Q, DM y TM a partir de la proteína LipJ mediante mutagénesis dirigida que presentan mayor especificidad para sustratos de cadena media y larga respecto a la proteína original.
- La variante H110N de la librería NNK muestra un cambio en la especificidad de sustrato. La falta de activación interfacial sugiere que la estructura de la *lid* de LipJ es la responsable de su comportamiento mesófilo.
- No se ha conseguido una variante termófila a pesar de haber analizado todos los factores que pueden influir en el comportamiento termófilo.
- *Escherichia coli* tiene una esterasa de 18 kDa aproximadamente, con una temperatura óptima de 50 ºC y un pH óptimo de 8, con un perfil cinético de Michaelis-Menten.
- Esta esterasa es termófila, pero presenta una baja estabilidad a temperaturas superiores a la óptima. Los iones Al^{3+}, Cu^{2+}, Fe^{2+}, Hg^{2+} y Zn^{2+} inhiben significativamente la actividad de esta enzima.
- Las matrices de celulosa bacteriana son un soporte adecuado para la inmovilización de enzimas por adsorción física.
- La lipasa Callera^{TM} Trans L fue inmovilizada en el papel de celulosa bacteriana (BCP) y en la suspensión acuosa de fibras de celulosa bacteriana (BCS) por adsorción física, reteniendo en ambas su actividad enzimática.
- En comparación a la lipasa libre, la lipasa inmovilizada sobre BCP amplió el rango de actuación de temperaturas y de pH, y presentó una estabilidad térmica más elevada.
- El nanocomposite Lipasa/BCP no presentó migración de la enzima, conservó la actividad enzimática por más de treinta días sin alterarse su estabilidad, y pudo reutilizarse hasta en diez ciclos.
- Es la primera vez que se ha descrito en la literatura la inmovilización de una enzima sobre papel compuesto íntegramente de celulosa bacteriana.
- Mediante la inmovilización de la enzima lisozima sobre el papel de celulosa bacteriana por adsorción física, se generó otro papel bioactivo, llamado Lys-BCP, descrito por primera vez en la literatura.
- La inmovilización no tuvo un efecto drástico ni en la actividad específica de la lisozima ni en la morfología ni la cristalinidad del soporte de CB.
- La lisozima inmovilizada presentó un rango de actuación de temperaturas más amplio que la enzima libre, mostrando una estabilidad más elevada que la lisozima libre.

- Lys-BCP exhibió actividad antimicrobiana contra bacterias grampositivas como *Staphylococcus aureus* y gramnegativas como *E.coli* con un 82 y un 72 %, respectivamente.
- La actividad antioxidante inherente de la CB no se vio disminuida, sino que al contrario, se ve ligeramente incrementada en un 30 %.
- Se han obtenido nanocristales de celulosa bacteriana mediante una hidrólisis exclusivamente enzimática. Estos nanocristales tienen un tamaño promedio de 700 nm de longitud y 9 nm de ancho. La elevada relación de aspecto longitud/ancho indicó que estos BCNC poseían una elevada área superficial. Adicionalmente, los BCNC mostraron una estabilidad térmica más elevada que la celulosa bacteriana nativa.
- Es el primer estudio en que se reporta el empleo de las enzimas LPMO en la obtención de nanocristales. Su acción conjunta genera unos BCNC con un tamaño ligeramente superior a los obtenidos únicamente con las celulasas.
- La oxidación de la CB por parte de SamC, previa digestión de las celulasas, genera cargas negativas en su superficie, que conducen a una buena dispersión en solución acuosa de los BCNC.
- El recubrimiento de soportes de celulosa de eucalipto con un 5 % de BCNC les aportó impermeabilidad al agua y a las grasas, además de unas propiedades mecánicas mejoradas.

7. REFERENCIAS BIBLIOGRÁFICAS

7. Referencias bibliográficas

Abral, H. *et al.* (2018) 'Preparation of nano-sized particles from bacterial cellulose using ultrasonication and their characterization', *Carbohydrate Polymers*, 191, pp. 161–167. doi: 10.1016/j.carbpol.2018.03.026.

Akoh, C. C. *et al.* (2004) 'GDSL family of serine esterases/lipases', *Progress in Lipid Research*, 43(6), pp. 534–552. doi: 10.1016/j.plipres.2004.09.002.

Angajala, G., Pavan, P. and Subashini, R. (2016) 'Lipases: An overview of its current challenges and prospectives in the revolution of biocatalysis', *Biocatalysis and Agricultural Biotechnology*, 7, pp. 257–270. doi: 10.1016/j.bcab.2016.07.001.

Antranikian, G., Bornscheuer, U. T. and Liese, A. (2010) 'Highlights in Biocatalysis', *ChemCatChem*, 2(8), pp. 879–880. doi: 10.1002/cctc.201000228.

Aravindan, R., Anbumathi, P. and Viruthagiri, T. (2007) 'Lipase applications in food industry', *Indian Journal of Biotechnology*.

Arca-Ramos, A. *et al.* (2016) 'Assessing the use of nanoimmobilized laccases to remove micropollutants from wastewater', *Environmental Science and Pollution Research*, 23(4), pp. 3217–3228. doi: 10.1007/s11356-015-5564-6.

Arpigny, J. L. and Jaeger, K. E. (1999) 'Bacterial lipolytic enzymes: Classification and properties', *Biochemical Journal*, 343(1), pp. 177–183. doi: 10.1042/0264-6021:3430177.

Asoodeh, A., Emtenani, Shirin and Emtenani, Shamsi (2014) 'Expression and Biochemical Characterization of a Thermophilic Organic Solvent-Tolerant Lipase from Bacillus sp. DR90', *Protein Journal*, 33(5), pp. 410–421. doi: 10.1007/s10930-014-9574-x.

Azeredo, H. M. C., Rosa, M. F. and Mattoso, L. H. C. (2017) 'Nanocellulose in bio-based food packaging applications', *Industrial Crops and Products*, 97, pp. 664–671. doi: 10.1016/j.indcrop.2016.03.013.

Bai, W., Holbery, J. and Li, K. (2009) 'A technique for production of nanocrystalline cellulose with a narrow size distribution', *Cellulose*, 16(3), pp. 455–465. doi: 10.1007/s10570-009-9277-1.

Bajpai, V. K. *et al.* (2018) 'Prospects of using nanotechnology for food preservation, safety, and security', *Journal of Food and Drug Analysis*, 26(4), pp. 1201–1214. doi: 10.1016/j.jfda.2018.06.011.

Balea, A. *et al.* (2018) 'Cellulose nanofibers from residues to improve linting and mechanical properties of recycled paper', *Cellulose*, 25(2), pp. 1339–1351. doi: 10.1007/s10570-017-1618-x.

Balea, A. *et al.* (2020) 'Industrial application of nanocelluloses in papermaking: A review of challenges, technical solutions, and market perspectives', *Molecules*, 25(3), p. 526. doi: 10.3390/molecules25030526.

Bassegoda, A. *et al.* (2010) 'Rational Protein Design of Paenibacillus barcinonensis Esterase EstA for Kinetic Resolution of Tertiary Alcohols', *ChemCatChem*, 2(8), pp. 962–967.

Bassegoda, A. *et al.* (2013) 'Special Rhodococcus sp. CR-53 esterase Est4 contains a GGG(A)X-oxyanion hole conferring activity for the kinetic resolution of tertiary alcohols', *Applied Microbiology and Biotechnology*, 97(19), pp. 8559–8568. doi: 10.1007/s00253-012-4676-x.

Bassegoda, A., Cesarini, S. and Diaz, P. (2012) 'Lipase improvement: goals and strategies', *Computational and Structural Biotechnology Journal*, 2(3), pp. 1–8. doi: 10.5936/csbj.201209005.

Bassegoda, Arnau, Pastor, F. I. J. and Diaz, P. (2012) 'Rhodococcus sp. strain CR-53 lipr, the first member of a new bacterial lipase family (Family X) displaying an unusual Y-type oxyanion hole, similar to the Candida antarctica lipase clan', *Applied and Environmental Microbiology*, 78(6), pp. 1724–1732. doi: 10.1128/AEM.06332-11.

Bassegoda, A, Pastor, F. I. J. and Diaz, P. (2012) '*Rhodococcus* sp. strain CR-53 lipR, the first member of a new bacterial lipase family (Family X) displaying an unusual Y-type oxyanion hole, similar to the Candida antarctica lipase clan', *Applied and Environmental Microbiology*, 78(6), pp. 1724–1732.

Bayazidi, P., Almasi, H. and Asl, A. K. (2018) 'Immobilization of lysozyme on bacterial cellulose nanofibers: Characteristics, antimicrobial activity and morphological properties', *International Journal of*

Biological Macromolecules, 107, pp. 2544–2551. doi: 10.1016/j.ijbiomac.2017.10.137.

Belbekhouche, S. *et al.* (2011) 'Water sorption behavior and gas barrier properties of cellulose whiskers and microfibrils films', *Carbohydrate Polymers*, 4(83), pp. 1740–1748. doi: 10.1016/j.carbpol.2010.10.036.

Bianchet, R. T. *et al.* (2020) 'Applicability of bacterial cellulose in cosmetics – bibliometric review', *Biotechnology Reports*, 27, p. e00502. doi: 10.1016/j.btre.2020.e00502.

Bielecki, S. *et al.* (2005) 'Bacterial Cellulose', in Vandamme, E. J., De Baets, S., and Steinbüchel, A. (eds) *Biopolymers Online*. Weinheim, Germany: Wiley-VCH Verlag GmbH & Co. KGaA. doi: 10.1002/3527600035.bpol5003.

Biundo, A. *et al.* (2016) 'Characterization of a poly(butylene adipate-co-terephthalate)-hydrolyzing lipase from Pelosinus fermentans', *Applied Microbiology and Biotechnology*, 100(4), pp. 1753–1764. doi: 10.1007/s00253-015-7031-1.

Biundo, A. *et al.* (2017) 'Engineering of the zinc-binding domain of an esterase from Clostridium botulinum towards increased activity on polyesters', *Catalysis Science & Technology*, 7(6), pp. 1440–1447. doi: 10.1039/C7CY00168A.

Biundo, A. *et al.* (2018) 'Synergistic effect of mutagenesis and truncation to improve a polyesterase from Clostridium botulinum for polyester hydrolysis', *Scientific Reports*, 8(1), pp. 1–7. doi: 10.1038/s41598-018-21825-9.

Blanco Parte, F. G. *et al.* (2020) 'Current progress on the production, modification, and applications of bacterial cellulose', *Critical Reviews in Biotechnology*, 40(3), pp. 397–414. doi: 10.1080/07388551.2020.1713721.

Bofill, C. *et al.* (2010) 'Differential behaviour of *Pseudomonas* sp. 42A2 LipC, a lipase showing greater versatility than its counterpart LipA.', *Biochimie*, 92(3), pp. 307–316.

Bornscheuer, U. T. (2002) 'Microbial carboxyl esterases: classification, properties and application in biocatalysis', *FEMS microbiology reviews*, 26(1), pp. 73–81. doi: 10.1111/j.1574-6976.2002.tb00599.x.

Bornscheuer, U. T. *et al.* (2002) 'Optimizing lipases and related enzymes for efficient application', *Trends in Biotechnology*, 20(10), pp. 433–437.

Bornscheuer, U. T. and Kazlauskas, R. J. (2006) *Hydrolases in organic synthesis: regio- and stereoselective biotransformations*. Wiley-VCH.

Branen, J. K. and Davidson, P. M. (2004) 'Enhancement of nisin, lysozyme, and monolaurin antimicrobial activities by ethylenediaminetetraacetic acid and lactoferrin', *International Journal of Food Microbiology*, 90(1), pp. 63–74. doi: 10.1016/S0168-1605(03)00172-7.

Brinchi, L. *et al.* (2013) 'Production of nanocrystalline cellulose from lignocellulosic biomass: Technology and applications', *Carbohydrate Polymers*, 94(1), pp. 154–169. doi: 10.1016/j.carbpol.2013.01.033.

Brown, A. J. (1886) 'XLIII. - On an acetic ferment which forms cellulose', *Journal of the Chemical Society, Transactions*, pp. 432–439. doi: 10.1039/CT8864900432.

Cabañas-Romero, L. V. *et al.* (2020) 'Bacterial Cellulose–Chitosan Paper with Antimicrobial and Antioxidant Activities', *Biomacromolecules*, 21(4), pp. 1568–1577. doi: 10.1021/acs.biomac.0c00127.

CAGRI, A., USTUNOL, Z. and RYSER, E. T. (2004) 'Antimicrobial Edible Films and Coatings', *Journal of Food Protection*, 67(4), pp. 833–848. doi: 10.4315/0362-028X-67.4.833.

Çakar, F. *et al.* (2014) 'Improvement production of bacterial cellulose by semi-continuous process in molasses medium', *Carbohydrate Polymers*, 106(1), pp. 7–13. doi: 10.1016/j.carbpol.2014.01.103.

Campano, C. *et al.* (2019) 'Hairy cationic nanocrystalline cellulose as retention additive in recycled paper', *Cellulose*, 26(10), pp. 6275–6289. doi: 10.1007/s10570-019-02494-x.

Cantarel, B. I. *et al.* (2009) 'The Carbohydrate-Active EnZymes database (CAZy): An expert resource for glycogenomics', *Nucleic Acids Research*, 37(SUPPL. 1). doi: 10.1093/nar/gkn663.

Cao, L., van Langen, L. and Sheldon, R. A. (2003) 'Immobilised enzymes: Carrier-bound or carrier-free?', *Current Opinion in Biotechnology*, 14(4), pp. 387–394. doi: 10.1016/S0958-1669(03)00096-X.

Carrasco-López, C. *et al.* (2009) 'Activation of bacterial thermoalkalophilic lipases is spurred by dramatic structural rearrangements.', *The Journal of biological chemistry*, 284(7), pp. 4365–72. doi: 10.1074/jbc.M808268200.

Carreño Pineda, L. D. (2011) 'Efecto de las condiciones de cultivo y purificación sobre las propiedades fisicoquímicas y de transporte en membranas de celulosa bacteriana', p. 138. Available at: http://www.bdigital.unal.edu.co/4303/ (Accessed: 12 August 2021).

Casas, C. *et al.* (2018) 'Development of Nanocomposites with Self-Cleaning', *Journal of the Society of Leather Technologies and Chemists*, 102, pp. 33–41.

Castilla, A. *et al.* (2017) 'A novel thermophilic and halophilic esterase from Janibacter sp. R02, the first member of a new lipase family (Family XVII)', *Enzyme and Microbial Technology*, 98, pp. 86–95. doi: 10.1016/j.enzmictec.2016.12.010.

Castro-Ochoa, L. D. *et al.* (2005) 'Screening, purification and characterization of the thermoalkalophilic lipase produced by Bacillus thermoleovorans CCR11', *Enzyme and Microbial Technology*, 37(6), pp. 648–654. doi: 10.1016/j.enzmictec.2005.06.003.

Castro, C. *et al.* (2011) 'Structural characterization of bacterial cellulose produced by Gluconacetobacter swingsii sp. from Colombian agroindustrial wastes', *Carbohydrate Polymers*, 84(1), pp. 96–102. doi: 10.1016/j.carbpol.2010.10.072.

Castro, C. *et al.* (2014) 'In situ production of nanocomposites of poly(vinyl alcohol) and cellulose nanofibrils from Gluconacetobacter bacteria: Effect of chemical crosslinking', *Cellulose*, 21(3), pp. 1745–1756. doi: 10.1007/s10570-014-0170-1.

Cesarini, S. *et al.* (2012) 'A thermostable variant of P. aeruginosa cold-adapted LipC obtained by rational design and saturation mutagenesis', *Process Biochemistry*, 47(12), pp. 2064–2071. doi: 10.1016/j.procbio.2012.07.023.

Chang, T. M. S. (1976) 'Biodegradable Semipermeable Microcapsules Containing Enzymes, Hormones, Vaccines, and Other Biologicals.', *J Bioeng*, 1(1), pp. 25–32. Available at: https://europepmc-org.sire.ub.edu/article/med/1052520 (Accessed: 9 August 2021).

Charreau, H., L. Foresti, M. and Vazquez, A. (2012) 'Nanocellulose Patents Trends: A Comprehensive Review on Patents on Cellulose Nanocrystals, Microfibrillated and Bacterial Cellulose', *Recent Patents on Nanotechnology*, 7(1), pp. 56–80. doi: 10.2174/187221013804484854.

Chawla, P. R. *et al.* (2009) 'Microbial cellulose: Fermentative production and applications', *Food Technology and Biotechnology*, 47(2), pp. 107–124.

Chen, L., Zou, M. and Hong, F. F. (2015) 'Evaluation of Fungal Laccase Immobilized on Natural Nanostructured Bacterial Cellulose', *Frontiers in Microbiology*, 6. doi: 10.3389/fmicb.2015.01245.

Cherry, J. R. and Fidantsef, A. L. (2003) 'Directed evolution of industrial enzymes: An update', *Current Opinion in Biotechnology*, 14(4), pp. 438–443. doi: 10.1016/S0958-1669(03)00099-5.

Chiu, E. *et al.* (2015) 'Structural basis for the enhancement of virulence by viral spindles and their in vivo crystallization', *Proceedings of the National Academy of Sciences of the United States of America*, 112(13), pp. 3973–3978. doi: 10.1073/pnas.1418798112.

Choi, M. M. F. (2004) 'Progress in Enzyme-Based Biosensors Using Optical Transducers', *Microchimica Acta*, 148(3–4), pp. 107–132. doi: 10.1007/s00604-004-0273-8.

Choi, S. M. and Shin, E. J. (2020) 'The nanofication and functionalization of bacterial cellulose and its applications', *Nanomaterials*, 10(3). doi: 10.3390/nano10030406.

Choi, W.-C. *et al.* (2005) 'Zinc in lipase L1 from Geobacillus stearothermophilus L1 and structural implications on thermal stability', *FEBS Letters*, 579(16), pp. 3461–3466. doi: 10.1016/j.febslet.2005.05.016.

Ciechańska, D. (2004) 'Multifunctional bacterial cellulose/chitosan composite materials for medical

applications', *Fibres and Textiles in Eastern Europe*, 12(4), pp. 69–72.

Coradi, M. *et al.* (2018) 'Production of antimicrobial textiles by cotton fabric functionalization and pectinolytic enzyme immobilization', *Materials Chemistry and Physics*, 208, pp. 28–34. doi: 10.1016/j.matchemphys.2018.01.019.

Coulet, P. R. and Gautheron, D. C. (1981) 'Enzymes immobilized on collagen membranes: A tool for fundamental research and enzyme engineering', *Journal of Chromatography A*, 215(C), pp. 65–72. doi: 10.1016/S0021-9673(00)81386-2.

Credou, J. and Berthelot, T. (2014) 'Cellulose: from biocompatible to bioactive material', *J. Mater. Chem. B*, 2(30), pp. 4767–4788. doi: 10.1039/c4tb00431k.

Cui, S. *et al.* (2016) 'Green preparation and characterization of size-controlled nanocrystalline cellulose via ultrasonic-assisted enzymatic hydrolysis', *Industrial Crops and Products*, 83, pp. 346–352. doi: 10.1016/j.indcrop.2016.01.019.

Dahman, Y. (2009) 'Nanostructured biomaterials and biocomposites from bacterial Cellulose nanofibers', *Journal of Nanoscience and Nanotechnology*, pp. 5105–5122. doi: 10.1166/jnn.2009.1466.

Dartois, V. *et al.* (1992) 'Cloning, nucleotide sequence and expression in Escherichia coli of a lipase gene from Bacillus subtilis 168', *BBA - Gene Structure and Expression*, 1131(3), pp. 253–260. doi: 10.1016/0167-4781(92)90023-S.

Dasgupta, N. *et al.* (2015) 'Nanotechnology in agro-food: From field to plate', *Food Research International*, 69, pp. 381–400. doi: 10.1016/j.foodres.2015.01.005.

Dogan, N. and McHugh, T. H. (2007) 'Effects of microcrystalline cellulose on functional properties of hydroxy propyl methyl cellulose microcomposite films', *Journal of Food Science*, 72(1), pp. E016–E022. doi: 10.1111/j.1750-3841.2006.00237.x.

Domínguez-Ramírez, L. and Tuena de Gómez-Puyou, M. (2005) 'Tip Revista Especializada en Ciencias', *Tip Revista Especializada en Ciencias Químico-Biológicas TIP Rev.Esp.Cienc.Quím.Biol*, 8(1), pp. 18–27. Available at: http://www.redalyc.org/articulo.oa?id=43211941004 (Accessed: 5 August 2021).

Domínguez, G. *et al.* (2021) 'Eco-Friendly Oleogels from Functionalized Kraft Lignin with Laccase SilA from Streptomyces ipomoeae: An Opportunity to Replace Commercial Lubricants', *ACS Sustainable Chemistry and Engineering*, 9(12), pp. 4611–4616. doi: 10.1021/acssuschemeng.1c00113.

Drepper, T. *et al.* (2006) 'Novel biocatalysts for white biotechnology', *Biotechnology Journal*, 1, pp. 777–786.

Dufresne, A. (2012) *Nanocellulose*, *Nanocellulose*. De gruyter. doi: 10.1515/9783110254600.

E, K. *et al.* (2005) 'Enzyme genomics: Application of general enzymatic screens to discover new enzymes', *FEMS microbiology reviews*, 29(2), pp. 263–279. doi: 10.1016/j.femsre.2004.12.006.

Eibinger, M. *et al.* (2017) 'Single-molecule study of oxidative enzymatic deconstruction of cellulose', *Nature Communications*, 8(1), pp. 1–7. doi: 10.1038/s41467-017-01028-y.

Elazzouzi-Hafraoui, S. *et al.* (no date) 'The Shape and Size Distribution of Crystalline Nanoparticles Prepared by Acid Hydrolysis of Native Cellulose'. doi: 10.1021/bm700769p.

Estevinho, B. N. *et al.* (2014) 'Microencapsulation of β-galactosidase with different biopolymers by a spray-drying process', *Food Research International*, 64, pp. 134–140. doi: 10.1016/j.foodres.2014.05.057.

Falcocchio, S. *et al.* (2005) 'Identification of a carboxylesterase-producing Rhodococcus soil isolate', *Canadian Journal of Microbiology*, 51(9), pp. 753–758.

Fang, Y. *et al.* (2011) 'Polymer materials for enzyme immobilization and their application in bioreactors', *BMB Reports*, 44(2), pp. 87–95. doi: 10.5483/bmbrep.2011.44.2.87.

Fernandes, I. de A. A. *et al.* (2020) 'Bacterial cellulose: From production optimization to new applications', *International Journal of Biological Macromolecules*, 164, pp. 2598–2611. doi: 10.1016/j.ijbiomac.2020.07.255.

Fernández, J. *et al.* (2019) 'Microbial Cellulose from a Komagataeibacter intermedius Strain Isolated from Commercial Wine Vinegar', *Journal of Polymers and the Environment*, 27(5), pp. 956–967. doi: 10.1007/s10924-019-01403-4.

Ferrer, M. *et al.* (2015) 'Biodiversity for biocatalysis: A review of the α/β-hydrolase fold superfamily of esterases-lipases discovered in metagenomes', *Biocatalysis and Biotransformation*, 33(5–6), pp. 235–249. doi: 10.3109/10242422.2016.1151416.

Fillat, A. *et al.* (2014) 'Improving enantioselectivity towards tertiary alcohols using mutants of *Bacillus* sp. BP-7 esterase EstBP7 holding a rare GGG(X)-oxyanion hole', *Applied Microbiology and Biotechnology*, 98, pp. 4479–4490.

Fillat, A. *et al.* (2015) 'Kinetic resolution of esters from secondary and tertiary benzylic propargylic alcohols by an improved esterase-variant from Bacillus sp. BP-7', *Catalysis Today*, 255, pp. 16–20.

Forsberg, Z. *et al.* (2014) 'Comparative study of two chitin-active and two cellulose-active AA10-type lytic polysaccharide monooxygenases.', *Biochemistry*, 53(10), pp. 1647–1656. doi: 10.1021/BI5000433.

Forsberg, Z. *et al.* (2014) 'Structural and functional characterization of a conserved pair of bacterial cellulose-oxidizing lytic polysaccharide monooxygenases', *Proceedings of the National Academy of Sciences of the United States of America*, 111(23), pp. 8446–8451. doi: 10.1073/pnas.1402771111.

Forsberg, Z. *et al.* (2019) 'Polysaccharide degradation by lytic polysaccharide monooxygenases', *Current Opinion in Structural Biology*. Elsevier Ltd, pp. 54–64. doi: 10.1016/j.sbi.2019.02.015.

Frazão, C. J. R. *et al.* (2014) 'Bacterial cellulose as carrier for immobilization of laccase: Optimization and characterization', *Engineering in Life Sciences*, 14(5), pp. 500–508. doi: 10.1002/elsc.201400054.

Fu, L., Zhang, J. and Yang, G. (2013) 'Present status and applications of bacterial cellulose-based materials for skin tissue repair', *Carbohydrate Polymers*, 92(2), pp. 1432–1442. doi: 10.1016/j.carbpol.2012.10.071.

Gama, F. M., Gatenholm, P. and Klemm, D. (2016) *Bacterial nanocellulose: A sophisticated multifunctional material*, *Bacterial NanoCellulose: A Sophisticated Multifunctional Material*.

Gao, C. *et al.* (2012) 'Immobilization of gelatin onto natural nanofibers for tissue engineering scaffold applications without utilization of any crosslinking agent', *Cellulose*, 19(3), pp. 761–768. doi: 10.1007/s10570-012-9698-0.

George, J. *et al.* (2011) 'Bacterial cellulose nanocrystals exhibiting high thermal stability and their polymer nanocomposites', *International Journal of Biological Macromolecules*, 48(1), pp. 50–57. doi: 10.1016/j.ijbiomac.2010.09.013.

George, J. and Sabapathi, S. N. (2015) 'Cellulose nanocrystals: Synthesis, functional properties, and applications', *Nanotechnology, Science and Applications*, 8, pp. 45–54. doi: 10.2147/NSA.S64386.

GILL, A. O. and HOLLEY, R. A. (2000) 'Surface Application of Lysozyme, Nisin, and EDTA to Inhibit Spoilage and Pathogenic Bacteria on Ham and Bologna', *Journal of Food Protection*, 63(10), pp. 1338–1346. doi: 10.4315/0362-028X-63.10.1338.

Gill, C. O. (2003) 'Active packaging in practice: Meat', in *Novel Food Packaging Techniques*. doi: 10.1016/B978-1-85573-675-7.50021-3.

Guerra, N. P. *et al.* (2005) 'Development of a bioactive packaging cellophane using NisaplinR as biopreservative agent', *Letters in Applied Microbiology*, 40(2), pp. 106–110. doi: 10.1111/j.1472-765X.2004.01649.x.

Gullo, M. *et al.* (2006) 'Characterization of acetic acid bacteria in "traditional balsamic vinegar"', *International Journal of Food Microbiology*, 106(2), pp. 209–212. doi: 10.1016/j.ijfoodmicro.2005.06.024.

Guncheva, M. and Zhiryakova, D. (2011) 'Catalytic properties and potential applications of Bacillus lipases', *Journal of Molecular Catalysis B: Enzymatic*, 68(1), pp. 1–21. doi: 10.1016/j.molcatb.2010.09.002.

Gupta, M. N. *et al.* (2011) 'Nanomaterials as matrices for enzyme immobilization', *Artificial Cells, Blood Substitutes, and Biotechnology*, 39(2), pp. 98–109. doi: 10.3109/10731199.2010.516259.

Gupta, R. *et al.* (2015) 'Molecular and functional diversity of yeast and fungal lipases: Their role in biotechnology and cellular physiology', *Progress in Lipid Research*, 57, pp. 40–54. doi: 10.1016/j.plipres.2014.12.001.

Gupta, R., Gupta, N. and Rathi, P. (2004) 'Bacterial lipases: an overview of production, purification and biochemical properties', *Applied Microbiology and Biotechnology*, 64(6), pp. 763–781.

Habibi, Y., Chanzy, H. and Vignon, M. R. (2006) 'TEMPO-mediated surface oxidation of cellulose whiskers', *Cellulose*, 13(6), pp. 679–687. doi: 10.1007/s10570-006-9075-y.

Hanušová, K. *et al.* (2013) 'Development of antimicrobial packaging materials with immobilized glucose oxidase and lysozyme', *Open Chemistry*, 11(7). doi: 10.2478/s11532-013-0241-4.

He, X. *et al.* (2020) 'Novel bacterial cellulose membrane biosynthesized by a new and highly efficient producer Komagataeibacter rhaeticus TJPU03', *Carbohydrate Research*, 493, p. 108030. doi: 10.1016/j.carres.2020.108030.

Heichal-Segal, O., Rappoport, S. and Braun, S. (1995) 'Immobilization in alginate-silicate sol-gel matrix protects β-Glucosidase against thermal and chemical denaturation', *Bio/Technology*, 13(8), pp. 798–800. doi: 10.1038/nbt0895-798.

Hernandez, K. and Fernandez-Lafuente, R. (2011) 'Control of protein immobilization: Coupling immobilization and site-directed mutagenesis to improve biocatalyst or biosensor performance', *Enzyme and Microbial Technology*, 48(2), pp. 107–122. doi: 10.1016/j.enzmictec.2010.10.003.

Hestrin, S. and Schramm, M. (1954) 'Synthesis of cellulose by Acetobacter xylinum. II. Preparation of freeze-dried cells capable of polymerizing glucose to cellulose.', *The Biochemical journal*, 58(2), pp. 345–352. doi: 10.1042/bj0580345.

Holden, M. A., Jung, S. Y. and Cremer, P. S. (2004) 'Patterning Enzymes Inside Microfluidic Channels via Photoattachment Chemistry', *Analytical Chemistry*, 76(7), pp. 1838–1843. doi: 10.1021/ac035234q.

Horn, S. J. *et al.* (2012) 'Novel enzymes for the degradation of cellulose', *Biotechnology for Biofuels*. BioMed Central, p. 45. doi: 10.1186/1754-6834-5-45.

Hu, W. *et al.* (2014) 'Functionalized bacterial cellulose derivatives and nanocomposites', *Carbohydrate polymers*, 101(1), pp. 1043–1060. doi: 10.1016/j.carbpol.2013.09.102.

Huang, Y. *et al.* (2014) 'Recent advances in bacterial cellulose', *Cellulose*, 21(1), pp. 1–30. doi: 10.1007/s10570-013-0088-z.

Huber, D. L. *et al.* (2003) 'Programmed adsorption and release of proteins in a microfluidic device', *Science*, 301(5631), pp. 352–354. doi: 10.1126/science.1080759.

Ibrahim, C. O. (2008) 'Development of applications of industrial enzymes from Malaysian indigenous microbial sources', *Bioresource Technology*, 99(11), pp. 4572–4582. doi: 10.1016/j.biortech.2007.07.040.

Ibrahim, H. R., Thomas, U. and Pellegrini, A. (2001) 'A Helix-Loop-Helix Peptide at the Upper Lip of the Active Site Cleft of Lysozyme Confers Potent Antimicrobial Activity with Membrane Permeabilization Action', *Journal of Biological Chemistry*. doi: 10.1074/jbc.M106317200.

Infanzón, B. *et al.* (2014) 'Unusual carboxylesterase bearing a GGG(A)X-type oxyanion hole discovered in Paenibacillus barcinonensis BP-23', *Biochimie*, 104, pp. 108–116. doi: 10.1016/j.biochi.2014.06.003.

Ishihara, M. *et al.* (2002) 'Utilization of D-xylose as carbon source for production of bacterial cellulose', *Enzyme and Microbial Technology*, 31(7), pp. 986–991. doi: 10.1016/S0141-0229(02)00215-6.

Islam, S. U. *et al.* (2021) 'Potential applications of bacterial cellulose and its composites for cancer treatment', *International Journal of Biological Macromolecules*, 168, pp. 301–309. doi: 10.1016/j.ijbiomac.2020.12.042.

Jaeger, K.-E. and Eggert, T. (2002) 'Lipases for biotechnology.', *Current opinion in biotechnology*, 13(4), pp. 390–7. Available at: http://www.ncbi.nlm.nih.gov/pubmed/12323363.

Jaeger, K.-E. and Reetz, M. T. (1998) 'Microbial lipases form versatile tools for biotechnology', *Trends in biotechnology*, 16, pp. 396–403.

Jaeger, K. E., Dijkstra, B. W. and Reetz, M. T. (1999) 'Bacterial biocatalysts: Molecular biology, three-dimensional structures, and biotechnological applications of lipases', *Annual Review of Microbiology*, 53(1), p. 315. doi: 10.1146/annurev.micro.53.1.315.

Jayani, T. *et al.* (2020) 'Bacterial Cellulose Nano Fiber (BCNF) as carrier support for the immobilization of probiotic, Lactobacillus acidophilus 016', *Carbohydrate Polymers*, 250. doi: 10.1016/j.carbpol.2020.116965.

Jeong, S.-T. *et al.* (2002) 'Novel Zinc-binding Center and a Temperature Switch in theBacillus stearothermophilus L1 Lipase', *Journal of Biological Chemistry*, 277(19), pp. 17041–17047. doi: 10.1074/jbc.M200640200.

Jesionowski, T., Zdarta, J. and Krajewska, B. (2014) 'Enzyme immobilization by adsorption: A review', *Adsorption*, 20(5–6), pp. 801–821. doi: 10.1007/s10450-014-9623-y.

Johansen, K. S. (2016) 'Lytic Polysaccharide Monooxygenases: The Microbial Power Tool for Lignocellulose Degradation', *Trends in Plant Science*, 21(11), pp. 926–936. doi: 10.1016/j.tplants.2016.07.012.

Jonas, R. and Farah, L. F. (1998) 'Production and application of microbial cellulose', *Polymer Degradation and Stability*, 59(1–3), pp. 101–106. doi: 10.1016/S0141-3910(97)00197-3.

Joshi, S. and Satyanarayana, T. (2015) 'In vitro engineering of microbial enzymes with multifarious applications: Prospects and perspectives', *Bioresource Technology*, pp. 273–283. doi: 10.1016/j.biortech.2014.10.151.

Kadokawa, J. (2012) 'Preparation and Applications of Amylose Supramolecules by Means of Phosphorylase-Catalyzed Enzymatic Polymerization', *Polymers*, 4(1), pp. 116–133. doi: 10.3390/polym4010116.

Kalashnikova, I. *et al.* (2012) 'Modulation of cellulose nanocrystals amphiphilic properties to stabilize oil/water interface', *Biomacromolecules*, 13(1), pp. 267–275. doi: 10.1021/bm201599j.

Kalia, S. *et al.* (2011) 'Cellulose-based bio- and nanocomposites: A review', *International Journal of Polymer Science*, 2011. doi: 10.1155/2011/837875.

Kalia, S. and Avérous, L. (2011) 'Biopolymers: Biomedical and Environmental Applications', *Biopolymers: Biomedical and Environmental Applications*, p. 614. doi: 10.1002/9781118164792.

Kapoor, M. and Gupta, M. N. (2012) 'Lipase promiscuity and its biochemical applications', *Process Biochemistry*, 47(4), pp. 555–569. doi: 10.1016/j.procbio.2012.01.011.

Karaki, N. *et al.* (2016) 'Enzymatic modification of polysaccharides: Mechanisms, properties, and potential applications: A review', *Enzyme and Microbial Technology*, 90, pp. 1–18. doi: 10.1016/j.enzmictec.2016.04.004.

Karim, Z. *et al.* (2017) 'Necessity of enzymatic hydrolysis for production and functionalization of nanocelluloses', *Critical Reviews in Biotechnology*. Taylor and Francis Ltd, pp. 355–370. doi: 10.3109/07388551.2016.1163322.

Karkehabadi, S. *et al.* (2008) 'The First Structure of a Glycoside Hydrolase Family 61 Member, Cel61B from Hypocrea jecorina, at 1.6 Å Resolution', *Journal of Molecular Biology*, 383(1), pp. 144–154. doi: 10.1016/j.jmb.2008.08.016.

Keller, M. B. *et al.* (2021) 'A comparative biochemical investigation of the impeding effect of C1-oxidizing LPMOs on cellobiohydrolases', *Journal of Biological Chemistry*, 296. doi: 10.1016/j.jbc.2021.100504.

Keshk, S. M. (2014) 'Bacterial Cellulose Production and its Industrial Applications', *Journal of Bioprocessing & Biotechniques*, 04(02), pp. 150–160. doi: 10.4172/2155-9821.1000150.

Kim, D. and Herr, A. E. (2013) 'Protein immobilization techniques for microfluidic assays', *Biomicrofluidics*, 7(4), p. 041501. doi: 10.1063/1.4816934.

Kim, H. J. *et al.* (2015) 'Biocompatible cellulose nanocrystals as supports to immobilize lipase', *Journal of Molecular Catalysis B: Enzymatic*, 122, pp. 170–178. doi: 10.1016/j.molcatb.2015.09.007.

Kim, J. H. *et al.* (2015) 'Review of nanocellulose for sustainable future materials', *International Journal of Precision Engineering and Manufacturing - Green Technology*, 2(2), pp. 197–213. doi: 10.1007/s40684-015-0024-9.

Kingkaew, J. *et al.* (2014) 'Effect of molecular weight of chitosan on antimicrobial properties and tissue compatibility of chitosan-impregnated bacterial cellulose films', *Biotechnology and Bioprocess Engineering*, 19(3), pp. 534–544. doi: 10.1007/s12257-014-0081-x.

Klemm, D. *et al.* (2001) 'Bacterial synthesized cellulose - Artificial blood vessels for microsurgery', *Progress in Polymer Science (Oxford)*, 26(9), pp. 1561–1603. doi: 10.1016/S0079-6700(01)00021-1.

Klemm, D. *et al.* (2011) 'Nanocelluloses: A new family of nature-based materials', *Angewandte Chemie - International Edition*, pp. 5438–5466. doi: 10.1002/anie.201001273.

Kourist, R. *et al.* (2017) 'Editorial: Applied Microbiology for Chemical Syntheses', *Frontiers in Microbiology*, 8, p. 1931. doi: 10.3389/fmicb.2017.01931.

Kourkoutas, Y. *et al.* (2004) 'Immobilization technologies and support materials suitable in alcohol beverages production: A review', *Food Microbiology*, 21(4), pp. 377–397. doi: 10.1016/j.fm.2003.10.005.

Lam, E. *et al.* (2012) 'Applications of functionalized and nanoparticle-modified nanocrystalline cellulose', *Trends in Biotechnology*, 30(5), pp. 283–290. doi: 10.1016/j.tibtech.2012.02.001.

Lee, K.-Y. *et al.* (2014) 'More Than Meets the Eye in Bacterial Cellulose: Biosynthesis, Bioprocessing, and Applications in Advanced Fiber Composites', *Macromolecular Bioscience*, 14(1), pp. 10–32. doi: 10.1002/mabi.201300298.

Li, X. *et al.* (2012) 'Structural basis for substrate targeting and catalysis by fungal polysaccharide monooxygenases', *Structure*, 20(6), pp. 1051–1061. doi: 10.1016/j.str.2012.04.002.

Lin, N. and Dufresne, A. (2014) 'Nanocellulose in biomedicine: Current status and future prospect', *European Polymer Journal*, 59, pp. 302–325. doi: 10.1016/j.eurpolymj.2014.07.025.

Lin, S. P. *et al.* (2013) 'Biosynthesis, production and applications of bacterial cellulose', *Cellulose*, pp. 2191–2219. doi: 10.1007/s10570-013-9994-3.

Liu, Z. *et al.* (2008) 'Polysaccharides-based nanoparticles as drug delivery systems', *Advanced Drug Delivery Reviews*, 60(15), pp. 1650–1662. doi: 10.1016/j.addr.2008.09.001.

Lorenzo, J. M., Batlle, R. and Gómez, M. (2014) 'Extension of the shelf-life of foal meat with two antioxidant active packaging systems', *LWT - Food Science and Technology*, 59(1), pp. 181–188. doi: 10.1016/j.lwt.2014.04.061.

Lu, H. *et al.* (2013) 'Morphological, crystalline, thermal and physicochemical properties of cellulose nanocrystals obtained from sweet potato residue', *Food Research International*, 50(1), pp. 121–128. doi: 10.1016/j.foodres.2012.10.013.

M, C. *et al.* (2018) 'Lytic xylan oxidases from wood-decay fungi unlock biomass degradation', *Nature chemical biology*, 14(3), pp. 306–310. doi: 10.1038/nchembio.2558.

M, L. *et al.* (2009) 'Crystal structure and biochemical properties of a novel thermostable esterase containing an immunoglobulin-like domain', *Journal of molecular biology*, 385(3), pp. 949–962. doi: 10.1016/J.JMB.2008.10.075.

MacPherson, I. S. and Murphy, M. E. P. (2007) 'Type-2 copper-containing enzymes', *Cellular and Molecular Life Sciences*, 64(22), pp. 2887–2899. doi: 10.1007/s00018-007-7310-9.

Makki, F. and Durance, T. D. (1996) 'Thermal inactivation of lysozyme as influenced by pH, sucrose and sodium chloride and inactivation and preservative effect in beer', *Food Research International*, 29(7), pp. 635–645. doi: 10.1016/S0963-9969(96)00074-9.

Mangalassary, S. *et al.* (2008) 'Effect of combining nisin and/or lysozyme with in-package pasteurization for control of Listeria monocytogenes in ready-to-eat turkey bologna during refrigerated storage', *Food Microbiology*, 25(7), pp. 866–870. doi: 10.1016/j.fm.2008.05.002.

Maria, L. C. S. *et al.* (2010) 'Preparation and antibacterial activity of silver nanoparticles impregnated in

bacterial cellulose', *Polimeros*, 20(1), pp. 72–77. doi: 10.1590/S0104-14282010005000001.

Mariotti, M. P. *et al.* (2008) 'Hydrolysis of whey lactose by immobilized β-galactosidase', *Brazilian Archives of Biology and Technology*, 51(6), pp. 1233–1240. doi: 10.1590/S1516-89132008000600019.

Martínez-Sanz, M., Lopez-Rubio, A. and Lagaron, J. M. (2012) 'Optimization of the dispersion of unmodified bacterial cellulose nanowhiskers into polylactide via melt compounding to significantly enhance barrier and mechanical properties', *Biomacromolecules*, 13(11), pp. 3887–3899. doi: 10.1021/bm301430j.

Masomian, M. *et al.* (2016) 'Analysis of comparative sequence and genomic data to verify phylogenetic relationship and explore a new subfamily of bacterial lipases', *PLoS ONE*, 11(3), p. e0149851. doi: 10.1371/journal.pone.0149851.

Matthysse, A. G. *et al.* (2005) 'The effect of cellulose overproduction on binding and biofilm formation on roots by Agrobacterium tumefaciens', *Molecular Plant-Microbe Interactions*, 18(9), pp. 1002–1010. doi: 10.1094/MPMI-18-1002.

Mazhari Mousavi, S. M. *et al.* (2017) 'Cellulose nanofiber/carboxymethyl cellulose blends as an efficient coating to improve the structure and barrier properties of paperboard', *Cellulose*, 24(7), pp. 3001–3014. doi: 10.1007/s10570-017-1299-5.

Miao, C. and Hamad, W. Y. (2013) 'Cellulose reinforced polymer composites and nanocomposites: A critical review', *Cellulose*, 20(5), pp. 2221–2262. doi: 10.1007/s10570-013-0007-3.

Mirhosseini, H. *et al.* (2008) 'Effect of Arabic gum, xanthan gum and orange oil contents on ζ-potential, conductivity, stability, size index and pH of orange beverage emulsion', *Colloids and Surfaces A: Physicochemical and Engineering Aspects*, 315(1–3), pp. 47–56. doi: 10.1016/J.COLSURFA.2007.07.007.

Mohamad, N. R. *et al.* (2015) 'An overview of technologies for immobilization of enzymes and surface analysis techniques for immobilized enzymes', *Biotechnology & Biotechnological Equipment*, 29(2), pp. 205–220. doi: 10.1080/13102818.2015.1008192.

Molinero-Abad, B. *et al.* (2014) 'Malate quinone oxidoreductase biosensors based on tetrathiafulvalene and gold nanoparticles modified screen-printed carbon electrodes for malic acid determination in wine', *Sensors and Actuators B: Chemical*, 202, pp. 971–975. doi: 10.1016/j.snb.2014.06.057.

Monosik, R. *et al.* (2012) 'Application of Enzyme Biosensors in Analysis of Food and Beverages', *Food Analytical Methods*, 5(1), pp. 40–53. doi: 10.1007/s12161-011-9222-4.

Moon, R. J. *et al.* (2011) 'Cellulose nanomaterials review: Structure, properties and nanocomposites', *Chemical Society Reviews*, 40(7), pp. 3941–3994. doi: 10.1039/c0cs00108b.

Morena, A. G. *et al.* (2019) 'Laccase/TEMPO-mediated bacterial cellulose functionalization: production of paper-silver nanoparticles composite with antimicrobial activity', *Cellulose*. doi: 10.1007/s10570-019-02678-5.

Mörseburg, K. and Chinga-Carrasco, G. (2009) 'Assessing the combined benefits of clay and nanofibrillated cellulose in layered TMP-based sheets', *Cellulose*, 16(5), pp. 795–806. doi: 10.1007/s10570-009-9290-4.

Müller, C. M. O., Laurindo, J. B. and Yamashita, F. (2009) 'Effect of cellulose fibers addition on the mechanical properties and water vapor barrier of starch-based films', *Food Hydrocolloids*, 23(5), pp. 1328–1333. doi: 10.1016/j.foodhyd.2008.09.002.

Nantel, G. and Proulx, P. (1973) 'Lipase activity in E. coli', *Biochimica et Biophysica Acta (BBA) - Lipids and Lipid Metabolism*, 316(2), pp. 156–161. doi: 10.1016/0005-2760(73)90005-2.

Narancic, T. *et al.* (2015) 'Recent developments in biocatalysis beyond the laboratory', *Biotechnology Letters*, 37(5), pp. 943–954. doi: 10.1007/s10529-014-1762-4.

Nardini, M. *et al.* (2000) 'Crystal structure of Pseudomonas aeruginosa lipase in the open conformation. The prototype for family I.1 of bacterial lipases', *Journal of Biological Chemistry*, 275(40), pp. 31219–31225. doi: 10.1074/jbc.M003903200.

Nascimento, E. S. *et al.* (2021) 'All-cellulose nanocomposite films based on bacterial cellulose nanofibrils

and nanocrystals', *Food Packaging and Shelf Life*, 29, p. 100715. doi: 10.1016/j.fpsl.2021.100715.

Nelson, J. M. and Griffin, E. G. (1916) 'Adsorption of invertase.', *Journal of the American Chemical Society*, 38(5), pp. 1109–1115. doi: 10.1021/ja02262a018.

Nguyen, H. H. *et al.* (2019) 'Immobilized enzymes in biosensor applications', *Materials*, 12(1). doi: 10.3390/ma12010121.

Nielsen, L. J. *et al.* (2010) 'Dual fluorescent labelling of cellulose nanocrystals for pH sensing', *Chemical Communications*, 46(47), pp. 8929–8931. doi: 10.1039/c0cc03470c.

Nigam, V. K. and Shukla, P. (2015) 'Enzyme Based Biosensors for Detection of Environmental Pollutants-A Review', *Journal of Microbiology and Biotechnology*, 25(11), pp. 1773–1781. doi: 10.4014/jmb.1504.04010.

Nishi, Y. *et al.* (1990) 'The structure and mechanical properties of sheets prepared from bacterial cellulose - Part 2 Improvement of the mechanical properties of sheets and their applicability to diaphragms of electroacoustic transducers', *Journal of Materials Science*, 25(6), pp. 2997–3001. doi: 10.1007/BF00584917.

Nordblad, M. *et al.* (2014) 'Identification of critical parameters in liquid enzyme-catalyzed biodiesel production', *Biotechnology and Bioengineering*, 111(12), pp. 2446–2453. doi: 10.1002/bit.25305.

Nthangeni, M. B. *et al.* (2001) 'Over-expression and properties of a purified recombinant Bacillus licheniformis lipase: A comparative report on Bacillus lipases', *Enzyme and Microbial Technology*, 28(7–8), pp. 705–712. doi: 10.1016/S0141-0229(01)00316-7.

Ogunyewo, O. A. *et al.* (2020) 'Synergistic Action of a Lytic Polysaccharide Monooxygenase and a Cellobiohydrolase from Penicillium funiculosum in Cellulose Saccharification under High-Level Substrate Loading', *Applied and Environmental Microbiology*, 86(23), pp. 1–21. doi: 10.1128/AEM.01769-20.

Okamoto, T. *et al.* (1994) 'Cloning of the Acetobacter xylinum cellulase gene and its expression in Escherichia coli and Zymomonas mobilis', *Applied Microbiology and Biotechnology*, 42(4), pp. 563–568. doi: 10.1007/BF00173921.

Okano, H. *et al.* (2015) 'Structural and biochemical characterization of a metagenome-derived esterase with a long N-terminal extension', *Protein Science : A Publication of the Protein Society*, 24(1), p. 93. doi: 10.1002/PRO.2591.

Omadjela, O. *et al.* (2013) 'BcsA and BcsB form the catalytically active core of bacterial cellulose synthase sufficient for in vitro cellulose synthesis', *Proceedings of the National Academy of Sciences of the United States of America*, 110(44), pp. 17856–17861. doi: 10.1073/PNAS.1314063110.

Omagari, Y. *et al.* (2009) 'Chemoenzymatic Synthesis of Amylose-Grafted Cellulose', *Macromolecular Bioscience*, 9(5), pp. 450–455. doi: 10.1002/mabi.200800237.

Pacheco, J. L. C.- *et al.* (2004) 'Celulosa bacteriana en gluconacetobacter xylinum: biosíntesis y aplicaciones', *Tip Revista Especializada en Ciencias Químico-Biológicas*, 7(1), pp. 18–25. Available at: https://www.redalyc.org/articulo.oa?id=43270103 (Accessed: 5 August 2021).

Palaninathan, V. *et al.* (2014) 'Acetosulfation of bacterial cellulose: An unexplored promising incipient candidate for highly transparent thin film', *Materials Express*, 4(5), pp. 415–421. doi: 10.1166/mex.2014.1191.

Panaitescu, D. M. *et al.* (2016) 'Structural and morphological characterization of bacterial cellulose nano-reinforcements prepared by mechanical route', *Materials and Design*, 110, pp. 790–801. doi: 10.1016/j.matdes.2016.08.052.

Panesar, P. S., Kumari, S. and Panesar, R. (2010) 'Potential applications of immobilized β-galactosidase in food processing industries', *Enzyme Research*, 2010. doi: 10.4061/2010/473137.

Paspaliari, D. K. *et al.* (2015) 'Listeria monocytogenes has a functional chitinolytic system and an active lytic polysaccharide monooxygenase', *The FEBS Journal*, 282(5), pp. 921–936. doi: 10.1111/FEBS.13191.

Peng, B. L. *et al.* (2011) 'Chemistry and applications of nanocrystalline cellulose and its derivatives: A nanotechnology perspective', *Canadian Journal of Chemical Engineering*, 89(5), pp. 1191–1206. doi:

10.1002/cjce.20554.

Perumal, A. B. *et al.* (2018) 'Development of polyvinyl alcohol/chitosan bio-nanocomposite films reinforced with cellulose nanocrystals isolated from rice straw', *Applied Surface Science*, 449, pp. 591–602. doi: 10.1016/j.apsusc.2018.01.022.

Picart, P., De María, P. D. and Schallmey, A. (2015) 'From gene to biorefinery: Microbial β-etherases as promising biocatalysts for lignin valorization', *Frontiers in Microbiology*, 6(SEP), p. 916. doi: 10.3389/fmicb.2015.00916.

Pirich, C. L. *et al.* (2015) 'Bacterial cellulose nanocrystals: impact of the sulfate content on the interaction with xyloglucan', *Cellulose*, 22(3), pp. 1773–1787. doi: 10.1007/s10570-015-0626-y.

Pohanka, M. (2019) 'Biosensors and Bioassays Based on Lipases, Principles and Applications, a Review', *Molecules*, 24(3), p. 616. doi: 10.3390/molecules24030616.

Prim, N. (2002) *Aïllament, producció i caracterització d'enzims bacterians d'interès biotecnològic. Avaluació de les lipases EstA de Paenibacillus sp. BP-23, EstA1 de Bacillus sp. BP-7, i LipA de Bacillus subtilis, i de la descarboxilasa d'àcids fenòlics PadA de Bacillus*.

Prim, N. *et al.* (2005) 'Isolation of lipolytic microorganisms from subtropical soils. cloning, purification and characterization of a novel esterase from strain Pseudomonas sp CR-611', *Journal of Biotechnology*, 118, pp. S120–S120.

Prim, N. *et al.* (2006) 'Esterase EstA6 from Pseudomonas sp CR-611 is a novel member in the utmost conserved cluster of family VI bacterial lipolytic enzymes', *Biochimie*, 88(7), pp. 859–867. doi: 10.1016/j.biochi.2006.02.011.

Rahman, M. Z. A. *et al.* (2012) 'Unlocking the mystery behind the activation phenomenon of T1 lipase: A molecular dynamics simulations approach', *Protein Science*, 21(8), pp. 1210–1221. doi: 10.1002/pro.2108.

Rämänen, P. *et al.* (2012) 'The effect of drying method on the properties and nanoscale structure of cellulose whiskers', *Cellulose*, 19(3), pp. 901–912. doi: 10.1007/s10570-012-9695-3.

Ramani, D. and Sastry, T. P. (2014) 'Bacterial cellulose-reinforced hydroxyapatite functionalized graphene oxide: A potential osteoinductive composite', *Cellulose*, 21(5), pp. 3585–3595. doi: 10.1007/s10570-014-0313-4.

Rånby, B. G. (1951) 'III. Fibrous macromolecular systems. Cellulose and muscle. The colloidal properties of cellulose micelles', *Discussions of the Faraday Society*, 11(0), pp. 158–164. doi: 10.1039/DF9511100158.

Reese, E. T., Siu, R. G. H. and Levinson, H. S. (1950) 'The biological degradation of soluble cellulose derivatives and its relationship to the mechanism of cellulose hydrolysis', *Journal of Bacteriology*, 59(4), pp. 485–497. doi: 10.1128/JB.59.4.485-497.1950.

Reetz, M. T. (2013) 'Biocatalysis in Organic Chemistry and Biotechnology: Past, Present, and Future', *Journal of the American Chemical Society*, 135(34), pp. 12480–12496. doi: 10.1021/ja405051f.

Reid, M. S., Villalobos, M. and Cranston, E. D. (2017) 'Benchmarking Cellulose Nanocrystals: From the Laboratory to Industrial Production', *Langmuir*, 33(7), pp. 1583–1598. doi: 10.1021/acs.langmuir.6b03765.

Revol, J. F. *et al.* (1992) 'Helicoidal self-ordering of cellulose microfibrils in aqueous suspension', *International Journal of Biological Macromolecules*, 14(3), pp. 170–172. doi: 10.1016/S0141-8130(05)80008-X.

Ribera, J. *et al.* (2017) 'Bacillus sp. JR3 esterase LipJ: A new mesophilic enzyme showing traces of a thermophilic past', *PLOS ONE*. Edited by M. Oberer, 12(7), p. e0181029. doi: 10.1371/journal.pone.0181029.

Ro, H. S. *et al.* (2004) 'Genome-wide cloning and characterization of microbial esterases', *FEMS Microbiology Letters*, 233(1), pp. 97–105. doi: 10.1016/j.femsle.2004.01.046.

Rocchitta, G. *et al.* (2016) 'Enzyme Biosensors for Biomedical Applications: Strategies for Safeguarding Analytical Performances in Biological Fluids', *Sensors*, 16(6), p. 780. doi: 10.3390/s16060780.

Roman, M. *et al.* (2009) 'Cellulose nanocrystals for drug delivery', *ACS Symposium Series*, 1017, pp. 81–91. doi: 10.1021/bk-2009-1017.ch004.

Roman, M. and Winter, W. T. (2004) 'Effect of sulfate groups from sulfuric acid hydrolysis on the thermal degradation behavior of bacterial cellulose', *Biomacromolecules*, 5(5), pp. 1671–1677. doi: 10.1021/bm034519+.

Romero-Fernández, M. *et al.* (2018) 'Preparation of a robust immobilized biocatalyst of β-1,4-endoxylanase by surface coating with polymers for production of xylooligosaccharides from different xylan sources', *New Biotechnology*, 44, pp. 50–58. doi: 10.1016/j.nbt.2018.04.007.

Römling, U. and Galperin, M. Y. (2015) 'Bacterial cellulose biosynthesis: Diversity of operons, subunits, products, and functions', *Trends in Microbiology*, 23(9), pp. 545–557. doi: 10.1016/j.tim.2015.05.005.

Rose, N. L. *et al.* (1999) 'Inactivation of Nisin by Glutathione in Fresh Meat', *Journal of Food Science*, 64(5), pp. 759–762. doi: 10.1111/j.1365-2621.1999.tb15906.x.

Ross, P., Mayer, R. and Benziman, M. (1991) 'Cellulose biosynthesis and function in bacteria', *Microbiological Reviews*, 55(1), pp. 35–58. doi: 10.1128/mmbr.55.1.35-58.1991.

Roy, D. *et al.* (2009) 'Cellulose modification by polymer grafting: A review', *Chemical Society Reviews*, 38(7), pp. 2046–2064. doi: 10.1039/b808639g.

Rudra, J. S., Dave, K. and Haynie, D. T. (2006) 'Antimicrobial polypeptide multilayer nanocoatings', *Journal of Biomaterials Science, Polymer Edition*, 17(11), pp. 1301–1315. doi: 10.1163/156856206778667433.

Ruiz, C. *et al.* (2002) 'Analysis of Bacillus megaterium lipolytic system and cloning of LipA, a novel subfamily I.4 bacterial lipase', *FEMS Microbiology Letters*, 217(2), pp. 263–267. doi: 10.1016/S0378-1097(02)01091-1.

Ruiz, C. *et al.* (2007) 'Helicobacter pylori EstV: Identification, cloning, and characterization of the first lipase isolated from an epsilon-proteobacterium', *Applied and Environmental Microbiology*, 73(8), pp. 2423–2431. doi: 10.1128/aem.02215-06.

Ruiz, C., Pastor, F. I. J. and Diaz, P. (2003) 'Isolation and characterization of Bacillus sp. BP-6 LipA, a ubiquitous lipase among mesophilic Bacillus species', *Letters in Applied Microbiology*, 37(4), pp. 354–359. doi: 10.1046/j.1472-765X.2003.01413.x.

Ruiz, C., Pastor, F. I. J. and Diaz, P. (2005) 'Isolation of lipid- and polysaccharide-degrading micro-organisms from subtropical forest soil, and analysis of lipolytic strain Bacillus sp CR-179', *Letters in Applied Microbiology*, 40(3), pp. 218–227. doi: 10.1111/j.1472-765X.2005.01660.x.

Sabbadin, F. *et al.* (2018) 'An ancient family of lytic polysaccharide monooxygenases with roles in arthropod development and biomass digestion', *Nature Communications*, 9(1). doi: 10.1038/s41467-018-03142-x.

Saibuatong, O. ard and Phisalaphong, M. (2010) 'Novo aloe vera-bacterial cellulose composite film from biosynthesis', *Carbohydrate Polymers*, 79(2), pp. 455–460. doi: 10.1016/j.carbpol.2009.08.039.

Saito, T. and Isogai, A. (2005) 'Ion-exchange behavior of carboxylate groups in fibrous cellulose oxidized by the TEMPO-mediated system', *Carbohydrate Polymers*, 61(2), pp. 183–190. doi: 10.1016/j.carbpol.2005.04.009.

Salari, M. *et al.* (2019) 'Preparation and characterization of cellulose nanocrystals from bacterial cellulose produced in sugar beet molasses and cheese whey media', *International Journal of Biological Macromolecules*, 122, pp. 280–288. doi: 10.1016/j.ijbiomac.2018.10.136.

Salle, A. *et al.* (2015) 'A Review on Extremozymes Biocatalysis: A Green Industrial Approach for Biomaterials Production', *Journal of Biomolecular Research & Therapeutics*, 04(01). doi: 10.4172/2167-7956.1000121

Sani, R. K. and Krishnaraj, R. N. (2017) *Extremophilic enzymatic processing of lignocellulosic feedstocks to bioenergy*, *Extremophilic Enzymatic Processing of Lignocellulosic Feedstocks to Bioenergy*. Edited by R. K. Sani and R. N. Krishnaraj. Cham: Springer International Publishing. doi: 10.1007/978-3-319-54684-1.

dos Santos, C. A. *et al.* (2018) 'Bacterial nanocellulose membranes combined with nisin: a strategy to prevent microbial growth', *Cellulose*, 25(11), pp. 6681–6689. doi: 10.1007/s10570-018-2010-1.

Santos, S. M. *et al.* (2015) 'Characterization of purified bacterial cellulose focused on its use on paper restoration', *Carbohydrate Polymers*, 116, pp. 173–181. doi: 10.1016/j.carbpol.2014.03.064.

Santos, S. M. *et al.* (2017) 'Paper reinforcing by in situ growth of bacterial cellulose', *Journal of Materials Science*, 52(10), pp. 5882–5893. doi: 10.1007/s10853-017-0824-0.

Satyamurthy, P. *et al.* (2011) 'Preparation and characterization of cellulose nanowhiskers from cotton fibres by controlled microbial hydrolysis', *Carbohydrate Polymers*, 83(1), pp. 122–129. doi: 10.1016/j.carbpol.2010.07.029.

Scherner, M. *et al.* (2014) 'In vivo application of tissue-engineered blood vessels of bacterial cellulose as small arterial substitutes: Proof of concept?', *Journal of Surgical Research*, 189(2), pp. 340–347. doi: 10.1016/j.jss.2014.02.011.

Schnellmann, J. *et al.* (1994) 'The novel lectin-like protein CHB1 is encoded by a chitin-inducible Streptomyces olivaceoviridis gene and binds specifically to crystalline α-chitin of fungi and other organisms', *Molecular Microbiology*, 13(5), pp. 807–819. doi: 10.1111/j.1365-2958.1994.tb00473.x.

Seth, S. *et al.* (2014) 'An insight into plant lipase research - Challenges encountered', *Protein Expression and Purification*, 95, pp. 13–21. doi: 10.1016/j.pep.2013.11.006.

Seves, A. *et al.* (2001) 'Characterization of Native Cellulose/Poly(ethylene glycol) Films', *Macromolecular Materials and Engineering*, 286(9), pp. 524–528. doi: 10.1002/1439-2054(20010901)286:9<524::AID-MAME524>3.0.CO;2-B.

Sharma, R., Chisti, Y. and Banerjee, U. C. (2001) 'Production, purification, characterization, and applications of lipases', *Biotechnology Advances*, 19(8), pp. 627–662. doi: 10.1016/S0734-9750(01)00086-6.

Sharma, S. and Kanwar, S. S. (2014) 'Organic Solvent Tolerant Lipases and Applications', *The Scientific World Journal*, 2014, pp. 1–15. doi: 10.1155/2014/625258.

Shi, Z. *et al.* (2014) 'Utilization of bacterial cellulose in food', *Food Hydrocolloids*, 35, pp. 539–545. doi: 10.1016/j.foodhyd.2013.07.012.

Siddiqui, K. S. (2015) 'Some like it hot, some like it cold: Temperature dependent biotechnological applications and improvements in extremophilic enzymes', *Biotechnology Advances*, 33(8), pp. 1912–1922. doi: 10.1016/j.biotechadv.2015.11.001.

Singhsa, P., Narain, R. and Manuspiya, H. (2018) 'Bacterial Cellulose Nanocrystals (BCNC) Preparation and Characterization from Three Bacterial Cellulose Sources and Development of Functionalized BCNCs as Nucleic Acid Delivery Systems', *ACS Applied Nano Materials*, 1(1), pp. 209–221. doi: 10.1021/acsanm.7b00105.

Skočaj, M. (2019) 'Bacterial nanocellulose in papermaking', *Cellulose*. Springer Netherlands, pp. 6477–6488. doi: 10.1007/s10570-019-02566-y.

Soleimani, M., Khani, A. and Najafzadeh, K. (2012) 'α-Amylase immobilization on the silica nanoparticles for cleaning performance towards starch soils in laundry detergents', *Journal of Molecular Catalysis B: Enzymatic*, 74(1–2), pp. 1–5. doi: 10.1016/j.molcatb.2011.07.011.

Spence, K. L. *et al.* (2010) 'The effect of chemical composition on microfibrillar cellulose films from wood pulps: Water interactions and physical properties for packaging applications', *Cellulose*, 17(4), pp. 835–848. doi: 10.1007/s10570-010-9424-8.

Stathopoulou, P. M. *et al.* (2013) 'Unraveling the lipolytic activity of thermophilic bacteria isolated from a volcanic environment', *BioMed Research International*, 2013. doi: 10.1155/2013/703130.

Stepanov, N. and Efremenko, E. (2018) '"Deceived" Concentrated Immobilized Cells as Biocatalyst for Intensive Bacterial Cellulose Production from Various Sources', *Catalysts*, 8(1), p. 33. doi: 10.3390/catal8010033.

Sulaiman, S. *et al.* (2015) 'A Review: Potential Usage of Cellulose Nanofibers (CNF) for Enzyme

Immobilization via Covalent Interactions', *Applied Biochemistry and Biotechnology*, 175(4), pp. 1817–1842. doi: 10.1007/s12010-014-1417-x.

Sung, K. *et al.* (2011) 'Lysozyme as a barrier to growth of Bacillus anthracis strain Sterne in liquid egg white, milk and beef', *Food Microbiology*, 28(6), pp. 1231–1234. doi: 10.1016/j.fm.2011.03.002.

Tahara, N. *et al.* (1998) 'Purification and characterization of exo-1,4-β-glucosidase from Acetobacter xylinum BPR2001', *Journal of Fermentation and Bioengineering*, 85(6), pp. 589–594. doi: 10.1016/S0922-338X(98)80010-X.

Tayeb, A. H. *et al.* (2018) 'Cellulose nanomaterials-binding properties and applications: A review', *Molecules*. MDPI AG. doi: 10.3390/molecules23102684.

Thomas, B. *et al.* (2018) 'Nanocellulose, a Versatile Green Platform: From Biosources to Materials and Their Applications', *Chemical Reviews*, 118(24), pp. 11575–11625. doi: 10.1021/acs.chemrev.7b00627.

Timucin, E. *et al.* (2015) 'Probing the roles of two tryptophans surrounding the unique zinc coordination site in lipase family I.5', *proteins*, 84, pp. 129–142.

Treichel, H. *et al.* (2010) 'A review on microbial lipases production', *Food and Bioprocess Technology*. doi: 10.1007/s11947-009-0202-2.

Troncoso, O. P. and Torres, F. G. (2020) 'Bacterial cellulose—graphene based nanocomposites', *International Journal of Molecular Sciences*, 21(18), pp. 1–17. doi: 10.3390/ijms21186532.

Ude, S. *et al.* (2006) 'Biofilm formation and cellulose expression among diverse environmental Pseudomonas isolates', *Environmental Microbiology*, 8(11), pp. 1997–2011. doi: 10.1111/j.1462-2920.2006.01080.x.

Vaaje-Kolstad, G. *et al.* (2010) 'An oxidative enzyme boosting the enzymatic conversion of recalcitrant polysaccharides', *Science*, 330(6001), pp. 219–222. doi: 10.1126/science.1192231.

Vaaje-Kolstad, G. *et al.* (2017) 'Structural diversity of lytic polysaccharide monooxygenases', *Current Opinion in Structural Biology*, 44, pp. 67–76. doi: 10.1016/j.sbi.2016.12.012.

Vaghari, H. *et al.* (2016) 'Application of magnetic nanoparticles in smart enzyme immobilization', *Biotechnology Letters*, 38(2), pp. 223–233. doi: 10.1007/s10529-015-1977-z.

Valenzuela, S. V. *et al.* (2017) 'Fast purification method of functional LPMOs from Streptomyces ambofaciens by affinity adsorption', *Carbohydrate Research*, 448, pp. 205–211. doi: 10.1016/j.carres.2017.02.004.

Valenzuela, S. V. *et al.* (2019) 'Differential activity of lytic polysaccharide monooxygenases on celluloses of different crystallinity. Effectiveness in the sustainable production of cellulose nanofibrils', *Carbohydrate Polymers*, 207, pp. 59–67. doi: 10.1016/j.carbpol.2018.11.076.

Valls, C. *et al.* (2019) 'Assessing the enzymatic effects of cellulases and LPMO in improving mechanical fibrillation of cotton linters', *Biotechnology for Biofuels*, 12(1), p. 161. doi: 10.1186/s13068-019-1502-z.

Vandamme, E. J. (1983) 'Peptide antibiotic production through immobilized biocatalyst technology', *Enzyme and Microbial Technology*, 5(6), pp. 403–416. doi: 10.1016/0141-0229(83)90021-2.

Varejão, N. *et al.* (2018) 'Structural Mechanism for the Temperature-Dependent Activation of the Hyperthermophilic Pf2001 Esterase.', *Structure (London, England : 1993)*, 26(2), pp. 199-208.e3. doi: 10.1016/j.str.2017.12.004.

Vasconcelos, N. F. *et al.* (2017) 'Bacterial cellulose nanocrystals produced under different hydrolysis conditions: Properties and morphological features', *Carbohydrate Polymers*, 155, pp. 425–431. doi: 10.1016/j.carbpol.2016.08.090.

Vasconcelos, N. F. *et al.* (2020) 'Oxidized bacterial cellulose membrane as support for enzyme immobilization: properties and morphological features', *Cellulose*, 27(6), pp. 3055–3083. doi: 10.1007/s10570-020-02966-5.

Vermaas, J. V. *et al.* (2015) 'Effects of lytic polysaccharide monooxygenase oxidation on cellulose structure and binding of oxidized cellulose oligomers to cellulases', *Journal of Physical Chemistry B*,

119(20), pp. 6129–6143. doi: 10.1021/acs.jpcb.5b00778.

Vermeiren, L. *et al.* (1999) 'Developments in the active packaging of foods', *Trends in Food Science & Technology*, 10(3), pp. 77–86. doi: 10.1016/S0924-2244(99)00032-1.

Vikhoreva, G. A., Gorbacheva, I. N. and Gal'braikh, L. S. (1994) 'Chemical modification of aquatic polysaccharides. A review', *Fibre Chemistry*, 26(5), pp. 326–334. doi: 10.1007/BF02396600.

Villares, A. *et al.* (2017) 'Lytic polysaccharide monooxygenases disrupt the cellulose fibers structure', *Scientific Reports*, 7. doi: 10.1038/srep40262.

Vu, V. V. *et al.* (2014) 'A family of starch-active polysaccharide monooxygenases', *Proceedings of the National Academy of Sciences of the United States of America*, 111(38), pp. 13822–13827. doi: 10.1073/pnas.1408090111.

Wang, J., Tavakoli, J. and Tang, Y. (2019) 'Bacterial cellulose production, properties and applications with different culture methods – A review', *Carbohydrate Polymers*, 219, pp. 63–76. doi: 10.1016/j.carbpol.2019.05.008.

Wang, P. (2006) 'Nanoscale biocatalyst systems', *Current Opinion in Biotechnology*, 17(6), pp. 574–579. doi: 10.1016/j.copbio.2006.10.009.

Wong, H. C. *et al.* (1990) 'Genetic organization of the cellulose synthase operon in Acetobacter xylinum (cellulose biogenesis/cloning/sequencing)', *Proc. Nati. Acad. Sci. USA*, 87, pp. 8130–8134.

Wu, S.-C., Wu, S.-M. and Su, F.-M. (2017) 'Novel process for immobilizing an enzyme on a bacterial cellulose membrane through repeated absorption', *Journal of Chemical Technology & Biotechnology*, 92(1), pp. 109–114. doi: 10.1002/jctb.4994.

Xue, Y., Mou, Z. and Xiao, H. (2017) 'Nanocellulose as a sustainable biomass material: Structure, properties, present status and future prospects in biomedical applications', *Nanoscale*, 9(39), pp. 14758–14781. doi: 10.1039/c7nr04994c.

Yamada, Y. *et al.* (2012) 'Subdivision of the genus Gluconacetobacter Yamada, Hoshino and Ishikawa 1998: The proposal of Komagatabacter gen. nov., for strains accommodated to the Gluconacetobacter xylinus group in the α-Proteobacteria', *Annals of Microbiology*, 62(2), pp. 849–859. doi: 10.1007/s13213-011-0288-4.

Yang, J. S., Xie, Y. J. and He, W. (2011) 'Research progress on chemical modification of alginate: A review', *Carbohydrate Polymers*, 84(1), pp. 33–39. doi: 10.1016/j.carbpol.2010.11.048.

Yang, W. *et al.* (2013) 'Genetic diversity and symbiotic evolution of rhizobia from root nodules of Coronilla varia', *Systematic and Applied Microbiology*, 36(1), pp. 49–55. doi: 10.1016/j.syapm.2012.10.004.

Yanto, D. H. Y., Tachibana, S. and Itoh, K. (2014) 'Biodecolorization of Textile Dyes by Immobilized Enzymes in a Vertical Bioreactor System', *Procedia Environmental Sciences*, 20, pp. 235–244. doi: 10.1016/j.proenv.2014.03.030.

Yao, W. *et al.* (2013) 'In vitro enzymatic conversion of γ-aminobutyric acid immobilization of glutamate decarboxylase with bacterial cellulose membrane (BCM) and non-linear model establishment', *Enzyme and Microbial Technology*, 52(4–5), pp. 258–264. doi: 10.1016/j.enzmictec.2013.01.008.

Yuan, H. *et al.* (2018) 'Evaluation of nanocellulose carriers produced by four different bacterial strains for laccase immobilization', *Carbohydrate Polymers*, 196, pp. 457–464. doi: 10.1016/j.carbpol.2018.05.055.

Zhang, Jingyan *et al.* (2010) 'Graphene oxide as a matrix for enzyme immobilization', *Langmuir*, 26(9), pp. 6083–6085. doi: 10.1021/la904014z.

Zhang, W. *et al.* (2011) 'Facile fabrication of flexible magnetic nanohybrid membrane with amphiphobic surface based on bacterial cellulose', *Carbohydrate Polymers*, 86(4), pp. 1760–1767. doi: 10.1016/j.carbpol.2011.07.015.

Zhao, X. *et al.* (2015) 'Lipase-catalyzed process for biodiesel production: Enzyme immobilization, process simulation and optimization', *Renewable and Sustainable Energy Reviews*, 44, pp. 182–197. doi: 10.1016/j.rser.2014.12.021.

Zhu, D., Wu, Q. and Wang, N. (2011) 'Industrial Enzymes', in *Comprehensive Biotechnology, Second Edition*. Elsevier, pp. 3–13. doi: 10.1016/B978-0-08-088504-9.00182-3.

Zhuang, J. *et al.* (2007) 'Economic Analysis of Cellulase Production Methods for Bio-Ethanol', *Applied Engineering in Agriculture*, 23(5), pp. 679–687. doi: 10.13031/2013.23659.

Zimmermann, T., Bordeanu, N. and Strub, E. (2010) 'Properties of nanofibrillated cellulose from different raw materials and its reinforcement potential', *Carbohydrate Polymers*, 79(4), pp. 1086–1093. doi: 10.1016/j.carbpol.2009.10.045.

Zinge, C. and Kandasubramanian, B. (2020) 'Nanocellulose based biodegradable polymers', *European Polymer Journal*, 133, p. 109758. doi: 10.1016/j.eurpolymj.2020.109758.

MICROBIAL ENZYMES GROUP

Delving into green technologies